International Journal of Air and Water Pollution

EDITORS

AIR POLLUTION SECTION

R. S. SCORER, *London*
G. NONHEBEL, *London*
C. M. FLETCHER, *London*
W. KLUG, *Darmstadt*
JAMES P. LODGE, *Boulder, Colo.*

WATER POLLUTION SECTION

B. A. SOUTHGATE, *Stevenage,*
W. WESLEY ECKENFELDER, *New York*
E. LECLERC, *Liège*

assisted by an international Editorial Advisory Board

VOL.
4
1961

Volume 4

1961

Copyright © 1961 Pergamon Press Ltd

PERGAMON PRESS Oxford London New York Paris

CONTENTS OF VOLUME 4

NUMBERS 1/2

F. Wipperman: Die Maximal-Konzentrationen eines sich in turbulenter Strömungausbreitenden Gases — *page* 1
K. D. Hage: The influence of size distribution on the ground deposit of large particles — 24
W. P. Elliot: The vertical distribution of gas from a continuous source — 33
G. T. Csanady: Some observations on smoke plumes — 47
C. L. Mateer: Effect of the weekly cycle of air pollution on solar radiation at Toronto — 52
A. P. Altshuller and I. Cohen: The gas phase reactions of nitrogen oxides with olefins — 55
A. P. Altshuller and A. F. Wartburg: Ozone interactions with plastic and metallic materials in a dynamic flow system — 70
E. R. Stephens, E. F. Darley, O. C. Taylor and W. E. Scott: Photochemical reaction products in air pollution — 79
G. H. Hepting and C. R. Berry: Needle blights of White Pine — the interpretation of fume damage — 101
N. Jaworski, G. W. Lawton and G. A. Rohlich: Aerobic sludge digestion — 106
J. M. Symons, R. E. McKinney, R. M. Smith and E. J. Donovan, Jr: Degradation of nitrogen-containing organic compounds by activated sludge — 115

Book Review: — 139

Papers to be published in future issues: — 140

NUMBERS 3/4

P. Stocks, B. T. Commins and K. V. Audrey: A study of smoke in Merseyside and other northern localities — 141
Tore Dalham and Lars Strandberg: Effects of sulphur dioxide on rabbit cilia — 154
Alexander Goetz: On the nature of the synergistic action of aerosols — 168
James Halitsky: Single-camera measurement of smoke plumes — 185
Francis Pooler Jr.: A prediction model of mean urban pollution for use with standard wind roses — 199
P. A. E. Crosse, D. H. Lucas and W. L. Snowsill: The measurement of dust nuisance emitted by chimneys — 212
Vitezslav Havlíček: The improvement of efficiency of fibrous dielectric filters — 225
R. T. Austin, R. W. Lewis and R. Donaldson Jr.: A new atmosphere irradiation chamber — 237
D. F. Adams: Limed filter paper technique for fluorine air pollution studies — 247
F. Rosenberg, N. Dondero and H. Heukelekian: Bacterial indicators of pollution in household well waters — 256

Abstracts of papers published in Staub: — 267

Air pollution bibliography: — 272

Book Reviews: — 275

News and Notes: — 276

AUTHOR INDEX

Adams, D. F.	247	Hurley, T. F.	272
Altshuller, A. P.	55, 70	Jaworski, N.	106
Audrey, K. V.	141	Lawton, G. W.	106
Austin, R. T.	237	Lewis, R. W.	237
Berry, C. R.	101	Lucas, D. H.	212
Crosse, P. A. E.	212	Mateer, C. L.	52
Cohen, I.	55	McKinney, R. E.	115
Commins, B. T.	141	Pooler, F. Jr.	199
Csanady, G. T.	47	Rohlich, G. A.	106
Dalhamn, T.	154	Rosenberg, F.	256
Darley, E. F.	79	Scott, W. E.	79
Donaldson, R. Jr.	237	Smith, R. M.	115
Dondero, N.	256	Snowsill, W. L.	212
Donovan, E. J. Jr.	115	Strauss, W.	267
Elliott, W. P.	33	Stephens, E. R.	79
Goetz, A.	168	Stocks, P.	141
G. B. C.	139 (B)	Strandberg, L.	154
Hage, K. D.	24	Symons, J. M.	115
Halitsky, J.	185	Taylor, O. C.	79
Havliček, V.	225	Wartburg, A. F.	70
Hepting, G. H.	101	Wipperman, F.	1
Heukelekian,	256		

(B) denote Book Reviews

VOL.
4
1961

Int. J. Air and Water Poll. Pergamon Press 1961. Vol. 4, Nos. 1/2, pp. 1–23. Printed in Great Britain.

DER EFFEKT DER MESSDAUER BEI DER ERMITTLUNG VON MAXIMAL-KONZENTRATIONEN EINES SICH IN TURBULENTER STRÖMUNG AUSBREITENDEN GASES

F. WIPPERMANN
Technische Hochschule Darmstadt, Meteorologisches Institut
(*Received* 21 *December* 1959)

Zusammenfassung—Die Brauchbarkeit der SUTTONschen Formel für die maximale Gaskonzentration am Boden kann experimentell nur geprüft werden, wenn die Gaskonzentration und die meteorologischen Parameter nicht nur simultan gemessen werden, sondern die dabei erhaltenen Mittelwerte auch aus Mittelbildungen über das gleiche Zeitintervall (Messdauer für die Konzentration, Beobachtungszeit für die meteorologischen Parameter) hervorgegangen sind. Soll diese Formel als Grundlage irgendwelcher Bestimmungen zum Zwecke der Schadensverhütung dienen, so gilt das gleiche – an die Stelle der Messdauer für die Konzentration tritt lediglich die sogenannte Immissionszeit. Diese wird von Biologen angegeben; der Mittelwert der Gaskonzentration über diese Zeit darf den ebenfalls von den Biologen angegebenen gerade noch zulässigen Grenzwert (MIK) nicht überschreiten. Wenn die Dauer der Konzentrationsmessung mit der Beobachtungszeit für die meteorologischen Parameter nicht übereinstimmt, bezw. die Immissionszeit für die Einwirkung des schädlichen Gases mit der Beobachtungszeit für die meteorologischen Parameter nicht übereinstimmt, ist die Anbringung einer Korrektur erforderlich. Diese wird mit Messdauereffekt bezeichnet.

Um quantitative Aussagen über diesen Messdauereffekt zu erhalten, wird eine statistiche Theorie entwickelt. Zu diesem Zwecke wird die Abhängigkeit der in die SUTTONsche Formel eingehenden meteorologischen Parameter von der Mittelbildungszeit untersucht. Es zeigt sich, dass sich ändernde Zeiten für die Mittelbildung über das Quadrat der Geschwindigkeitsfluktuationen in vertikaler Richtung für den Messdauereffekt praktisch bedeutungslos sind. Eine starke Abhängigkeit von der Mittelbildungszeit zeigen jedoch die durch die Mittelbildung selbst erhaltene Grundströmung wie auch der Mittelwert des Quadrates der Geschwindigkeitsfluktuationen quer dazu. Da die SUTTON-Formel eine Orientierung des Koordinatensystems nach der mittleren Windrichtung vorsieht, hängt auch die Orientierung des Koordinatensystems von der Mittelbildungszeit ab.

Eine Anwendung der Theorie setzt die Kenntnis einiger Kenngrössen des atmosphärischen Strömungsfeldes voraus, nämlich: Beständigkeit des Windes, Turbulenzniveau (sowohl für eine unendlich lange als auch für irgendeine endliche Mittelbildungszeit) und eine charakteristische Zeit. Diese Grössen wurden so weit wie möglich aus Beobachtungen entnommen, für den Rest wurden die plausibelsten Werte angenommen. Das Ergebnis ist in einer Tabelle im Anschluss an Gleichung (87) zusammengestellt. Ein Vergleich des theoretischen Ergebnisses mit Messdaten ist nur in beschränktem Masse möglich, da hierfür geeignete Messdaten bislang nur von STEWART u.a. (1954) erhalten wurden. Diese zeigen jedoch eine befriedigende Übereinstimmung.

Abstract—The usefulness of the Sutton formula for the maximum concentration of gases at the surface can be checked by experiment only, if the gas concentration and the meteorological parameters are not only measured simultaneously, but that the so-obtained mean values are means over the same interval of time (time of sampling for the concentration, observation time for the meteorological parameters). The same holds true if this formula shall be used as basis for regulations for preventing any damages; the time of measurement is then replaced by the so-called " Immissionszeit ". This time is stated by the biologists; the mean of the gas concentration taken over this interval may not exceed the maximum allowable concentration (MIK), which is also stated by the biologists. If the interval of concentration measurement is not in agreement with the observation time of the meteorological parameters, respectively, the " Immissionszeit " for the influence of the noxious gas is not in agreement with the observation time of the meteorological parameters, a correction factor has to be used. This is called the effect of sampling time.

VOL. 4 1961

A statistical theory is presented to obtain quantitative statements for this effect of sampling time. For this purpose the dependence of the meteorological parameters of the Sutton formula on the time interval over which the means are taken is investigated. It is shown, that different mean intervals for the square of the velocity fluctuations in vertical direction are insignificant for the effect of sampling time. A strong dependence on the mean intervals is shown for the mean velocity as well as for the square of the velocity fluctuations perpendicular to it. Because the Sutton formula requires an orientation of the co-ordinate system in the direction of the mean flow, the orientation of the co-ordinate system depends also on the mean interval.

An application of the theory requires knowledge of some characteristic values of the atmospheric flow. These are: Steadiness of the wind, level of turbulence (for infinitely long mean interval), level of turbulence (for any finite time interval) and a characteristic time. These values were taken—as far as possible—from observations, the rest are the most plausible values. The results are shown in a table following equations (87). A comparison of the theoretical results with experimental data is restricted, because suitable data were published only by STEWART *et al.* (1954). The agreement with these data is satisfactory.

EINLEITUNG

In dem Bemühen, die Abgabe schädlicher Industrieabgase in die Atmosphäre auf ein erträgliches Mass zu reduzieren, lässt man sich zweckmässigerweise von der Vorstellung leiten, dass im Bereiche möglicher Schädigungen – also vorwiegend am Erdboden oder in dessen unmittelbarer Nähe – gewisse Maximalkonzentrationen nicht überschritten werden dürfen. Letztere werden von Medizinern, Biophysikern, Biologen, Botanikern und Pflanzenphysiologen zugleich mit einer sogenannten Immissionszeit so festgesetzt, dass Schädigungen erst dann auftreten, wenn die über die angegebene Immissionszeit gemittelte Konzentration den festgelegten Maximalwert überschreitet. Für interessierende Emissionsgrössen (Schornsteinhöhe, Quellstärke, Austrittstemperatur und Austrittsgeschwindigkeit) lässt sich dann bei Vorgabe bestimmter Kenngrössen der atmosphärischen Turbulenz mittels einer der hierfür hergeleiteten Formeln feststellen, ob die festgelegte Maximalkonzentration erreicht wird oder nicht. Der Grad der Sicherheit, mit dem diese Entscheidung getroffen werden kann, hängt selbstverständlich davon ab, wieweit im Einzelfalle diejenigen Voraussetzungen und Vereinfachungen erfüllt sind, die bei der Ableitung der benutzten Formel notwendigerweise gemacht werden mussten.

Die Verwendung derartiger Maximalkonzentrationen (z.B. bei den angedeuteten Luftreinhaltungs-Massnahmen) wirft sofort ein neues, bislang ungelöstes Problem auf: dasenige des Effektes der Messdauer. Es besteht Einhelligkeit in der Meinung darüber, dass dieses ein sehr wichtiges Problem ist – vergl. z.B. FRENKIEL und SHEPPARD (1959) – ohne dessen Lösung viele Fragen der Luftverunreinigung nur mangelhaft beantwortet werden können. In dieser Untersuchung wird der Versuch unternommen mit Hilfe einer statistischen Theorie zu quantitativen Aussagen über den Effekt der Messdauer zu gelangen.

ZUR DEFINITION DES EFFEKTES DER MESSDAUER

Eine gewisse Verwirrung – zumindest im deutschsprachigen Bereich – der Begriffe Messdauer, Beobachtungszeit und Immissionszeit macht es notwendig, zunächst eine präzise Definition des genannten Effektes zu geben. Hierzu wiederum ist es erforderlich, eine saubere Unterscheidung zwischen Mittelbildungen über verschieden lange

Zeiten zu treffen, wie auch die Abweichungen von Mitteln über verschieden lange Zeiten zu unterscheiden. Dies geschehe durch eine Indizierung der Mittelwerte; für eine beliebige Grösse a gelte

$$\bar{a}_T(t) = \frac{1}{T}\int_{-T/2}^{+T/2} a(t+\vartheta)\,d\vartheta \tag{1}$$

und entsprechend

$$\bar{a}_\infty = \lim_{A\to\infty} \frac{1}{2A}\int_{-A}^{+A} a(t)\,dt \tag{2}$$

Die Abweichungen vom jeweiligen Mittel sollen mit einem Apostroph bezeichnet werden:

$$a'_T(t) = a(t) - \bar{a}_T(t) \tag{3}$$

beziehungsweise

$$a'_\infty(t) = a(t) - \bar{a}_\infty \tag{4}$$

Definitionsgemäss ist

$$\overline{[a'_\infty(t)]}_\infty \equiv 0 \tag{5}$$

während jedoch

$$\overline{[a'_T(t)]}_T = \bar{a}_T(t) - \overline{(\bar{a}_T)}_T(t) \tag{6}$$

im allgemeinen nicht verschwindet.

Es liefern nun alle praktisch verwendbaren Theorien für die Ausbreitung eines Gases in turbulenter Strömung nur Verteilungen der zeitlich gemittelten Konzentration des Gases. Dies ist bei beiden, sowohl bei den analytischen wie auch bei den statistischen Theorien leicht einzusehen, besonders leicht bei letzteren: Man geht von einer Normalverteilung† für die Konzentration aus und identifiziert das Streuungsquadrat (d.h. das mittlere Quadrat der Partikelverschiebungen) dieser Verteilung mit dem Diffusionskoeffizienten. Das bedeutet aber, dass es sich nur um die Verteilung einer zeitlich gemittelten Konzentration handeln kann, und zwar gemittelt über die gleiche Zeit über die das mittlere Verschiebungsquadrat der Partikel gebildet wurde. Bezeichnen wir letzteres in den drei Koordinatenrichtungen mit $\overline{(\xi)^2}_T$, $\overline{(\eta)^2}_T$, $\overline{(\zeta)^2}_T$ und die Konzentration des Gases mit s, so gilt für den Fall einer momentan freigesetzten Gasmenge

$$\bar{s}_T = f(x, y, z, t, \overline{(\xi)^2}_T, \overline{(\eta)^2}_T, \overline{(\zeta)^2}_T) \tag{7}$$

Eine Nachprüfung jeglicher Ausbreitungstheorie käme einer Verifikation der Beziegung (7) gleich. Hierzu müssen die Grössen $\overline{(\xi)^2}_T$, $\overline{(\eta)^2}_T$, $\overline{(\zeta)^2}_T$ aus meteorologischen Beobachtungen entnommen werden, wobei die Theorie angibt, welcher Zusammen-

† In diesem Zusammenhange ist es unerheblich, dass eine Normalverteilung gewählt wird (d.h. der Diffusionsvorgang als einfacher MARKOV-prozess im Konfigurationsraum aufgefasst wird). Bei einer etwas wirklichkeitsnäheren Beschreibung eines turbulenten Diffusionsvorganges (z.B. eines einfachen MARKOV-prozesses im Phasenraum) wird eine Verteilung erhalten, die der Lösung einer Diffusionsgleichung vom Typ der Telegraphengleichung entspricht (GOLDSTEIN, 1951). Für die Konzentration gilt auch dann das oben gesagte.

VOL. 4 1961

hang zwischen diesen mittleren Verschiebungsquadraten und irgendwelchen messbaren Kenngrössen für die atmosphärische Turbulenz hierfür ausgenutzt wird. Auf der andern Seite muss die Konzentration s gemessen und ihr Mittelwert festgestellt werden. Dabei ist wesentlich, dass die Dauer der Konzentrationsmessung mit der Dauer der Messung der meteorologischen Parameter (Beobachtungszeit) übereinstimmt. Ist die Konzentrationsmessung zwar simultan mit der Messung der meteorologischen Parameter erfolgt, ist jedoch die Dauer beider Messungen verschieden ($T_K \neq T_M$), so ist eine Verifikation der Beziehung (7) nur möglich bei Verwendung eines Korrekturfaktors V derart, dass

$$V(T_M \mid T_K) \cdot \overline{s_{T_K}} = f(x, y, z, t, \overline{(\xi)^2}_{T_M}, \overline{(\eta)^2}_{T_M}, \overline{(\zeta)^2}_{T_M})$$

Dieser Faktor $V(T_1 \mid T_2)$

$$V(T_M \mid T_K) = \frac{\overline{s_{T_M}}}{\overline{s_{T_K}}} = f(x, y, z, t, \overline{(\xi)^2}_{T_M}, \overline{(\xi)^2}_{T_K}, \overline{(\eta)^2}_{T_M}, \overline{(\eta)^2}_{T_K}, \overline{(\zeta)^2}_{T_M}, \overline{(\zeta)^2}_{T_K}) \qquad (8)$$

werde als Effekt der Messdauer bezeichnet; es ist V = 1·0, wenn die Dauer der Konzentrationsmessung mit der Messdauer der meteorologischen Parameter (Beobachtungszeit) übereinstimmt.

Bei der zu Anfang genannten Problemstellung der Luftreinhaltung übernimmt die angegebene Immissionszeit die Rolle der Konzentrationsmessdauer. Wenn also die meteorologischen Parameter nicht als Mittelwerte über die Zeitspanne zur Verfügung stehen, die zusammen mit der Maximalkonzentration als Immissionszeit für das betreffende schädliche Gas angegeben wird, kann eine Formel (der Ausbreitungstheorie) nur bei zusätzlicher Verwendung des vorgenannten Korrekturfaktors V benutzt werden. Gerade deshalb ist eine quantitative Erfassung dieses Messdauereffektes so wichtig.

DER EFFEKT DER MESSDAUER FÜR MAXIMALE BODENKONZENTRATIONEN IM FELDE EINER KONTINUIERLICHEN PUNKTQUELLE

Im Hinblick auf die anfänglich genannte Problemstellung der Luftreinhaltung ist es sinnvoll festzustellen, wie gross der Effekt der Messdauer für maximale Bodenkonzentrationen im Felde einer kontinuierlichen Punktquelle ist. SUTTON (1932) gibt für die Maximalkonzentration folgende Beziehung

$$s^* = \frac{Q}{\pi e h^2} \frac{2 C_z}{\overline{u} C_y} \qquad (9)$$

worin Q die Quellstärke [g sec^{-1}], h die effektive Höhe der Quelle, u die räumlich konstant vorausgesetzte Grundgeschwindigkeit, C_z und C_y die virtuellen Diffusionskoeffizienten in vertikaler Richtung und senkrecht zur Richtung der mittleren Windgeschwindigkeit sind. Dass für die Gültigkeit der Beziehung (9) noch eine Reihe von Voraussetzungen erfüllt sein muss, wie z.B. das Vorhandensein eines völlig ebenen, das Gas nicht absorbierenden Erdbodens, ist im Zusammenhang mit dem Effekt der Messdauer unwesentlich.

Für die virtuellen Diffusionskoeffizienten C_z und C_y erhält SUTTON durch Verwendung eines aus Dimensionsüberlegungen gewählten Ansatzes für die LAGRANGEsche Korrelationsfunktion folgende Beziehungen zu messbaren Grössen für die atmosphärischen Turbulenzverhältnisse

$$C^2_z = \frac{4N^n}{(1-n)(2-n)} \frac{1}{(\bar{u})^n} \left[\frac{\overline{(w')^2}}{(\bar{u})^2}\right]^{1-n} \tag{10a}$$

$$C^2_y = \frac{4N^n}{(1-n)(2-n)} \frac{1}{(\bar{u})^n} \left[\frac{\overline{(v')^2}}{(\bar{u})^2}\right]^{1-n} \tag{10b}$$

worin N die Makroviskosität, w die vertikale Geschwindigkeitskomponente und v diejenige in Richtung senkrecht zur mittleren Windgeschwindigkeit bedeuten. Der Parameter n charakterisiert die Stabilität der atmosphärischen Schichtung und ist nach SUTTON aus dem gemessenen vertikalen Profil der mittleren Windgeschwindigkeit zu bestimmen.

Mit (10a) und (10b) ergibt sich für die Maximalkonzentration (9)

$$s^* = \frac{Q}{\pi e h^2} \frac{2}{\bar{u}} \left[\frac{\overline{(w')^2}}{\overline{(v')^2}}\right]^{\frac{1-n}{2}} \tag{11}$$

Wie bereits angedeutet, wird zum Erhalt dieser Beziehung ein Ansatz für die LAGRANGEsche Korrelationsfunktion benutzt; infolge ihrer Definition bedingt diese Mittelbildungen über eine unendlich lange Zeit. Mit der vorgesehenen Indizierung der gemittelten Grössen zur Kennzeichnung der Länge der Mittelbildungsintervalle lautet Gl. (11) also

$$(\overline{s^*})_\infty = \frac{Q}{\pi e h^2} \frac{2}{\bar{u}_\infty} \left[\frac{\overline{(w'_\infty)^2}_\infty}{\overline{(v'_\infty)^2}_\infty}\right]^{\frac{1-n_\infty}{2}} \tag{12}$$

In dieser Form, in der das SUTTONsche Ergebnis eigentlich gültig ist, ist es aber gleichzeitig aus zwei Gründen unanwendbar: Erstens ist $\overline{s^*}_\infty$ ein für alle Zeiten konstanter Wert, bei dem der interessierende Einfluss sich zeitlich verändernder Turbulenzverhältnisse durch die unendlich lange Mittelbildungszeit unerkennbar bleibt, zum andern können auch wegen der unendlich langen Mittelbildungszeit die für die Gültigkeit von Gl. (11) bezw. (12) notwendigen Voraussetzungen nie erfüllt werden. $\overline{s^*}_\infty$ wird sich aber trotzdem als Bezugsgrösse sehr nützlich erweisen.

Man sichert dem SUTTONschen Ergebnis seine vielseitigen Anwendungsgemöglichkeiten erst dadurch, dass man anstelle von (12)

$$(\overline{s^*})_T = \frac{Q}{\pi e h^2} \frac{2}{\bar{u}_T} \left[\frac{\overline{(w'_T)^2}_T}{\overline{(v'_T)^2}_T}\right]^{\frac{1-n_T}{2}} \tag{13}$$

setzt. Die beiden Maximalkonzentrationen (12) und (13) werden sich dabei um einen von der Mittelbildungszeit T abhängigen Faktor

$$\Psi(T) = \frac{\overline{s^*}_T}{\overline{s^*}_\infty} = \frac{\bar{u}_\infty}{\bar{u}_T} \left[\frac{\overline{(w'_T)^2}_T}{\overline{(w'_\infty)^2}_\infty} \frac{\overline{(v'_\infty)^2}_\infty}{\overline{(v'_T)^2}_T}\right]^{\frac{1-\hat{n}}{2}} \tag{14}$$

unterscheiden. Dieser Faktor führt unmittelbar zur Definition des Messdauereffektes $V(T_1 \mid T_2)$

$$V(T_1 \mid T_2) = \frac{\Psi(T_1)}{\Psi(T_2)} \tag{15}$$

Es gilt also $V(T \mid \infty) = \Psi(T)$

VOL. 4 1961

Aus Gründen der Vereinfachung wurde in der Beziehung (14) angenommen

$$\bar{n}_T = \bar{n}_x = \hat{n}$$

d.h. der Stabilitätsgrad der atmosphärischen Schichtung wird über alle Zeit als konstant vorausgesetzt. Der Einfluss der Nichterfüllung dieser Voraussetzung wird an späterer Stelle diskutiert.

Die SUTTONsche Formel (9) bezw. (11) setzt eine derartige Orientierung des Koordinatensystemes voraus, dass die X-Achse in Richtung des Vektormittels der horizontalen Windgeschwindigkeit liegt. Das bedeutet, dass eine Veränderung der Mittelbildungsdauer eine Neuorientierung des Koordinatensystemes zur Folge haben kann. Gerade dieser Umstand ist es, der das Problem erschwert; relativ einfach ist lediglich die Behandlung der Geschwindigkeitsfluktuationen in Richtung der für alle Zeiten unveränderten Vertikalkoordinate. Für die horizontalen Bewegungen bleibt aber die Verwendung von Vektoren unumgänglich. Es wird mithin statt (14) geschrieben:

$$\Psi(T) = \frac{|\,\bar{\mathbf{v}}_x\,|}{|\,\bar{\mathbf{v}}_T\,|} \left[\frac{\overline{(w'_T)^2}_T \; \overline{(\mathbf{i}_x \times \mathbf{v}'_x)^2}_x}{\overline{(w'_x)^2}_T \; \overline{(\mathbf{i}_T \times \mathbf{v}'_T)^2}_T} \right]^{\frac{1-\hat{n}}{2}} \tag{16}$$

mit den Einheitsvektoren

$$\mathbf{i}_T = \frac{\bar{\mathbf{v}}_T}{|\,\bar{\mathbf{v}}_T\,|}$$

Es erscheint zweckmassig an dieser Stelle zwei verschiedene Möglichkeiten einer Betrachtungsweise zu unterscheiden:

(*a*) Für eine hinreichend lange Messdauer T^* werde der Maximalwert der Bodenkonzentration am Punkte seines Auftretens ermittelt, es ergibt sich der Wert $\overline{(s)}_{T^*}$.† Falls die Messung durch eine fortlaufende Registrierung vorgenommen wird, so ist es möglich auch die Konzentration für gleichgrosse Teilintervalle von T^* zu bestimmen. Die Werte für die einzelnen Teilintervalle werden um den Wert $\overline{(s)}_{T^*}$ schwanken, das Mittel über alle Teilintervalle ergibt jedoch wieder diesen Wert. Dies ist unabhängig von der Dauer der (gleich langen) Teilintervalle. Das gleiche Resultat erhält man auch, wenn man nicht die Konzentration misst, sondern die durch eine Formel vorgeschriebenen meteorologischen Parameter, und aus diesen die Konzentrationen berechnet. Erst wenn die Länge der Teilintervalle so klein gemacht wird, dass ein merklicher Teil des Spektrums der turbulenten kinetischen Energie unberücksichtigt bleibt, werden Unterschiede zwischen den so errechneten und gemessenen Konzentrationen auftreten; die durch die Ungenauigkeiten der verwendeten Formel bedingten Unterschiede sind dabei ausser Betracht geblieben. Da alle Messungen an einem festen Punkt (nämlich demjenigen der maximalen Konzentration im Gesamtzeitraum) vorgenommen werden, das Maximum aber in jedem Teilintervall an einem andern Punkte zu finden sein wird, verbietet sich die Anwendung der Formel für die Maximalkonzentration zur Bestimmung der Konzentration in den Teilintervallen. Da quantitative Aussagen über den Messdauereffekt – wie noch gezeigt werden wird – wiederum nur im Mittel über unendlich viele Fälle gelten, ist für diesen Fall A das Problem ohnehin gegenstandslos; das Mittel aller Konzentrationen in den Teilintervallen ergibt wieder die Maximalkonzentration im Gesamtintervall.

(*b*) Bei der Bewältigung des anfänglich erwähnten Problemes der Luftreinhaltung interessiert vielmehr der Fall, bei dem die Konzentrationsmessungen nicht nur am Punkte des Auftretens der Maximalkonzentration für den Gesamtzeitraum T^* vorgenommen werden, sondern zugleich an den Punkten, an denen die Maximalkonzentration in den einzelnen Teilintervallen der Länge T ermittelt werden kann. Es gilt dann sicher

$$\overline{(s_T)}_{T^*} > \overline{s}_{T^*} \tag{17}$$

† Für die maximale Konzentration am Erdboden wird künftig statt s^* nur noch s gesetzt.

Das Verhältnis dieser beiden Konzentrationen ist nahezu das, was zuvor als Messdauereffekt definiert worden ist. Eine experimentelle Bestimmung dieses Verhältnisses durch Konzentrationsmessungen ist eine nur unter grossen Schwierigkeiten zu lösende Aufgabe. STEWART, GALE und CROOKS (1954) haben durch eine sehr geschickte Anordnung zur Messung der Ausbreitung radioaktiver Gase einige quantitative Aussagen über dieses Verhältnis – wenn auch nicht dasjenige der Bodenkonzentrationen – machen können. Es sind die einzigen Daten dieser Art, die dem Autor bislang bekannt wurden. Leichter dürfte es jedenfalls sein, dieses Konzentrationsverhältnis indirekt durch Messung der meteorologischen Parameter zu bestimmen; diese – wegen der vorausgesetzten homogenen Turbulenz im ganzen Felde konstant angesehen – brauchen nur an einem Punkte ermittelt zu werden. Aber selbst derartige Messungen und Auswertungen stehen noch aus.

Für den Einzelfall lässt sich zunächst nur die Aussage machen

$$\overline{(s)}_T \neq \overline{(s)}_{T^*}$$

Ueber das Verhältnis dieser beiden Konzentrationen ist nur eine statistische Aussage in der Form der Erwartung möglich. Dabei wäre am wünschenswertesten die Grösse

$$\overline{\mathrm{V}}_{T^*}(T \mid T^*) = \frac{\overline{(s_T)}_{T^*}}{\overline{s}_{T^*}}$$

doch ist diese der Theorie zunächst unzugänglich. Eine Aussage gestattet die Theorie jedoch über die Grösse

$$\overline{V}_\infty(T \mid T^*) = \frac{\overline{(s_T)}_\infty}{\overline{(s_{T^*})}_\infty} \tag{18}$$

mit andern Worten über das Verhältnis zweier, über verschieden lange Zeiten gemessener Maximalkonzentrationen, und zwar als Mittelwert über unendlich viele gleichartige Konzentrationsverhältnisse.

Es erscheint wichtig festzustellen, dass die im Folgenden gemachten quantitativen Angaben über den Messdauereffekt nicht für einen bestimmten Einzelfall gelten können, sondern als statistische Aussagen vielmehr ein mittleres Verhalten dieses Effektes angeben.

Anstelle von (15) ist also nunmehr zu setzen

$$\overline{\mathrm{V}}_x(T \mid T^*) = \frac{\overline{\Psi}_x(T)}{\overline{\Psi}_x(T^*)} \tag{19}$$

wobei jetzt

$$\overline{\Psi}_x(T) = \frac{|\,\overline{\mathbf{v}}_x\,|}{|\,\overline{\mathbf{v}}_T\,|_\infty}\left[\frac{\overline{(w'_T)^2}_x}{\overline{(w'_x)^2}_\infty}\,\frac{\overline{(\mathbf{i}_\infty \times \mathbf{v}'_x)^2}_\infty}{\overline{(\mathbf{i}_T \times \mathbf{v}'_T)^2}_x}\right]^{\frac{1-\hat{n}}{2}} \tag{20}$$

Mit den Abkürzungen

$$B_T = \frac{|\,\overline{\mathbf{v}}_\infty\,|}{|\,\overline{\mathbf{v}}_T\,|_\infty} \tag{21}$$

und

$$G_T = \frac{\overline{(w'_T)^2}_x}{\overline{(w'_x)^2}_\infty} \qquad H_T = \frac{\overline{(\mathbf{i}_T \times \mathbf{v}'_T)^2}_\infty}{\overline{(\mathbf{i}_\infty \times \mathbf{v}'_x)^2}_x} \tag{22}$$

lautet (20)

$$\overline{\Psi}_x(T) = B_T\left[\frac{G_T}{H_T}\right]^{\frac{1-\hat{n}}{2}} \tag{23}$$

B_0 gibt die Beständigkeit des Windes an, so wie sie als klimatologische Masszahl definiert ist (Skalarwert des Vektormittels im Verhältnis zum Mittel der Skalarbeträge der horizontalen Windgeschwindigkeit). Allerdings werden in der Klimatologie zur Bestimmung der Beständigkeit des Windes gemessene Geschwindigkeitsvektoren – also bereits Mittelwerte über die Dauer der Windmessung

VOL. 4 1961

verwendet, sodass tatsächlich anstelle von B_0 ein B_t angegeben wird (t sei die Dauer der Windmessung).

Mit wachsendem T steigt B_T von B_0 aus monoton an und erreicht asymptotisch den Wert 1.0

$$\lim_{T\to\infty} B_T = 1{\cdot}0$$

Da $v'_0 \equiv 0$, steigt die Grösse H_T monoton von Null aus an und erreicht asymptotisch den Wert 1·0

$$H_0 = 0; \quad \lim_{T\to\infty} H_T = 1{\cdot}0$$

Der Anteil G_T als Funktion der Mittelbildungszeit T

Zu den fundamentalen Voraussetzungen der SUTTON-Formel (9) gehört diejenige, dass die Grundströmung rein horizontal sei

$$\overline{w}_\infty = 0 \tag{24}$$

Hiermit wird folgende Identität erhalten

$$\overline{(w'_\infty)^2}_\infty = \overline{(w'_T)^2}_\infty + \overline{(\overline{w}_T)^2}_\infty + \overline{2(\overline{w}_T w'_T)}_\infty \tag{25}$$

Verwendet man hierin die weitere Identität [unter nochmaliger Benutzung von (24)]

$$\overline{w}_T = \overline{(\overline{w}_\infty + w'_\infty)}_T = \overline{(w'_\infty)}_T \tag{26}$$

so ergibt sich

$$\overline{(w'_T)^2}_\infty = \overline{(w'_\infty)^2}_\infty - \overline{\left[\overline{(w'_\infty)}_T\right]^2}_\infty - 2\overline{\left[\overline{(w'_\infty)}_T w'_T\right]}_\infty \tag{27}$$

Einsetzen von (4) in (3) unter Verwendung von (24) liefert

$$w'_T = w'_\infty - \overline{w}_T$$

beziehungsweise mit (26)

$$w'_T = w'_\infty - \overline{(w'_\infty)}_T$$

Wendet man dies im letzten Term von (27) an

$$\overline{\left[\overline{(w'_\infty)}_T w'_T\right]}_\infty = \overline{\left[\overline{(w'_\infty)}_T w'_\infty\right]}_\infty - \overline{\left[\overline{(w'_\infty)}_T\right]^2}_\infty$$

so erhält (27) die folgende Form

$$\overline{(w'_T)^2}_\infty = \overline{(w'_\infty)^2}_\infty + \overline{\left[\overline{(w'_\infty)}_T\right]^2}_\infty - 2\overline{\left[\overline{(w'_\infty)}_T w'_\infty\right]}_\infty \tag{28}$$

Definitionsgemäss ist

$$\overline{\left[\overline{(w'_\infty)}_T\right]^2}_\infty = \lim_{A\to\infty} \frac{1}{2AT^2} \int_{-A}^{A} \int_{-T/2}^{T/2} \int_{-T/2}^{T/2} w'_\infty(t+\vartheta_1) w'_\infty(t+\vartheta_2)\, d\vartheta_1\, d\vartheta_2\, dt$$

oder mit Verwendung der EULERschen Korrelationsfunktion

$$R_x(\vartheta) = \lim_{A\to\infty} \frac{1}{2A} \int_{-A}^{A} w'(t) w'(t+\vartheta)\, dt \tag{29}$$

folgt nach Vertauschung der Integrationen

$$\overline{\left[\overline{(w'_\infty)}_T\right]^2}_\infty = \frac{1}{T^2} \int_{-T/2}^{T/2} \int_{-T/2}^{T/2} R_x(\vartheta_1 - \vartheta_2)\, d\vartheta_1\, d\vartheta_2$$

Dieser Ausdruck lässt sich umformen zu

$$\overline{\left[\overline{(w'_\infty)}_T\right]^2}_\infty = \frac{1}{T^2} \int_0^T (T-\vartheta)\{R_x(\vartheta) + R_x(-\vartheta)\}\, d\vartheta$$

sodass man wegen

$$R_z(\vartheta) = R_z(-\vartheta) \tag{30}$$

schliesslich erreicht:

$$\overline{\left[\overline{(w'_\infty)_T}\right]^2}_\infty = \frac{2}{T^2}\int_0^T (T-\vartheta) R_z(\vartheta)\, d\vartheta \tag{31}$$

Anstelle der EULERschen Korrelationsfunktion $R_z(\vartheta)$ werde deren FOURIERtransformierte, die Spektralfunktion $F_z(\nu)$ mit ν der Frequenz verwendet:

$$R_z(\vartheta) = \overline{(w'_\infty)^2}_\infty \int_0^\infty F(\nu)\cos(\nu\vartheta)\, d\nu \tag{32}$$

wodurch (31) die folgende Form erhält

$$\overline{\left[\overline{(w'_\infty)_T}\right]^2}_\infty = \overline{(w'_\infty)^2}_\infty \int_0^\infty F_z(\nu)\left(\frac{\sin(\nu/2)T}{(\nu/2)T}\right)^2 d\nu \tag{33}$$

In ähnlicher Weise lässt sich auch der letzte Term von (28) umformen. Es ist definitionsgemäss

$$\overline{\left[\overline{(w'_\infty)_T} w'_\infty\right]}_\infty = \lim_{A\to\infty}\frac{1}{2AT}\int_{-A}^{A}\int_{-T/2}^{T/2} w'(t)w'(t+\vartheta)\, d\vartheta\, dt$$

Eine Vertauschung der Integrationen liefert unter Berücksichtigung von (30)

$$\overline{\left[\overline{(w'_\infty)_T} w'_\infty\right]}_\infty = \frac{2}{T}\int_0^{T/2} R_z(\vartheta)\, d\vartheta$$

Mit der Spektralfunktion als der FOURIER-Transformierten von $R_z(\vartheta)$ gem. (32) erhält man

$$\overline{\left[\overline{(w'_\infty)_T} w'_\infty\right]}_\infty = \overline{(w'_\infty)^2}_\infty \int_0^\infty F_z(\nu)\,\frac{\sin(\nu/2)T}{(\nu/2)T}\, d\nu \tag{34}$$

Einsetzen von (33) und (34) in (28) liefert mit der Abkürzung (22)

$$G_T = \int_0^\infty F_z(\nu)\left\{1 - 2\frac{\sin(\nu/2)T}{(\nu/2)T} + \left(\frac{\sin(\nu/2)T}{(\nu/2)T}\right)^2\right\} d\nu \tag{35}$$

Der Klammerausdruck in (35) als diejenige Gewichtsfunktion, die angibt in welchem Masse ein bestimmter Spektralbereich der kinetischen Energie der turbulenten Vertikalbewegung zur Funktion G_T beiträgt, ist in der Abb. 1 dargestellt. Man sieht, dass diese Gewichtsfunktion die Wirkung eines high-pass-Filters hat, Wirbel mit Frequenzen, die kleiner sind als $2\pi/T$ bleiben nahezu unberücksichtigt; andere Spektralbereiche steuern etwas mehr zum Integral (35) bei als ihrer tatsächlichen kinetischen Energie entspricht.

Unter der Voraussetzung

$$\overline{(w'_T)_T} = 0 \tag{36}$$

entfällt in (28) der letzte Term, während der vorletzte sein Vorzeichen wechselt; man erhält die Beziehung

$$G_T = \int_0^\infty F_z(\nu)\left\{1 - \left(\frac{\sin(\nu/2)T}{(\nu/2)T}\right)^2\right\} d\nu$$

(vergl. z.B. OGURA 1957). Die Gewichtsfunktion in diesem Ausdruck ist zu Vergleichszwecken ebenfalls in Abb. 1 als gestrichelte Kurve dargestellt; sie kommt den Eigenschaften eines idealen Filters

VOL. 4 1961

noch näher. Man erkennt, dass die unterschiedliche Wirksamkeit der Filter mit zunehmender Mittelbildungszeit abnimmt – ein Ausdruck dafür, dass die Voraussetzung (36) um so eher erfüllt ist, je grösser die Mittelbildungszeit ist.

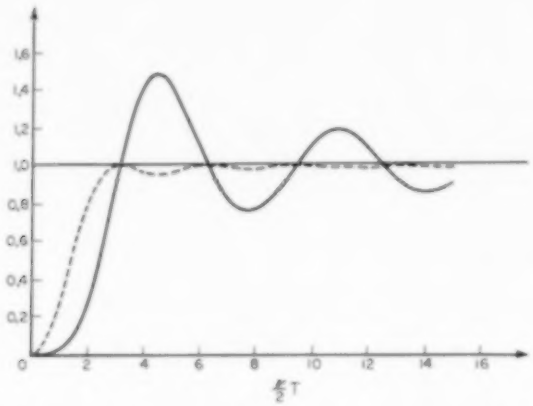

ABB. 1. Gewichtsfunktion (ausgezogene Kurve) gem. Klammerausdruck in Gl. (35); als gestrichelte Kurve ist die Gewichtsfunktion mit der Vereinfachung (36) dargestellt.

Der Anteil B_T als Funktion der Mittelbildungszeit T

Die Bestimmung von $B_T = f(T)$ ist wesentlich schwieriger, da – wie bereits auseinandergesetzt – die horizontalen Koordinaten ihre Orientierung in Abhängigkeit von der Mittelbildungszeit T ändern.

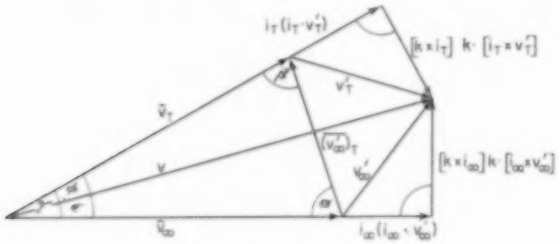

ABB. 2.

Die Verwendung von (4) für $\mathbf{v}$ unter der Mittelbildung in $\bar{\mathbf{v}}_T$ gibt die Beziehung

$$\bar{\mathbf{v}}_T = \bar{\mathbf{v}}_\infty + \overline{(\mathbf{v}'_\infty)_T}$$

Die folgenden Bezeichnungsweisen werden aus der Abbildung 2 ersichtlich:

$$\sphericalangle\{\bar{\mathbf{v}}_T, \overline{(\mathbf{v}'_\infty)_T}\} = \beta$$

$$\sphericalangle\{\bar{\mathbf{v}}_\infty, \overline{(\mathbf{v}'_\infty)_T}\} = \pi - \alpha$$

Es gilt

$$\frac{|\bar{\mathbf{v}}_T|}{|\bar{\mathbf{v}}_\infty|} = \frac{\sin\alpha}{\sin\beta} = q \tag{37}$$

Mithin ist

$$\frac{1}{B_T} = \frac{\overline{|\bar{\mathbf{v}}_T|}_\infty}{|\bar{\mathbf{v}}_\infty|} = \overline{(q)}_\infty \tag{38}$$

Aussagen über das Verhalten der Grösse q für den Einzelfall können nicht gemacht werden, wohl aber solche über eine Häufigkeitsverteilung dieser Grösse. Bei der Mittelbildung (38) soll dieser Umstand zu Nutze gemacht werden

$$\overline{(q)}_\alpha = \lim_{A\to\infty} \frac{1}{2A} \int_{-A}^{A} q(t)\,dt = \lim_{a\to\infty} \int_{-a}^{a} q h_T(q)\,dq \tag{39}$$

Welche Informationen liegen nun zur Bestimmung der Verteilungsfunktion $h_T(q)$ vor?

(*a*) Der Winkel α ist zufällig verteilt im Bereiche $0 \leqslant \alpha \leqslant \pi$; die Verteilung von α ist unabhängig von der Mittelbildungszeit.

(*b*) Der Winkel β ist verteilt im Bereiche $0 \leqslant \beta \leqslant \pi$; die Verteilung ist von T derart abhängig, dass für grosse Werte von T kleine Winkel γ häufiger auftreten. Dies bedingt, dass für grosses T ein Winkel $\beta > \pi/2$ häufiger ist als ein $\beta < \pi/2$.

(*c*) $\alpha = 0$ ist nur möglich, wenn gleichzeitig $\beta = 0$ oder $\beta = \pi$.

(*d*) $\alpha = \pi/2$ erfordert gleichzeitig $\beta = 0$.

(*e*) Wegen $B_\alpha = 1{\cdot}0$ muss gelten.

$$\lim_{T\to\infty} \overline{(q)}_\alpha(T) = 1{\cdot}0 \tag{40}$$

Aus (*c*) und (*d*) lässt sich für die Häufigkeitsverteilung $h_T(q)$ folgern

$$h_T(0) = 0 \tag{41}$$

$$\lim_{q\to\infty} h_T(q) = 0 \tag{42}$$

$$h_T(1) = \text{Max} \tag{43}$$

Aus der Information (*b*) und (*e*) folgt:

$$\lim_{T\to\infty} h_T(q) = \delta(q-1) \tag{44}$$

$$\lim_{a\to\infty} \int_{-a}^{a} h_T(q)\,dq = 1{\cdot}0 \tag{45}$$

worin δ die DIRAC-Funktion bedeutet. Es können sicher sehr viele Verteilungsfunktionen angegeben werden, welche die Bedingungen (41)–(45) befriedigen. Nimmt man an, dass durch diese Bedingungen das Wesentlichste der Häufigkeitsverteilung $h_T(q)$ festgelegt ist, und zwar so festgelegt ist, dass nach Ausführung der Integration gem. (39) bei der Benutzung verschiedener Verteilungsfunktionen keine merklichen Unterschiede auftreten, so kann man sich für eine bestimmte Funktion entscheiden. Mitbestimmend für die Auswahl dieser Funktion ist der Umstand, dass die Integration gem. (39) ausführbar bleiben soll. Unter diesem Gesichtspunkt wurde als Verteilungsfunktion, die den Bedingungen (41)–(45) genügt, folgende gewählt:

$$h_T(q) = \frac{\mu^{\mu+1}}{\Gamma(\mu+1)} q^\mu e^{-\mu q} \tag{46}$$

worin der Parameter μ eine lineare Abhängigkeit von der Mittelbildungszeit aufweist

$$\mu = c_1 + c_2 T \tag{47}$$

Diese Festsetzung ist zunächst unbegründet. Die Uebereinstimmung von Auswertungen der Funktion $\Psi_\alpha(T)$ mit den Ergebnissen von Konzentrationsmessungen scheint diese Annahme jedoch zu rechtfertigen. Eine vollständige Begründung könnte nur durch umfangreiche Windmessungen und deren Auswertung nach der Grösse B_T gem. (38) geliefert werden.

Die Verwendung von (46) in (39) liefert mit

$$\int_{-\infty}^{+\infty} q^{\mu+1} e^{-\mu q}\,dq = \frac{\Gamma(\mu+2)}{\mu^{\mu+2}}$$

VOL. 4 1961

die Beziehung

$$B_T = \frac{\mu}{\mu + 1} \tag{48}$$

Zur Bestimmung der Konstanten c_1 und c_2 entnimmt man der umgeschriebenen Form (48)

$$\mu = \frac{B_T}{1 - B_T} \tag{49}$$

für $T = 0$ mit (47)

$$c_1 = \mu_0 = \frac{B_0}{1 - B_0} \tag{50}$$

Mit (49) und (50) liefert (47)

$$c_2 \cdot T = \frac{B_T}{1 - B_T} - \frac{B_0}{1 - B_0}$$

woraus für den Fall $c_2 T = 1 \cdot 0$ folgt

$$B_* = \frac{1}{2 - B_0} \tag{51}$$

beziehungsweise

$$c_2 = \frac{1}{T^*}$$

Unter T^* ist diejenige Mittelbildungszeit zu verstehen, die angewandt werden muss, damit das zugehörige B_{T^*} den durch (51) gegebenen Wert annimmt. Somit ergibt sich endgültig

$$B_T = \frac{\mu_0 + (T/T_*)}{\mu_0 + 1 + (T/T_*)} \tag{52}$$

Der Anteil H_T als Funktion der Mittelbildungszeit T

Der Abbildung (2) lassen sich die Beziehungen

$$|\mathbf{i}_T \times \mathbf{v}'_T| = |\mathbf{v}| \sin\phi$$
$$|\mathbf{i}_\infty \times \mathbf{v}'_\infty| = |\mathbf{v}| \sin\epsilon$$

entnehmen. Es folgt

$$\overline{(\mathbf{i}_T \times \mathbf{v}'_T)^2}_\infty = \overline{\left[(\mathbf{i}_\infty \times \mathbf{v}'_\infty)^2 \frac{\sin^2\phi}{\sin^2\epsilon}\right]}_\infty = \overline{(p^2)}_\infty$$

Nunmehr wird wie im vorangehenden Abschnitt verfahren. Auch über die Grösse p sind keine Aussagen im Einzelfalle möglich, wohl aber solche über die Häufigkeitsverteilung von p. Dies soll bei der Mittelbildung wieder benutzt werden. Analog zu (39) erhält man

$$\overline{(p^2)}_\infty = \lim_{A\to\infty} \frac{1}{2A} \int_{-A}^{A} p^2(t)\,dt = \lim_{a\to\infty} \int_{-a}^{a} p^2 h_T(p)\,dp \tag{53}$$

Welche Informationen liegen nun zur Bestimmung der Verteilungsfunktion $h_T(p)$ vor?

(*a*) Der Winkel ϵ ist zufällig verteilt im Bereiche $0 \leqslant \epsilon \leqslant \pi$. Diese Verteilung ist unabhängig von T.

(*b*) Der Winkel ϕ ist verteilt im Bereiche $0 \leqslant \phi \leqslant \pi$; diese Verteilungist von T derart abhängig, dass für kleines T kleine Winkel ϕ bevorzugt auftreten.

(*c*) $\epsilon = 0$ ist nur möglich, wenn gleichzeitig auch $\mathbf{i}_\infty \times \mathbf{v}'_\infty = 0$.

(*d*) Für $T = 0$ muss $\overline{(p^2)}_\infty$ verschwinden.

(*e*) Für $T \to \infty$ muss sein $\overline{(p^2)}_\infty = \overline{(\mathbf{i}_\infty \times \mathbf{v}'_\infty)^2}_\infty$.

Für die Häufigkeitsverteilung $h_T(q)$ wird aus (*b*) und (*d*) gefolgert

$$h_T(0) = \text{Max} \tag{54}$$

$$\lim_{T\to 0} h_T(p) = \delta(0) \tag{55}$$

aus (*c*) folgt

$$\lim_{p\to\infty} h_T(p) = 0 \tag{56}$$

sowie aus (*e*)

$$\lim_{T\to\infty} \int_{-\infty}^{+\infty} p^2 h_T(p)\, dp = \overline{(\mathfrak{i}_\infty \times \mathfrak{v}'_\infty)^2}_\infty \tag{57}$$

Unter Hinweis auf die bei der Wahl von $h_T(q)$ bereits vorgebrachten Argumente wird als die die Bedingungen (54)–(57) befriedigende Verteilungsfunktion

$$h_T(p) = \sqrt{\frac{\lambda}{\pi}} \exp.\{-\lambda p^2\} \tag{58}$$

gewählt. Für den Parameter λ wird wieder eine lineare Abhängigkeit von der Mittelbildungszeit T [siehe Bemerkung zu Gl. (47)] festgelegt

$$\lambda = c_3 + \frac{c_4}{T} \tag{59}$$

worin die Konstanten c_3 und c_4 noch zu bestimmen sind. Die Verwendung von (58) und (53) liefert

$$\overline{(p^2)}_\infty = \frac{1}{2\lambda} \tag{60}$$

(59) in (60) liefert mit der Bedingung (57)

$$c_3 = \frac{1}{2\overline{(\mathfrak{i}_\infty \times \mathfrak{v}'_\infty)^2}_\infty} = \lambda_\infty$$

Mithin ergibt sich für die gesuchte Grösse H_T

$$\frac{1}{H_T} = \frac{\overline{(\mathfrak{i}_\infty \times \mathfrak{v}'_\infty)^2}_\infty}{\overline{(\mathfrak{i}_T \times \mathfrak{v}'_T)^2}_\infty} = \frac{\lambda}{\lambda_\infty} = 1 + \frac{c_4}{\lambda_\infty \cdot T} \tag{61}$$

Zur Bestimmung der Konstanten c_4 werde die Turbulenzmasszahl τ benutzt, die folgendermassen definiert sei

$$\tau_{y,T} = \frac{\overline{(\mathfrak{i}_T \times \mathfrak{v}'_T)^2}_\infty}{(\bar{\mathfrak{v}}_\infty)^2}; \quad \tau_{x,T} = \frac{\overline{(\mathfrak{i}_T \cdot \mathfrak{v}'_T)^2}_\infty}{(\bar{\mathfrak{v}}_\infty)^2} \tag{62a}$$

Hiermit ergibt sich

$$\frac{c_4}{\lambda_\infty} = \left(\frac{\tau_{y;\infty}}{\tau_{y;T}} - 1\right) T.$$

Soll c_4/λ_∞ aus dieser Beziehung mittels Beobachtungen von $\tau_{y,T}$ bestimmt werden, so ist dem Umstand Rechnung zu tragen, dass durch die Beobachtung eine etwas von der Definition (62) verschiedene Kenngrösse $\hat{\tau}$ geliefert wird:

$$\hat{\tau}_{y,T} = \overline{\left[\frac{\overline{(\mathfrak{i}_T \times \mathfrak{v}'_T)^2}_T}{(\bar{\mathfrak{v}}_T)^2}\right]}_\infty \tag{62b}$$

Setzt man jedoch

$$\overline{\left[\frac{\overline{(\mathfrak{i}_T \times \mathfrak{v}'_T)^2}_T}{\overline{(\mathfrak{v}'_T)^2}}\right]}_\infty \approx \frac{\overline{\left[(\mathfrak{i}_T \times \mathfrak{v}'_T)^2\right]}_\infty}{\overline{(\bar{\mathfrak{v}}_T)^2}_\infty} = \frac{\overline{(\mathfrak{i}_T \times \mathfrak{v}'_T)^2}_\infty}{\overline{(\bar{\mathfrak{v}}_T)^2}_\infty}$$

so ergibt sich nach einer Erweiterung mit $(\bar{\mathfrak{v}}_\infty)^2$

$$\hat{\tau}_{y,T} = \tau_{y,T}(B_T)^2.$$

Diese Beziehung wird in der Bestimmungsgleichung für c_4/λ_∞ verwandt, man erhält

$$\frac{c_4}{\lambda_\infty} = \left\{(B_T)^2 \frac{\tau_{y,\infty}}{\hat{\tau}_{y,T}} - 1\right\} T \tag{63}$$

VOL. 4 1961

Ist aus Messungen für irgendeine Mittelbildungszeit $\hat{T}$ die Turbulenzmasszahl $\hat{\tau}_{y,\hat{T}}$ ermittelt worden, so liefert (63) unter Verwendung von (52)

$$\frac{c_4}{\lambda_x} = \left\{ (B_T)^2 \frac{\tau_{y,\infty}}{\hat{\tau}_{y,\hat{T}}} - 1 \right\} \hat{T}$$

bezw. (61) lautet

$$\frac{1}{H_T} = 1 + \left\{ (B_T)^2 \frac{\tau_{y,\infty}}{\hat{\tau}_{y,\hat{T}}} - 1 \right\} \frac{\hat{T}}{T} \tag{64}$$

Hierin kann der Wert des Klammerausdruckes aus den genannten Beobachtungen ermittelt werden – für die Grösse $\tau_{y,\infty}$ wird dies im Folgenden noch gezeigt –; die Mittelbildungszeit T ist in den Einheiten der Mittelbildungszeit $\hat{T}$ anzugeben, welche bei der Bildung des vorliegenden Wertes von $\hat{\tau}_{y,\hat{T}}$ benutzt wurde.

Eine Beziehung zwischen der Windbeständigkeit B_0 und dem Turbulenzniveau τ_x im Falle isotroper Turbulenz

Für $T \to \infty$ geht die in (62) definierte Turbulenzmasszahl τ in das sogenannte Turbulenzniveau τ_∞ über, eine Grösse, die zur Bestimmung der Konstanten c_4/λ_x gem. (63) bekannt sein muss. Es kann gezeigt werden, dass im Falle isotroper Turbulenz mit B_0 auch τ_∞ gegeben ist, ein Umstand, von welchem in (63) Gebrauch gemacht werden soll.

Aus der Identität (vergl. Abbildung 2)

$$(\bar{v}_T)^2 + (\mathbf{i}_T \cdot \mathbf{v}_T')^2 + (\mathbf{i}_T \times \mathbf{v}_T')^2 + 2\bar{v}_T v'_T = (\bar{v}_\infty)^2 + (\mathbf{i}_\infty \cdot \mathbf{v}'_\infty)^2 + (\mathbf{i}_\infty \times \mathbf{v}'_\infty)^2 + 2\bar{v}_\infty v'_\infty$$

folgt nach der Mittelbildung über eine unendlich lange Zeit unter Benutzung der Definition (21) und (62)

$$\frac{\overline{(\bar{v}_T)^2}_x}{(\bar{v}_x)^2} + 2\frac{\overline{(\bar{v}_T \cdot v'_T)}_x}{(\bar{v}_x)^2} + \tau_{x,T} + \tau_{y,T} = 1 + \tau_{x,\infty} + \tau_{y,\infty} \tag{65}$$

Selbstverständlich ist der erste Term in (65) von der durch B_T definierten Grösse verschieden

$$\frac{\overline{(\bar{v}_T)^2}_x}{(\bar{v}_x)^2} \neq \frac{(\overline{|\bar{v}_T|}_x)^2}{(\bar{v}_x)^2} = \frac{1}{B^2_T}$$

jedoch lässt sich entsprechend der in 4.2 gegebenen Bestimmung von B_T ein Zusammenhang mit dieser Grösse angeben:

$$\frac{\overline{(\bar{v}_T)^2}_x}{(\bar{v}_x)^2} = \overline{(q^2)}_x = \lim_{a \to \infty} \int_{-a}^{a} q^2 h_T(q)\, dq.$$

Verwendet man für die Verteilungsfunktion $h_T(q)$ die mit Gl. (46) gegebene, so folgt

$$\frac{\overline{(\bar{v}_T)^2}_x}{(\bar{v}_x)^2} = 1 + \frac{3}{\mu} + \frac{2}{\mu^2}$$

oder mit (49)

$$\frac{\overline{(\bar{v}_T)^2}_\infty}{(\bar{v}_\infty)^2} = \frac{2 - B_T}{(B_T)^2}$$

Für $T \to 0$ verschwindet in (65) sowohl $\tau_{x,T}$ und $\tau_{y,T}$, als auch $2\overline{(\bar{v}_T v'_T)}_x/(\bar{v}_\infty)^2$. Da für isotrope Turbulenze gilt

$$\tau_{x,\infty} = \tau_{y,\infty}$$

resultiert aus (65)

$$\frac{2 - B_0}{(B_0)^2} = 1 + 2\tau_\infty$$

oder

$$\tau_\infty = \frac{1}{B_0^2} - \frac{1}{2B_0} - \frac{1}{2} \tag{66a}$$

beziehungsweise

$$\tau_\infty = \frac{1}{\mu_0^2} + \frac{3}{2\mu_0} \tag{66b}$$

Diese Beziehung für das Torbulenzniveau soll in (64) verwendung finden.

Die Funktion $\overline{\Psi}_\infty(T)$

Für die gesuchte Funktion $\overline{\Psi}_\infty(T)$ ergibt sich aus (23) mit (35), (52) und (64) mit (66) folgender Ausdruck:

$$\overline{\Psi}_\infty(T) = \frac{\mu_0 + (T/T^*)}{\mu_0 + 1 + T/T^*} \left\{ \left[1 + \left(\frac{\mu_0 + \hat{T}/T^*}{\mu_0 + 1 + \hat{T}/T^*} \right) \frac{1}{\hat{\tau}_{v,\hat{T}}} \left(\frac{1}{\mu_0^2} + \frac{3}{2\mu_0} \right) \frac{\hat{T}}{T} \right] \times \right.$$
$$\left. \times \int_0^\infty F_{z,\infty}(v) \left[1 - 2 \frac{\sin(v/2)\,T}{(v/2)\,T} + \left(\frac{\sin(v/2)\,T}{v/2\,T} \right)^2 \right] dv \right\}^{\frac{1-\hat{n}}{2}} \tag{67}$$

Eine Auswertung der Funktion $\overline{\Psi}_\infty(T)$ setzt also die Kenntnis der folgenden Grössen voraus:

die Spektralfunktion $F_{z,\infty}(v)$, (68a)

die Beständigkeit des Windes B_0, aus welcher gem. (49) der Wert für μ_0 folgt. (68b)

diejenige Zeit T^*, für welche gem. (51) $B_{T^*} = 1/(2 - B_0)$, (68c)

die Turbulenzkenngrösse $\hat{\tau}_{v,\hat{T}}$ für irgendeine Mittelbildungszeit $\hat{T}$ gem. (62b) (68d)

die mittlere Stabilitätsgrösse $\hat{n}$ der atmosphärischen Schichtung. (68e)

Man entnimmt der angegebenen Bezienung (67) sofort

$$\lim_{T \to \infty} \overline{\Psi}_\infty(T) = 1$$

ob jedoch die Funktion mit wachsender Mittelbildungszeit zu diesem Wert monoton abfällt – wie dies von der Physik her gefordert werden muss – wird eine Auswertung mit Messwerten zeigen müssen.

DIE AUSWERTUNG DER FUNKTION $\overline{\Psi}_\infty(T)$

Einer Auswertung der mit (67) gegebenen Funktion $\overline{\Psi}_\infty(T)$ stehen insofern unerwartete Schwierigkeiten entgegen, als praktisch für keinen der benötigten Parameter (68a)–(68e) befriedigende Messungen vorliegen. Obwohl solche zum grössten Teile als durchaus möglich angesehen werden müssen, wird dieser Umstand nur dadurch verständlich, dass einmal derartige Werte bislang kaum benötigt wurden, zum andern ihre Auswertung einen ziemlichten Arbeitsaufwand erfordert. Bei einer Auswertung der Funktion $\overline{\Psi}_\infty(T)$ muss also neben einer möglichst vollständigen Ausschöpfung dessen, was an brauchbaren Messergebnissen vorliegt, ein Einsetzen plausibler Werte weiterhelfen.

Die Auswertung der Funktion G_T gem. Gl. (35)

Eine Auswertung der Funktion

$$G_T = \int_0^\infty F_{z,\infty}(v) \left\{ 1 - 2 \frac{\sin(v/2)\,T}{(v/2)\,T} + \left(\frac{\sin(v/2)\,T}{(v/2)\,T} \right)^2 \right\} dv \tag{69}$$

stezt die Kenntnis der Spektralfunktion $F_{z,\infty}(v)$ voraus. Aus jüngster Zeit liegen verschiedene Angaben über die Form des Spektrums vor, wenn auch nicht als das Resultat einer unendlich langen,

VOL. 4 1961

oder zumindest sehr langen Messreihe, wie dies von der Theorie gefordert wird. Einen zusammenfassenden Ueberblick geben PANOFSKY und DELAND (1958). Es zeigt sich, dass die Form des Spektrums abhängt von der Höhe über Grund, der mittleren Windgeschwindigkeit und deren Scherung, der Rauhigkeit und der Stabilität der Schichtung. Es wäre eine sehr schwierige Aufgabe, wollte man aus Teilmessungen zu jedesmal verschiedenen äusseren Bedingungen diejenige Form des Spektrums festlegen, die man über eine unendlich lange Messzeit erhielte.

Aus diesem Grunde wird hier ein anderes Vorgehen für nützlich gehalten: Die Spektralfunktion $F_{z,u}(\nu)$ soll in analytischer Form vorgeben und durch nur wenige – etwa zwei – Parameter den Beobachtungen angepasst werden. Zieht man zur Bestimmung dieser Parameter die am besten feststellbaren Eigenschaften der Spektralverteilung heran, so dürfte unter den gegeben Umständen die Form des Spektrums in der zweckmässigsten Weise festgelegt sein. Als Spektralfunktion erscheint geeignet:

$$F_{z,u}(\nu) = \frac{k^{m+1}}{\Gamma(m+1)} e^{-k\nu} \nu^m \tag{70}$$

Diese Funktion erfüllt die an sie zu stellenden folgenden Bedingungen

$$F_{z,u}(0) = 0$$

$$\lim_{\nu \to \infty} F_{z,u}(\nu) = 0$$

$$\int_0^\infty F_{z,u}(\nu) d\nu = 1{\cdot}0$$

Zur Festlegung der Parameter k und m bieten sich mehrere Möglichkeiten an. Bezeichnet ν_M die Frequenz mit der maximalen Energie, ν_W diejenige mit einem Wendepunkt in der Spektralfunktion, ν_S die dem Schwerpunkt des Spektrums zugeordnete Frequenz, und ν_T eine für den Bereich charakteristische Frequenz, in welchem das 5/3-Gesetz erfüllt ist (inertial subrange), so gilt

$$\nu_M = \frac{m}{k} \tag{71a}$$

$$\nu_W = \frac{m}{k} \pm \frac{\sqrt{m}}{k} \tag{71b}$$

$$\nu_S = \frac{m}{k} + \frac{1}{k} \tag{71c}$$

$$\nu_T = \frac{m}{k} + \frac{5}{3k} \tag{71d}$$

Für (71a) und (71b) ist dies leicht zu erkennen, für (71c) folgt es aus der Definition

$$\nu_S = \frac{\int_0^\infty \nu F_u(\nu) d\nu}{\int_0^\infty F_u(\nu) d\nu}$$

und (71d) ergibt sich aus folgender Ueberlegung. Aus

$$\frac{F(\nu_1)}{F(\nu_2)} = \left(\frac{\nu_2}{\nu_1}\right)^{\frac{5}{3}}$$

folgt mit (70)

$$k = \frac{m + \frac{5}{3}}{\nu_2 - \nu_1} \ln \frac{\nu_2}{\nu_1}$$

Beim Uebergang $\nu_2 \to \nu_1$ und der Bezeichnung $\nu_1 = \nu_T$ (als der die Inertial subrange charakterisierenden Frequenz) erhält man (71d). Zweifelsohne ist den Beobachtungen am leichtesten ν_M zu entnehmen. Die Wendepunkte der Spektralfunktion und der Schwerpunkt des Spektrums sind nur schwer festzulegen; für letzteres wäre eine numerische Integration erforderlich, die ihrerseits wieder den Verlauf der Spektralfunktion als bekannt voraussetzt. Zweckmässigerweise verwendet man als zweit Information noch diejenige über die Inertial-Subrange.

Aus (71a) und (71d) folgt:

$$k = \frac{5}{3(\nu_T - \nu_M)} \tag{72a}$$

$$m = \frac{5\nu_M}{3(\nu_T - \nu_M)} \tag{72b}$$

Für ν_T findet man z.B. eine Angabe bei McCready (1953). Danach soll das 5/3-Gesetz (im Falle einer sehr bodennahen Strömung) in dem Spektralbereich von 2·5 cyl/sec bis 40 cyl/sec erfüllt sein. Dementsprechend werde als charakteristischer Wert angesetzt:

$$\nu_T = 10 \text{ cyl/sec}$$

Für die Frequenz mit dem Maximalbetrag der kinetischen Energie (der Vertikalbewegungen) entnimmt man den verschiedenen Darstellungen den Wert von rund 100 cyl/hr, Fluktuationen mit einer Periode von 36 sec entsprechend; es wird also gesetzt:

$$\nu_M = 2{\cdot}\overline{7} \times 10^{-2} \text{ cyl/sec}$$

Mit diesen Werten liefert (72a) und (72b)

$$k \approx 0{\cdot}15 \text{ sec} \tag{73a}$$

$$m \approx 4{\cdot}2 \cdot 10^{-3} \tag{73b}$$

VOL. 4 1961

Unter Einsetzen dieser Werte in die Spektralverteilung der Form (70) soll die Integration (69) durchgeführt werden. Nach Umformung des dritten Termes in (69) erhält man

$$G_T = \frac{k^{m+1}}{\Gamma(m+1)} \left\{ \int_0^\infty e^{-k\nu} \left(\nu^m + \frac{2\nu^{m-2}}{T^2} \right) d\nu - \frac{4}{T} \int_0^\infty e^{-k\nu}\, \nu^{m-1} \sin\left(\frac{\nu}{2} T\right) d\nu - \frac{2}{T^2} \int_0^\infty e^{-k\nu}\, \nu^{m-2} \cos(\nu T)\, d\nu \right\}$$

Führt man noch die Abkürzung

$$\frac{T}{k} \equiv \rho \tag{74}$$

ein, so ergibt sich nach Ausführung der Integrationen für G_T

$$G_T = 1 + \frac{2}{\rho m} \left\{ \frac{1}{\rho(m-1)} - 2\, \frac{\sin[m \operatorname{arctg}(\rho/2)]}{[1+(\rho/2)^2]^{m/2}} - \frac{1}{\rho(m-1)}\, \frac{\cos[(m-1)\operatorname{arctg}\rho]}{(1+\rho^2)^{(m-1)/2}} \right\} \tag{75}$$

Mit den in (73a) und (73b) festgelegten Werten gilt

$$\rho \gg 1{\cdot}0 \tag{76a}$$

$$m \ll 1{\cdot}0 \tag{76b}$$

sofern ein festzulegender Wert für die Mittelbildungszeit T nicht unterschritten wird. (Z.B. nimmt für $T = 3$ min die Grösse ρ bereits den Wert $1{\cdot}2\ 10^3$ an und erfüllt damit sicher die Bedingung (76a).) Mit (76a) und (76b) folgt aus (75):

$$G_T \approx 1 + \frac{2}{\rho m} \left\{ \frac{1}{\rho} - m\pi \right\}$$

Hierin ist wieder wegen (76a) und (76b) der zweite Term gegenüber dem Wert 1·0 vernachlässigbar klein, sodass

$$G_T = 1 \tag{77}$$

gesetz werden kann. Dieses Ergebnis kann physikalisch folgendermassen interpretiert werden: Nimmt man als untere Grenze der Mittelbildungszeit $T = 3$ min, so werden bei Durchführung einer

Mittelbildung die Energiebeträge ausgefiltert und unberücksichtigt gelassen, die Frequenzen zugeordnet sind, welche kleiner als 20 cyl/hr sind. [Das setzt noch voraus, dass der Klammerausdruck in (35) als idealer Filter wirksam ist.] Der auf diese Weise ausgefilterte Spektralanteil ist aber bereits sehr klein, seine Berücksichtigung würde das Ergebnis praktisch nicht ändern.

Die Auswertung der Funktion B_T gem. Gl. (52)

Die Verwendung der Funktion (52) setzt die Kenntnis von μ_0 und T^* voraus, wobei μ_0 gem. (50) und T^* über B_* gem. (51) von B_0 abhängt. Auswertungen von Windregistrierungen zur Bestimmung der Beständigkeit B sind dem Verfasser kaum irgendwelche bekannt geworden. Neben einer hier nicht brauchbaren Angabe für die Tropen von CONRAD ist nur eine von WEGENER (1919) für 20 Balkanstationen durchgeführte Auswertung der Windbeobachtungen vom Juli 1917 hier verwendbar. WEGENER gibt für die Beständigkeit des Bodenwindes $B=0{\cdot}47$ an. Der Veröffentlichung sind keinerlei Details über die Art der vorgenommenen Windmessung zu entnehmen. Da jedoch durch die Windmessung selbst bereits eine Mittelbildung durchgeführt wird, ist dieser Wert selbstverständlich einer von Null verschiedenen Mittelbildungszeit (etwa 5 min) zuzuordnen. Eine Voraussetzung für die Auswertung von B_0 wäre also eine Reihe von Windregistrierungen in einer solchen Art, dass diesen der Windvektor als Mittelwert über verschieden lange (absolut jedoch kurze) Mittelbildungszeiten entnommen werden könnte. Derartige Auswertungen müssten den Grenzwert erkennen lassen, dem B_T für $T\to 0$ zustrebt. Da derartige Auswertungen aber noch ausstehen, bleibt nur die Möglichkeit einen plausiblen Wert anzunehmen. Für diesen wird unter Berücksichtigung des zuvor genannten WEGENERschen Wertes gesetzt:

$$B_0 = 0{\cdot}400 \tag{78}$$

Hiermit folgt aus (51)

$$B_* = 0{\cdot}625$$

Ordnet man – wie zuvor erwähnt – den von WEGENER gegeben Wert $B_T=0{\cdot}47$ einer Mittelbildungszeit (Dauer der Windmessung) von 5 min zu, so gehörte bei einer linearen Abhängigkeit der Grösse B_T von der Mittelbildungszeit T zum Werte $B_*=0{\cdot}625$ die Zeit von 16·07 min. Die Kenntnis, dass diese Abhängigkeit nicht linear ist, gestattet den Schluss: $T^*>16{\cdot}07$ min. Das ist der einzige Anhalt, der zur Festsetzung von T* gegeben ist; als vernünftig erscheinender Wert wird daher gesetzt:

$$T^* = 1/2 \text{ hr} \tag{79a}$$

Für den andern Parameter folgt aus (50) mit (78)

$$\mu_0 = 0{\cdot}\overline{6} \tag{79b}$$

Hiermit, sowie mit (79a) ist die Funktion B_T festgelegt, sie lautet:

$$B_T = \frac{\frac{2}{3}+\frac{T}{30\text{ min}}}{\frac{5}{3}+\frac{T}{30\text{ min}}} \tag{80}$$

Die Auswertung der Funktion H_T gem. Gl. (64)

Eine Auswertung der Funktion H_T setzt die Kenntnis der folgenden Grössen voraus: $(B\hat{\tau})^2$, $\hat{\tau}_{v,u}; \hat{\tau}_{v,\hat{v}}$ sowie $\hat{T}$. Die l etzte dieser Grössen $\hat{T}$ bestimmt sich aus den zur Verfügung stehenden Auswertungen für $\hat{\tau}_{v,\hat{v}}$. Hierzu scheinen diejenigen von LETTAU und DAVIDSON (1957) am geeignetsten. Den Tabellen 5.2.a. der einzelnen Messperioden wurden die Werte $\overline{(v'_{T_1})^2}_{T_1}$ für $T_1=10$ min und den Tabellen 4.1.8. die korrespondierenden Werte $\bar{u}_{T_2}$ für $T_2=15$ min (beides in 12 m Höhe) entnommen und der Quotient $\overline{(v'\hat{\tau})^2}\hat{\tau}/(\bar{u}\hat{\tau})^2$ gebildet. Als zugehörige Mittelbildungszeit wurde $\hat{T}=12$ min ($T_1<\hat{T}<T_2$) gesetzt. Sodann stehen zur endgültigen Mittelbildung (eigentlich über eine unendlich lange Mittelbildungszeit) 55 derartiger Quotienten zur Verfügung. Es wird daher anstelle von (62b) gesetzt:

$$\hat{\tau}_{v,\hat{v}} = \overline{\left[\frac{\overline{(v'\hat{\tau})^2\hat{\tau}}}{(u\hat{\tau})^2}\right]}_{\infty} \approx \overline{\left[\frac{\overline{(v'\hat{\tau})^2\hat{\tau}}}{(u\hat{\tau})^2}\right]}_{55}$$

der so erhaltene Wert lautet:

$$\hat{\tau}_{v,\hat{v}} = 1{\cdot}103\times 10^{-2} \tag{81}$$

$$\hat{T} = 12 \text{ min} \tag{82}$$

Aus (78) in (66a) folgt unter der Voraussetzung horizontaler Isotropie

$$\tau_{y,\infty} = 4{\cdot}500 \tag{83}$$

sowie mit (79a) und (79b) in (52)

$$(B\hat{T})^2 = 0{\cdot}2663 \tag{84}$$

Benutzt man die in (81)–(84) festgelegten Werte, so gilt

$$(B\hat{T})^2 \frac{\tau_{y,\infty}}{\hat{n}_{y,\hat{T}}} = 1{\cdot}0866 \times 10^2 \approx 1{\cdot}10^2$$

und gemäss (64) erhält man

$$\frac{1}{H_T} = 1 + 1 \times 10^2 \frac{12\ \text{min}}{T} \tag{85}$$

Die Festlegung des Wertes $\hat{n}$

$\hat{n}$ ist der für alle Zeiten voraussetzungsgemäss als konstant anzusehende meteorologische Exponent, der (nach dem SUTTONschen Ansatz) den Abfall der LAGRANGEschen Korrelationsfunktion bestimmt. Am zweckmässigsten verwendet man hierfür einen Mittelwert von n über eine möglichst lange Messperiode. Die von LETTAU und DAVIDSON (1957) mitgeteilten Messergebnisse gestatten auch eine Festlegung von n (z.B. aus den mittleren Windgeschwindigkeiten in 8 m und 16 m Höhe). Aus 57 derartig festgelegten n-Werten ergibt sich ein Mittel von 0·329. Ebenso gestatten die Angaben von BARAD (1958) im gleichen Höhenbereich die Bestimmung von 71 n-WERTEN, deren Mittel 0·331 ist. In Uebereinstimmung mit diesen beiden Auswertungen wird

$$\hat{n} = 1/3 \tag{86}$$

gesetzt.

VOL. 4 1961

DER VERLAUF DER FUNKTION $\overline{\Psi}_x(T)$ GEM. GL. (67)

Mit den Festlegungen (77), (80), (85) und (86) erhält man aus (67) für die gesuchte Funktion

$$\overline{\Psi}_x(T) = \frac{\frac{2}{3} + (T/30)}{\frac{5}{3} + (T/30)} \left\{1 + \frac{1{\cdot}2 \times 10^3}{T}\right\}^{\frac{1}{3}};\quad [T] = \text{min}. \tag{87}$$

Der Verlauf dieser Funktion ist in Abbildung 3 als ausgezogene Kurve dargestellt; Einzelwerte enthält die nachfolgende Tabelle:

T	$\overline{\Psi}_x$	T	$\overline{\Psi}_x$
2 min	3·57	25 min	2·20
3 min	3·20	30 min	2·16
4 min	2·97	45 min	2·07
5 min	2·83	1 hr	2·01
6 min	2·72	1·5 hr	1·91
8 min	2·56	2 hr	1·83
10 min	2·47	3 hr	1·71
12 min	2·40	4 hr	1·63
15 min	2·33	5 hr	1·56
20 min	2·25	6 hr	1·51
		12 hr	1·33
Der gesuchte Messdauereffekt $\overline{V}_x(T_1 \mid T_3)$ kann gem. (15) durch einfache Verhältnisbildung aus dieser Tabelle erhalten werden		1 d	1·20
		2 d	1·11
		3 d	1·08
		4 d	1·06

DER EINFLUSS DER ATMOSPHÄRISCHEN SCHICHTUNG AUF DEN MESSDAUEREFFEKT

Es waren Gründe der Vereinfachung, die zu der Voraussetzung zwangen, den Exponenten n (als Masszahl für die atmosphärische Schichtung) konstant zu halten und durch einen Mittelwert $\hat{n}$ zu ersetzen. Es ist zunächst keine Möglichkeit zu erkennen, bei der statistischen Erfassung der Funktionen G_T und H_T eine Variation des Exponenten n zu berücksichtigen.

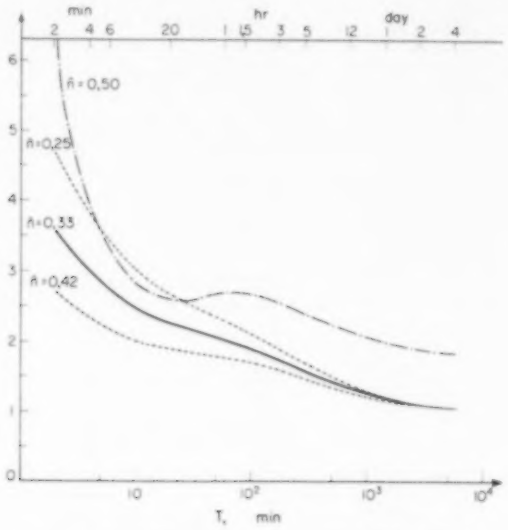

ABB. 3. Verlauf der Funktion $\overline{\Psi}_\varepsilon(T)$ gem. Gl. 87 (ausgezogene Kurve) sowie für weitere Werte von $\hat{n}$ gem. Abschn. 7.

Zumindest qualitativ wird jedoch der Einfluss der Schichtung zu erkennen sein, wenn man für $\hat{n}$ andere Werte als den mit (86) festgelegten benutzt. Derartige Auswertungen wurden durchgeführt für $n = 0{\cdot}25$ (nach SUTTON der Fall der adiabatischen Schichtung), für $n = 0{\cdot}42$ und für $n = 0{\cdot}50$. Die Ergebnisse für $\overline{\Psi}_\varepsilon(T)$ sind ebenfalls in Abbildung 3 dargestellt. Man erkennt, dass die Funktion $\overline{\Psi}_\varepsilon(T)$ im Falle $n = 0{\cdot}50$ nicht mehr monoton abfällt, wie dies von der Physik des Vorganges her gefordert werden muss; offensichtlich ist für diesen Fall einer sehr grossen Stabilität (als Mittel über eine unendlich lange Zeit) die vorstehende Theorie überfordert. Eine naheliegende Erklärung ist diejenige, dass für einen so hohen Wert von n auch mit andern Masszahlen für die atmosphärischen Strömungsverhältnisse (B_0, τ_ε u.s.w.) eingegangen werden muss.

Bei einer Anwendung des Ergebnisses z.B. im Falle adiabatischer Schichtung ($n = 0{\cdot}25$) erscheint es jedoch untunlich, die für $n = 0{\cdot}25$ ermittelte Kurve zu benutzen. Diese deutet vielmehr nur an, in welcher Richtung der Messdauereffekt unter den gegebenen Verhältnissen abweicht, die Abweichung selbst ist sicher wesentlich geringer. Der Messdauereffekt, so wie er angegeben ist, gilt eben definitionsgemäss nur als Mittel über unendlich viele Fälle; nur zu einem kleinen Teil dieser Fälle wird der gerade beobachtete Exponent n (z.B. der im adiabatischen Falle) auftreten.

DIE UEBEREINSTIMMUNG MIT MESSERGEBNISSEN

In der Abbildung 4 ist der Messdauereffekt für die drei Bezugszeiten 2 min, 3 min und 4 min in drei entsprechenden Kurvenzügen dargestellt. Weiterhin enthält die Abbildung als Punkte die Messergebnisse von STEWART u.a. (1954), welche – wie schon vorher erwähnt – als einzige zur Prüfung der vorliegenden Theorie geeignete Messdaten dem Verfasser bekannt geworden sind. Gegen einen Vergleich dieser Daten mit dem in Abb. 4 dargestellten Massdauereffekt erhob Dr. PASQUILL den berechtigten Einwand, dass erstere für die Konzentration in Höhe der Quelle gelten, während der Messdauereffekt für maximale Bodenkonzentrationen berechnet wurde. Lässt man gelten, dass mit zunehmender Messdauer das Verhältnis der Konzentration zu derjenigen bei der ursprünglichen Messdauer in gleicher Weise abnimmt, so erscheint ein Vergleich mit den genannten Daten dennoch gerechtfertigt. Da gegen diese Annahme zunächst kein gewichtiger physikalischer Grund spricht, auf der andern Seite auch keine andern Daten als die genannten verfügbar sind, sollten sie wenigstens um eines Anhaltes willen zum Vergeich herangezogen werden können.

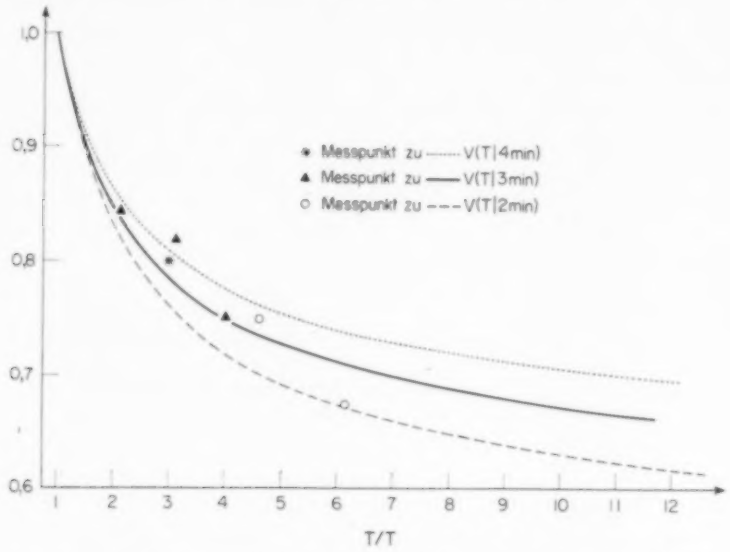

ABB. 4. Prüfung de Theorie an den Messergebnissen von STEWART u.a. (1954).

Die Ubereinstimmung ist besser als erwartet, sie darf als eine mögliche Bestätigung der vorgelegten Theorie angesehen werden.

Auf der andern Seite lässt diese gute Uebereinstimmung sofort die Frage aufkommen, welche Veränderungen der Verlauf der Funktion $\overline{\Psi}_z(T)$ bei einer andern Wahl der meteorologischen Parameter erfährt, und inwieweit durch eine geschickte Wahl dieser Parameter eine Uebereinstimmung erzwungen werden kann. Eine Prüfung dieser Frage würde einen erheblichen Aufwand an numerischen Auswertungen bedingen; diese wurden nicht durchgeführt. Da man infolge des Mangels an den erforderlichen meteorologischen Beobachtungen zur Annahme plausibler Werte

VOL. 4 1961

gezwungen ist, dürften gewisse „ Freiheitsgrade " für eine Adaption des theoretischen Ergebnisses an die Vergleichsmessungen vorhanden sein. Ob tatsächlich ein derartiger Spielraum existiert, und wie gross er ggf. ist, könnte wiederum nur durch eine Reihe numerischer Auswertungen festgestellt werden. Die im Vorangehenden im einzelnen gegebenen Begründungen werden erkennen lassen, dass tatsächlich die plausibelsten Werte eingesetzt wurden und deren Wahl nicht durch eine möglichst hohe Güte des Ergebnisses bestimmt war. Vielmehr lässt der Umstand der guten Uebereinstimmung des theoretischen Ergebnisses mit den Vergleichsmessungen vermuten, dass auch bei der Wahl etwas geänderter Parameter, der Verlauf der Funktion $\overline{\Psi}_z(T)$ keine wesentliche Aenderung erfährt.

Die beiden unsichersten Angaben sind ohne Zweifel diejenigen für B_0 in (78) und für T^* in (79a). Hier müssen durch Auswertungen von Windregistrierungen noch fundiertere Werte erhalten werden, mit welchen dann die Theorie an Vergleichsmessungen zu prüfen wäre. Es wäre wünschenswert, wenn auch letztere zu dem vorgesehenen Zweck etwas zahlreicher als bisher zur Verfügung ständen. Dann erst können gültige Aussagen gemacht werden; bis zu diesem Zeitpunkt aber wolle man die in der Tabelle angegebenen Werte nur als Anhalt für den Messdauereffekt benutzen.

Note added in proof

In der kürzlich erschienenen Arbeit von G. NONHEBEL " Recommendations on heights for new industrial chimneys " (Druck des Institute of Fuel, London W 1, Mai 1960) befindet sich eine von P. J. MEADE gegebene Tabelle über den Messdauereffekt. Leider lässt die Veröffentlichung nicht erkennen, wie die Werte erhalten wurden. Ein Vergleich dieser Werte mit dem vorstehenden Ergebnis zeigt eine befriedigende übereinstimmung.

Messdauer	Relative Konzentration (als zeitliches Mittel)	
	nach MEADE	nach vorstehender Theorie
3 min	1·00	1·00
15 min	0·82	0·73
1 hr	0·61	0·63
3 hr	0·51	0·53
24 hr	0·36	0·38

LITERATURHINWEISE

BARAD M. L. (1958) Project Prairie Grass, a Field Program in Diffusion. *Geophys. Res. Pap.* **2**, 59.

FRENKIEL F. N. and SHEPPARD P. A. (1959) Atmospheric diffusion and air pollution. *Advances in Geophysics* **6**, 459. Academic Press, London.

GOLDSTEIN S. (1951) On Diffusion by continuous movements and on the telegraph equation. *Quart. J. Mech. Appl. Math.* **4**, 129–156.

LETTAU H. and DAVIDSON B. (1957) *Exploring the Atmosphere's First Mile* **2**. Pergamon Press, Oxford.

MCCREADY P. B. (1953) Atmospheric turbulence measurements and analysis. *J. Met.* **10**, 434–49.

OGURA Y. (1957) The influence of finite observation intervals on the measurement of turbulent diffusion. *J. Met.* **14**, 176–81.

PANOFSKY H. A. and DELAND R. J. (1958) *One-dimensional spectra of atmospheric turbulence in the lowest* 100 *metres.* Preprint Intern. Sympos. on Turb. Diffus. and Air Poll., Oxford, 1958.

STEWART N. G. u.a. (1954) The atmospheric diffusion of gases discharged from the chimney of the HARWELL pile (BEPO). A.E.R.E.-H.P./R.1452.

SUTTON O. G. (1932) The theory of eddy diffusion in the atmosphere. *Proc. Roy. Soc.* A **135,** 143–65.

WEGENER A. (1919) Klimatische Windkarten. *Zeitschr. f. Meteor.* **36,** 53–5.

VOL.
4
1961

Int. J. Air and Water Poll. Pergamon Press 1961. Vol. 4, Nos. 1/2, pp. 24–32. Printed in Great Britain.

THE INFLUENCE OF SIZE DISTRIBUTION ON THE GROUND DEPOSIT OF LARGE PARTICLES EMITTED FROM AN ELEVATED SOURCE†

K. D. HAGE‡
Suffield Experimental Station
Ralston, Alberta, Canada
(*Received* 16 *March* 1960)

Abstract—A non-turbulent fallout model is found to be inadequate for the prediction of the time-averaged ground deposit of nearly homogeneous nominal 100μ diameter particles emitted from a point source at 15 m. As the heterogeneity of the particle size distribution increases, the turbulent effects are obscured by the effects of size distribution so that, for mass-diameter distributions with large standard deviations such as those commonly encountered in practice, the non-turbulent fallout model may provide acceptable predictions of mass deposit even though individual particles are influenced appreciably by turbulent dispersion. In this circumstance, however, the range of particle sizes to be found at a fixed distance from the source according to the non-turbulent fallout model will be much too narrow. In experiments which are designed to test theoretical models incorporating the effects of turbulence on the dispersion of large particles it is essential that nearly homogeneous particles be used.

INTRODUCTION

IN practical problems concerned with the turbulent dispersion of particles in the atmosphere one is often faced with complex and wide distributions of mass as functions of particle size. In such problems and in the design of experiments to test various theoretical approaches it is of interest to investigate the effects of the mass-diameter distribution on ground deposition.

As a basis for the investigation of particle size range effects, in the present report ground-level particle deposit data obtained under approximately neutral stability conditions are compared to ROUNDS' (1955) solution of the Fickian diffusion equation. The basic assumption, the merits, and the shortcomings of this approach to the turbulent diffusion problem have been discussed at length by many authors including SUTTON (1953) and GODSON (1958). No additional comments on these points are included here. Of the numerous models which have been proposed in the literature, it appears that ROUNDS' analytic solution is the only one which rigorously satisfies continuity requirements and surface boundary conditions for falling particles from a fixed source. Furthermore, if the gravitational settling speed of the particles is taken to be the still air terminal velocity, all parameters which appear in the solution can be evaluated without recourse to the deposition data which is to be predicted.

Numerous difficulties are encountered in attempts to obtain accurate deposit data in the field. For this reason, relatively large glass spheres of nominal diameter 100μ were used in the initial experimental studies. It is hoped that the experience and techniques which have evolved from this work will aid in future studies with smaller particles and that the deposit data will provide a useful reference for comparison with other particle sizes.

† Contribution from the Physics and Meteorology Section, Defence Research Board of Canada, Suffield Experimental Station, Ralston, Alberta, Canada, as Suffield Technical Paper No. 172. (DRB project Bo. D89-16-01-08.)

‡ Seconded to Suffield Experimental Station from the Department of Transport, Meteorological Branch.

THEORY

If the horizontal turbulent flux in the direction of the wind is neglected in comparison with transport by the mean wind, the two-dimensional Fickian diffusion equation takes the form

$$U\frac{\partial\psi}{\partial x}=\frac{\partial}{\partial z}\left(K_z\frac{\partial\psi}{\partial z}\right)+W\frac{\partial\psi}{\partial z} \tag{1}$$

For a point source, ψ represents crosswind-integrated concentration, K_z is the coefficient of vertical eddy diffusion, W is the gravitational settling speed of the particles, z is height above ground, U is the horizontal wind speed, and x is distance from the source in the direction of the wind. A solution to Eqn. (1) was obtained by ROUNDS (1955) for the special case in which U is approximated by a power function of the form

$$U=v_*c(z/z_0)^\alpha$$

where v_* is the friction velocity, c and α are constants which are used to fit the approximate power law to the logarithmic wind profile within the appropriate atmospheric layer, and z_0 is the roughness parameter. For a source emitting particles at a rate Q from an elevated point at height h above ground, the solution at ground level takes the form

$$D=\frac{W\psi_0}{Q}=\frac{W\gamma}{hU_h\Gamma(1-p)}\,(x/A)^{1-p}\quad\exp -A/x \tag{2}$$

where D = relative crosswind-integrated deposit
ψ_0 = crosswind-integrated concentration at ground level
U_h = wind speed at the height of emission
Γ = gamma function

and where

$$A=\frac{h^2U_h}{\gamma^2K_h},\quad \gamma=2+\alpha,\quad p=\frac{-W}{kv_*\gamma} \tag{3}$$

In Eqn. (3), K_h is the coefficient of vertical eddy diffusion at height h, and k is von KARMAN's constant. The solution for falling particles is valid only under neutral stability conditions.

In the event that turbulent effects on the motion of the particles are negligible

$$x=\frac{\bar{U}h}{W} \tag{4}$$

where $\bar{U}$ is the mean wind from the surface to the height of emission. Eqn. (4) represents the single point of deposit which corresponds to the solution of the degenerate form of Eqn. (1) with $K_z=0$ and W constant.

For a heterogeneous particle size distribution

$$D=\frac{1}{Q}\frac{\Delta Q}{\Delta x}=\frac{-1}{Q}\frac{\Delta Q}{\Delta r}\frac{\Delta r}{\Delta x} \tag{5}$$

where, as before, D is the relative crosswind-integrated deposition per unit distance in the direction of the wind, and r is particle radius. In general, it is necessary to compute the non-turbulent fallout deposition in an approximate manner at discrete intervals from a specified mass-diameter distribution. However, for particles which

VOL. 4 1961

are nearly uniform in size, it is reasonable to approximate the terminal velocities of the particles by a linear relation of the form

$$W = ar + b$$

where a and b are constants. In some instances, the mass-radius distribution may be approximated by a normal distribution

$$\frac{dQ}{dr} = \frac{Q}{\sqrt{2\pi}\,\sigma_r} \exp - \frac{(r - \bar{r})^2}{2\sigma_r^2} \tag{6}$$

where $\bar{r}$ is the mean radius, and σ_r is the standard deviation. With these approximations, in the limit as Δr and Δx tend to zero, Eqn. (5) becomes

$$D = \frac{\bar{U}h}{\sqrt{2\pi}\,\sigma_r a x^2} \exp - \frac{(\overline{W}x - \bar{U}h)^2}{2\sigma_r^2 a^2 x^2} \tag{7}$$

where $\overline{W}$ is the settling speed of particles of mean radius $\bar{r}$. Similar expressions may be derived for certain other mass-diameter distributions. In order to incorporate particle size variations into the K theory equation for deposit it is necessary to sum (Eqn. (2) over successive discrete size intervals.

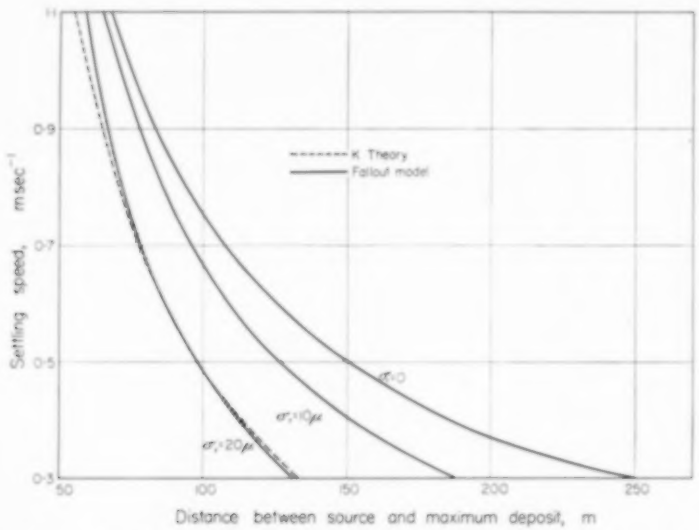

FIG. 1. Effect of variations in the mass-diameter distribution on the position of maximum ground deposit for a non-turbulent fallout model ($\bar{U} = 5{\cdot}0$ m.sec.$^{-1}$, $r = 53{\cdot}4$ μ, $h = 15{\cdot}0$ m.).

It will be seen from Eqns. (4) and (7) that the deposition of polydisperse particles differ in two principal ways from that of monodisperse particles under non-turbulent conditions. In the first place, the particles are spread over a finite swath in the direction of the wind, and, in the second place, the position of maximum deposit is displaced towards the source. These effects are precisely those produced by turbulence if we accept Eqn. (2). Consequently, for large values of σ_r, it is conceivable that the effects of size variation equal or dominate the effects of turbulence and that Eqn. (7) and Eqn. (2) yield comparable results.

The displacement of the position of maximum deposition may be considered quantitatively as an illustration. For convenience, Eqn. (2) will be referred to as the K theory and Eqn. (7) will be termed the fallout model. The positions of maximum deposit, x_m, are as follows

$$K\text{-theory} \qquad x_m = \frac{hU_h}{\gamma(\overline{W} + kv_*\gamma)} \tag{8}$$

$$\text{Fallout model} \qquad x_m = \frac{\overline{U}h}{4\sigma_r^2 a^2}\{(\overline{W}^2 + 8\sigma_r^2 a^2)^{\frac{1}{2}} - \overline{W}\} \tag{9}$$

Values of x_m which were obtained from Eqns. (8) and (9) for various values of σ_r and $\overline{W}$ are shown in Fig. 1. Meteorological parameters corresponding to neutral stability conditions and a mean wind speed of 5 m.sec.$^{-1}$ from ground level to the emission height of 15 m were used in the equations. Over the selected range of settling speeds, the parameter a appropriate to particles of density 2·4 gms cm^{-3} ranged from $1{\cdot}4 \times 10^4$ sec^{-1} to $1{\cdot}8 \times 10^4$ sec^{-1}. The important role of the parameter σ_r on the position of maximum deposit in this particular example is clearly demonstrated in Fig. 1.

EXPERIMENTAL

Before further consideration can be given to the effects of size distribution on the deposit of particles it is necessary to examine the validity of the model described by Eqn. (2). The results of a number of experiments with glass spheres of nominal diameter 100μ are available for comparison with the prediction of the theory. In the

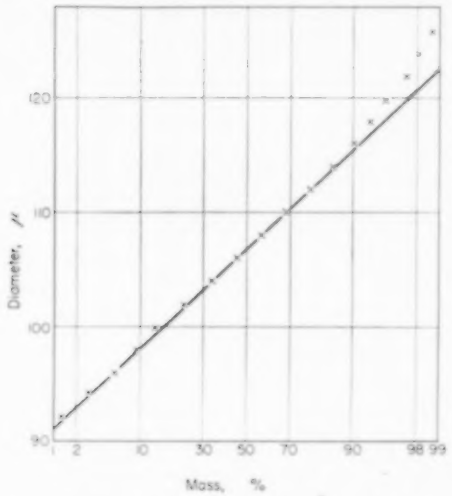

FIG. 2. Measured mass-diameter distribution of glass microspheres and fitted normal distribution.

experiments, microspheres† were emitted continuously from a 15 m tower for periods ranging from 45 to 60 minutes. The spheres were previously coated with fluorescent dye and samples of deposit were assessed under ultraviolet light in the laboratory. Details of the experiments have been discussed by HAGE, DIEHL, and DUDLEY (1960).

† 3M Superbrite manufactured by the Minnesota Mining and Manufacturing Company, St. Paul.

Samples of bulk microspheres were sized by microscope and the results are shown in Fig. 2. In order to facilitate comparison with a normal mass-diameter distribution the data are shown on linear-probability scales. The distribution is a narrow one with a mass median diameter of 106·7μ and a standard deviation of 6·8μ.

Terminal velocities were computed for the size range shown in Fig. 2 using successive approximations based on standard equations (see, for example, JOHNSON, 1954).

$$W = \frac{2(\rho_s - \rho_a)}{9\mu}\left(\frac{24}{C_D R_e}\right) r^2 \tag{10}$$

$$R_e = \frac{2\rho_a r W}{\mu} \tag{11}$$

where W = terminal velocity in still air
ρ_s = density of glass microspheres = 2·42 gms cm^{-3}
ρ_a = density of air = 1·15 × 10^{-3} gms cm^{-3}
μ = coefficient of viscosity = 174 × 10^{-6} poises
C_D = drag coefficient
R_e = Reynolds number
r = radius of the sphere

The values of ρ_a and μ represent average values for the experiments under consideration and correspond to a temperature of +6° C, a dew-point temperature of −1° C, and a pressure of 920 mb. Empirical drag coefficients were obtained from Langmuir and Blodgett (1946) From Fig. 2 and Eqns. (10) and (11), for a size range which includes 98 per cent of the mass of particles used in the experiments, the parameters σ_r and a which appear in Eqn. (7) have the values

$$\sigma_r = 3{\cdot}4 \times 10^{-4} \text{ cm.}$$

$$a = 1{\cdot}7 \times 10^{4} \text{ sec}^{-1}$$

Eqn. (7) may be refined for a continuous source by taking into account variations in the mean wind $\bar{U}$ over time intervals which are small compared to the total emission time but greater than or equal to the time of flight of the particles. Eqn. (7) becomes

$$D = \frac{h}{\sqrt{2\pi}\,\sigma_r a x^2} \sum_{i=1}^{n} f_i \bar{U}_i \quad \exp - \frac{(\bar{W}x - \bar{U}_i h)^2}{2\sigma_r^2 a^2 x^2} \tag{12}$$

$$\sum_{i=1}^{n} f_i = 1 \tag{13}$$

Assuming a constant rate of emission, f_i represents the fraction of the total emission time in which the mean wind remains within specified limits with a mean value $\bar{U}_i$. In connection with the experiments under consideration one-minute mean winds were used in the evaluation of Eqn. (12). The modifications to the original deposition curves were found to be negligible for the trial results given in this report.

The meteorological parameters which occur in Eqns. (2) and (3) were evaluated along the lines suggested by GODSON (1958). The observed wind profile was matched to the power law to obtain equivalence in the ratios of wind speed U_h at height h to the mean wind speed over h, $\bar{U}$ so that

$$\frac{U_h}{\bar{U}} = 1 + \alpha \tag{14}$$

The friction velocity v_* was obtained from the theoretical expression for the neutral wind profile

$$U_h = \frac{v_*}{k} \ln h/z_0 \tag{15}$$

A total of 25 wind profiles of duration 30 to 60 minutes from the surface to 15 m was used to obtain a value for the roughness parameter z_0. The ratios of mean wind speed in the upper half of the layer to the mean wind in the lower half of the layer were arranged according to corresponding vertical temperature gradients. The observed ratio appropriate to zero vertical temperature difference between 8 m and 0·5 m was entered into the theoretical ratio of logarithms to obtain z_0. A constant value $z_x = 8{\cdot}7$ cm was adopted for the experimental terrain and height of emission. A value of 0·4 was used for von KARMAN'S constant. The settling speed W was assumed to be the still air settling speed of glass spheres. Appropriate values were computed from Eqns. (10) and (11).

RESULTS

The results of three trials, which were conducted under approximately neutral stability conditions, have been analyzed for comparison with the theoretical models. In each trial glass microspheres of mass mean diameter 106·7 μ were emitted continuously from a point source at 15 m over gently rolling prairie terrain. The trial conditions are listed in Table 1.

VOL. 4 1961

TABLE 1. TRIAL PARAMETERS

Parameter	Trial 1	Trial 2	Trial 3
Local Time (hrs)	1217	1120	1530
Duration of Emission (min)	60	60	44
Emission Amount (gms)	672·7	427·5	497·0
Surface Conditions	Snow 3–8 cm	Ice patches	Ice patches

One-minute average winds at 6 heights were obtained with calibrated Sheppard-Casella electric contact cup anemometers. Temperature differences between these heights were measured with shielded copper-constantan thermocouples. Arithmetic mean winds were computed for each level for the period of emission. The mean winds for the layer between ground level and the height of emission were evaluated by graphical methods. A data summary is given in Table 2.

The microspheres were counted on adhesive sampling surfaces of dimensions 6·5 by 13 inches. The crosswind distribution of particles on each sampling arc was approximated by rectangular elements of width 1·0 m, length equal to the spacing between samples, and height equal to the deposit density as measured by the sample at the central point. Crosswind-integrated deposits were obtained by summing the mass content of all such rectangular elements on each sampling arc. The area under the curve of crosswind-integrated deposit as a function of distance from the source provided an estimate of the total recovery.

TABLE 2. METEOROLOGICAL PARAMETERS

Height (m.)	Mean Wind Speed (m.sec^{-1}) Trial 1	Trial 2	Trial 3
0·5	2·32	2·90	2·49
1·0	2·83	3·47	3·05
2·0	3·31	4·16	3·65
4·0	4·02	4·87	4·24
8·0	M	5·72	5·23
16·0	6·05	7·10	6·76
Mean Wind (m.sec.$^{-1}$)	4·57	5·41	4·93
Temperature Difference 4m–0·5m (° C.)	+0·6	+0·1	+0·4
Friction Velocity v_* m.sec.$^{-1}$)	0·46	0·54	0·51
Power Law Exponent α	0·30	0·28	0·33
Emission Height Wind (m.sec.$^{-1}$)	5·94	6·93	6·57

In Table 3, the predicted deposits D_K of the K theory, and the deposits D_F of the fallout model are compared to the observed deposits D. All deposits have been divided by the source strength Q. The fitted normal mass-diameter distribution defined by the straight line in Fig. 2 was used in the computation of $D_K$and D_F.

TABLE 3. DEPOSIT DATA (mg/gm/m)

Trial		Distance from Source (m) 27·4	45·7	73·2	100·6	128·0	205·7	402·3
Trial 1	D	—	—	5·8	9·3	6·5	1·4	0·1
	D_K	0·3	3·1	6·1	5·7	4·5	2·0	0·4
	D_F	0·0	0·0	0·0	15·0	16·6	0·0	0·0
Trial 2	D	0·0	0·0	1·1	6·3	6·0	2·5	0·2
	D_K	0·1	1·8	4·5	4·9	4·3	2·3	0·6
	D_F	0·0	0·0	0·0	0·0	28·1	0·0	0·0
Trial 3	D	0·0	0·0	1·5	7·6	6·8	1·6	0·2
	D_K	0·3	2·6	5·3	5·2	4·3	2·1	0·5
	D_F	0·0	0·0	0·0	2·3	30·6	0·0	0·0

Although the predictions of ROUNDS' solution to the K theory are far from perfect they are clearly superior to the predictions of the non-turbulent fallout model. In each instance the K theory deposit curve is not as sharply peaked as the observed

curve; a result which may be due in part to the circumstance that all of the experiments were carried out under slightly stable conditions.

The effect of variable size distributions on the position of maximum ground deposit was illustrated in Fig. 1. If, on the basis of the results in Table 3, the K theory is accepted as a reasonable approximation to the observed ground deposit, it is possible to examine the effect of variable size distribution on the magnitude of the peak deposit or on the degree of spreading of particles in the direction of the wind. In Table 4, D_K and D_F are compared for various values of σ_r under conditions which are otherwise identical to those of Trial 1.

TABLE 4. DEPOSIT DATA (mg/gm/m)

		Distance from Source (m)							
		45·7	73·2	86·9	100·6	115·0	128·0	160·0	205·7	402·3
$\sigma_r = 3{\cdot}4\mu$	D_K	3·1	6·1	6·1	5·7	5·1	4·5	3·3	2·0	0·4
	D_F	0·0	0·0	0·2	15·0	37·1	16·6	0·2	0·0	0·0
$\sigma_r = 10\mu$	D_K	2·9	5·2	5·1	4·8	4·2	3·8	2·8	1·8	0·4
	D_F	0·0	3·9	10·1	12·9	11·6	9·4	4·4	1·4	0·0
$\sigma_r = 20\mu$	D_K	4·0	5·3	5·0	4·5	3·9	3·5	2·6	1·8	0·6
	D_F	1·3	8·6	8·3	7·2	5·8	4·8	3·0	1·6	0·3

Normal mass-radius distributions with standard deviations $\sigma_r = 3{\cdot}4\mu$, 10μ, and 20μ and mean size $\bar{r} = 53{\cdot}4\mu$ were used in the deposit calculations for Table 4. The true distributions were approximated by 30 discrete elements with appropriate mean radii, and with mean settling speeds derived from Eqns. (10) and (11).

It will be seen in Table 4 that, as σ_r increases, D_F approaches D_K both in regard to the position of maximum deposit and in regard to the magnitude of maximum deposit or the degree of spreading along the x axis. It is evident that the dispersive effects of turbulence on the ground deposit of particles under neutral conditions *may* be obscured to a large extent by the effects of the non-uniformity of the particle sizes. Consequently, in experimental studies which are designed to study turbulent dispersion or to test dispersion theories, it is essential that σ_r be kept small. Conversely, under certain circumstances, a simple fallout model may provide adequate predictions of mass deposit of particles even though individual particles are markedly affected by turbulence.

The foregoing conclusions are based on limited data and on quantitative arguments for special cases only and, as a result, are severely restricted. It is hoped, however, that the results are indicative of some of the possible dangers involved in the interpretation of heterogeneous particle data from the viewpoint of turbulent diffusion.

Acknowledgement—The experimental results which have been reported in this paper would not have been possible without the zeal and patience of Mr. C. H. H. DIEHL and Mr. M. G. DUDLEY. Their efforts are gratefully acknowledged. Thanks are due to Mr. K. F. STYLES for meteorological measurements and data reduction and to Mr. S. A. CYGANIK for drafting the figures.

VOL. 4 1961

REFERENCES

GODSON W. L. (1958) The diffusion of particulate matter from an elevated source. *Arch. F. Meteor., Geoph., U. Biokl.*, **10A**, 305–27.

HAGE K. D., DIEHL C. H. and DUDLEY M. G. (1960) On horizontal sampling of solid particles in the atmosphere. *A.M.A. Arch. Ind. Health*, **21**, 124–31.

JOHNSON J. C. (1954) *Physical Meteorology*. The Technology Press of M.I.T., and John Wiley, New York, 393 pp.

LANGMUIR I. and BLODGETT K. B. (1946) A mathematical investigation of water droplet trajectories. *U.S. Army Air Force, Tech. Rep.* No. 5418, Washington, D.C., 68 pp.

ROUNDS W., Jr. (1955) Solutions of the two-dimensional diffusion equations. *Trans. Amer. Geoph. Union*, **36**, 395–405.

SUTTON O. G. (1953) *Micrometeorology*. McGraw-Hill, New York, 333 pp.

Int. J. Air and Water Poll. Pergamon Press 1961. Vol. 4, Nos. 1/2, pp. 33–46. Printed in Great Britain

THE VERTICAL DIFFUSION OF GAS FROM A CONTINUOUS SOURCE

WILLIAM P. ELLIOTT
Geophysics Research Directorate
(*Received* 4 *June* 1960)

Abstract—An empirical investigation of the form of the vertical profile of gas concentration indicates that Sutton's suggested parameters have somewhat limited applicability. The term $\exp(-z^a/B)$ is examined for values of a and B. The findings indicate that the value of 2·0 for a, as suggested by SUTTON, is an overestimate except in fairly stable conditions. Values of 1·5 seem more appropriate for near neutral conditions and values less than 1·5 for unstable conditions.

The data used for this study were obtained during Project Prairie Grass, a field program in diffusion conducted over short grass on level prairie land. The observations were made at 100 metres from the source to a height of 17·5 metres. Forty-one cases are discussed during which the wind speeds at two metres varied from 1·4 to 9·4 metres/sec.

1. INTRODUCTION

THE most frequently quoted hypothesis for describing diffusion from a continuous point source is that due to SUTTON (1953). One of the features embodied in this hypothesis is the assumption that the vertical distribution of concentration χ at any point (x, y) in the horizontal plane downwind of the source (located at (0, 0, 0)) follows a Gaussian curve. That is

$$\chi(z) = \chi_0 \exp(-z^2/2\sigma_z^2) \tag{1}$$

where $\chi(z)$ is the concentration at height z,
χ_0 is the concentration at the ground and
σ_z^2 is the vertical variance of the concentration.

SUTTON has pointed out, however, that Equation 1 is not a unique solution of the theoretical equations from which it stems. Actually the exponential term could be of the form $\exp(-z^a/B)$ (with certain restrictions on a and B which need not concern us here) and still satisfy the theory. The purpose of this paper is to examine the values of a and B obtained from some experimental data to see if, in fact, the Gaussian assumption is supported.

The data used in this study were taken during Project Frairie Grass. This project was a field program designed to investigate diffusion from a continuous point source in natural conditions. Descriptions of the program have appeared elsewhere in the literature (a brief description can be found in ELLIOTT (1959) and a complete one in BARAD (1958)), so that only the part of this program germane to the present study will be discussed.

2. OBSERVATIONS

The sampling network consisted of ground samplers along arcs at various distances from the source and 6 towers on which samplers were also placed. These towers were located 14° apart on an arc 100 m from the source with samplers at heights of 0·5, 1·5, 2·5, 4·5, 7·5, 10·5, 13·5 and 17·5 m above the ground. Sulphur dioxide was emitted

for 10 minutes at a height of 46 cm for 64 releases and 150 cm during the last 6 releases. The observing site was flat prairie land with a 5–6 cm grass cover.

Of the total of 70 gas releases data from the towers were available for only 50 releases. During 3 of these 50 releases the cloud just barely touched one of the towers and these 3 were not included in the study. One more release was rejected because data were missing from some of the samplers. Five more releases were not included; 3 because the height of the cloud was too low to be recorded on enough samplers to allow computations to be made and 2 because the vertical distributions were too erratic to permit meaningful calculations. Thus in all 41 of the available 50 releases were used in this study. Of these 41, 20 were made during unstable conditions and 21 during stable conditions.

3. METHOD OF ANALYSIS

In the following analysis, the vertical concentration of gas at any point is assumed to be given by

$$\chi(z) = \chi_0 \exp(-z^a/B) \tag{2}$$

where a and B are to be determined from the data.

Considering the concentrations at two separate levels z_1 and z_2 values of

$$\ln \frac{\chi(z_1)}{\chi(z_2)} = \frac{z_2^a - z_1^a}{B} \tag{3}$$

can be computed. B can be eliminated by computing another ratio from a different pair of heights, say z_2 and z_3. Thus

$$\ln \frac{\chi(z_1)}{\chi(z_2)} \Big/ \ln \frac{\chi(z_2)}{\chi(z_3)} = \frac{z_2^a - z_1^a}{z_3^a - z_2^a} \tag{4}$$

Equation 4 can be solved for values of a by trial and error methods. Once a is obtained, values of B can be calculated for any pair of heights using Equation 3.

4. RESULTS

Values of a and B were computed in the above manner for each of the 41 runs. In order to determine the effect of computing these values at specified heights, two sets of heights were chosen.

In one set observations at 1·0, 2·5 and 7·5 m were used and in the other set observations at 1·5, 4·5 and 10·5 m were used. The mean value of a for the lower set was 1·50 with a standard deviation of 0·34. For the higher set the mean value was 1·45 with a standard error of 0·28. The medians for both sets were 1·50. For the lower set 3 individual values equaled or exceeded 2·0 and 1 individual value exceeded 2·0 in the higher set. In the lower set 3 values were less than 1·0 and in the higher set 2 values were less than 1·0. These results indicate practically no variation of a over the height range used. When the two sets were combined the average value of a was 1·49 with a standard deviation of 0·28.

When these values of a were plotted against the Stability Ratio (defined as

$$SR = \frac{T_4 - T_1}{U_2^2} \times 10^5 \quad ^\circ\text{C/(cm/sec)}^2 \tag{5}$$

where the subscripts refer to the height in metres of the temperature (T) and wind speed (U) observations) a slight indication that the value increased with increasing

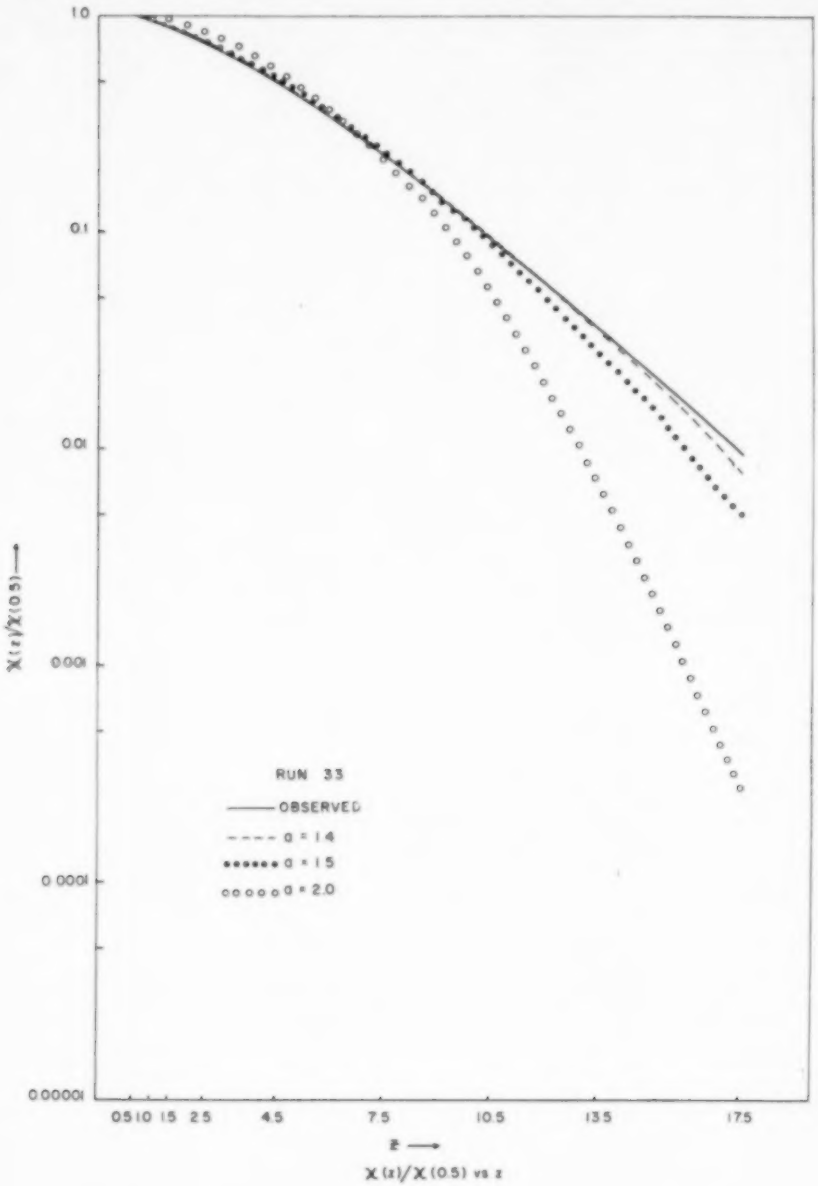

FIG. 1

stability was found but the scatter was much too great to define a functional relationship.

In order to represent the results graphically values of B were computed for values

VOL. 4 1961

of $a = 1{\cdot}4$, $1{\cdot}5$ and $2{\cdot}0$ using equation 3. Values of B showed little tendency to vary with height when computed using $a = 1{\cdot}4$ or $1{\cdot}5$ being about 10 per cent higher in the

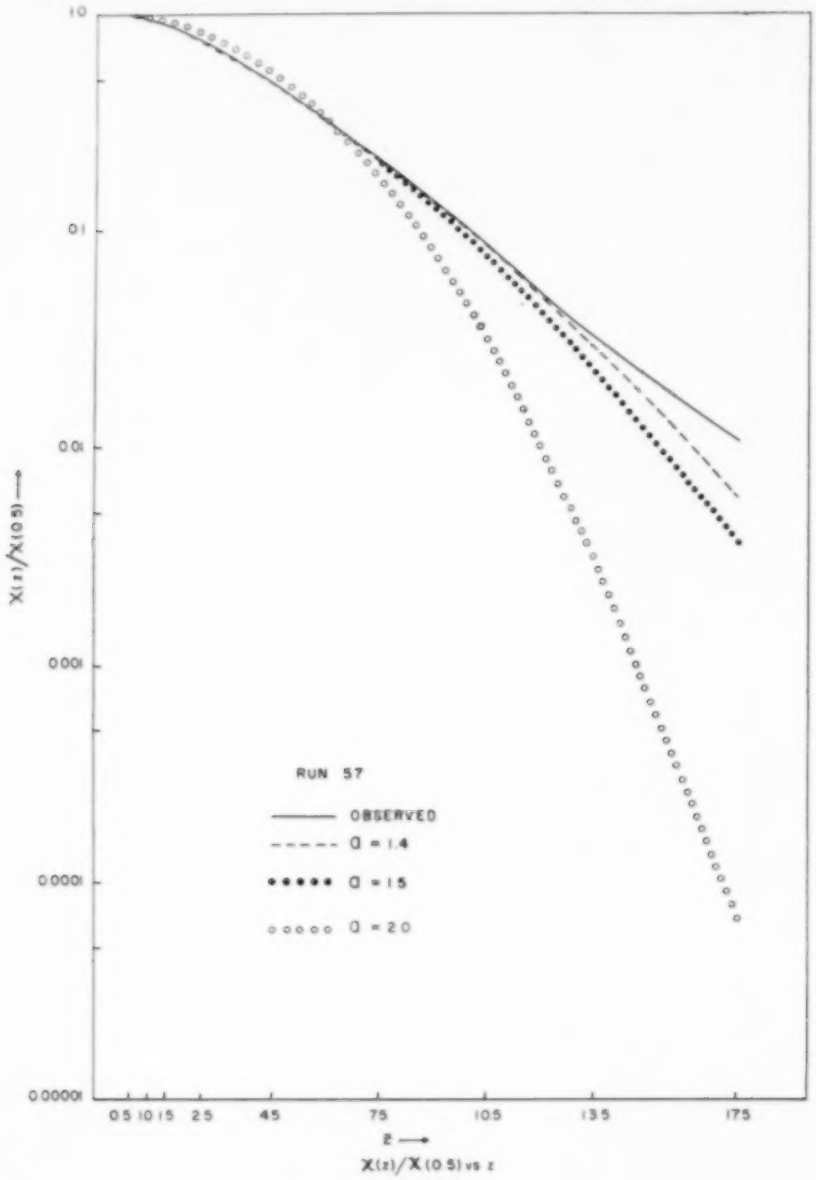

FIG. 2

latter case. However using $a = 2{\cdot}0$ produced values of B distinctly varying with height; the averages for the 41 cases being 22·8, 28·8, 37·0 and 50·7 for the height intervals 1·0–2·5, 1·5–4·5, 2·5–7·5, 4·5–10·5 metres respectively.

These results can be seen more clearly by examining Figs. 1–4 where the ratios of the

concentrations at height z to the concentration at 0·5 m have been plotted.* The four lines represent the observed ratios and the ratios computed from $a = 1{\cdot}4$, 1·5 and

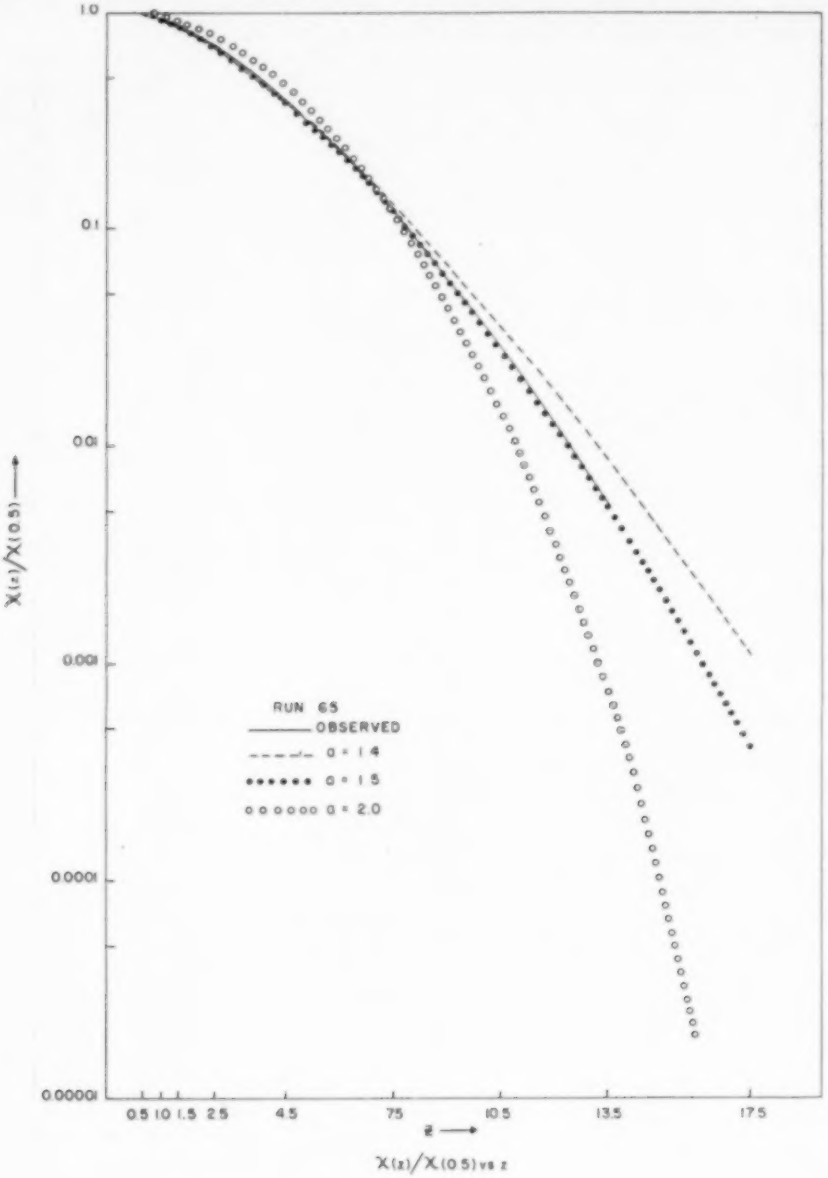

FIG. 3

2·0. In computing the ratios with $a = 2{\cdot}0$, an average value of B for the four height pairs was used. The fact that the $a = 2{\cdot}0$ line crosses the observed line near 7·5 m

* The appendix contains data for 22 of the 41 cases. These cases represent the smoothest observed profiles.

VOL. 4 1961

is a result of the particular choice of B. Had some other value of B been chosen a different crossover point would result. However, one can easily see that a value of 2·0 with B adjusted to give some sort of best fit will result in an overestimate of the concentration in the lower levels and an underestimate in the upper levels.

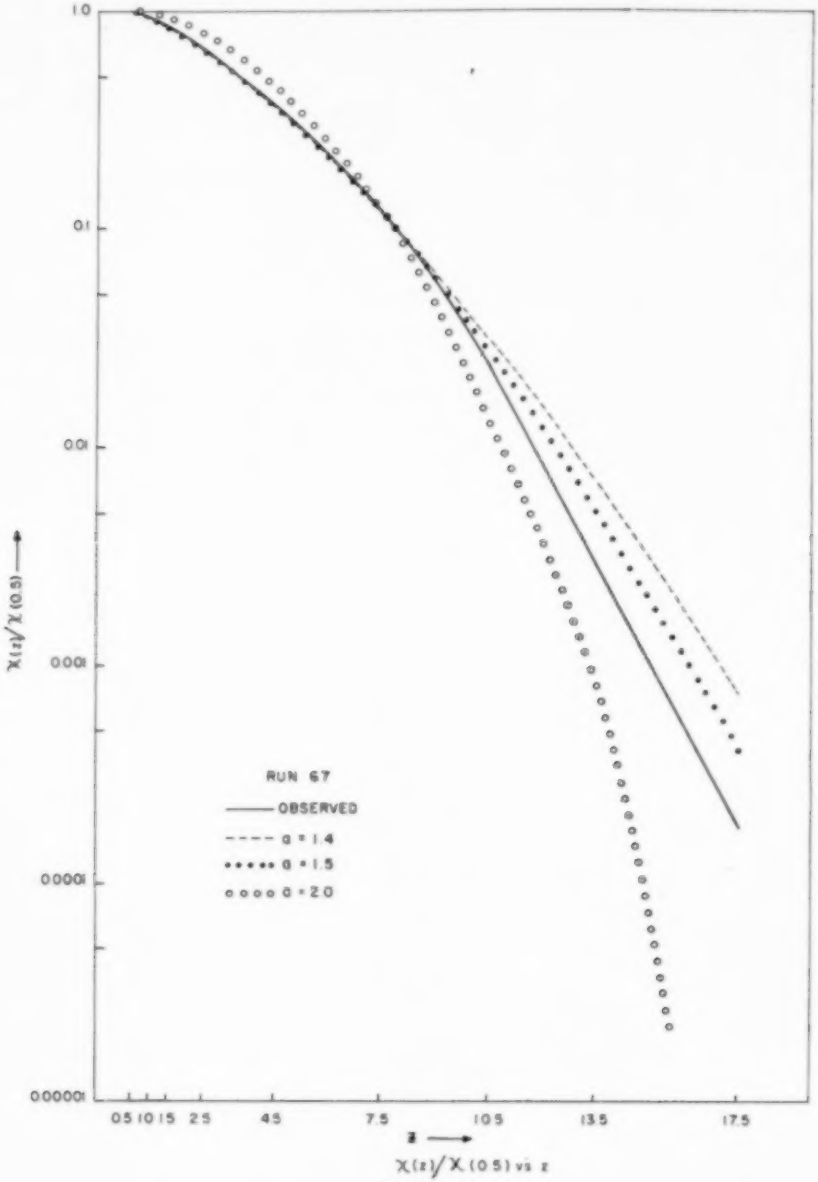

FIG. 4

Figs. 1–4 clearly show that an exponent of 1·4 or 1·5 fits the data better than 2·0. Figs. 1 and 2 present data taken during unstable conditions and Figs. 3 and 4 stable

conditions. Figs. 1 and 3 are runs where one or the other line was a close fit to the data and Figs. 2 and 4 present some of the poorer fits. In general, most of the runs fell somewhere in between these sets of examples with respect to goodness of fit. In 4 of the total of 41 cases, the plot based on an $a = 2{\cdot}0$ was a closer fit to the observed ratios than $a = 1{\cdot}5$ or $1{\cdot}4$.

In examining these graphs the reader can see that $a = 1{\cdot}4$ seems to fit data better for the unstable runs and $a = 1{\cdot}5$ better for the stable runs. In general, this pattern was noticed for all the runs. Graphs, such as those shown, were plotted for all 41 cases. When these 41 runs were (subjectively) split into two categories – $a = 1{\cdot}4$ better, or $a = 1{\cdot}5$ better – it was found that $a = 1{\cdot}4$ was better in 14 unstable cases and 4 stable cases, and $a = 1{\cdot}5$ was better in 15 stable cases and 4 unstable cases. Two stable and two unstable cases were indeterminate. This evidence points to at least a slight dependence on stability of the exponent a.

As an alternative to allowing a to vary we can consider using a fixed value of a and allowing B to vary. If the values of B calculated using $a = 1{\cdot}5$ are plotted against the Stability Ratio, the variation shown in Figure 5 results. Although the scatter is large, B evidently decreases with increasing stability.

5. DISCUSSION OF RESULTS

Two main questions concerning the above analysis need to be answered. These questions are (1) Sutton's original form presumes the source to be at the ground while the source was elevated during these runs. Does neglect of source height correction affect the results? (2) Was there appreciable deposition of the gas between the source and the 100 m arc during the runs?

VOL. 4 1961

Question 1 will be treated first. For an elevated source Sutton transforms Equation 1 to

$$\chi(z) = \chi_0[\exp(-(z+h)^2/2\sigma_z^2) + \exp(-(z-h)^2/2\sigma_z^2)] \tag{6}$$

where h is the height of the source.

If the method of images employed in arriving at Equation 6 is applied to Equation 2, we get

$$\chi(z) = \chi_0[\exp(-(z+h)^a/B) + \exp(-(z-h)^a/B)] \tag{7}$$

If the terms $(z+h)^a$ are written $z^a(1 \pm h/z)^a$ and expanded in series with only the first three terms retained, Equation 7 can be written (for h less than z)

$$\chi(z) = \chi_0\left\{\exp\left[-\frac{z^a}{B}\left\{1+\frac{ah}{z}+\frac{a(a-1)}{2}\left(\frac{h}{z}\right)^2\right\}\right] + \exp\left[-\frac{z^a}{B}\left\{1-\frac{ah}{z}+\frac{a(a-1)}{2}\left(\frac{h}{z}\right)^2\right\}\right]\right\} \tag{8}$$

After some manipulations, Equation 8 can be reduced to

$$\chi(z) = \chi_0 \exp\left[-\frac{z^a}{B}\left\{1+\frac{a(a-1)}{2}\left(\frac{h}{z}\right)^2\right\}\right] 2\cosh\left(\frac{ahz^{a-1}}{B}\right) \tag{9}$$

So if the ratio of $\chi(z_1)$ to $\chi(z_2)$ is formed, the result is

$$\frac{\chi(z_1)}{\chi(z_2)} = \exp\left[\frac{z_2^a - z_1^a}{B}\right]\left\{\frac{\cosh[(a/2B)z_1^{a-1}]}{\cosh[(a/2B)z_2^{a-1}]}\exp\left[\frac{a(a-1)}{2B}\frac{z_1^{a-2} - z_2^{a-2}}{4}\right]\right\} \tag{10}$$

if h is taken as 50 cm. The term in braces represents the effect of the elevated source. A few trial-and-error solutions for a and B using Equation 10 were obtained. These

values of a and B were compared with values obtained by using Equations 3 and 4, and there was no essential difference. Thus, for our particular case, the fact that the source height was not at the ground made little difference in the calculations. In fact, using average values of a and B obtained from the trial-and-error methods, it can be shown that the term in braces represents only at worst a 2 per cent correction to $\chi(z_1)/\chi(z_2)$ for the heights used.

Question 2 above, concerning the amount of deposition, cannot be answered conclusively. However, several factors indicate that deposition is probably negligible.

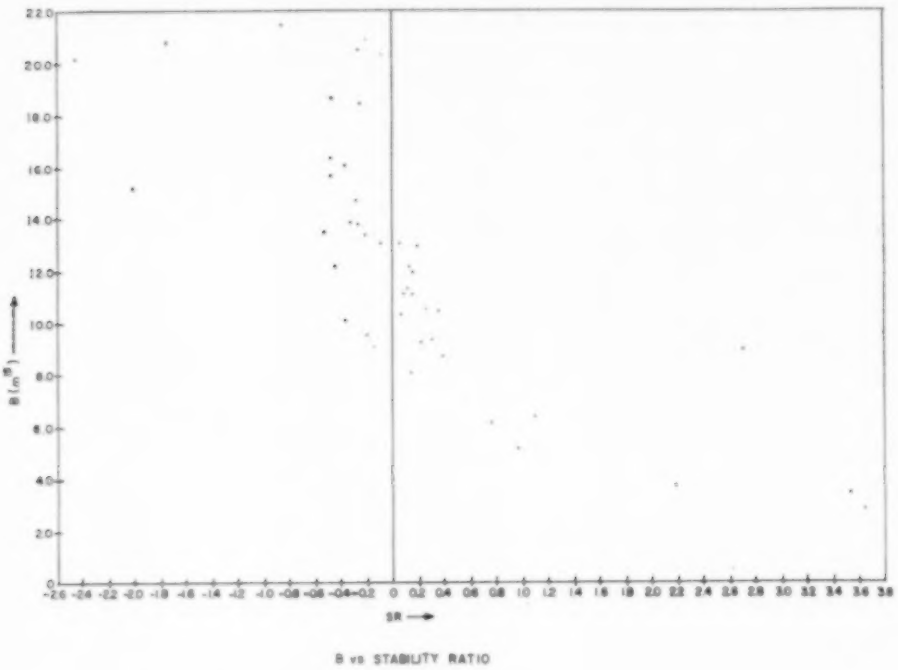

FIG. 5

If deposition were appreciable the total amount of gas passing the 100 m arc should be smaller than the total emitted. One could calculate the total amount Q passing the 100 m arc if one knew the terms in the integral

$$Q = \int_{-\infty}^{\infty} \int_{0}^{\infty} \overline{u\chi}\, dz\, dy \tag{11}$$

Since simultaneous observations of the wind speed, u, and the concentration, χ, at the 100 m arc were not available, the term $\overline{u\chi}$ can be only approximated by $\overline{u}\,\overline{\chi}$ which, since u and χ are probably inversely related, would result in an overestimate of $\overline{u\chi}$ and, hence, of Q. Nevertheless, numerical integration of Equation 11 was carried out with this approximation. If the results of this integration were values of Q less than or equal to the source strength we would have had an indication that deposition was important. However, the results gave Q's from -10 per cent–25 per cent greater (with a median of 13 per cent) than the source strength. Thus, all we can

conclude from this is that the error in Q would probably have to be greater than 10–15 per cent in order to indicate deposition.

Two other points are worth mentioning. BARAD and HAUGEN (1959), who were concerned with deposition, state that visual inspection of the site revealed no evidence of grass damage due to uptake of SO_2 after the actual experiments were begun. Furthermore, if Sutton's form were correct in the absence of deposition we would expect, if deposition were important, the data near the ground to show a less rapid decrease with height than Sutton's form. Inspection of Figs. 1–4 indicate just the reverse–a greater decrease with height than predicted by Sutton. These observations indicate, at least to the present writer, that the shape of the vertical profiles of concentration was relatively unaffected by deposition of SO^2.

6. SUMMARY AND CONCLUSIONS

The major purpose of this paper has been to investigate the validity of Sutton's original assumption concerning the value of a. The assumption that this value is 2·0 seems to be valid, based on these results, only for moderate values of positive stabilities. In the above comparisons it was found that for only 4 of the 41 cases available for study was a value of 2·0 better than 1·5. Also it will be recalled that 5 of the original 50 cases were rejected for reasons other than lack of data. Of these, 3 were rejected because the height of the cloud was not sufficient to calculate a value of a. This would indicate a rapid decrease in concentration with height and probably, were it possible to compute an a, their values would also have been close to 2·0. In examining these 7 cases collectively they represent 7 of 9 most stable periods during which vertical measurements were made. On this basis one concludes that the value of 2·0 for a may be valid during cases where the Stability Ratio is greater than 1·0 (this corresponds to a Richardson Number at 2 metres of roughly 0·04).

This study indicates further that a value closer to 1·5 would be more appropriate, during slightly stable and near neutral conditions and values less than 1·5, perhaps as low as 1·0, in extremely unstable cases, than the usual assumption of Gaussian distribution throughout the entire range of stability conditions.

In closing, the conditions under which the observations were made should be stressed. Observations were available only at 100 m from the source and the highest observation was at 17·5 metres. The experiments were conducted over quite level land with short grass. The wind speeds varied from a low of 1·4 m/sec to a high of 9·4 m/sec (measured at 2 metres).

Acknowledgements—Dr. MORTON L. BARAD and Mr. DUANE A. HAUGEN of the Geophysics Research Directorate offered many suggestions which were most helpful. Mr. ROGER LANDERS of the Geophysics Research Directorate drew the figures and Miss MARGO SYLVESTER and Miss HELEN SCOTT helped prepare the manuscript. All these people here receive the author's thanks for their assistance.

REFERENCES

BARAD, MORTON L. (Editor) (1958) *Project Prairie Grass, A Field Program in Diffusion, Vol.* 1. Geophysics Research Paper No. 59, Geophysics Research Directorate, Air Force Cambridge Research Center.

BARAD, MORTON L. and DUANE A. HAUGEN (1959) A preliminary analysis of Sutton's hypothesis for diffusion from a continuous point source. *J. Met.* **16,** 12–20.

ELLIOTT, WILLIAM P. (1959) The areas within concentration isopleths downwind of a continuous point source. *Int. J. Air. Poll.* **2,** 115–26.

SUTTON, O. G. (1953) *Micrometeorology*, McGraw-Hill, New York.

VOL. 4 1961

APPENDIX

Table A contains the computed data for 22 of the runs used in this study. Values of B computed for both $a = 1{\cdot}4$ and $a = 1{\cdot}5$ together with the Stability Ratio are shown along with the ratios $\chi(z)/\chi(0{\cdot}5)$ computed from the data (R_0) and computed using $a = 1{\cdot}4$ ($R_{1\cdot4}$) and $a = 1{\cdot}5$ ($R_{1\cdot5}$).

TABLE A1

Run	S.R.	$B_{1\cdot4}$	$B_{1\cdot5}$
17	·37	8·4	10·5
19	−·46	14·6	18·7
20	−·28	11·7	14·7
21	·09	9·2	11·2
22	·07	8·5	10·4
26	−·44	9·9	12·2
27	−·47	12·5	15·7
30	−·36	12·6	16·1
31	−·26	18·5	20·0
33	−·26	11·3	13·8
37	·18	9·8	12·0
40	2·70	7·4	9·0
43	−·85	15·7	20·0
45	−·19	7·8	9·6
49	−·52	10·2	13·5
55	·12	9·4	11·4
56	·20	10·5	13·0
57	−·08	10·7	13·1
60	·27	8·7	10·6
65	·31	8·0	9·4
67	·23	7·6	9·3
68	·97	4·3	5·2

TABLE A2.

$R_o = \chi(z)/\chi(0{\cdot}5)$ observed
$R_{1\cdot4} = \chi(z)/\chi(0{\cdot}5)$ computed with $a = 1{\cdot}4$
$R_{1\cdot5} = \chi(z)/\chi(0{\cdot}5)$ " " $a = 1{\cdot}5$

	Run 17			Run 19			Run 20		
ht(m)	R_o	$R_{1\cdot4}$	$R_{1\cdot5}$	R_o	$R_{1\cdot4}$	$R_{1\cdot5}$	R_o	$R_{1\cdot4}$	$R_{1\cdot5}$
0·5	1·0	1·0	1·0	1·0	1·0	1·0	1·0	1·0	1·0
1	·96	·93	·94	·96	·96	·97	·98	·95	·96
1·5	·87	·87	·87	M	·92	·92	·96	·91	·91
2·5	·70	·68	·71	·73	·80	·83	·84	·76	·79
4·5	·42	·40	·42	·52	·58	·61	·55	·51	·53
7·5	·14	·14	·15	·30	·33	·34	·28	·25	·25
10·5	·046	·043	·041	·14	·16	·16	·11	·10	·10
13·5	M	·011	·0092	·069	·075	·072	·042	·040	·035
17·5	·0021	·0015	·0010	·019	·024	·020	·0092	·0093	·0070

VOL. 4 1961

	Run 21			Run 22			Run 26		
ht(m)	R_o	$R_{1\cdot4}$	$R_{1\cdot5}$	R_o	$R_{1\cdot4}$	$R_{1\cdot5}$	R_o	$R_{1\cdot4}$	$R_{1\cdot5}$
0·5	1·0	1·0	1·0	1·0	1·0	1·0	1·0	1·0	1·0
1	·94	·93	·94	·94	·93	·94	·92	·94	·95
1·5	·87	·89	·88	·88	·88	·87	·88	·90	·89
2·5	·74	·70	·73	·70	·68	·70	·71	·73	·74
4·5	·44	·43	·44	·39	·40	·42	·44	·45	·47
7·5	·16	·17	·16	·14	·14	·14	·20	·19	·19
10·5	·044	·057	·049	·050	·045	·039	·070	·069	·063
13·5	·0075	·012	·012	·015	·012	·0087	·047	·022	·018
17·5	·00094	·0027	·0015	·0023	·0017	·00091	·018	·0041	·0025

	Run 27			Run 30			Run 31		
ht(m)	R_0	$R_{1\cdot4}$	$R_{1\cdot5}$	R_0	$R_{1\cdot4}$	$R_{1\cdot5}$	R_0	$R_{1\cdot4}$	$R_{1\cdot5}$
0·5	1·0	1·0	1·0	1·0	1·0	1·0	1·0	1·0	1·0
1·0	·94	·95	·96	·98	·95	·96	·93	·97	·97
1·5	·85	·91	·91	·94	·91	·91	·88	·94	·93
2·5	·69	·77	·80	·79	·77	·80	·85	·84	·84
4·5	·48	·53	·55	·58	·54	·57	·56	·66	·63
7·5	·26	·27	·28	·29	·27	·29	·36	·41	·36
10·5	·11	·12	·12	·12	·12	·12	·21	·24	·19
13·5	·068	·048	·043	·045	·50	·047	·12	·13	·085
17·5	·026	·013	·0097	·028	·013	·011	·050	·052	·026

	Run 33			Run 37			Run 40		
ht(m)	R_0	$R_{1\cdot4}$	$R_{1\cdot5}$	R_0	$R_{1\cdot4}$	$R_{1\cdot5}$	R_0	$R_{1\cdot4}$	$R_{1\cdot5}$
0·5	1·0	1·0	1·0	1·0	1·0	1·0	1·0	1·0	1·0
1·0	·94	·94	·95	·95	·94	·95	·91	·92	·93
1·5	·88	·90	·90	·86	·89	·89	·83	·86	·84
2·5	·77	·75	77	·76	·72	·74	·65	·65	·67
4·5	·48	·50	·51	·47	·45	·46	·37	·35	·36
7·5	·22	·23	·23	·17	·19	·19	·12	·11	·11
10 5	·093	·094	·087	·047	·067	·060	·018	·028	·024
13·5	·035	·035	·028	·0094	·021	·017	·0014	·0061	·0042
17·5	·0097	·0078	·0051	·0024	·0037	·0023	·000048	·00061	·0003

	Run 43			Run 45			Run 49		
ht(m)	R_0	$R_{1\cdot4}$	$R_{1\cdot5}$	R_0	$R_{1\cdot4}$	$R_{1\cdot5}$	R_0	$R_{1\cdot4}$	$R_{1\cdot5}$
0·5	1·0	1·0	1·0	1·0	1·0	1·0	1·0	1·0	1·0
1·0	·95	·96	·97	·95	·92	·93	·94	·94	·95
1·5	·90	·93	·93	·86	·86	·86	·91	·90	·90
2·5	·86	·81	·84	·67	·66	·68	·69	·73	·76
4·5	·63	·61	·63	·36	·37	·38	·53	·46	·51
7·5	·32	·35	·36	·12	·12	·12	·21	·20	·22
10·5	·19	·18	·19	·040	·034	·030	·071	·075	·083
13·5	·10	·090	·085	·012	·0079	·0059	·023	·025	·026
17·5	·048	·031	·026	·0012	·00091	·00050	·0079	·0048	·0045

VOL. 4 1961

	Run 55			Run 56			Run 57		
ht(m)	R_0	$R_{1\cdot4}$	$R_{1\cdot5}$	R_0	$R_{1\cdot4}$	$R_{1\cdot5}$	R_0	$R_{1\cdot4}$	$R_{1\cdot5}$
0·5	1·0	1·0	1·0	1·0	1·0	1·0	1·0	1·0	1·0
1·0	·96	·93	·94	·98	·94	·95	·96	·94	·95
1·5	·89	·89	·88	·96	·90	·90	·92	·90	·90
2·5	·73	·71	·73	·59	·73	·76	·76	·74	·76
4·5	·43	·44	·44	·51	·47	·49	·49	·48	·50
7·5	·17	·17	·17	·22	·21	·21	·21	·21	·21
10·5	·064	·060	·053	·047	·080	·075	·086	·084	·077
13·5	·018	·018	·013	·0092	·027	·023	·032	·029	·023
17·5	·0033	·0030	·0017	—	·0055	·0037	·011	·0060	·0037

	Run 60			Run 65			Run 67		
ht(m)	R_0	$R_{1\cdot4}$	$R_{1\cdot5}$	R_0	$R_{1\cdot4}$	$R_{1\cdot5}$	R_0	$R_{1\cdot4}$	$R_{1\cdot5}$
0·5	1·0	1·0	1·0	1·0	1·0	1·0	1·0	1·0	1·0
1·0	·98	·93	·94	·96	·92	·93	·90	·92	·93
1·5	·94	·88	·87	·88	·87	·85	·84	·86	·85
2·5	·76	·67	·71	·73	·67	·68	·65	·66	·68
4·5	·45	·41	·42	·39	·38	·38	·38	·36	·37
7·5	·16	·15	·15	·12	·13	·12	·12	·12	·11
10·5	·039	·048	·042	·029	·036	·028	·024	·031	·027
13·5	·0095	·013	·0096	·0056	·0088	·0053	·0028	·0069	·0050
17·5	·000099	·0019	·0010	—	·0011	·00041	·00018	·00075	·00041

Run 68

ht(m)	R_0	$R_{1\cdot4}$	$R_{1\cdot5}$
0·5	1·0	1·0	1·0
1·0	·91	·86	·89
1·5	·78	·76	·75
2·5	·55	·47	·50
4·5	·20	·16	·17
7·5	·020	·022	·021
10·5	·00061	·0020	·0015
13·5	·000055	·00014	·000075
17·5	—	—	—

Int. J. Air and Water Poll. Pergamon Press 1961. Vol. 4, Nos. 1/2, pp. 47–51. Printed in Great Britain.

SOME OBSERVATIONS ON SMOKE PLUMES

G. T. CSANADY
University of New South Wales
(*Received* 13 *June* 1960)

Abstract—The plume at Tallawarra power station was photographed many times to obtain the mean position. The observations were plotted in terms of appropriate nondimensional variables and compared with the observations of BOSANQUET *et al.*, as well as the theoretical results of PRIESTLEY and SUTTON. Within about 1500 ft. from the source good agreement with theory was found. The asymptotic plume height was found to be given crudely by the formula:

$$z_a = 250 \frac{F}{U^3}$$

where U is wind speed, F " flux of buoyancy ", a variable proportional to heat flux.

METHOD OF OBSERVATIONS

THE smoke plume of Tallawarra power station was photographed a number of times, the negatives projected on a screen and the mean plume path traced. Superimposing several photographs taken under identical conditions a " time-mean path " was found. The minimum number of photos used to obtain one curve was 3, the maximum 31. The length scale of the photographs was obtained from the 288 ft. tall chimney stack of the station, which appeared in all exposures.

VOL. 4 1961

Wind velocities were measured by noting the time taken by a given configuration in the plume to travel a known distance. This was done several times on each occasion, using a stopwatch, the distance timed being of the same order of magnitude as the maximum distance at which the plume was observed. If there was variation of wind with height, the figures represent mean values. Other atmospheric variables were not measured, but all observations were carried out on clear spring days in moderately strong wind. Most plumes were photographed over substantially the same piece of flat terrain which could be observed from a conveniently situated range of hills. One plume (curve *d* in Fig. 2) was travelling in a roughly 180° opposite direction, where the terrain dropped somewhat just past the power station.

Tallawarra is a base-load station and during the observations carried an approximately constant load of 130 MW. Operational data of interest were:

gas flow 3950 ft³/sec
gas temperature 290° F
gas flow reduced to NTP 2765 ft³/sec
gas velocity in chimney 12 ft/sec

The station is situated in a rural area, on the shores of the Tallawarra lake.

DIMENSIONAL ANALYSIS

Let vertical distances, z, be measured from chimney top, horizontal distances along wind, x, from the chimney centre. The mean path of the plume is then a function $z(x)$ and it may be assumed to depend on (SCORER, 1959; BATCHELOR, 1954):

(i) Wind speed, U;
(ii) Gas velocity in chimney, w;
(iii) Chimney radius, R;
(iv) Buoyant acceleration at chimney:

$$b = g\frac{\rho_a - \rho}{\rho}$$

where ρ = density of effluent,
ρ_a = density of atm. air.

(v) Atmospheric variables, such as scale and intensity of turbulence and temperature gradient. As no data were recorded, these will be assumed to have been constant, i.e. they will be left out of the analysis.

The effect of the ground on plume rise will be neglected, which means that chimney height will not be regarded a significant parameter. This assumption is justified as long as plume diameter is small compared with height above ground. This was approximately true in the observations reported herein, except those concerning asymptotic height.

Using the buoyant acceleration b, we first define " flux of buoyancy " F, proportional to the total heat flux, which, at large distances, is the only " source variable " of importance:

$$F = wR^2b$$

and then a characteristic length l:

$$l = \frac{F}{U^3}.$$

This is the better choice for a length-scale: the alternative, the chimney radius, cannot have an influence on plume path at large distances. With the aid of this length-scale the distance variables may be made nondimensional: z/l; x/l; R/l. An appropriate variable containing efflux velocity is the " Froude-number ":

$$\frac{w^2}{Rb} = \frac{Rw^3}{F}.$$

The physical meaning of this combination is: ratio of inertia forces to buoyancy forces at the chimney. With these variables one may write:

$$\frac{z}{l} = f\left(\frac{x}{l};\ \frac{Rw^3}{F};\ \frac{R}{l}\right) \tag{1}$$

At large x/l one may expect that the influence of R/l and Rw^3/F becomes negligible, i.e.:

$$\frac{z}{l} = f\left(\frac{x}{l}\right) \tag{2}$$

At still larger distances the plume often turns horizontal, i.e.:

$$\frac{z}{l} = \text{const.} \tag{3}$$

It must be recalled here that atmospheric variables have been assumed constant. The asymptotic height, if any, must be strongly influenced by atmospheric conditions.

Theoretical formulae (e.g. BOSANQUET *et al.*, 1950; SUTTON, 1953; PRIESTLEY, 1956) suggest that the asymptotic height in a neutral atmosphere is infinite.

Where the asymptotic formulae, Eqns. (2) and (3) hold, the effective origin of z may have to be moved to allow for a " momentum rise ".

RESULTS

(*a*) At $x/l \leqslant 2{,}000$. Fig. 1 shows the observations at Tallawarra (dots) and also those of BOSANQUET *et al.* (1950; triangles) in a graph z/l against x/l. The values of the " Froude number " were:

	Tallawarra	BOSANQUET: (1)	(2)	(3)	(4)
Rw^3/F	11·3	11·4	19·2	134	1·11

The dots separate from the rest represent the one plume observed in the 180° opposite direction, and the peculiar shape may be attributed to the drop of the terrain. The remaining dots and the triangles representing the plants BOSANQUET (1) and (2)

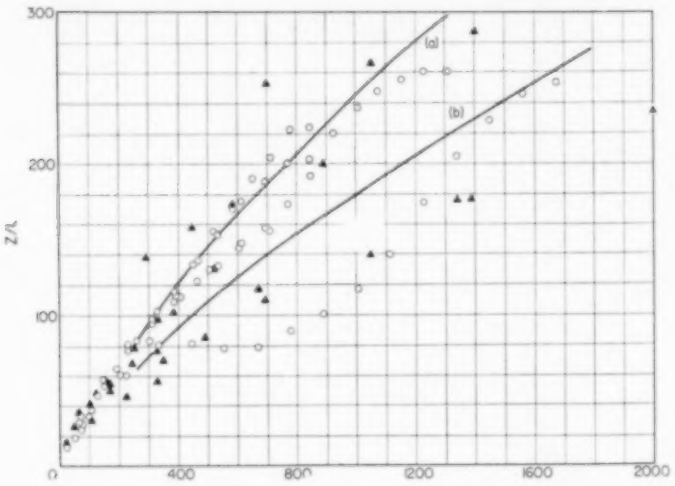

FIG. 1

group around a single curve up to about $x/l = 300$. At higher x/l only the plume BOSANQUET (3) remains with the Tallawarra plume, the BOSANQUET (1) plume being much lower. At $x/l = 1200$, for example, $z/l = 260$ for Tallawarra, 160 for BOSANQUET (1). This discrepancy must be attributed to different eddy diffusivity.

The plumes BOSANQUET (3) and (4), but particularly the former, show the effects of the Froude number, Rw^3/F. The black triangles well above the Tallawarra plume belong to the plume BOSANQUET (3); deviations on the low side represent the plant BOSANQUET (4). The excess temperature in plant BOSANQUET (3) was only 25° C and the relevance of the length-scale l must in this case be doubted. That plume is dominated by initial momentum and the readings do not fit well into the scheme of (Fig. 1).

VOL. 4 1961

(*b*) At large x/l. The limits of the photographic observations were set by the plume becoming too diffuse to be located accurately on the film. This, however, did not seem to be an entirely gradual process; much rather a certain instability seemed to set in at some distance from the source, leading to a relatively rapid break-up of the plume into separate smaller parcels of smoke.

As far as one could tell by crude visual observation (which however, extended to many miles downwind distance on some occasions) the plume reached an asymptotic height soon after break-up and turned horizontal at levels where an inversion " lid " could not be suspected. An order of magnitude estimate of the asymptotic height reached, in function of wind speed is:

Wind speed, ft/sec	20	26	48
Asymptotic height ft	450	250	50

Applying Eqn. (3) to the asymptotic height one may write:

$$z_a = 250 \frac{F}{U^3}. \tag{4}$$

For the three wind speeds quoted above this gives asymptotic heights of 500, 230 and 37 feet respectively, in reasonable agreement with observation.

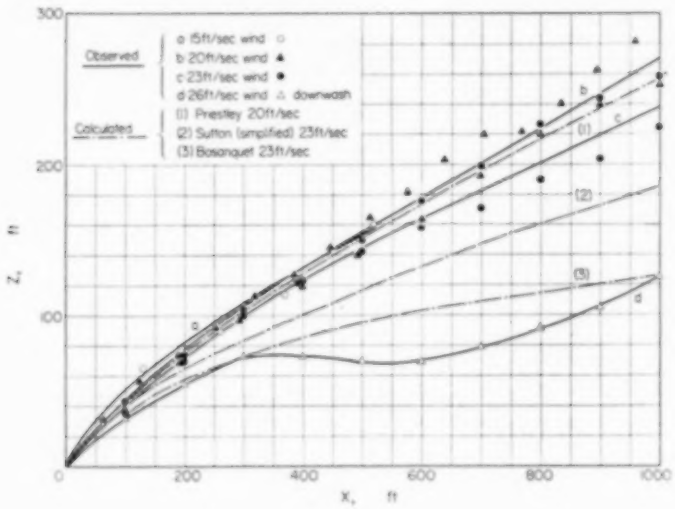

FIG. 2

(*c*) Comparison with theory. The observed results are in Fig. 2 compared with the predictions of three different theoretical formulae, due to PRIESTLEY (1956), SUTTON (1953; simplified formula see CSANADY (1956) and BOSANQUET *et al.* (1950) respectively. In the case of PRIESTLEY's theory only the " first phase theory " has been used, because his " second phase " theory did not yield realistic results. The asymptotic form of PRIESTLEY's formula may be expressed as:

$$\frac{z}{l} = \frac{1{\cdot}38}{\sqrt{c}} \left(\frac{x}{l}\right)^{\frac{1}{3}} \tag{5}$$

where c is an atmospheric turbulence constant, of order unity.

In Fig. 1 the full curves shown are according to PRIESTLEY's theory, with $c = 1{\cdot}0$ and $1{\cdot}87$ respectively. In Fig. 2 $c = 1{\cdot}1$ has been used. It is clear that this theory is qualitatively correct and that the constant c is a useful device for taking into account atmospheric influences.

The simplified Sutton theory may be expressed as:

$$\frac{z}{l} = K\left(\frac{x}{l}\right)^{\frac{2}{3}} \tag{6}$$

where the constant K has the value of $1{\cdot}7$ when fitted to the observations of BOSANQUET *et al.*

Again this theory is qualitatively correct, but in order to fit the Tallawarra observations the constant K has to be assigned the value $2{\cdot}2$.

The Bosanquet formula is asymptotically equal to

$$\frac{z}{l} = \text{const.}' \log \frac{x}{l} \tag{7}$$

This formula fits the observations less well, particularly at larger distances.

It is to be noted that all theoretical formulae are only valid in a neutral atmosphere and that they all predict an infinitely rising plume. It is certain, however, that with the " break-up " of the plume a new flow-regime sets in and the above formulae cease to hold. PRIESTLEY (1956) has recognized this and proposed his " second phase " theory. The practical application of this theory is defeated by the lack of a rational estimate for the transition point.

Acknowledgment—The courtesy of the Electricity Commission of N.S.W. in placing the operational data at the author's disposal is gratefully acknowledged.

VOL. 4 1961

REFERENCES

BATCHELOR G. K. (1954) *Quart. J. Roy. Meteor. Soc.* **80,** 339.
BOSANQUET C. H., CAREY W. F. and HALTON E. M. (1950) *Proc. I Mech. E.* **162,** 355.
CSANADY G. T. (1956) *Aust. J. Appl. Sci.* **7,** 23.
PRIESTLEY C. H. B. (1956) *Quart. J. Roy. Meteor. Soc.* **82,** 165.
SCORER R. S. (1959) The behaviour of chimney plumes. *Int. J. Air Poll.* **1,** 198.
SUTTON O. G. (1953) *Micrometeorology*, McGraw Hill, New York.

Int. J. Air and Water Poll. Pergamon Press 1961. Vol. 4, Nos. 1/2, pp. 52–54. Printed in Great Britain.

NOTE ON THE EFFECT OF THE WEEKLY CYCLE OF AIR POLLUTION ON SOLAR RADIATION AT TORONTO*

C. L. MATEER
Meteorological Service of Canada, Toronto
(*Received* 9 *March*, 1960)

Abstract—Over 20 years of solar radiation measurements at Toronto are analysed to detect any possible difference between average Sunday and average weekday radiation and thereby estimate the magnitude of the weekly cycle of air pollution. Sundays are found to average higher by nearly 3 per cent, and a χ^2 test indicates significance at the 99·5 per cent level. There is also some evidence for a decrease in the difference in recent years.

THE effects of air pollution on radiation in the atmosphere have been discussed recently by SHEPPARD (1958). Solar radiation measurements may be used as a crude index of air pollution by comparing measurements taken at adjacent polluted and unpolluted places and or by comparing variations at one place from time to time (Leicester Survey, 1945). HAND (1949) and CHURCH (1952) have presented clear evidence of the pollution effect using the former technique. The latter type of study, however, requires a rather lengthy series (10–20 years) of measurements so that the random effect of day to day weather changes may be removed.

Fairly continuous measurements of total solar and sky radiation have been made at the Meteorological Office, Toronto, since October 20, 1937, with an Eppley 180° pyrheliometer (sensing surface horizontal and exposed to the entire sky hemisphere). The metropolitan area of Toronto stretches for some 20 miles along the north shore of Lake Ontario, reaching about 10 miles inland at some points. The lake is 245 feet above sea level and the terrain rises irregularly to the north, attaining an elevation of about 560 feet within 5 miles of the shore. The main railway yards and a good deal of industry are located just north of the lake shore. The area of rising terrain adjacent to the lake provides a natural location for inversions and the accumulation of air pollutants. The Meteorological Office is located very near the east–west centre of the city and 2 miles north of the lake at an elevation of 379 feet. Although very centrally located, it is not immediately adjacent to any pronounced source of industrial pollution.

In order to detect the existence of a weekly cycle of industrial pollution at this site, one may compare the radiation on Sundays with that on weekdays. Throughout the period of record, the average radiation on Sundays was 313·8 langleys (1 langley = 1 gm cal/cm²) and on weekdays was 305·2 langleys, a difference of 8·6 langleys, or 2·8 per cent. As a test of significance, the average Sunday and the average weekday radiation were computed for each month of each year of record. For the 262 months of record, the Sunday radiation was greater than the weekday in 154 cases. Computing χ^2, we get:

$$\chi^2 = \frac{(154-131)}{131} + \frac{(108-131)}{131} = 8{\cdot}08.$$

* Published with the permission of the Director, Meteorological Service of Canada.

Thus, with no difference between Sundays and weekdays, the chance of getting a χ^2 as great as 8·08 is less than 0·5 per cent. We would, therefore, reject the null hypothesis and conclude that there is a real difference in radiation between Sundays and weekdays, although the magnitude is rather small.

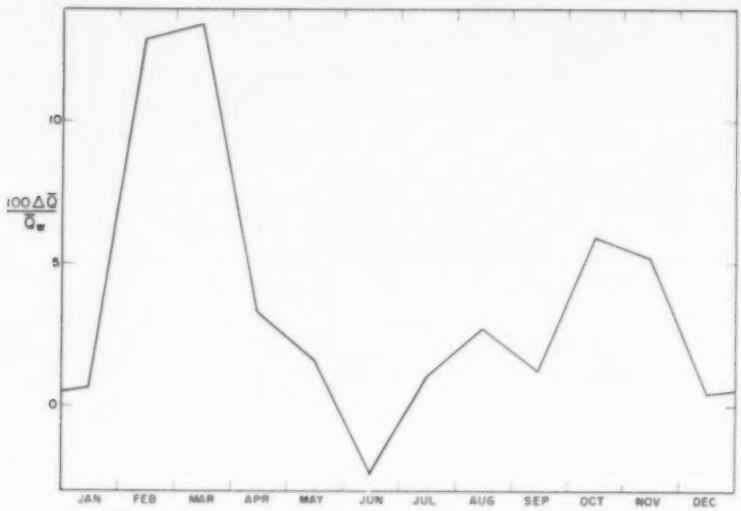

FIG. 1. Average increase in solar radiation on Sundays ($\Delta\bar{Q}$) as percentage of average weekday radiation ($\bar{Q}_w$) for each month of the year.

VOL. 4 1961

Fig. 1 shows the increase in radiation on Sundays ($\Delta\bar{Q}$) as a percentage of the average weekday radiation ($\bar{Q}_w$) during each month of the year. For the heating season (October–April, inclusive), the increase averages 6·0 per cent, and only 0·8 per cent during the remainder of the year. In an attempt to detect any possible change with

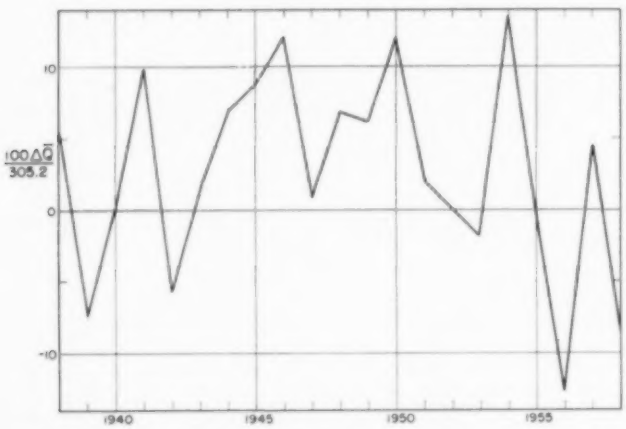

FIG. 2. Average increase in solar radiation on Sundays ($\Delta\bar{Q}$) as a percentage of the annual average weekday radiation (305·2) for each complete year of record.

time, the difference between average Sunday and average weekday radiation was calculated for each complete year of record (1938–58, inclusive). Results are plotted in Fig. 2 which shows the Sunday increase as a percentage of the annual average weekday radiation (305·2). The linear regression coefficient was calculated to be −0·47 langleys/day/year. Thus the difference between Sunday and weekday radiation appears to be decreasing slowly.

In considering changes with time, it may be more instructive to divide Fig. 2 into three periods. The first period, from the beginning of record up to about 1945, suggests a gradual increase with time of the amplitude of the weekly pollution cycle. This might be associated with a gradual increase in industrial activity through the war years. The second period, from 1945–46 through to about 1954 is one of little change in amplitude and may be associated with the gradual introduction of the 5-day week, starting about 1945–46, so that Saturday has become an off-day for industrial pollution and the heating of office buildings. Since Saturday is included in the week-day averages, any increase in Saturday radiation will result in an apparent decrease in the amplitude of the weekly cycle. The third period, from 1954 to the present appears to be one of decreasing amplitude (1959 value, not plotted in Fig. 2, is +12·6 per cent). This may be associated with the gradual changeover from coal-steam to diesel locomotives in the railway yards, which started in 1954 and was completed in late 1959.

Acknowledgment—The author wishes to acknowledge many helpful discussions with Mr. R. E. MUNN, Air Pollution Meteorologist, Meteorological Service of Canada, who suggested the investigation, and the considerable clerical assistance of Miss R. INOUYE and Mr. J. LORTIE.

REFERENCES

ANON. (1945) *Atmospheric pollution in Leicester—a scientific survey*. Tech. Paper No. 1, Department of Scientific and Industrial Research, 161 pp.

CHURCH P. E. (1952) Some new developments in micrometeorological studies of the atmosphere. *Proceedings of the Second National Air Pollution Symposium*, Pasadena, 5–6 May, 47–53.

HAND I. F. (1949) Atmospheric contamination over Boston. *Bull. Amer. Met. Soc.* 7, 252–254.

SHEPPARD P. A. (1958) The effect of pollution on radiation in the atmosphere. *Int. J. Air Poll.*, 1, 31–43.

Int. J. Air and Water Poll. Pergamon Press 1961. Vol. 4, Nos. 1/2 pp. 55–69. Printed in Great Britain.

THE GAS PHASE REACTIONS OF NITROGEN OXIDES WITH OLEFINS*

AUBREY P. ALTSHULLER and ISRAEL COHEN
Air Pollution Engineering Research,
Robert A. Taft Sanitary Engineering Center,
Public Health Service
U.S. Department of Health, Education, and Welfare,
Cincinnati 26, Ohio
(*Received* 9 *November* 1959)

Abstract—The nature of the condensation products formed in the gas phase reactions of nitrogen dioxide and nitric oxide with pentene-1, 2-methylbutene-2, and 2-methylbutadiene-1,3 was investigated. The reactants were combined at partial pressures in the range of 0·1 to 2·5 mm with the total pressure at one atmosphere. The products were determined by infrared and ultraviolet spectroscopy and colorimetry.

The condensates included primary and secondary nitro compounds and alkyl nitrates. Strong hydroxyl and single bond carbon to oxygen stretching vibrations indicate the presence of either nitroalcohols or simple aliphatic alcohols formed through oxidation reactions. Carbonyl stretching frequencies observable in some of the reactions support the conclusion that a portion of the reactants disappear by oxidation rather than by nitration processes. The available results do not indicate the presence of appreciable amounts of *tert.*-nitrocompounds, conjugated nitro-olefins, or *gem*-dinitroalkanes. The reactivities of the olefins with the nitrogen oxides are in the decreasing order: 2-methylbutadiene-1,3, 2-methylbutene-2, pentene-1.

VOL.
4
1961

INTRODUCTION

ALTHOUGH a considerable amount of work has been done on the liquid phase reactions of nitrogen oxides and olefins (RIEBSOMER, 1945; GRAY and YOFFE, 1955; BROWN, 1957) relatively little consideration has been given to the corresponding gas phase reactions (GRAY and YOFFE, 1955; COTTRELL and GRAHAM, 1953, 1954; BROWN, 1957). There appears to be little information on these reactions at low partial pressures of reactants in the gas phase. The dark reactions of nitrogen oxides and olefins at low concentrations may be of considerable importance in both high temperature combustion processes and atmospheric reactions. Furthermore, the reactions which may occur in automobile exhaust mixtures containing nitrogen oxides and olefins can present serious analytical problems (HURN *et al.*, 1958a) if grab or adsorption samples are allowed to stand prior to analysis.

Some preliminary measurements were made on the products of the reactions between nitric oxide and various olefins. Most of the work was concerned with the reaction of nitrogen dioxide with 2-methylbutadiene-1,3, 2-methylbutene-2, and pentene-1 at room temperature. Owing to the small amount of products formed, isolation was not practical. Even when fractionation and liquid chromatography over alumina were possible, decomposition and explosion resulted (BROWN, 1957). Instead, the products were identified by use of infrared spectroscopy, colorimetry, ultraviolet spectroscopy, and gas phase chromatography applied to the entire reaction mixture.

* Presented at the 134th Annual Meeting of the American Chemical Society, Chicago, Illinois, September 1958.

The major difference between liquid phase nitration processes and gas phase reactions at high concentrations is the presence of oxidation as well as nitration products (MICHAEL and CARLSON, 1940; COTTRELL and GRAHAM, 1953, 1954; BROWN, 1957). For example, carbon monoxide and carbon dioxide are major products in the gas reaction of nitrogen dioxide with ethylene (COTTRELL and GRAHAM, 1953). The formation of carbon dioxide and of various carbonyl-type products also has been reported in the reactions of nitric oxide and nitrogen dioxide with isobutylene (MICHAEL and CARLSON, 1940; BROWN, 1957).

In the present study it was found that a film of condensate was usually formed on the surface of the reaction flasks during the course of the reactions. These condensates were washed out with the appropriate solvents and analyzed.

EXPERIMENTAL PROCEDURE

The nitric oxide and nitrogen dioxide were obtained from Matheson cylinders. The nitric oxide had 2%–3% nitrogen dioxide impurity and a few tenths per cent of nitrous oxide. Similarly the nitrogen dioxide had a small amount of nitric oxide (which oxidized partly to nitrogen dioxide in the reactions, using air as a diluent) and a trace of nitrous oxide. The olefins used were Phillips Petroleum " pure grade " 2-methylbutadiene-1,3, 2-methylbutene-2, and pentene-1, all of 99+ mole per cent purity.

Concentrations of olefins between 0·1 and 0·5 p.p.m. were obtained by use of a diffusion cell apparatus operation at room temperature. The olefin was diluted in various experiments either with prepurified nitrogen or with air and was mixed dynamically with the nitric oxide in a Venturi-type mixing chamber. The mixture was passed into a 5-liter glass reaction vessel which was flushed with the reaction mixture. The stop-cocks were then closed (no grease or a minimum amount of silicone grease was used) and the mixture was allowed to remain in the flask 15 minutes to several days. The condensates were found to be soluble in acetonitrile and acetone, somewhat soluble in carbon tetrachloride and hydrocarbons, and slightly soluble in carbon disulfide. The condensation products were therefore washed out with carbon tetrachloride, cyclohexane, or acetone. It was discovered, after several runs, that acetone was reacting with the condensate. Therefore acetonitrile was substituted for acetone in subsequent work.

Infrared measurements of the liquids were made using 0·1-mm thickness cells with sodium chloride windows. These windows were slowly attacked, probably by a small amount of dissolved dinitrogen tetroxide and by water in the condensate. Repolishing of cell windows was necessary periodically. After almost all the work reported here was completed, barium fluoride windows were received. Barium fluoride is considerably more resistant to nitrogen oxides and water and the deposits can be washed off with water (ALTSHULLER and COHEN, 1959).

Infrared measurement on the gas phase products was made by evacuating a Perkin-Elmer ten-meter optical path-length gas cell and introducing successively the gas phase of the contents of three 5-liter reaction flasks. All infrared determinations were made with a Beckman IR-4 Spectrophotometer.

Colorimetric determinations for primary and secondary nitroparaffins were made by a number of procedures (SCOTT and TREON, 1940; JONES and RIDDICK, 1952;

TURBA, *et al.*, 1959; Altshuller and Cohen, 1960.) The spectra were run on a Cary Model 11 Spectrophotometer.

The condensate was taken up in several solvents and the mixture injected into a Perkin-Elmer gas chromatograph for analysis. Owing to the high boiling nature of some of the oily condensate, it was difficult to be sure that the chromatograms were completely representative of the condensate.

RESULTS

Most of the measurements were made of the infrared spectra of the condensation products. The infrared absorption bands observed and their approximate relative intensities for the nitrogen dioxide reactions with 2-methylbutadiene-1,3, 2-methylbutene-2, and pentene-1 are given in Tables 1, 3, and 5.

The absorption bands listed are with one exception believed to arise from the infrared absorption of the reaction products. The strongest nitrogen dioxide band at 6·2 microns was not observed, but a band was observed repeatedly at 5·75 microns which can be assigned to the absorption in carbonyl type compounds. However, dinitrogen tetroxide also has its strongest band at 5·7 microns and, in the liquid state or in solution, dinitrogen tetroxide should be the predominant species. It is felt that a portion of the absorption at 5·75 microns may be caused at times by dinitrogen tetroxide being carried down or adsorbed by the condensate, but that the dinitrogen tetroxide is present in very small amounts in the condensate. The very gradual attack on the sodium chloride windows with the occurrence of a nitrate band at 7·3 microns supports this assumption.

2-Methylbutadiene-1,3-Nitrogen Dioxide Reaction. The spectra of the condensate from the nitrogen dioxide reaction with 2-methylbutadiene-1,3 are characterized by absorption bands at 6·08, 7·80, 11·7–11·8, and 14·2 microns (Table I). All of these bands are absorption frequencies of alkyl nitrates. The 13·3-micron band of alkyl nitrates is covered by solvent bands of carbon tetrachloride and acetonitrile. It is not possible to distinguish between simple alkyl nitrates and nitronitrates on the basis of these data. However, it has been shown that certain types of nitronitrates exhibit bands at both 7·70 and 7·90 microns rather than at 7·80 microns (BROWN, 1955). The absence of the 7·70–7·90-micron band splitting does exclude a 1-nitro-2-methylbutyl nitrate type of compound.

The presence of nitro groups is clearly shown by the appearance of bands at 6·40 and 7·28 microns in the condensate. Conjugated nitro-olefins are excluded by the absence of bands at 6·5–6·6 and 7·4–7·5 microns (BROWN, 1955). Similarly, dinitroalkanes with the two nitro groups on the same carbon atom are excluded by the absence of bands in the 6·30- to 6·35- and 7·5-micron regions. Tertiary nitro compounds have an asymmetrical NO_2 stretching vibration at 6·50 microns (BROWN, 1955, KORNBLUM, *et al.*, 1958); consequently, the absence of this band in the condensate spectra also excludes tertiary nitro compounds as detectable products. The presence of an appreciable amount of product having nitro groups attached to internal carbon atoms in either tertiary or secondary type positions is doubtful, in view of the absence of the multiple absorption bands in the 7·0- to 7·5-micron region. Splitting into two to four bands is characteristic of structures in which alkyl and nitro groups are attached to the same carbon atom. Further evidence for the predominance of primary nitro compounds is substantiated by the presence of the absorption band at 6·9–7·0 microns resulting from methylene bending vibrations in primary nitro compounds. Unconjugated primary nitro-olefins such as 1-nitro-2-methyl-2-butene could also be present.

Alkyl nitrites are usually found in liquid phase reactions of nitrogen oxides with olefins, often as nitro alkyl nitrites (MICHAEL and CARLSON, 1940; LEVY and SCAIFE, 1946; BALDOCK, *et al.*, 1949). In gas phase reactions in which oxidation processes also occur, the presence of nitrite groups on product molecules is less likely. The infrared spectra showed no indication of the 6·05- and 6·20-micron bands of primary and secondary alkyl nitrites (HASZELDINE and MATTINSON, 1955), nor were the strong bands at 12·7 and 12·9 microns found in the infrared spectra of primary and secondary butyl nitrites observable (TARTE, 1951). Tertiary alkyl nitrites have a very weak N-O stretching band at 6·20 microns owing to the small proportion of the cis-form of the molecule. However, in a small number of spectra run in cyclohexane, there was no indication of the combination of a strong band at 12·4 microns and of a very strong absorption band at 13·2 microns, which has been reported in the

VOL. 4 1961

literature for the *tert.*-butyl nitrite molecule (TARTE, 1951). It is believed that very little if any of the product is in the form of alkyl nitrites.

The infrared spectra of the condensate from the nitrogen dioxide-2-methylbutadiene-1,3 reaction also show a band near 2·8 microns, which corresponds to an O-H stretching vibration in water, alcohol, or ketoxime. Most of the absorption at 2·8 microns certainly arises from water. The 2·8 micron band is present only in spectra run with acetonitrile as solvent. Alcohols and many simple nitro alcohols are about as soluble in carbon tetrachloride as in acetonitrile, but water, while very soluble in acetonitrile, is only slightly soluble in carbon tetrachloride. Also the weaker 1·83-micron water band is observed when the 2·8-micron band is very intense, owing to a large amount of water in the condensate in these runs. Finally, the absorption band in the 6·1-micron region is uniformly more intense, broader, and shifted 0·02 to 0·05 microns compared to the band in carbon tetrachloride. Some indication of two bands is occasionally observed. Their appearance results from the superposition of the water band at 6·1 microns on the NO_2 asymmetrical stretching band of alkyl nitrates at 6·06 microns. The bands at 8·3, 8·6, and 9·0 microns are most readily associated with C-O stretching or CO-H bending vibrations, although the $C(CH_3)_2$ rocking vibration does occur near 8·6 microns. It seems reasonable to assume that the absorptions at 8·6 and 9·0 microns should be associated in part with the C-O stretching or CO-H bending vibration in a secondary or tertiary alcohol or nitroalcohol whose O-H stretching vibration occurs at 2·8 microns. However, the absorption at 8·3 and 9·0 microns could possibly be associated also with formic acid, and those at 8·3 and 8·6 microns with pyruvic acid. These two substances are organic end oxidation products of 2-methylbutadiene-1,3. Pyruvic acid has a strong absorption peak near 7·4–7·5 microns, which does not appear in the condensate spectra. The gas phase spectra show no indication of these oxidation products.

The band at 5·75 microns is believed to result largely from a carbonyl stretching vibration in a saturated aldehyde, ketone, or acid. The weak band at 5·9 microns lies in the carbonyl stretching region of unsaturated aldehydes, acids, or ketones. Such a compound could result from the oxidation of one of the two double bonds of the 2-methylbutadiene-1,3 molecule. The three most likely compounds which could be formed, depending on which double bond is attacked and to what extent, are methyl acrylic acid, methyl acrolein, and methyl vinyl ketone. The remaining absorption band as yet undiscussed is the one at 10·3–10·6 microns. This band lies in a region in which not too many compounds absorb. A possible assignment is to a ketoxime, $R_2C{=}NOH$. Ketoximes have a strong sharp O-H stretching band at 2·8 microns and a strong N-O stretching vibration in the 10·3 to 10·8 micron region (BROWN, 1955). This class of compounds has been reported to be formed in the liquid phase reaction between nitric oxide and isobutylene (BROWN, 1957).

Gas chromatographic results. A number of gas chromatograms were run on the condensate from the 2-methylbutadiene-1,3-nitrogen dioxide reaction using a silicone grease on firebrick column at 110° C and 210° C. For the condensate-sample runs carbon tetrachloride, acetone, and acetonitrile were used as solvents. As many as five peaks were found in addition to the solvent peak. One of the peaks preceding the solvent appears to be 2-methylbutadiene-1,3. The gas chromatographic method would be considerably more sensitive than the infrared method in detecting small amounts of 2-methylbutadiene-1,3. One other peak preceding the solvent may have been nitrogen dioxide although this gas tends to be difficult to desorb. However, the three remaining peaks, including one on the shoulder of the acetone and carbon tetrachloride peaks and one which was retained 5 to 10 times as long as the solvents, are assignable to reaction products. The 30- to 60-minute retention time falls between that found for 1-nitropentane and 1-nitrohexane. Nitroethane and the nitropropanes were retained about the same time as the peak observed on the shoulder of the solvent peak.

2-*Methylbutadiene*-1,3-*Nitric Oxide Reaction.* The infrared spectra of a number of condensates from the 2-methylbutadiene-1,3-nitric oxide reaction were run using carbon tetrachloride, carbon disulfide, and ethylene tetrachloride (Table 2). The absorption spectra of the condensates show the same type of nitration products, nitroalkanes, and alkyl nitrates as those found in the condensates from the 2-methylbutadiene-1,3-nitrogen dioxide reaction. The band at 8·2–8·3 microns may be associated with a C-O vibration. A weak band appears around 10·6 microns which again can be associated with a ketoxime.

2-*Methylbutene*-2-*Nitrogen Dioxide Reaction.* The infrared spectra of the condensate from the nitrogen dioxide-2-methylbutene-2 reaction (Table 3) show many of the general features of the condensate spectra from the nitrogen dioxide-2-methylbutadiene-1,3 reaction. Thus, bands at 6·08, 7·8, 11·7–11·8, and 14·2 microns all indicate the presence of alkyl nitrate. The formation of products

containing nitro groups is shown by the presence of bands at 6·40 and 7·28 microns. Similarly, the band at 2·8 microns and those at 8·85 and 9·30 microns indicate the presence of branched chain alcohols (or nitroalcohols) as products.

Although the infrared spectra clearly show the presence of nitroalkanes, there is only a weak indication of the secondary and tertiary nitroalkanes expected from the nitration of a molecule with the double bond in an internal position. Consequently, several colorimetric procedures were used to confirm the presence of primary and secondary nitroalkanes (Table 4). The less sensitive tests gave negative results, but the more sensitive procedures capable of detecting 10–100 μg/ml gave fairly good positive tests for both primary and secondary nitroalkanes.

One very interesting feature of the spectra is the appearance of a medium to strong band at 7·70 microns, which is always somewhat less intense than the adjacent band at 7·80 microns. The 7·80-micron band is the NO_2 asymmetrical stretching vibration of an alkyl nitrate. With nitro-alkyl nitrates such as 1-nitro-2-methyl-2-propyl nitrate, the NO_2 asymmetrical stretching band shifted down to 7·70 microns. However, this shift is due to band splitting, so this band is accompanied by another fairly strong one at 7·90 microns. The complete absence of the 7·90-micron band from the product spectra would seem to eliminate the assignment of the 7·70-micron band to a nitro-alkyl nitrate. Another possible and logical assignment of the 7·70-micron band is to an acetic acid dimer vibration. This is a very strong vibration of acetic acid, and acetic acid is the reasonable end product for the 2-carbon fragment in the oxidation of 2-methylbutene-2. The weak absorption bands at $8{\cdot}6 \pm 0{\cdot}1$ and $10{\cdot}45 \pm 0{\cdot}1$ micron also coincide with vibrations of the acetic acid molecule and its dimer. It is true that the 5·77-micron band in a number of the spectra is less intense than the 7·7-micron band. In acetic acid spectra, the 5·77-micron band usually is equally or more intense than that at 7·7 microns. However, no other type of compound appears at all reasonable as a product that will absorb strongly at 7·70 microns and at the other wavelengths.

The gas phase spectrum of the nitrogen dioxide-2-methylbutene-2 reaction indicated the complete or nearly complete disappearance of the olefin. Strong absorption bands of the excess nitrogen dioxide were the major feature of the spectra. However, four weak bands did appear which are not assignable to reactants. Three which appeared at 5·75, 7·3, and 8·2 microns are almost certainly due to acetone. No indication was observed of the absorption bands of isopropyl alcohol in the 8·5 to 9·0 micron region nor at 10·5 microns. None of the strong absorption bands of ethyl alcohol, acetaldehyde, or acetic acid was observed. The fourth absorption band appeared at 9·75 microns and barely gave indications of a resolvable PQR vibrational-rotational fine structure. These facts lead to the conclusion that this band is the strong C-O vibration of methyl alcohol.

VOL. 4 1961

Any traces of acetone in the condensate would be detectable only by means of the 8·2-micron absorption band since the 5·75 micron C=O band is nonspecific and the 7·3-micron band would be obscured by the symmetrical NO_2 vibrations of nitroalkanes. A weak absorption, detected at 8·25 microns, can be assigned to acetone. The other possible assignment would be to the C-O stretch in methyl formate or to formic acid, which also has a strong band at 8·2 microns as well as a slightly weaker absorption at just above 9·0 microns. Consequently, there is some evidence for acetone, formic acid or methyl formate in solution. In addition there are several bands at 7·55, 8·85, 9·3 and possibly at 10·45 microns assignable to other vibrations in alcohols. Finally, the weak band at 5·93 microns suggests the presence of a small amount of an unsaturated aldehyde or ketone. Most of the strong absorption at 2·8 microns is again attributable to water carried down with the condensate.

The absorption bands given in Table 3 are observed in condensates resulting from the reaction of 0·5 mm of 2-methylbutene-2 with 2·5 mm of nitrogen dioxide, and of 0·1 mm of 2-methylbutene-2 with 2·5 mm of nitrogen dioxide. In the gas spectra, product formation was detectable only at the 0·5 mm level of olefin.

Pentene-1-Nitrogen Dioxide Reaction. The reaction between 0·5 mm of pentene-1 and 2·5 mm of nitrogen dioxide proceeds much more slowly than the corresponding reactions of 2-methylbutadiene-1,3 and 2-methylbutene-2 with nitrogen dioxide. The infrared bands for the condensate from six 5-liter flasks are similar to but much less intense than those in the other reactions, since the contents of no more than four such flasks were required for similar measurements in the other reactions. These bands are listed in Table 5. Strongest are the band at 6·10 microns assignable to a symmetrical stretching vibration in an alkyl nitrate and the O-H stretching band at 2·77 microns. In a few condensates more than 2 per cent water was observed, assuming that essentially all of the absorption at 2·8 microns is due to water. Since no indication is observed of C-O stretching vibrations in the 8 to 9 micron

region, it is felt that in this reaction water is usually the major component of the condensate. The NO_2 stretching bands of nitroalkanes at 7·25 microns and 6·39 microns were very weak. A very weak band at 5·73 microns may be due to a trace of a carbonyl compound or of a nitrogen oxide. A weak band at 5·83 microns observed once in the strongest spectra in carbon tetrachloride probably is the result of carbonyl absorption.

Unlike the gas spectra for the nitrogen dioxide reaction with 2-methylbutadiene-1,3 and 2-methylbutene-2, strong olefin absorption bands remain after even 24 hours of reaction time. The results for two runs are compared with the pentene-1 spectra in Table 6. Very little reaction appears to occur after 15 minutes and much of the olefin is unreacted after 16 hours. The band at 5·75 microns does intensify as reaction proceeds. This absorption can be ascribed to the carbonyl absorption of butyraldehyde, formaldehyde, or both aldehydes, which are likely gas state products.

2-Methylbutene-2 and Pentene-1 with Nitric Oxide Reactions. Only a few infrared spectra were obtained of condensates from the reaction of 2-methylbutene-2 with nitric oxide and pentene-1 with nitric oxide. Only a very weak absorption was discernible in the C-H stretching region for a condensate from the 2-methylbutene-2 reaction with nitric oxide in a single 5-liter flask. In the pentene-1 reaction with nitric oxide the infrared absorption of the condensate from a single flask showed only weak or very weak bands in the C-H stretching region, in the carbonyl stretching region near 5·8 microns, and in the CH_2 bending region. No bands assignable to NO_2 or ONO_2 vibrations were detectable.

Quantitative Infrared Analysis of Reaction Products. Approximate average values and range for the weight percentages of water, total organic nitro compounds, total organic nitrates, and total saturated carbonyl compounds are listed in Table 7. These values represent the average weight percentages and weight-percentage ranges for bands in carbon tetrachloride and acetonitrile, reaction times, and reactant concentrations.

The calculations are based on an average molecular weight of 150 for the nitro compounds and organic nitrates, and on an assumed molecular weight of 75 for the carbonyl compound. The molar absorption coefficients are taken as follows: water, $\lambda = 2{\cdot}8$ microns, $\epsilon = 100$; nitro compounds, $\lambda = 7{\cdot}2$–$7{\cdot}3$ microns, $\epsilon = 150$; nitrate compounds, $\lambda = 7{\cdot}8$ microns, $\epsilon = 600$; and carbonyl compounds $\lambda = 5{\cdot}8$ microns, $\epsilon = 300$, mole^{-1} liter^{-1} cm. The molecular weights used are assumed averages which could readily be 25 or 50 per cent in error. Similarly the molecular absorption coefficients for the 7·2–7·3 micron range from about 100 to 200 mole^{-1} liter^{-1} cm (BROWN, 1955). An average absorption coefficient of 600 mole^{-1} liter^{-1} cm for the 7·8-micron band of the organic nitrates is assumed on the basis of the small amount of intensity data available (BROWN, 1955). The carbonyl intensities vary widely. Aliphatic ketones have molecular coefficients around 200, aliphatic aldehydes between 100 and 200, aliphatic acids around 600, and esters also around 600 mole^{-1} liter^{-1} cm (BELLAMY, 1954). In view of these wide variations, an average value of 300 mole^{-1} liter^{-1} cm was assumed. The molar absorption coefficients of the 1·83, 2·8, and 6·1 microns of water in acetonitrile were determined. The absorption bands obey Beer's Law between at least 0·5 and 2·0 weight per cent. The molar absorption coefficients of the water bands in acetonitrile are as follows: $\lambda = 1{\cdot}83$ microns, $\epsilon = 4{\cdot}3$ mole^{-1} liter^{-1} cm; $\lambda = 2{\cdot}8$ microns, $\epsilon = 100$ mole^{-1} liter^{-1} cm; and $\lambda = 6{\cdot}1$ microns, $\epsilon = 57$ mole^{-1} liter^{-1} cm.

Since a number of assumptions necessarily are involved in the above discussion, the numerical values listed in Table 6 should be understood as giving only a rough quantitative idea of the composition of the condensate when dissolved in carbon tetrachloride or acetonitrile. In most of the runs the solvent was reduced to between 0·25 and 0·5 ml before injection into the infrared cell. For example, in terms of product weight in 0·25 ml of solvent for one run of 2-methylbutene-2-NO_2 reaction, approximately 1·5 mg of water, 5 mg of total organic nitro compounds, 2 mg of organic nitrates and 0·8 mg of carbonyl compounds were present in the condensate in carbon tetrachloride. This weight of material represented the combined condensate from four flasks of 5-liter capacity.

DISCUSSION OF RESULTS

In the present investigation with reactant concentrations in the 0·1- to 2·5-mm range it has been found that oxidation as well as nitration occurs. The same two processes have been observed at higher concentrations in the gas phase reactions of olefins with

nitrogen oxides (MICHAEL and CARLSON, 1940; BROWN, 1957). In liquid phase reactions, nitration appears to be the only type of reaction leading to products.

In liquid phase nitration reactions, the products often include organic nitrites and nitroso compounds (MICHAEL and CARLSON, 1940; RIEBSOMER, 1945; BROWN, 1957). We also have observed the greenish-blue solutions indicating nitroso compounds and the ultraviolet spectra of alkyl nitrites when adding nitrogen dioxide to liquid olefins (ALTSHULLER, *et al.*, 1958). However, in the gas phase reaction products no positive indications are found of either alkyl nitrites or nitroso derivatives.

The oxidation products appear to be the stable ketone or acid which is the end product of the oxidation. Thus in the 2-methylbutene-2 reaction with nitrogen dioxide, acetone and acetic acid appear as oxidation products.

A very clear cut difference in reactivity exists between the 2-methylbutadiene-1,3 and 2-methylbutene-2, and the much less reactive pentene-1. This greater reactivity of diolefins and internally double bonded olefins with nitrogen oxides has been observed previously (HURN, *et al.*, 1958a). The rate of disappearance of various olefins in the presence of nitrogen dioxide and nitric oxide was observed using gas chromatography to follow the disappearance of the hydrocarbons (HURN, *et al.*, 1958a). It has also been observed that internally bonded olefins are more reactive than terminally bonded olefins, paraffinic hydrocarbons, and acetylenic hydrocarbons in the photolytic reaction with nitrogen dioxide in automobile exhaust studies (MADER and CHAMBERS, 1957) and in reactions with atomic oxygen and ozone (FORD and ENDOW, 1957; CADLE, 1956).

VOL. 4 1961

The diolefin, 2-methylbutadiene-1,3, appears to be somewhat more reactive with nitrogen dioxide and nitric oxide than the internally bonded olefin, 2-methylbutene-2, based on its incomplete disappearance at lower partial pressures, 0·1 mm of olefin and 0·5 mm of nitrogen dioxide. The 2-methylbutadiene-1,3 is completely reacted at both this lower concentration and at 0·5 mm of olefin and 2·5 mm of nitrogen dioxide. The diolefin also appears quite reactive with nitric oxide. This appreciable reactivity does not appear explainable by the presence of a few per cent of nitrogen dioxide impurity. In contrast, at all concentrations of pentene-1 and nitrogen dioxide, up to the 0·5 mm of pentene-1 and 2·5 mm of nitrogen dioxide, a large part of the pentene-1 remains even after 24 hours (Table 6). In several other runs of nitrogen dioxide with pentene-1, an even larger part of the olefin remained after reaction.

The nitration products observed in these reactions include nitro compounds and organic nitrates. Certain types of organic nitrogen compounds including conjugated nitro-olefins, *gem*-dinitroalkanes, organic nitrites, and nitroso compounds are not present in detectable quantities. It is more difficult to ascertain whether the nitro and nitrate groups are present as nitroparaffins, alkyl nitrates, nitroalcohols, nitronitrates, or dinitrocompounds with the nitro groups on adjacent carbons. Some types of nitronitrates are excluded by the absence of the 7·7- and 7·9-micron bands in the infrared. The absence of O—H stretching bands of the products in carbon tetrachloride would seem to reduce considerably the possibility of major amounts of simple nitro monoalcohols. 2-Nitro-1-butanol and 2-nitro-2-methyl propanol-1 are soluble enough in carbon tetrachloride to give strong bands in the infrared spectra. Furthermore, the O—H bands appear at 2·77 and 2·90 microns in carbon tetrachloride and at 2·86 microns in acetonitrile. (In acetonitrite the weak solvent bands in this region distort the O—H band positions of the solute.) On the other hand, the nitro-alcohols

with two and three OH groups are insoluble in carbon tetrachloride. However, the C—O stretching bands of nitroalcohols are far stronger than the O—H stretching bands, so that the weak bands in the 8–9 microns observed in the condensate from the 2-methylbutene-2 and 2-methylbutadiene reactions with nitrogen dioxide could be the strong C—O bands in the infrared spectra of pure nitroalcohols. The presence of 1,2- or 2,3-dinitro compounds cannot be proved conclusively, but these are extremely likely products and their infrared spectra are in agreement with the observed spectra of the condensates.

A number of types of carbonyl compounds are indicated by the infrared spectra. The infrared absorption bands of acetone, acetic acid, and formic acid appear in the infrared analysis of the gaseous products and condensate. Traces of aliphatic esters and possibly of ketones are present in the condensate. Very small quantities of α, p-unsaturated carbonyl compounds are also indicated by the infrared spectra of the condensate. Semiquantitative determinations gave values for the amounts of carbonyl compounds in twenty-one condensates using varying olefin and nitrogen dioxide condensations ranging from 0·0- to 0·15-weight per cent in the condensates diluted up to 0·25 to 0·5 ml with carbon tetrachloride.

A trace of methanol was indicated by the infrared spectra in the gas phase of the 2-methylbutene-2-nitrogen dioxide reaction. Traces of alcohols were probably present in the condensates from both the 2-methylbutene-2 and 2-methylbutadiene-1,3 reactions with nitrogen dioxide. Small amounts of ketoximes also were present in the condensates from both of these reactions.

CONCLUSIONS

Results of gas phase reactions of nitrogen oxides with olefins indicate the risks involved in grab sampling automobile exhaust products or other combustion effluent streams for analysis at a future time. Such products cannot be kept at room temperature for more than a few minutes before appreciable amounts of reaction products are formed. Since these reactions would not occur in the ordinary operation of automobiles or other combustion devices during which the concentrated products are rapidly diluted in the atmosphere, they give a false impression of the actual reactions. Storage of grab samples at reduced temperatures is an obvious alternative. Use of liquid nitrogen temperatures in the handling of automobile exhaust products prior to gas chromatography has been useful (HURN, 1958a). Dry-ice acetone temperature or, less probably, iced-water temperature may be a convenient compromise. The immediate removal of the nitrogen oxides is another possibility. However, this does not seem possible at present without also removing the oxygenated products of reaction.

Since the reactions discussed in this paper were performed at room temperature, they do not answer the question of the desired temperature for storage of grab samples. To gain such information further work will be necessary. Also of interest is the possible formation of some organic nitrogen reaction products in the short periods of passage, and at the elevated temperatures existing in the automobile exhaust system and in some other combustion devices. Organic nitrites and nitrates tend to decompose at 300° C to 400° C, but nitroparaffins are more resistant (POWLING and SMITH, 1957).

These as well as previous experiments point up the importance not only of internally

bonded olefins but also of diolefins in the overall automotive exhaust problem. The very reactive diolefins may be present in exhaust products in almost the same amounts as the internally bonded mono-olefins (HURN and DAVIS, 1958b). The diolefins should be carefully investigated, not only in terms of the overall automotive exhaust emission and photolysis reactions, but also of their reactions with ozone and atomic oxygen.

Acknowledgment—The authors wish to thank Mr. CLARENCE CLEMONS for running the gas chromatographic determinations.

REFERENCES

ALTSHULLER A. P., STEPHANS D. and SCHWAB C. M. (1958) Electronic absorption spectra of inorganic and organic compounds of nitrogen. I. Nitrogen dioxide-dinitrogen tetroxide in solution. *J. Phys. Chem.* **62,** 607–10.

ALTSHULLER A. P. and COHEN I. R. (1959) Window materials for use in infrared analyses involving nitrogen dioxide. *Anal. Chem.* **31,** 628–9.

ALTSHULLER A. P. and COHEN I. R. (1960) Determination of Primary Nitroparaffins by the Nitrous Acid Reaction. *Anal. Chem.* **32,** 881.

BALDOCK H., LEVY N. and SCAIFE C. W. (1949) Addition of dinitrogen tetroxide to olefins. V. Cyclohexene and the octenes. *J. Chem. Soc.*, 26–27–33.

BELLAMY L. J. (1954) The infrared Spectra of Complex Molecules. John Wiley, New York.

BROWN J. F. (1955) The infrared spectra of nitro and other oxidized nitrogen compounds. *J. Amer. Chem. Soc.* **77,** 6341–51.

BROWN J. F. (1957) The reaction of nitric oxide with isobutylene. *J. Amer. Chem. Soc.* **79,** 2480–9.

CADLE R. D. (1956) *Experimental studies of Los Angeles air and kinetics of atmospheric reactions*, Proceedings Conference on Chemical Reactions in Urban Atmospheres. ROGERS L. H. (Ed.). Report No. 15, Air Pollution Foundation.

COTTRELL T. L. and GRAHAM T. E. (1953) The kinetics of the oxidation of ethylene by nitrogen dioxide. *J. Chem. Soc.*, 556–63.

COTTRELL T. L. and GRAHAM T. E. (1954) Kinetics of oxidation of propylene by NO_2. *J. Chem. Soc.* 3644.

FORD H. W. and ENDOW N. (1957) Rate constants at low concentrations. IV. Reactions of atomic oxygen with various hydrocarbons. *J. Chem. Phys.* **27,** 1277–9.

GRAY P. and YOFFE A. D. (1955) The reactivity and structure of nitrogen dioxide. *Chem. Rev.* **55,** 1069–1154.

HASZELDINE R. N. and MATTINSON B. J. H. (1955) Spectroscopy IX. Further studies on nitrosamines and nitrites. *J. Chem. Soc.*, 4172–85.

HURN R. W., HUGHES K. J. and CHASE J. O. (1958a) *Application of gas chromatography to analysis of exhaust gas.* SAE Annual Meeting, Detroit, Michigan.

HURN R. W. and DAVID T. C. (1958b) *Gas chromatographic analyses show influence of fuel on composition of automotive engine exhaust.* API-COAR Group Session on Analytical Research, Los Angeles.

JONES L. R. and RIDDICK J. A. (1952) Colorimetric Determination of Nitroparaffins. *Anal. Chem.* **24,** 1533–6.

KORNBLUM N., UNGUADE H. E. and SMILEY R. A. (1956) The infrared absorption spectra of nitroparaffins and alkyl nitrates. *J. Org. Chem.* **21,** 377–9.

LEVY N. and SCAIFE C. W. (1946) Addition of dinitrogen tetroxide to olefins. I. General Introduction. III. Propylene. *J. Chem. Soc.*, 1093–6, 1100–4.

MADER P. P. and CHAMBER L. A. (1957) *Motor exhaust composition in relation to selected fuels.* First Technical Meeting, West Coast Section, Air Pollution Control Association, Los Angeles, California.

MICHAEL A. and CARLSON G. H. (1940) 1,2- and 1,4- Addition. IV. Nitrogen tetroxide and isobutylene. *J. Org. Chem.* **5,** 1–13.

VOL. 4 1961

TABLE 1. INFRARED ABSORPTION BANDS OBSERVED IN CONDENSATE FROM NITROGEN DIOXIDE-2-METHYLBUTADIENE-1,3

Wavelengths, microns	Relative intensities (*a*)	Type of Vibration	Possible assignments (*b*)
2·8	(s)	O—H str.	(1) Water (2) Alcohol or nitroalcohol (3) Ketoxime
3·42, 3·51	(m)	C—H str.	paraffinic chain
5·75 ± 0·05	(m to w)	C = O str. (*c*)	sat. aldehyde, acid, or ester
5·9 ± 0·05	(w)	C = O str.	unsat. aldehyde, acid, or ester
6·06 ± 0·02	(s)	NO_2 asym. str.	alkylnitrate
6·40 ± 0·02	(s)	NO_2 asym. str.	(1) primary nitroalkane (2) secondary nitroalkane
6·9	(w)	CH_2 bend	paraffinic chain
7·0	(w)	CH_3 bend	primary nitro compound
7·28 ± 0·02	(s)	NO_2 sym. str.	nitroalkane
7·80 ± 0·02	(s)	NO_2 sym. str.	alkyl nitrate
8·3	(m to w)	C—O str.	(1) ester (2) formic acid (3) pyruvic acid
8·6	(m)	C—O str. or CO—H bend $C(CH_3)_2$ rock	(1) sta. tert. alcohol (2) symmetrical secondary alcohol (3) isopropyl group (4) pyruvic acid
9·0	(m)	C—O str. or CO—H bend	(1) unsat. tert. alcohol (2) sat. secondary alcohol (3) formic acid
10·6 ± 0·1	(m)	N—O str.	ketoxime
11·7 ± 0·1	(s)	C—NO_2 str.	alkyl nitrate
13·2 ± 0·1 (*d*)	(m)	NO_2 out of plane bend	alkyl nitrate
14·2 ± 0·1	(m)	NO_2 bend	alkyl nitrate

(*a*) Approximate relative intensities: (s) strong, (m) medium, (w) weak.

(*b*) The compounds are numbered in the order of assumed decreasing probability of occurrence.

(*c*) Occasionally some dinitrogen tetroxide may be carried down with the condensate, then N-O str. at 5·75 microns will add to C = O str. from Carbonyl compounds.

(*d*) Observed only when cyclohexane is used as infrared solvent since carbon tetrachloride and acetonitrile have absorption bands in this region.

MICHAEL A. and CARLSON G. H. (1940) 1,2- and 1,4- Addition. V. Nitrogen tetroxide and tetramethylethylene. *J. Org. Chem.* **5,** 14–23.

POWLING J. and SMITH W. A. W. (1957) Flame decomposition of the propyl nitrates. *Combustion and Flame* **1,** 308–20.

RIEBSOMER J. L. (1945) The reaction of N_2O_4 with organic compounds. *Chem. Rev.* **36,** 157–233.

SCOTT E. W. and TREON J. F. (1940) Colorimetric determination of primary mononitroparaffins. *Ind. Eng. Chem.*, Anal. Ed., **12,** 189–90.

TARTE P. (1951) Spectroscopic studies of esters of nitrous acid. II. Infrared spectra of alkyl nitrites. *Bull. soc. chim. belges* **60,** 240–250.

TURBA F., HAUL R. and UHLEN G. (1949) Colorimetric determination of nitroparaffins. *Angew. Chem.* **61,** 74–5.

TABLE 2. INFRARED ABSORPTION BANDS OBSERVED IN CONDENSATE FROM NITRIC OXIDE-2-METHYLBUTADIENE-1,3 REACTION

Wavelengths, microns	Relative intensities (*a*)	Type of vibration	Possible assignments (*b*)
3·38, 3·50	(m), (w)	C—H str.	paraffinic chain
5·73 ± 0·02 (*c*)	(w)	C = O str.	sat. aldehyde, acid, or ester
6·06 ± 0·02	(s)	NO_2 asym. str.	alkyl nitrate
6·40 ± 0·02	(s)	NO_2 asym. str.	(1) primary nitroalkane (2) secondary nitroalkane
6·9	(w)	CH_2 str.	(1) paraffinic chain (2) primary nitroalkane
7·28	(m)	NO_2 sym. str.	nitroalkane
7·82 ± 0·02	(s)	NO_2 sym. str.	alkyl nitrate
8·3	(w)	C—O str.	ester
10·6	(w)	N—O str.	ketoxime
11·7 ± 0·1	(m)	O—NO_2 str.	alkyl nitrate

(*a*) Approximate relative intensities: (s) strong, (m) medium, (w) weak.

(*b*) The compounds are numbered in the order of assumed decreasing probability of occurrence.

(*c*) Occasionally some dinitrogen tetroxide may be carried down with the condensate, then N-O str. at 5·75 microns will add to C = O str. from carbonyl compounds.

VOL. 4 1961

TABLE 3. INFRARED ABSORPTION BANDS OBSERVED IN CONDENSATE FROM NITROGEN DIOXIDE-2-METHYLBUTENE-2 REACTION

Wavelengths, microns	Relative intensities (*a*)	Type of vibration	Possible assignments (*b*)
2·8	(s)	O—H str.	(1) water (2) alcohol or nitroalcohol
3·36 sh, 3·42, 3·50	(m)	C—H str.	paraffinic chain
5·77 ± 0·05 (*c*)	(m)	C = O str.	sat. aldehyde, ketone, acid, or ester
5·93 ± 0·02	(w)	C = O str.	unsat. aldehyde or ketone
6·08 ± 0·01	(s)	NO_2 asym. str.	alkyl nitrate
6·41 ± 0·02	(s)	NO_2 asym. str.	(1) primary nitroalkane (2) secondary nitroalkane
6·5 (*d*)	(w)	NO_2 asym. str.	(1) tertiary nitroalkane
6·88	(w)	CH_2 bend	paraffinic chain
6·98	(w)	CH_2 bend C—O—H str.	(1) primary nitroalkane (2) carboxylic acid dimer
7·15–7·20 (*d*)	(w)	CH_3 sym. bend	(1) *i*-propyl group, secondary nitroalkane (2) *t*-butyl group, tertiary nitroalkane
7·28 ± 0·02	(s)	NO_2 sym. str.	nitroalkane
7·33 ± 0·02	(w)	NO_2 sym. str. C—C str.	(1) secondary nitroalkane (2) acetone
7·48 ± 0·02	(w)	NO_2 sym. str. CH_2 wag.	(1) tertiary nitroalkane (2) paraffinic chain
7·55 ± 0·05	(w)	CO—H bend or CO st.	alcohol
7·70 ± 0·02	(m, s)	dimer vib.	acetic acid dimer
7·80 ± 0·02	(s)	NO_2 asym. str.	(1) alkyl nitrate
8·25 ± 0·05	(w)	C—O str.	(1) acetone (2) formic acid or methyl formate

TABLE 3 (cont.). INFRARED ABSORPTION BANDS OBSERVED IN CONDENSATE FROM NITROGEN DIOXIDE-2-METHYLBUTENE-2 REACTION

Wavelengths, microns	Relative intensities (*a*)	Type of vibration	Possible assignments (*b*)
8·6 ±0·1	(w)	C—O str. or CO—H bend	(1) acetic acid (2) sat. tert. alcohol (3) sym. secondary alcohol (4) isopropyl group
8·85±0·05	(w)	C—O str. or CO—H bend	(1) sat. tert. alcohol (2) sym. sec. alcohol
9·03±0·02	(m, w)	C—O str. or CO—H bend	(1) unsat. tert. alcohol (2) sat. sec. alcohol (3) formic acid
9·30±0·05	(w)	C—O str. or CO—H bend	unsat. sec. alcohol
10·45±0·1	(w)	O—H bend N—O str.	(1) acetic acid (2) ketoxime
11·4	(m)	C—N str.	nitro compd.
14·2	(w)	NO_2 bend	alkyl nitrate

(*a*) Approximate relative intensities: (s) strong, (m) medium, (w) weak.
(*b*) The compounds are numbered in the order of assumed decreasing probability of occurrence.
(*c*) Occasionally some dinitrogen tetroxide may be carried down with the condensate, then N—O str. at 5·75 microns will add to C=O str. from carbonyl compounds.
(*d*) Shoulder on strong peak.

TABLE 4. COLORIMETRIC TESTS FOR PRIMARY AND SECONDARY NITROALKANES ON CONDENSATE FROM NITROGEN DIOXIDE-2-METHYLBUTENE-2 REACTION

Method	Class of nitro compds. detectable	μg/ml of nitro compd. giving absorbance of 1	Test on nitrogen dioxide-2-methyl-butene-2 condensate
Ferric chloride procedure (*a*)	primary nitroalkanes	260–480	negative
nitrolic acid extracted with alkaline ether (*b*)	primary nitroalkanes	20–30	positive
resorcinol procedure (*c*)	secondary nitroalkanes	~70	positive
nitrolic acid extracted with alkaline ether (*b*) (*d*)	secondary nitroalkanes	$\sim 10^4$	negative

(*a*) SCOTT and TREON (1940).
(*b*) ALTSHULLER and COHEN (1960).
(*c*) JONES and RIDDICK (1952).
(*d*) TURBA, *et al.* (1949).

VOL. 4 1961

TABLE 5. INFRARED ABSORPTION BANDS OBSERVED IN CONDENSATE FROM NITROGEN DIOXIDE PENTENE-1 REACTION

Wavelengths, microns	Relative intensities (*a*)	Type vibration	(*b*) Possible assignments
2·8	(m)	O—H str.	(1) water (2) alcohol
5·75	(vw)	C=O str. N—O str.	(1) dinitrogen tetroxide (2) sat. aldehyde, acid, or ester
5·83	(vw)	O=O str.	sat. aldehyde, acid, or ester
6·08	(s)	NO_2 asym. str.	alkyl nitrate
6·39	(w)	NO_2 asym. str.	(1) primary nitroalkane (2) secondary nitroalkane
7·25	(vw)	NO_2 sym. str.	nitroalkane
7·79	(w)	NO_2 sym. str.	alkyl nitrate

(*a*) Approximate relative intensities: (s) strong, (m) medium, (w) weak, (vw) very weak.
(*b*) The compounds are numbered in the order of assumed decrease in probable occurrence.

TABLE 6. UNREACTED PENTENE-1 IN GAS STATE DURING REACTION OF PENTENE-1 WITH NITROGEN DIOXIDE

Concentration—mm			Infrared Peaks of Pentene		
Pentene-1	Nitrogen Dioxide	Time Minutes	10·0 microns	10·9 microns	% unreacted Pentene-1
0·5	0	—	0·27	0·65	100
0·5	2·5	15	0·23	0·58	87
0·5	2·5	960	0·13	0·33	49

TABLE 7. ESTIMATES FROM INFRARED ANALYSIS OF REACTION PRODUCT AMOUNTS

Product	Weight percent of products in carbon tetrachloride or acetonitrile		
	2-methylbutadiene-1,3-NO_2	2-methylbutene-2-NO_2	Pentene-1-NO_2
water (*a*)			
max. ave. value (*b*)	0·7	0·4	>0·9
range	0·2 to 1·7	0·2 to 1·0	0·2 to >·2
no. of runs	16	13	8
nitro group (*c*)			
average value	1·2	1·6	0·25
range	0·4 to 2·7	0·6 to 2·2	0·1 to 0·45
no. of runs	10	3	3
nitrate group (*d*)			
average value	0·5	0·5	0·06
range	0·15 to 0·7	0·12 to 0·8	0·03 to 0·12
no. of runs	10	3	3
carbonyl group (*e*)			
max. ave. value (*f*)	0·06	0·25	0·05
range	0·0 to 0·15	0·0 to 0·6	0·0 to 0·075
no. of runs	10	8	3

(*a*) Based on intensity of 2·8 micron band; (*b*) maximum values arrived at by assuming all absorption at 2·8 microns is due to water and not partially due to alcohols, nitro alcohols, or ketoximes; (*c*) based on intensity of 7·2- to 7·3-micron band; (*d*) based on intensity of 7·8-micron band; (*e*) based on 5·8-micron band; (*f*) maximum values arrived by assuming all absorption at 5·8 microns is due to carbonyl groups and not partially to dinitrogen tetroxide.

VOL. 4 1961

Int. J. Air and Water Poll. Pergamon Press 1961. Vol. 4, Nos. 1/2, pp. 70–78. Printed in Great Britain.

THE INTERACTION OF OZONE WITH PLASTIC AND METALLIC MATERIALS IN A DYNAMIC FLOW SYSTEM

A. P. ALTSHULLER and A. F. WARTBURG
Air Pollution Engineering Research,
Robert A. Taft Sanitary Engineering Center,
Public Health Service,
U.S. Department of Health, Education, and Welfare,
Cincinnati, Ohio
(*Received* 14 *July* 1960)

Abstract—The loss of ozone in the p.p.h.m. range after passing through or over various plastic and metallic substances has been investigated. The materials used include Teflon, glass, stainless steel, aluminium, polyethylene and polyvinyl tubing, Mylar film, and aluminium foil.

Unused Teflon passes ozone without loss. Glass tubing, after a short exposure to ozone, passes ozone without loss. Stainless steel tubing, aluminum tubing or foil and Mylar film must be exposed to ozone in the p.p.h.m. range for several hours before 90 per cent or more of the ozone initially present can be passed through or over these materials. More rapid conditioning to ozone can be achieved by several five to fifteen-minute exposures to about 10 p.p.m. of ozone. Polyethylene and Nalgon tubing even after many hours of exposure to ozone will pass only 75 to 80 per cent of the ozone initially present in the gas stream. Some types of polyvinyl tubing are unsatisfactory for use with ozone irrespective of the amount of exposure to ozone.

Flowrates below 1000 c^3/min. will increase losses of ozone. Except for Teflon and glass, materials should not be used in ozone analysis under any circumstances at low flowrates until they are thoroughly conditioned. Results obtained with stainless steel, aluminium and polyethylene indicate that conditioning to ozone once obtained will persist for at least two weeks.

INTRODUCTION

THE interaction of gases with the surfaces of tubing and piping, and with the walls of sampling containers and reaction chambers is of high importance to work involving trace quantities of various reactive gases. Physical and chemical adsorption and reaction can have significant, and sometimes disastrously large, effects on chemical and physical determinations of composition. BAKER and DOERR (1959), THUMAN (1958), and WILSON and BUCHBERG (1958) have made measurements on the decrease in concentration of various species with time in large static chambers and in flasks. In these investigations the gases studied included ozone, nitrogen dioxide, sulfur dioxide, carbon monoxide, hydrogen sulfide, hydrogen fluoride, hydrogen cyanide, ammonia, sulfuric acid, several aldehydes and ketones, acetic acid, methanol and several aliphatic and aromatic hydrocarbons.

For various reasons, including its high toxicity, ozone is a particularly important gaseous component in urban atmospheres and in the upper atmosphere. Data are available on the decomposition of ozone and in the 1 to 10 p.p.m. range under static conditions in large glass flasks (WILSON and BUCHBERG, 1959). Some results also have been obtained on the decomposition of ozone in a large steel chamber (THUMAN, 1958). No detailed study appears to have been published on the reactivity of ozone in the part per hundred million range with tubing materials or with added surfaces in glass flasks under dynamic flow conditions. The percentage of ozone removed from the gas

phase by contact with the surfaces of Teflon, glass, stainless steel, aluminium, polyethylene, aluminium, and two vinyl chloride-vinyl acetate copolymer tubing materials and with aluminum foil and Mylar film strips in a glass flask has been investigated. The ozone concentration was determined by use of a continuously monitoring colorimetric type ozone instrument.

EXPERIMENTAL DETAILS

The ozone was generated by an ultraviolet type ozonizer consisting of a small bulb, producing ultraviolet radiation in the appropriate wavelength range, sealed into a glass base which in turn fitted into a glass flask by means of ground glass joints. The lengths of tubing used were connected directly to the outlet of the ozonizer apparatus when the flow rates through the tubing were 1000 or 2000 ml/min. At flow rates of 200 or 500 ml/min, the ozone was pulled out of a Mylar bag which served as an ozone reservoir. The five-liter pyrex flask used in the experiments involving aluminum foil and Mylar plastic strips was connected to the ozonizer and detector by short lengths of Teflon tubing.

Large plastic bags of both Mylar and Saran were investigated as ozone reservoirs. The Saran plastic decomposed the ozone so rapidly as to be unsatisfactory as a possible reservoir material. However, the ozone concentration in a Mylar bag ($4ft^3$) was essentially unchanged over three or four hours. In one determination over a sixteen hour period the ozone concentration in the Mylar bag did decrease from 90 and 55 p.p.h.m. The use of this Mylar bag served to smooth out the short-time fluctuations in ozone concentration experienced when the ozone was obtained directly from the ozonizer.

VOL. 4 1961

The ozone detection instrument used is produced by the Mast Development Co., Inc., Davenport, Iowa. The ozone sensor is based on the oxidation-reduction reaction of the iodide ion. The current needed to satisfy the electrode reaction can be detected with a galvanometer or a recorder. The liquid reagent flows continuously by gravity through the sensor unit, in which it contacts the ozone-containing gas stream. The response time of this ozone instrument is much shorter than the response times of the continuous recording colorimetric type " oxidant " instruments because of the small liquid volume involved. Irrespective of the flow rate through the tubing under investigation, the flow rate through the ozone instrument was maintained at 200 ml/min by splitting the total gas flow appropriately.

The calibration curve for ozone concentration in p.p.h.m. was linear, corresponding very closely to scale reading on the recorder up to about 70 p.p.h.m. of ozone. Above about 70 p.p.h.m. of ozone the scale reading increased much more slowly than does the ozone concentration. For example, a scale reading of 83 corresponded to 100 p.p.h.m. of ozone. The instrument was calibrated by use of the colorimetric neutral buffered potassium iodide method (BYERS and SALTZMAN, 1958).

RESULTS

All of the data were obtained on a relative basis. Each of the tube lengths used was added on to a reference line consisting of four feet of Teflon tubing and about one foot of glass tubing. Much longer lengths of both Teflon and glass tubing were tested

and showed little or no reactivity with the ozone after little or no conditioning. Consequently, very little loss of ozone should have occurred in flowing through the reference line.

The term conditioning is used throughout this paper to include such chemical or physical changes occurring on a surface exposed to ozone as to render the surface comparatively inert to ozone. Conditioning occurs to varying extents throughout the exposure periods to ozone. However, exposure to high concentrations of ozone appears to accelerate the conditioning process appreciably.

Fourteen additional feet of 3/8 inch i.d. Teflon tubing was added to the reference line. At a flow rate of 200 ml/min the inlet ozone concentration was 16 p.p.h.m. and the outlet ozone concentration was 15 p.p.h.m. When the same length of Teflon tubing was used at an ozone flow rate of 2000 ml/min, the inlet concentration was 51 p.p.h.m. and the outlet concentration was 51 p.p.h.m. No conditioning period was therefore necessary in any ozone measurements for which Teflon tubing was used.

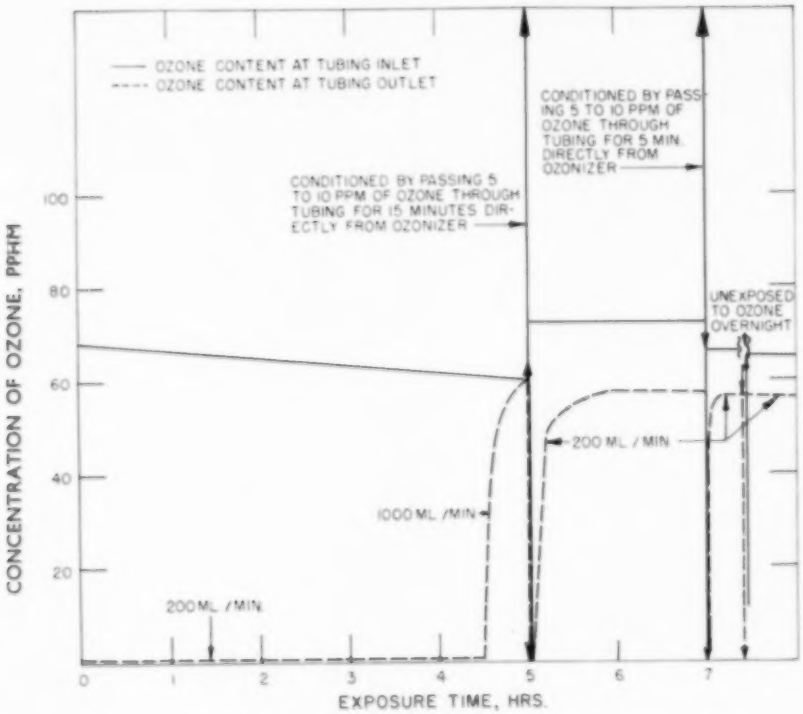

FIG. 1. Six foot length ($\frac{1}{16}$" i.d.) of 304 stainless steel exposed to ozone

A 12-foot piece of 3/8 inch i.d. glass tubing, when added to the line, took less than an hour to condition. With an inlet ozone concentration of 61 p.p.h.m., and a flow rate of 1000 ml/min, the outlet ozone concentration was 54 p.p.h.m. after 15 minutes, 58 p.p.h.m. after 30 minutes and 61 p.p.h.m. after 45 minutes. These results would indicate that glass is not quite as good a tubing material for use with ozone as is Teflon, but glass tubing certainly should be completely satisfactory at flow rates of

above one liter/min. Previous preliminary results obtained at about a one liter/min flow rate also indicated that glass tubing was about as satisfactory as teflon tubing for the passage of ozone.

A twelve-foot length of 304 type stainless steel tubing (7/16 inch i.d.) was cut into two 6 foot lengths. One of these lengths would not pass any ozone at 200 ml/min after four hours of exposure to 60 p.p.h.m. of ozone (Fig. 1). However, after 4½ hours practically all of the ozone could be recovered from the outlet of this tubing at a flow rate of 1000 ml/min. After conditioning with excess ozone, about 70 per cent of the ozone at an inlet concentration of 72 p.p.h.m. would pass through the tubing even at a flow rate of 200 ml/min. Following a second short period of conditioning by about a ten-fold excess of ozone, 85 per cent of the ozone passed through the tubing at 200 ml/min. After the tubing remained unexposed to ozone overnight, the stainless steel tubing still would pass 85 per cent of the ozone.

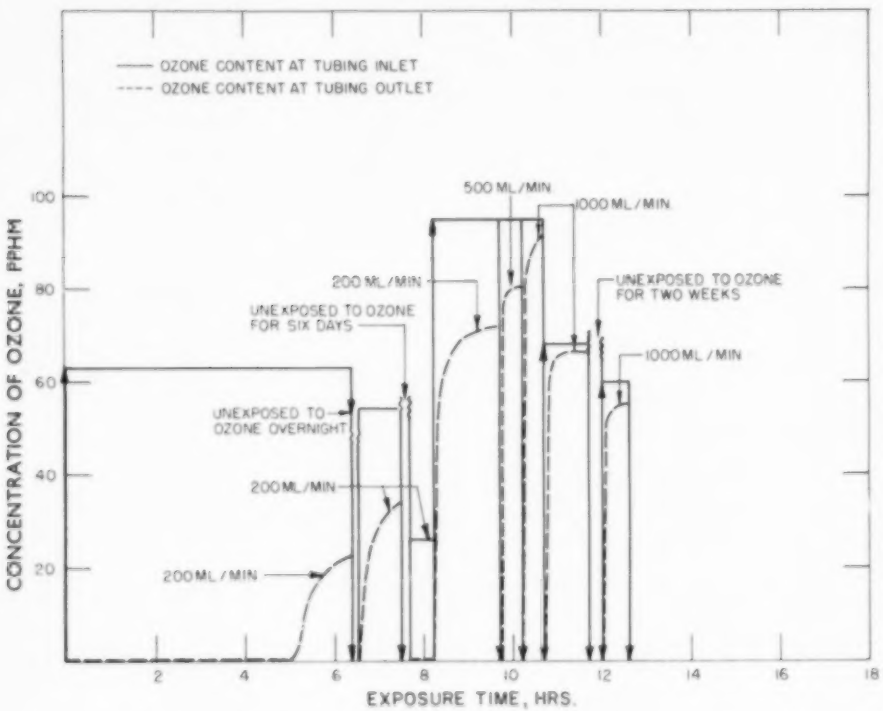

FIG. 2. Six foot length ($\frac{7}{16}$" i.d.) of 304 stainless steel exposed to ozone

The second length of stainless tubing began to condition after 4½ hours using only a 200 ml/min flow rate (Fig. 2). After seven hours of exposure, despite being unexposed and open to the atmosphere overnight, 60 per cent of the ozone at an inlet concentration of 56 p.p.h.m. passed through the tubing at 200 ml/min. However, after standing unexposed and open to the atmosphere for six days, the tubing would not pass any ozone for about one-half hour; subsequently, it conditioned rapidly. After ten hours of exposure, 75 per cent of the ozone passed through the tubing at 200 ml/min, and

VOL. 4 1961

85 per cent of the ozone passed through the tubing at 500 ml/min. At a flow rate of 1000 ml/min, over 95 per cent of the ozone passing into the tubing could be detected at the tubing outlet. After a 12 hour period of exposure, 90 per cent of the ozone passed into this tubing at 1000 ml/min came through the tubing even after the tubing remained unexposed and open to the atmosphere for two weeks.

A twelve-foot length of type 316 stainless steel tubing (3/8 inch i.d.) also was exposed to low concentrations of ozone. This tubing started conditioning rapidly after a little over a half hour exposure to the ozone. At a flow rate of 1000 ml/min and with an inlet ozone concentration of 73 p.p.h.m., the outlet ozone concentrations observed at various exposure times were as follows: 0·5 hr, 1 p.p.h.m.; 1 hr, 49 p.p.h.m.; 1·5 hr, 60 p.p.h.m.; 2 hr, 63 p.p.h.m.; 3 hr, 67 p.p.h.m.

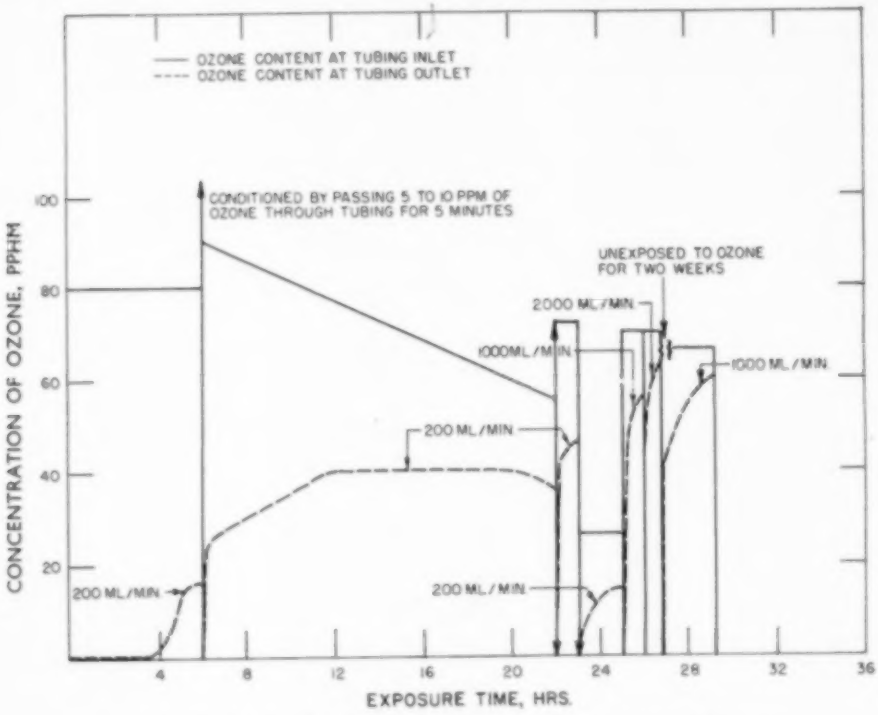

FIG. 3. Twelve foot length of aluminium tubing ($\frac{1}{2}$" i.d.) exposed to ozone

A twelve-foot length of aluminum tubing ($\frac{1}{2}$ inch i.d.) upon exposure to 80 p.p.h.m. of ozone at 200 ml/min passed no ozone for about 4 hr (Fig. 3). After an additional two-hour exposure to the same ozone concentration at the same flow rate, only about 20 per cent of the ozone flowing in could be determined at the outlet of the tubing. The tubing then was conditioned by flowing 5 to 10 p.p.m. of ozone through for 5 minutes. Subsequent to this treatment, about 60 per cent of the ozone could be detected after passing through the aluminum tubing despite over 24 hours of total exposure at 200 ml/min. However, when the flow rate was increased to 1000 ml/min, 85 per cent of the ozone passed through the tubing. At a flow rate of 2000 ml/min,

90 per cent of the ozone passed through the aluminum tubing. Even after the tubing remained unexposed to ozone and open to the atmosphere for two weeks, 90 per cent of the ozone passed through the tubing at a flow rate of 1000 ml/min after an additional two-hour exposure time.

Six- and twelve-foot lengths of polyethylene tubing (3/8 inch i.d.) conditioned slowly, but continuously, to ozone over a five-hour exposure period (Fig. 4). After the twelve-foot length of tubing remained unexposed to ozone and open to the atmosphere for two weeks, almost 75 per cent of the ozone remained intact at a flow rate of 1000 ml/min. When the flow rate was increased up to 2000 ml/min, 80 per cent of the ozone passed through the polyethylene tubing.

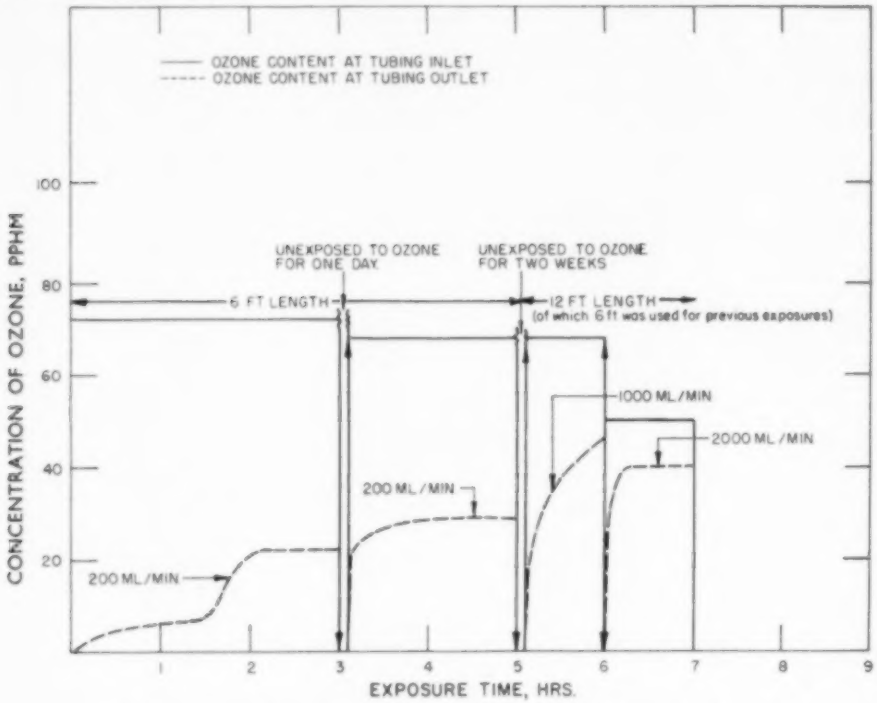

FIG. 4. Various lengths of polyethylene tubing ($\frac{3}{8}$" i.d.) exposed to ozone

A twelve-foot length of " Nalgon " tubing, a variety of polyvinyl chloride plastic, conditioned to ozone only slowly at flow rate of 1000 and 2000 ml/min (Fig. 5). A six-foot length of this tubing after 7·5 hours of exposure to 60 to 64 p.p.h.m. of ozone at flow rates of 1000 and 2000 ml/min would pass only about 80 per cent of the inlet ozone concentration.

Various lengths of " Tygon " tubing, another commercial variety of polyvinyl, chloride plastic, conditioned poorly (Fig. 6). A six-foot length of " Tygon " after over eight hours of exposure to 70 p.p.h.m. of ozone at flow rates of 1000 and 2000 ml/min would pass only about 30 per cent of the inlet ozone concentration.

Measurements made in the 5 liter glass flask used in the present study involved high surface-to-volume ratios. As much as 10 square feet of Mylar film (in small strips)

VOL. 4 1961

was placed in the flask which had a volume of only about 1/6 ft³. Under these conditions, and at flow rates as low as 100 ml/min, no significant loss of ozone could be observed. Similarly, 2 ft² of aluminum foil (cut into small strips) were placed in the 5-liter flask. The flask when filled with aluminum foil allowed as much ozone to pass through as when it was empty, once the foil had been exposed to ozone at 100 p.p.h.m. for several hours. This behavior persisted despite vigorous scrubbing with steel wool or cleaning of the foil with detergent solution or acetone. Even after the previously exposed aluminum foil remained unexposed for several days, the same ozone concentration was reached rapidly as was attained at the time of conditioning.

DISCUSSION

These results indicate that Teflon and glass tubing are the most satisfactory materials to use for the sampling of ozone. Static measurements showed appreciable decomposition in a 250-ml glass flask, about 3–4 per cent/hr (WILSON and BUCHBERG, 1958).

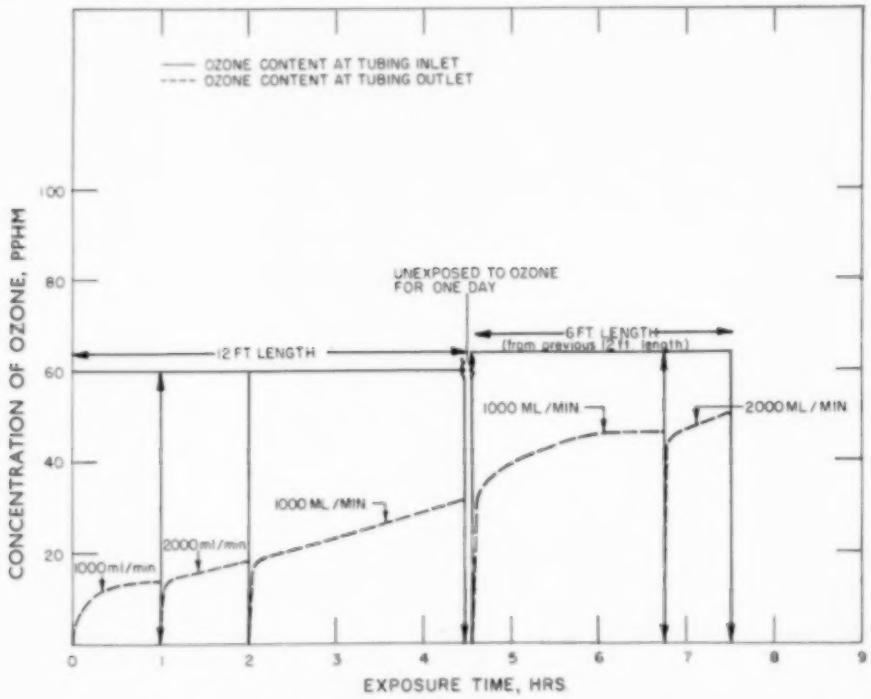

FIG. 5. Various lengths of Nalgon tubing ($\frac{1}{4}$" i.d.) exposed to ozone

In 12-liter glass flasks very little decomposition of ozone was observed in 100 hours. WILSON and BUCHBERG (1958) consider the rate of disappearance of ozone at glass and Teflon surfaces to be of the same order of magnitude.

Stainless steel and polyethylene tubing were less satisfactory than glass and Teflon in the dynamic experiments presented here, in agreement with observations in the static measurements (WILSON and BUCHBERG, 1958). Stainless steel tubing was found

to be better than polyethylene for dynamic ozone measurements. The static data show a one-third decrease in ozone concentration in ten hours with 80 in² of stainless steel surface in a 12-liter glass flask, or about 0·04 per cent/hr-in², while they show about seven hours with the same area of polyethylene in the glass flask, or about 0·06 per cent/hr-in². Thus, the two sets of data again seem to give generally comparable results.

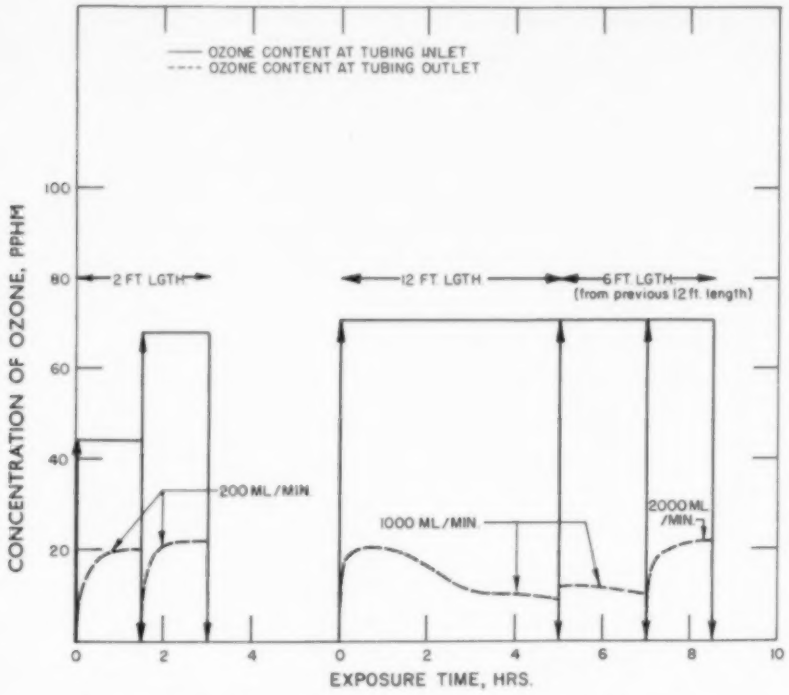

FIG. 6. Various lengths of Tygon tubing ($\frac{5}{16}$" i.d.) exposed to ozone

The results in the static measurements using 60 in² of aluminum surface in the glass flask indicate that about 25 hours will be required for a one-third decrease in ozone concentration, or about 0·02 per cent/hr-in². Our dynamic measurements on aluminum tubing, and on aluminum foil in 5-liter flasks, also show aluminum to be useable.

Some vinyl chloride copolymer tubings are unsatisfactory for use with gas mixtures containing ozone. The static experiments show an extremely rapid decrease in ozone concentration in the presence of two vinyl chloride copolymer-type films. In static measurements ozone is far more reactive with these particular vinyl chloride copolymer-type materials than with cellophane, Saran, Mylar, aluminum, or stainless steel (WILSON and BUCHBERG, 1958). The dynamic measurements given in this paper confirm the undesirability of using some plastic tubings of vinyl chloride copolymer formulation in the presence of ozone. Data presented by WILSON and BUCHBERG (1958) also show that one type of polyvinyl chloride tubing is very reactive with nitrogen

VOL. 4 1961

dioxide. Qualitative observations in this study indicate that the high concentrations of both nitrogen dioxide and sulfur dioxide cause rapid deterioration of " Tygon " tubing. The more satisfactory results with " Nalgon " tubing may mean that the substance reacting avidly with the ozone is a plasticizer rather than polyvinyl chloride copolymer. Alternatively, the difference in results must be due to some detail in manufacturing processes.

Data obtained on the reactivity of a series of materials with one gas should not be used for another gas. For example, while glass seems slightly more satisfactory than stainless steel with ozone in the 1–10 p.p.m. range, with 70 p.p.m. of nitrogen dioxide, stainless steel is a better storage container than glass (BAKER and DOERR, 1959). Furthermore, although no loss of nitrogen dioxide occurred in 24 hours at 74 p.p.m. in a 34-liter stainless steel tank (BAKER and DOERR, 1959), at 5·5 p.p.m. of nitrogen dioxide in a glass flask with an aluminum-foil surface to gas-volume ratio of 13 ft.$^{-1}$, 15 per cent of the nitrogen dioxide disappeared from the gas phase (WILSON and BUCHBERG, 1958). Consequently, considerable caution must be used in extrapolating data on reactivities of a given gas with various materials over a range of concentrations and surface-to-volume ratios.

The combined results of this work and those of WILSON and BUCHBERG (1958) indicate that stainless steel, aluminum, Mylar, and polyethylene should be satisfactory materials for dynamic measurements of ozone and for static measurements extending over several hours.

Conditioning by exposure for several hours before to ozone concentrations at or above those to be used in the actual experiments of interest and at flow rates of 1000 ml/min or above is recommended for all of the materials investigated except possibly Teflon. Once a given system is conditioned, the conditioning appears to remain for at least two weeks (Figs. 2, 3, 4) for many of the materials tested. Tubing and other materials made from vinyl chloride copolymer, if they must be used in contact with dilute ozone gas mixtures, should be used with caution and in the minimum lengths or areas possible. Conditioning of materials composed of vinyl chloride copolymer should be carried out at least eight hours, and the highest flow rates practically useable should be employed.

REFERENCES

BAKER R. A. and DOERR R. C. (1959) Methods of Sampling and Storage of Air Containing Vapors and Gases, *Int. J. Air Poll.* **2**, 142–58.

BYERS D. H. and SALTZMAN B. E. (1958) Determination of Ozone in Air by Neutral and Alkaline Iodide Procedures. *Am. Ind. Hyg. Assoc. Quart.* **19**, 251–7.

THUMAN W. C. (1958) *Development of Technology for Production, Sampling and Assay of Simulated Atmospheres in Closed Chambers*, Stanford Research Institute Project No. SU-2285.

WILSON K. W. and BUCHBERG (1958) Evaluation of Materials for Controlled Air Reaction Chambers, *Ind. Eng. Chem.* **50**, 1705–8.

Int. J. Air and Water Poll. Pergamon Press 1961. Vol. 4, Nos. 1/2, pp. 79–100. Printed in Great Britain.

PHOTOCHEMICAL REACTION PRODUCTS IN AIR POLLUTION *

E. R. STEPHENS,† E. F. DARLEY,‡ O. C. TAYLOR‡ and W. E. SCOTT†

Abstract—When low concentrations of simple olefins and nitrogen oxides in air are irradiated with artificial sunlight, the olefin molecule splits at the double bond. One end forms a carbonyl compound, and the other yields a variety of products. Among these is a highly oxidized, unstable organic nitrogen compound previously described as compound X or peroxyacetyl nitrite (PAN) and detected in polluted atmospheres. This compound has now been purified by gas chromatographic techniques, and its chemical, physical, and physiological properties have been examined. At concentrations well below 1p.p.m. in air, this compound produces damage symptoms on plants, similar to those observed from oxidant air pollution but different in some respects from the phytotoxicant from ozone-olefin reactions. PAN is the first pure compound isolated from photochemical reaction mixtures which has been found to produce the characteristic oxidant damage symptoms. It is also a strong eye irritant at concentrations in the 1 p.p.m. range and is therefore probably responsible, along with acrolein and formaldehyde, for the eye irritation in photochemical air pollution.

VOL. 4 1961

INTRODUCTION

PLANT damage and eye irritation are two important manifestations of air pollution arising from photochemical reactions in the atmosphere. The early studies of HAAGEN-SMIT, *et al.* (1952) demonstrated that plant damage similar to that found on leafy vegetable crops in the Los Angeles Basin could be reproduced by treatment with the reaction products of ozone and many olefins. They indicated also that similar results could be obtained with photolyzed mixtures of nitrogen dioxide and gasoline vapors. Peroxidic organic compounds were suggested as the phytotoxicants; organic acids and aldehydes were shown not to be toxic.

The characteristic injury, since called oxidant damage, consists of glazing or bronzing of the under surface of the affected leaves of a variety of plants. MIDDLETON, DARLEY, and BREWER (1956) have reviewed the effects of oxidants on plants. DARLEY, *et al.* (1958) further studied the effects of ozone-olefin reaction products on plants and suggested the zwitter-ion or an ozone-olefin addition complex as possible phytotoxicants. Ozonides, and again formic acid and aldehydes, were shown not to be toxic. ARNOLD (1959) demonstrated that the half-lives of the phytotoxicants produced by reacting ozone with 2-pentene or 3-heptene were very short (3 min and 15 min, respectively).

Ozone, a product of the photochemical reaction of oxides of nitrogen and organic materials in air (HAAGEN-SMIT and FOX, 1956) is also a phytotoxicant, but its effects

* Presented, by E. R. STEPHENS, to a session on automobiles, hydrocarbons, and clean air during the 25th Midyear Meeting of the American Petroleum Institute's Division of Refining, in the Sheraton-Cadillac Hotel, Detroit, Mich., May 11, 1960; presiding, JERRY MCAFEE, Gulf Oil Corp., Pittsburgh, Pa.

† W. E. SCOTT and Associates. Perkasie, Pa.

‡ University of California, Riverside, Calif.

on many plants are distinguishable from those of so-called " oxidants " in air pollution (SCHUCK and DOYLE, 1959). Ozone produces a stippling, mottling, or bleaching on the upper surface of affected leaves. Ozone damage has been found in the field on grapes (RICHARDS, *et al.*, 1958) and tobacco (HEGGESTAD and MIDDLETON, 1959). Although ozone is itself an oxidant, the term " oxidant " damage has been reserved for those as-yet-unidentified toxicants produced by the ozone-olefin reaction or by the photochemical nitrogen oxide-hydrocarbon reaction.

TAYLOR, *et al.* (1960), recently compared injury symptoms produced on pinto bean and petunia foliage by the following four toxicants: 1, ozone; 2, ozone-olefin reaction products; 3, photolyzed mixtures of olefin and nitrogen dioxide; and, 4, oxidants in polluted ambient air (in Riverside, Calif.). They found that the first three of these each produced readily distinguishable injury symptoms. Plant species and age of leaf tissues were important in distinguishing the toxicants. Ozone produced chlorosis or bleaching symptoms on the oldest petunia leaves and on 14-day-old pinto bean leaves. Ozone-olefin reactions caused glazing or bronzing on 14-day-old pinto bean leaves but did not damage 7-day-old pinto bean leaves or petunias. Photochemical reactions of nitrogen dioxide and 1-*n*hexene caused typical oxidant bronzing of 7-day-old pinto bean and petunia leaves but did not injure 14-day-old pinto bean leaves. The plants exposed to ambient air showed the symptoms ascribed to each of the three toxicants, but the most prevalent damage during the period of the experiments on both beans and petunias was the type caused by photolyzed nitrogen dioxide and olefin.

Eye irritation has been studied in several laboratories using irradiated mixtures of oxides of nitrogen and organic materials. An early study was made by HARTON and BOLZE (1958) with the use of natural sunlight irradiation. SCHUCK (1957) and STEPHENS and SCHUCK (1958) reported eye irritation from a variety of irradiated automobile exhaust mixtures and indicated that the irritant was relatively long lived. For this and other reasons, it was suggested (DARLEY, *et al.*, 1958) that the eye irritant and the phytotoxicant were different materials. DARLEY, MIDDLETON, and GARBER (1960) reported plant damage but no eye irritation from ozone-olefin mixtures reacted for relatively short residence periods. More recently, SCHUCK and DOYLE (1959) reported irritation from irradiated mixtures of nitrogen dioxide and pure olefins. Formaldehyde and acrolein were products of some of the reactions. From the irritation indices for these two aldehydes in pure form and their concentrations as measured in the irradiated mixtures, they were able to predict the eye-irritation index with a high degree of accuracy. Several minor products of the reaction were shown not to be irritating. They concluded that formaldehyde and acrolein are the principal eye irritants in oxidant air pollution.

HAAGEN-SMIT and FOX (1956) and STEPHENS, *et al.* (1957, 1956) have elucidated the mechanisms by which ozone is formed from the photooxidation of nitrogen dioxide with organic compounds in air. The long-path infrared techniques used by the latter investigators also revealed the presence of an unstable organic nitrogen compound which was tentatively identified as peroxyacetyl nitrite (PAN) and assigned the structure:

$$CH_3C(=O)—OONO.$$

This compound was also detected, with the use of long-path infrared, in photolyzed automobile exhaust and in natural oxidant air pollution (SCOTT *et al.*, 1957). Although evidence presented in this paper indicates that the correct formula may be peroxyacetyl *nitrate* (rather than *nitrite*), it will be referred to herein as PAN, an abbreviation suitable for either formula.

The ultraviolet radiation present in natural sunlight causes photolytic dissociation of nitrogen dioxide into nitric oxide and atomic oxygen. The latter species can then react with molecular oxygen to form ozone. In the absence of other components, only small concentrations of ozone could form in this way because the back reaction of ozone with nitric oxide to regenerate nitrogen dioxide is extremely rapid:

$$NO_2 + O_2 \overset{h\nu}{\rightleftharpoons} O_3 + NO$$

In the presence of organic material the ozone does accumulate to higher concentrations, presumably because nitric oxide is converted to nitrogen dioxide at some stage in the oxidation of the organic material. At one time, it was thought that formation of PAN from nitric oxide and its photolysis to yield nitrogen dioxide would account for this conversion. Studies of automobile exhaust photolysis (SCHUCK *et al.*, 1958; STEPHENS and SCHUCK, 1958) directly confirmed the conversion of nitric oxide to nitrogen dioxide and provided evidence that the rate of this conversion is dependent on the amount and type of hydrocarbon present. However, this conversion was much too fast in comparison with the rate of formation of PAN for the photolysis of this compound to account for the conversion. Therefore, it is apparent that there is a mechanism which involves hydrocarbon by which nitric oxide is converted to nitrogen dioxide.

VOL. 4 1961

THE OLEFIN REACTION

In the studies of the photochemical reaction, it became apparent that the olefins were appreciably more active than hydrocarbons of any other type. Olefins disappear more rapidly than hydrocarbons of other types and are also more active in promoting the photochemical conversion of nitric oxide to nitrogen dioxide in air. It has long been known that olefins react rapidly with ozone, a reaction leading to rupture of the molecule at the double bond. Detailed studies of this reaction in air at low concentration in the gas phase (STEPHENS *et al.*, 1959) showed that the reaction is stoichiometric and of the second order. One end of the olefin molecule yields a carbonyl compound (aldehyde or ketone); the other end yields a variety of fragments (ketene, methanol, carbon monoxide, carbon dioxide). At first it seemed possible that this reaction might account for the disappearance of olefin in the photolytic reaction with nitrogen oxides, inasmuch as ozone is a product of the reaction. This proved not to be the case, however, when the rates of olefin disappearance were compared with rates calculated on the basis of the measured ozone concentrations and known rate constants.

Because cleavage occurs at the double bond, the number of possible products is halved by working with symmetrical olefins. Ethylene, the simplest olefin, reacts slowly and does not yield some of the more interesting products, such as PAN. Since 2-butene and 3-hexene react much more rapidly, more work was done with these two olefins. A few experiments were also made with *iso*butylene.

The long-path infrared cell, which was previously used for atmospheric analysis (SCOTT *et al.*, 1957) and automobile exhaust studies (SCHUCK *et al.*, 1958; STEPHENS and SCHUCK, 1958), was used to study the photolytic reaction with pure olefins and nitrogen oxides. This instrument is housed in a laboratory trailer.

A series of experiments which were primarily designed to measure the aldehyde yield are summarized in Table 1. The main conclusion to be drawn from these data is that one mole of carbonyl compound is formed by rupture of the olefin at the double bond whether nitric oxide or nitrogen dioxide is used as starting material. The times

TABLE 1. PHOTOLYSIS OF NITROGEN OXIDE-OLEFIN MIXTURES

Reactants (p.p.m.)					
Nitrogen Dioxide	Nitric Oxide	Olefin	Carbonyl Product (p.p.m.)	Other Products (p.p.m.)	Time (min)
cis-3-Hexene (all consumed in every experiment)					
10·6	—	11·2	11·1 propionaldehyde	—	40
9·9	—	11·2	11·4 propionaldehyde	—	19
10·6	—	11·8	11·7 propionaldehyde	—	20
10	—	5·0	4·8 propionaldehyde	—	22
10	—	2·1	1·9 propionaldehyde	—	20
—	10	1·9	1·7 propionaldehyde	—	40
—	10	10·0	9·7 propionaldehyde	—	45
cis-2-Butene (all consumed in every experiment)					
—	9·2	10·9	10·9 acetaldehyde	3·0 PAN*	30
—	9·4	11·0	11·2 acetaldehyde	*	30†
10	—	10·6	8·6 acetaldehyde	2·3 PAN*	25
*Iso*butylene					
10	—	9·7	5·1 acetone 3·0 formaldehyde	(0·6 *iso*butylene)	83
—	11	10·2	5·8 acetone 4·6 formaldehyde	(0·7 *iso*butylene)	90
10	—	10·0	4·8 acetone 3·5 formaldehyde	(0·5 *iso*butylene)	90
Ethylene					
10	—	11·2	4·9 formaldehyde	(5·0 ethylene)	270

* Other products are ketene, methanol, and methyl nitrate.

† Ozone detected after 18 min.

listed in the last column serve to illustrate the relative rates of these reactions. Whereas 2-butene and 3-hexene are completely consumed in 20 min to 30 min, half the ethylene remained after 4½ hours. The other end of the olefin molecule is only partly accounted for among the products. With *cis*-2-butene, the acetaldehyde yield accounted for one end of the olefin molecule; the other end produced the PAN, methyl nitrate, ketene, and methanol. Fig. 1 illustrates the formation of aldehyde by the photolysis of nitrogen dioxide or nitric oxide with *cis*-2-butene. The initial rate of aldehyde formation is faster when nitrogen dioxide is the starting material, probably because this is the light absorber and its concentration is higher when it is used as the starting material. The concentration of ozone necessary to form acetaldehyde from *cis*-2-butene at the observed rate was estimated with the use of the rate

constant for this reaction previously measured (STEPHENS *et al.*, 1959). The calculated amounts far exceed the actual ozone concentration. In fact, when nitric oxide was the starting material, ozone could not be detected until 18 min had elapsed and the reaction was nearly completed. This illustrates clearly that ozone attack cannot be the sole reaction causing olefin disappearance. SCHUCK and DOYLE (1959) have calculated the expected rate of disappearance for various olefins from the known rates of their reaction with ozone and with oxygen atoms. Under some circumstances the observed rate was in good agreement with the calculated rate, but under other conditions the observed rate exceeded that calculated. This was interpreted as indicating the occurrence of a third reaction of olefin, the nature of which is not known.

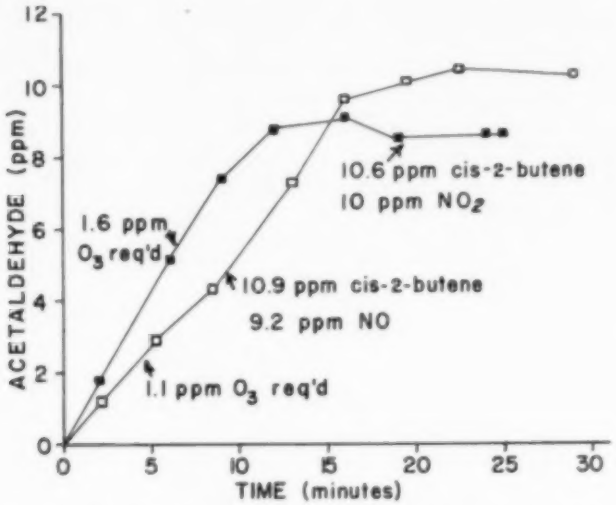

FIG. 1. Formation of Acetaldehyde by Irradiation of *cis*-2-Butene with Nitrogen Oxides

Because aldehydes are major products of the reaction, it was of interest to see whether or not they would react under the conditions of their formation. Accordingly, dilute mixtures of aldehydes with nitric oxide and nitrogen dioxide were irradiated under conditions similar to those used for the olefins. In every case, the reaction was much slower than with olefin as the starting material. For example, 3 hours to 4 hours were required to reduce the concentrations of propionaldehyde or formaldehyde by half when 10 p.p.m. were irradiated with 10 p.p.m. of nitric oxide or nitrogen dioxide. Acetone reacted still more slowly; barely 10 per cent reacted in 3 hours of irradiation with 10 p.p.m. of nitrogen dioxide. This clearly shows that aldehyde is not an intermediate in the formation of the other products so far identified (PAN, methyl nitrate, etc.). However, PAN was formed slowly as the photolysis of aldehyde-nitrogen oxide mixtures proceeded.

It will be noted that there is a striking resemblance between the products of the ozone-olefin reaction and those of the photolytic olefin-nitrogen oxide reaction. In both cases aldehyde is formed in stoichiometric yield, and in both cases ketene and methanol are minor products (when 2-butene is the olefin). Furthermore, the rates of the photolytic reaction parallel those in the ozone-olefin reaction in regard to the

VOL. 4 1961

effect of olefin structure. This suggests that the attack of an oxygen atom on the double bond is closely followed by reaction with molecular oxygen to produce the same intermediate as addition of ozone to the double bond.

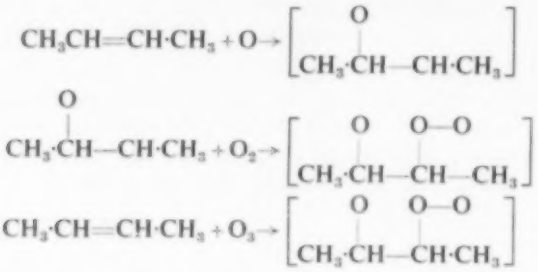

This complex then splits at the original location of the double bond to yield aldehyde and a zwitter ion. The aldehyde is relatively stable under the conditions of the experiment, but the zwitter ion reacts further to produce the other observed products. Presumably, this process results in the conversion of more than one molecule of nitric oxide to nitrogen dioxide (on the average). This is necessary to account for the net conversion of nitric oxide to nitrogen dioxide since one nitrogen dioxide molecule must be photolyzed to provide the oxygen atom or ozone molecule necessary to react with one olefin molecule.

PRODUCT SEPARATION

With the possible exception of the peroxyacetyl nitrite, none of the reaction products identified by long-path infrared could be responsible for eye irritation or plant damage. To determine whether or not PAN could be responsible for these effects,

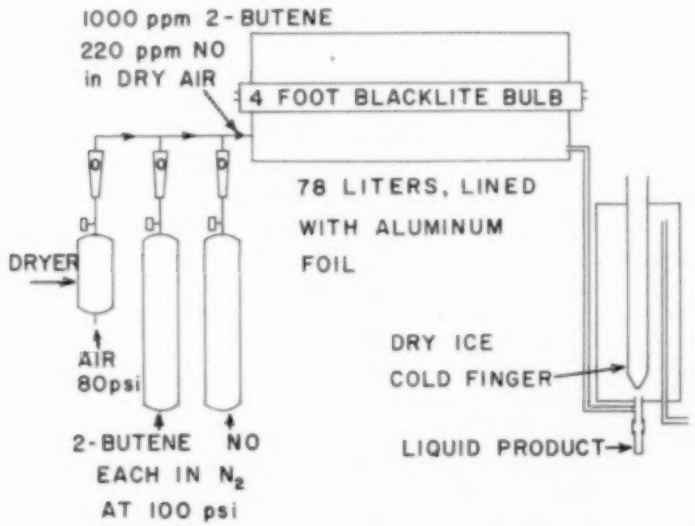

FIG. 2. Photochemical Reactor

it was necessary to devise a method for preparing and purifying samples of this compound. Some years ago (STEPHENS *et al.*, 1956), samples were prepared by photolyzing a mixture of diacetyl and nitrogen dioxide in air and condensing the products at dry-ice temperature. Some chemical properties were studied with the use of samples prepared in this way, but no means were then available for purifying the compound or for conducting eye-irritation tests or plant-damage studies.

A new photochemical reactor was constructed to prepare larger amounts of PAN for purification and study. This apparatus is shown schematically in Fig. 2. The reactor itself was made of galvanized iron and was lined with aluminum foil. It was 1 ft in diameter and just long enough so that the ends of an axially mounted 4-ft " blacklite " fluorescent bulb just protruded from the reactor. Compressed air was dried over silica gel and then fed into one end of the reactor along with small concentrations of reactants (2-butene and nitric oxide) supplied from pressurized tanks at a

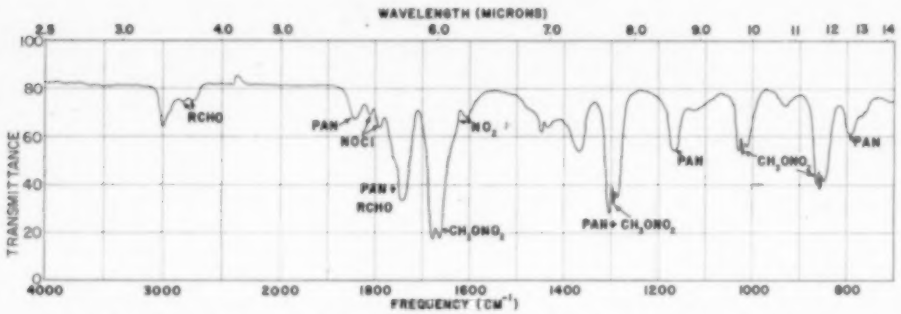

FIG. 3. Vapor Spectrum (10-Cm Cell) of Liquid Products from Photochemical Reactor

$\frac{1}{10}$ dilution in nitrogen. Concentrations of approximately 1,000 p.p.m. of 2-butene and 220 p.p.m. of nitric oxide were generally used at a total flow rate of 2·8 liters per minute, giving a residence time of approximately 30 min. The effluent from the reactor was passed into a 40-liter box containing a cold finger filled with a freezing mixture of dry ice and acetone. Upon warming the cold finger, the mixture of liquid products drained into a receiver. The infrared spectrum (see Fig. 3) of the vapors from this liquid sample showed the same products as were observed when the same reactants were irradiated in the long-path cell at parts-per-million concentrations (i.e., aldehyde, methyl nitrate, and PAN). Crude samples prepared in this way could be stored for days at dry-ice temperature.

After a number of trials, the gas chromatograph shown in Fig. 4 was evolved to effect the separation of these products so that the PAN could be obtained in pure form. The separating column was made of pyrex glass (4 ft long by $\frac{3}{8}$ in. ID) and was filled with C-22 fire brick coated with 20 per cent of polyethylene glycol (carbowax 600). The column was operated at room temperature and was not thermostated. Helium flowing at 300 ml per minute was used as carrier gas. The most unusual feature of this chromatograph is the splitting of the carrier gas stream after it leaves the column. The glass capillaries shown in Fig. 4 serve to feed approximately 10 per cent of the stream to the thermal conductivity detector and the remainder to the glass trap which could be chilled in a mixture of dry ice and acetone. This was done so that any decomposition products produced by the hot filaments in the detector

VOL. 4 1961

would not be collected in the dry-ice trap. A small portion of the column effluent was also bled into a time-of-flight mass spectrometer to aid in the identification of peaks. The pressure upstream of the capillaries was measured on a silicon oil manometer as an indication of flow rate.

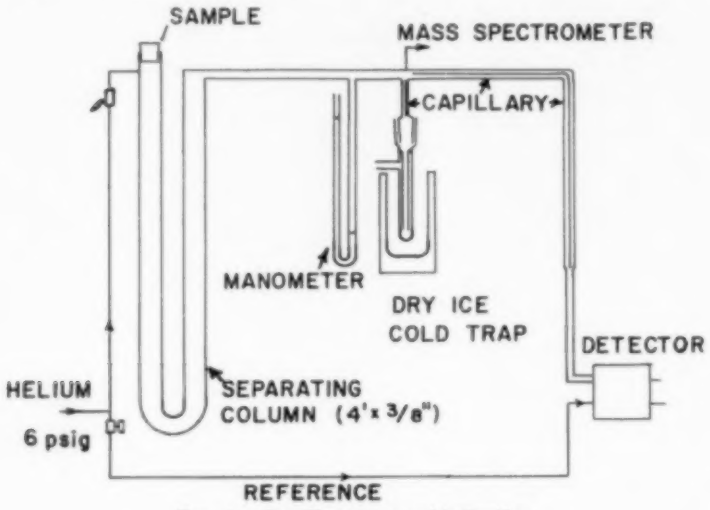

FIG. 4. Gas Chromatographic Purifier

A typical chromatogram produced by the product mixture from the reactor is shown in Fig. 5. The PAN began to emerge approximately 40 min after injection of the sample (approximately 200 microliters of liquid). It was fairly well separated from the other components of the mixture. The other major components—acetaldehyde and methyl nitrate—emerged before the PAN. A number of minor components are also evident in this chromatogram. Methylethyl ketone was one of these (partly super-

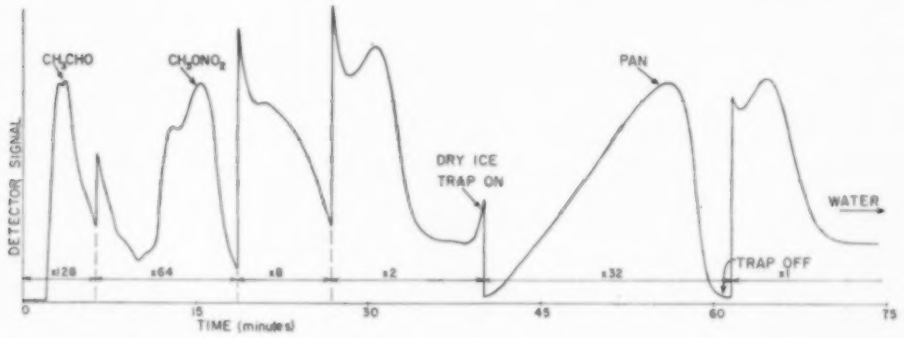

FIG. 5. Chromatogram of Liquid Products from Photochemical Reactor

imposed on the methyl nitrate). The mass spectrum suggested that the peak emerging at 30 min is a six-carbon keto-alcohol.

The PAN peak yielded approximately 30 mg of a colorless liquid in the dry-ice freeze trap. This liquid could be reintroduced into the column and chromatographed a

second and a third time to demonstrate the substantially complete removal of the impurities. Most of the experiments reported here were performed with samples obtained after a single pass. This preparation and purification are now on a semi-routine basis.

PAN PROPERTIES

Infrared Spectrum

The purified PAN has a vapor pressure at room temperature of approximately 10 mm of mercury (Hg), which is sufficient to produce a good infrared spectrum in a 10-cm absorption cell (see Fig. 6). Table 2 gives the frequencies and wave lengths observed for the purified material as compared with the spectrum of the PAN pre-

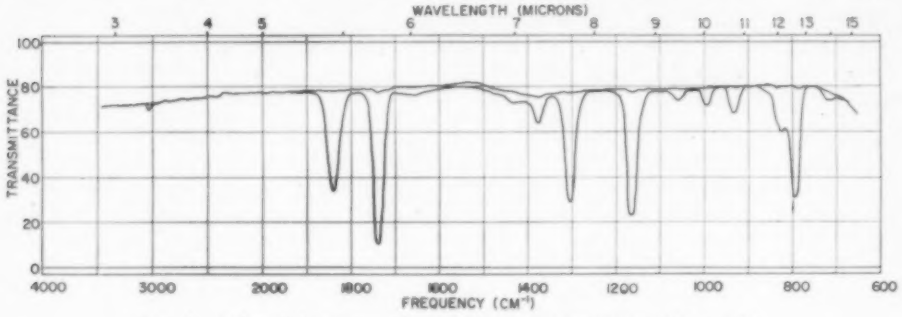

FIG. 6. Infrared Spectrum of PAN Vapor (6 Mm Hg in 10-Cm Cell)

pared from diacetyl and nitrogen dioxide and previously published (STEPHENS *et al.*, 1956). There can be no doubt that these two materials are identical—the one difference between the two spectra is the diacetyl band at 8.9μ in the spectrum of the sample prepared from this material.

Stability

This compound has been known to be unstable for some time, although data on its stability in a pure state were lacking. In the 1956 paper (STEPHENS *et al.*, 1956) the violent explosion of a one- or two-drop liquid sample was reported. During the

TABLE 2. INFRARED SPECTRUM OF PAN

Frequency (Cm^{-1})	Wave Length (Microns)	1956 Spectrum (Microns)	Strong (S), Medium (M)
3027	3·30	3·30	M
1839	5·44	5·42	S
1736	5·76	5·75	S
1371	7·30	7·30	M
1302	7·68	7·65	S
1163	8·60	8·57	S
1056	9·47	9·45	M
992	10·08	10·10	M
931	10·74	10·75	M
793	12·61	12·60	S
717	13·95	13·85	M

VOL. 4 1961

present studies six samples have exploded. One of these was an impure liquid mixture from the photochemical reactor; four others were small liquid samples of the chromatographically purified material; and the sixth was a one-liter vapor sample at a pressure of approximately 8 mm Hg, which exploded while nitrogen gas was being bled in to bring the pressure to 1 atm. This explosion (presumably initiated by compression heating of the PAN vapor) did not break the flask, but was evidenced by a sharp sound and the appearance of nitrogen dioxide in the flask. The infrared spectrum of the products of the explosion showed, in addition to nitrogen dioxide, approximately 15·5 mm Hg of carbon monoxide and 2·9 mm Hg of carbon dioxide (total = 18·4 mm Hg). This is slightly larger than the total of 16 mm Hg which would be expected if the original molecule contained two carbon atoms and if it were all converted to carbon monoxide and carbon dioxide by the explosion. The cause of the explosion of the four liquid samples is not known, which serves to illustrate the extreme sensitivity of this compound. It should be handled with the respect due an extremely dangerous high explosive.

On the other hand, vapor samples of PAN, when left undisturbed at room temperature, did not show appreciable decomposition over periods of many hours or even days. A vapor sample kept for 16 hours in a 10-cm infrared cell showed no detectable decomposition. Decomposition took place slowly when vapor samples were held at approximately 50 C for several hours.

TABLE 3. INFRARED SPECTRUM AND DECOMPOSITION OF PAN

(Concentration of PAN in Millimeters of Mercury)

Wave Length:	5·44μ	5·76μ	7·68μ	8·60μ	12·61μ
Absorptivity ($mm\ Hg^{-1}m^{-1}$)*:	0·62	1·45	0·78	0·89	0·70
I. Initial	3·3	3·4	†	3·4	3·2
2 hours at 40 C to 65 C	2·6	2·9	†	2·9	2·9
20 hours at 40 C to 65 C	0·34	0·28	†	0·37	0·32
II. 1 hour at 50 C	2·7	2·8	†	2·8	2·8
16 hours at 40 C to 50 C	0·9	0·9	†	0·9	0·9
III. See reference No. 16, Fig. 2 (1-meter path).	0·33	0·41	0·35	0·33	0·35

* To convert to $p.p.m.^{-1}\ m^{-1}$ multiply by (7·6) (10^{-1}).
† Methyl nitrate produced interferes.

Data on these decomposition experiments and on the infrared spectrum are given in Table 3. The concentration of PAN was measured at four of the five major absorption bands (product methyl nitrate interferes at 7·7μ) with very consistent results. This further substantiates the assignment of all these bands to a single compound. The concentrations in the 1956 sample (STEPHENS *et al.*, 1956) prepared from diacetyl were also calculated for all five major bands with the use of the absorptivities derived from the new samples. The good agreement among four of the five values (the

carbonyl is high because of the diacetyl impurity) further confirms the identity of the two materials.

Methyl nitrate and carbon dioxide were the principal products of this slow decomposition. Variable amounts of nitromethane were also produced, but no carbon monoxide could be detected. Formation of methyl nitrate and carbon dioxide in stoichiometric yield would indicate that the original molecule contained five oxygen atoms, but it has not been possible to demonstrate this as yet. None of the proposed structures contain more than four atoms of oxygen. Peroxyacetyl *nitrate* would therefore account for the observed decomposition products better than peroxyacetyl *nitrite*.

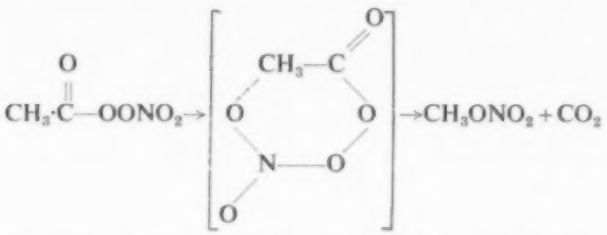

The ring structure in brackets is suggested as a plausible intermediate in this decomposition.

Ultraviolet Spectrum

In an earlier publication (Scott, *et al.*, 1957) an ultraviolet spectrum of PAN in solution in pentane was reported. This showed a rather weak and featureless absorption in the sunlight region from 3000 Å to 4000 Å, rising steeply for wave lengths

VOL. 4 1961

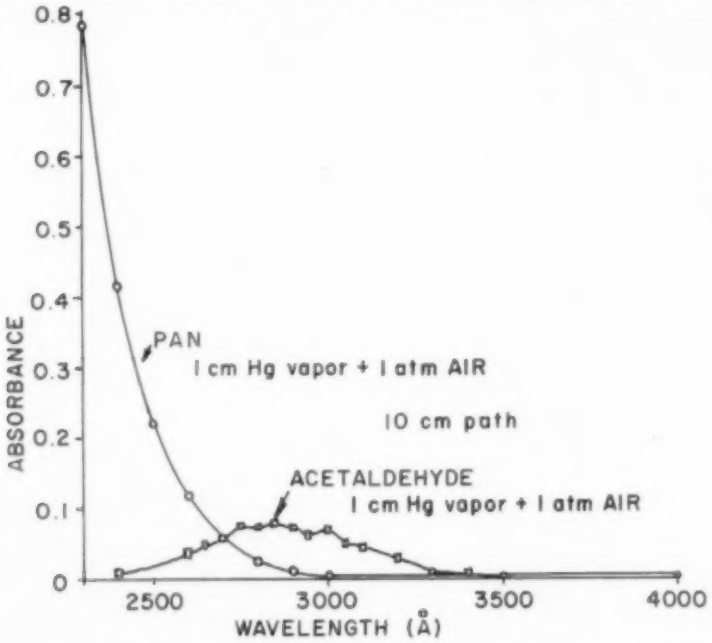

Fig. 7. Ultraviolet Spectrum of PAN Vapor (10-Cm Cell)

shorter than this. A vapor spectrum of the purified material is shown in Fig. 7 along with an acetaldehyde spectrum taken at the same concentration (10-cm path). Both samples were pressurized to 1 atm with nitrogen. The PAN spectrum is similar to the solution spectrum published earlier but is quite weak in the sunlight region. Acetaldehyde and PAN are both products of the photochemical *cis*-2-butene-nitrogen oxide reaction; however, of the two, the former is the stronger absorber of sunlight ultraviolet. Approximately 2·6 p.p.m. of PAN was subjected to ultraviolet photolysis in the long-path cell in air of normal humidity. Disappearance was relatively slow, the half life being approximately 1½ hours, and the remaining PAN could still be detected after 6½ hours. No ozone was detected, nor any other products.

Mass Spectrum

The mass spectrum of PAN was recorded as it emerged from the gas chromatograph by bleeding a portion of the effluent into a time-of-flight mass spectrometer (see Table 4). No peak corresponding to a mass/charge ratio greater than 46 could be detected above background levels in the spectrum.

Table 4. Mass spectrum of PAN

(Mass/Charge Ratio = 43 Taken as 100)

Mass/Charge Ratio	Height	Assignment	Mass/Charge Ratio	Height	Assignment
46	17	NO_2^+	30	13	NO^+
45	1		29	3·6	
44	5	CO_2^+	15	39	CH_3^+
43	100	CH_3CO^+	14	6	CH_2^+
42	3	CH_2CO^+	13	2	CH^+
41	1	$CHCO^+$	12	0·6	C^+

The main features of this spectrum are consistent with the various proposed structures, with the assignments shown in the table. The presence of an acetyl group along with oxidized nitrogen is confirmed. The small peaks at 45 and 29 do not follow the major peaks and may therefore be ascribed to a trace of impurity. Mass spectra of PAN samples were reported in 1957 (Scott *et al.*, 1957). At that time, it was suspected that extensive decomposition took place in the spectrometer inlet system so that the PAN spectra were reported as residues after subtraction of the spectra of the decomposition products. Qualitatively these spectra are similar to the new spectrum, except for the absence of mass 46.

Both the proposed structures for PAN have a peroxide link and so would be expected to release iodine from potassium iodide solution. To verify this, vapor samples of PAN were treated with 2 per cent of potassium iodide solution in a 2-liter flask. Although oxidation of the potassium iodide occurred, it was appreciably slower than would be expected for a similar amount of ozone. The iodine liberated was measured colorimetrically with the use of the calibrations established for ozone. In two trials, 0·46 and 0·63 moles of iodine were liberated per mole of PAN. A yield of 0·50 would indicate transfer of one electron per mole of PAN.

SCHUCK and DOYLE (1959) have recently prepared samples of acetyl nitrate following the procedure of PICTET and KHOTINSKY (1907):

$$CH_3{\cdot}\overset{\overset{O}{\|}}{C}{\cdot}O{\cdot}\overset{\overset{O}{\|}}{C}{\cdot}CH_3 + N_2O_2 \rightarrow 2CH_3{\cdot}\overset{\overset{O}{\|}}{C}ONO_2$$

The acetyl nitrate was purified by distillation at reduced pressure, its infrared spectrum recorded, and its eye irritation measured. On the basis of the infrared spectrum. SCHUCK and DOYLE suggested that it is the same as PAN. We are indebted to R. H. WADE and E. A. SCHUCK of Stanford Research Institute for giving us a sample of this compound.

Study of the properties of this sample led to the conclusion that it was not the same as the PAN produced in the photochemical reactor and separated chromatographically, Evidence for this was obtained in a variety of ways:

(1) Acetyl nitrate hydrolyzed more quickly than PAN; with liquid water, the reaction was virtually instantaneous. It fumed markedly when exposed to humid air, a property noted by PICTET and KHOTINSKY (1907). Liquid PAN persisted as a separate phase when mixed with aqueous potassium iodide solution and did not fume when exposed to laboratory air.

(2) Acetyl nitrate failed to emerge from the gas chromatograph under the conditions used to purify PAN.

(3) Acetyl nitrate has a higher vapor pressure than PAN at room temperature.

(4) The infrared spectrum of acetyl nitrate (see Fig. 8), although, superficially similar in some respects to that of PAN, is clearly not the same. The infrared spectrum of acetyl nitrate showed strong acetic acid bands, as marked in Fig. 8. This

VOL. 4 1961

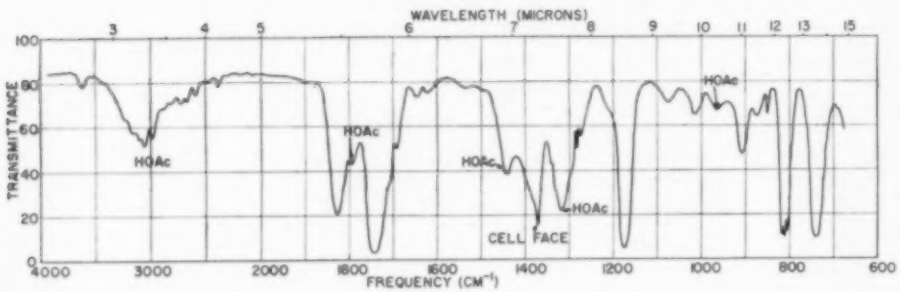

FIG. 8. Infrared Spectrum of Acetyl Nitrate Vapor (10-Cm Cell)

probably originated in hydrolysis occurring during transfer of the sample. Three of the five major bands in the PAN spectrum have counterparts in the acetyl nitrate spectrum at approximately the same wave lengths, i.e., at 5·75μ, at 8·6μ, and at 12·6μ. However, the acetyl nitrate band at 12·6 μ shows structure which is completely absent in the PAN spectrum. The acetyl nitrate band at 5·5 μ is at a somewhat longer wave length than the corresponding band in the PAN spectrum. The strong 7·7 μ band in the PAN spectrum is not present in the acetyl nitrate spectrum, but the

latter does have a strong band at 13·9 μ which is not present in the PAN spectrum. Finally, the weak bands between 9 μ and 12 μ are different in the two spectra. A single test of eye irritation and two plant fumigations with acetyl nitrate are reported elsewhere in this paper.

EYE IRRITATION

Experiments were made to determine and compare the eye-irritating qualities of several of the irradiated mixtures, and products thereof, discussed in the previous sections. Three eye-irritation booths, patterned after those developed by Stanford Research Institute (Schuck, 1957) and described in detail elsewhere (Darley *et al.*, 1960), were employed for these studies with some modifications. The air flow lines of the irritation booths were connected with the air flow system of the long-path infrared spectrometer housed in the mobile laboratory mentioned in the foregoing. This laboratory was parked adjacent to the glasshouse in which the booths were located. A system of valves was installed so that, unknown to the subjects, either polluted air from the long-path cell or carbon-filtered (clean) air from the glasshouse could be passed over their eyes. The system also permitted clean air to be drawn into the cell for purposes of flushing and of obtaining background spectra. In addition, the loose-fitting plastic face masks used in previous studies were replaced by snugly fitting eye goggles. This permitted a slower air flow over the eyes and conserved pollutant mixtures prepared statically in the long-path cell so that dilution during a given test was held to a minimum. Flow rate through the goggles was approximately 1·5 liters per minute. An exhaust hood over the booths carried pollutants out of the glasshouse as they emerged from the goggles.

Subjects for these tests were students, both male and female, at the University of California at Riverside. Students were selected from a group whose medical records showed freedom from chronic upper respiratory or eye troubles. For most exposures, the subjects received 5 min of clean air and 5 min of polluted air, the order being alternated in a random fashion. At times, the exposure to pollutants was increased to 10 min to 15 min. Each subject reported his eye irritation every 30 sec as none, medium, or severe. If a subject recorded either medium or severe, his response was recorded as positive. The ratio of the subjects giving a positive response to the total number of subjects exposed was recorded as the response to a given fumigant. From 13 to 20 subjects were exposed in a test, and most tests were replicated several times.

Fumigants used in these experiments were of two types: 1, mixtures of compounds resulting from either the photochemical reaction of nitrogen oxides with olefins or aldehydes or from the reaction of ozone with olefins; and, 2, selected pure compounds identified as products of these reactions. With mixtures, the reactants were introduced at desired concentrations into the long-path cell and reacted statically for approximately an hour until the reaction was complete, as indicated by the infrared spectrum. The products were then pumped slowly through the eye goggles. The ratio of the flow rate to the volume of the cell was such that the change in concentration during an experiments as a result of dilution was less than 10 to 15 per cent. Compounds—either prepared in the small photochemical reactor and purified by gas chromatography, as described in earlier sections, or proprietary ones—were introduced into the long-path cell at measured concentrations under static or dynamic flow conditions, their infrared spectra recorded, and then passed over the subject's eyes.

The results of these experiments are given in Table 5 (mixtures) and Table 6 (pure compounds). The photochemical reaction products which emerged from the chromatograph before and after the PAN peak were collected as two mixtures and tested for eye irritation.

TABLE 5. EYE IRRITATION FROM PRODUCTS OF IRRADIATED MIXTURES OF OLEFINS AND NITRIC OXIDE AND FROM PRODUCTS OF OLEFIN-OZONE DARK REACTIONS (EYES EXPOSED 5 MIN; STATIC EXPERIMENTS)

Reactants	Concentration (p.p.m.)	Number of Experiments	Positive Responses	
			Number*	Per Cent
cis-2-Butene Nitric oxide (Ultraviolet)	5 2 (1 hour)	8	44/80	55
cis-2-Butene Nitric oxide (Ultraviolet)	2 1 (1 hour)	5	9/68	13
trans-3-Hexene Nitric oxide (Ultraviolet)	5 2 (1 hour)	4	29/40	72
2-Heptene Nitric oxide (Ultraviolet)	5 2 (1 hour)	6	29/58	50
cis-3-Methyl, 2-pentene Nitric oxide (Ultraviolet)	5 2 (1 hour)	2	13/16	81
Butadiene-1, 3 Nitric oxide (Ultraviolet)	5 2 (1 hour)	2	16/16	100
Butadiene-1, 3 Nitric oxide (Ultraviolet)	0·5 0·5 (1 hour)	4	24/60	40
Acetaldehyde Nitric oxide (Ultraviolet)	5 2 (1 hour)	6	5/45	11
cis-2-Butene Ozone (Reacted)	5 5 (1 hour)	5	2/44	5
Butadiene-1, 3 Ozone (Reacted)	5 2 (1 hour)	2	10/14	71

* Numerator is number of exposures for which eye irritation was reported; denominator is total number of exposures of from 13 to 20 panel members.

From the earlier studies of the photochemical nitrogen oxide-olefin reaction it was clear that aldehydes were major reaction products. Two aldehydes were known to be powerful eye irritants: acrolein and formaldehyde. To determine whether or not

VOL. 4 1961

additional irritants were formed in the photochemical reaction, attention was concentrated on the internally bonded olefins which produce little or none of these two known irritants. It is clear from the data of Table 5 that the products from these reactions are definitely irritating to the eyes.

Fifty per cent or more of the responses were positive when olefin-nitric oxide concentrations of 5 p.p.m. and 2 p.p.m. respectively, were irradiated. Reducing the concentrations of *cis*-2-butene and nitric oxide to 2 p.p.m. and 1 p.p.m., respectively, reduced irritation markedly. Products of the irradiation of *cis*-2-butene and nitric oxide include acetaldehyde, PAN, methyl nitrate, ketene, and methanol. A number of the corresponding compounds have been identified among the products of irradiation of the higher internal olefins with nitrogen oxides.

TABLE 6. EYE IRRITATION FROM PURE COMPOUNDS DERIVED FROM PRODUCTS OF IRRADIATED MIXTURE OF OLEFINS AND OXIDES OF NITROGEN OR FROM OLEFIN-OZONE REACTIONS

Fumigant	Concentration (p.p.m.)	Static (S), Dynamic (D)	Number of Experiments	Time of Exposure (Min)	Positive Responses	
					Number *	Per Cent
Formaldehyde	5	S	3	5	18/27	67
Formaldehyde	2 to 4	S	4	5	10/47	33
Formaldehyde	4	D	1	5	7/7	100
Formaldehyde	2	D	4	12	9/37	24
Formaldehyde	1	S	8	5	6/75	8
Acrolein	1 to 2	S	3	5	20/23	87
Acrolein	1	S	2	5	14/17	82
Acrolein	0·5	S	8	5	25/72	35
Acrolein	0·5	D	4	5	7/36	19
Acrolein	0·5	D	4	12	30/33	91
PAN	5	S	3	5	18/19	95
PAN	2	D	8	10	20/63	32
PAN	1	S	4	5	3/36	8
PAN	1	D	8	10 to 15	38/61	62
PAN	0·5	D	6	12	9/56	18
Acetyl nitrate	4	S	2	12	3/17	18
Acetaldehyde	5 to 7	S	3	5	0/27	0
Gas chromatographic peaks:						
Before PAN	7	S	2	10	2/17	12
After PAN	14	S	1	10	1/7	14
Clean air		D	9	10	5/72	7

* Numerator is number of exposures for which eye irritation was reported; denominator is total number of exposures of from 13 to 20 panel members.

Acetaldehyde alone, in concentrations comparable to the product of irradiated reactions, produced no irritation. Eleven per cent of the responses from the irradiated mixture of acetaldehyde and nitric oxide were positive. This small response might be attributable to small amounts of PAN or formaldehyde formed. Reaction in the

dark of *cis*-2-butene and ozone gives as much acetaldehyde and more ketene and methanol than the irradiated *cis*-2-butene and nitric oxide. This dark reaction resulted in a positive response of only 4 per cent. It thus appeared that the irradiated reaction produced an irritant which was not formed by the reaction of ozone with *cis*-2-butene. Methyl nitrate and PAN were the only two products which were known to be present in the irradiated mixtures but not in the dark reaction. When pure samples of PAN became available, it was tested and found to be irritating at concentrations as low as 2 p.p.m. for 5-min exposures and 1 p.p.m. for 10- to 15-min exposures (see Table 6). The threshold for detection is approached at 0·5 p.p.m. for 12-min exposures.

Formaldehyde and acrolein were definitely irritating in the present investigation. Five p.p.m. of formaldehyde and 1 p.p.m. to 2 p.p.m. of acrolein gave rather severe irritation. Threshold values for detection in 5-min exposures appeared to be approximately 1 p.p.m. for formaldehyde and somewhat less than 0·5 for acrolein. Increasing the time of exposures from 5 to 12 min at the lower concentrations markedly increased the irritation. Acrolein appears to be two to three times more irritating than formaldehyde. Threshold limit values recommended by the American Conference of Governmental Industrial Hygienists (1958) are 5 p.p.m. for formaldehyde and 0·5 p.p.m. for acrolein (time-weighted-average concentration for a normal work day).

The photochemical butadiene-nitric oxide reaction (see Table 5) yielded a severely irritating mixture of products, a not unexpected result inasmuch as this reaction yields both acrolein and formaldehyde. Even when the starting concentrations were reduced to 0·5 p.p.m., 40 per cent of the responses were still positive. The reaction of ozone with butadiene-1, 3 also produces the two aldehllde s but oo PAN; and when the reaction is completed, considerable irritation is observed. A previous report (DARLEY *et al.*, 1960) indicated that this reaction did not produce irritating products. The reason for the difference in results is to be found in the longer reaction time of the present experiment.

VOL. 4 1961

The present results are in agreement with those reported by SCHUCK and DOYLE (1959) as to the concentrations of formaldehyde and acrolein necessary to produce moderate eye irritation. Very limited tests of acetyl nitrate are also in agreement, but SCHUCK and DOYLE did not test PAN. They concluded that formaldehyde and acrolein were the principal materials responsible for eye irritation because they could account for all the irritation they observed on the basis of measured concentrations of acrolein and formaldehyde. It should be noted that most of their work was done with olefins which produced either formaldehyde or acrolein or both, whereas our work has been concentrated on the internal olefins which do not yield significant amounts of either aldehyde.

Those compounds produced by the *cis*-2-butene–nitric oxide reaction which emerged from the chromatographic column before and after PAN were tested collectively and found to be not irritating.

From these results, it is concluded that the photochemical reaction between nitric oxide and certain olefins produces three eye irritants: formaldehyde, acrolein, and PAN. Acrolein is two or three times as irritating as formaldehyde, while PAN is intermediate in activity. Which of these three irritants contributes most to the irritation caused by a given reaction mixture obviously depends on the particular reactants in question. At the present time, there is not sufficient data on the concentrations of these three irritants in natural air pollution to evaluate their relative importance.

PLANT DAMAGE

Concurrent with eye-irritation experiments, several of the reactions and their products noted in the foregoing were also studied to determine if they caused plant damage and, if so, to compare such damage with that occurring in the field. In exploratory experiments three mercury vapor sterilamps, emitting radiation at 2537 Å, were used to irradiate certain mixtures in a box with a volume of 120 cu ft provided with a dynamic air flow system. With a residence time (volume of the box divided by the rate of air flow) of only 2 min, extensive reaction was obtained when nitrogen dioxide and *n*hexane, a comparatively unreactive hydrocarbon, were irradiated. These irradiated mixtures caused severe injury, indistinguishable from injury caused by phytotoxicants in the polluted ambient atmosphere (Haagen-Smit, 1952; Noble, 1955; Taylor *et al.*, 1960) on leaves of pinto bean, petunia, tobacco, head lettuce, endive, Swiss chard, mangel, bell pepper, spinach, and annual blue grass. Because the sterilamps emitted ultraviolet light of shorter wave length than that found in sunlight, these lights were replaced in succeeding experiments by 48 blacklit fluorescent tubes which do not emit radiation shorter than 3000 Å. The mixtures of nitrogen dioxide with hydrocarbon were less reactive with the blacklite irradiation, but the characteristics of plant response to the reacted mixtures appeared to be the same as when sterilamps were used.

Rooted petunia cuttings and 8- and 14-day-old pinto bean seedlings were used extensively in attempts to identify the phytotoxicants formed in the photolysis of nitrogen dioxide plus hydrocarbon and automobile exhaust. In recent studies using these plants, Taylor *et al.* (1960) reported at least three phytotoxicants resulting from irradiated hydrocarbon-nitrogen dioxide mixtures and ozone-olefin reactions.

Irradiated Nitrogen Dioxide Plus Hydrocarbons

Several experiments were conducted with irradiated mixtures of nitrogen dioxide and hydrocarbons (5 p.p.m. of each) under static conditions in the long-path cell. The plants were exposed in the box on top of the cell (Darley *et al.*, 1958) only after the reaction was complete, as indicated by the infrared spectrum. All the hydrocarbons used gave the typical plant response noted for photochemical reactions (Taylor *et al.*, 1960), and the severity of damage bore a direct relationship to the speed of reaction: *cis*-2-butene, severe (1-hour reaction); propylene, moderate (2-hour reaction); 1-hexene, moderate (2-hour reaction); and cumene, light (5-hour reaction).

Irradiated Automobile Exhaust

Previous attempts to produce plant damage from irradiated automobile exhaust resulted in no more than a trace of oxidant-type plant damage (Schuck *et al.*, 1958). This failure may have occurred because the selectivity of the phytotoxicants for a specific physiological age of leaf tissue and species of test plant was not recognized. More recently, however, automobile exhaust samples were collected in an evacuated tank directly from the tail pipe of a 1957 Chevrolet, diluted one part to 600 to 700 parts of air, and irradiated for 40 min with 48 blacklite fluorescent tubes. Irradiated exhausts from an idling automobile (high in hydrocarbon but with little or no oxides of nitrogen) and from a steady 40-mph uphill cruise (low in hydrocarbon and high in oxides of nitrogen) produced no plant damage (Schuck, 1957; Stephens *et al.*, 1959). Irradiated

products from a 50-50 mixture of an uphill and downhill cruise (the latter with alternating acceleration and deceleration) produced extensive oxidant-type damage on 8-day-old primary and trifoliate leaves of pinto beans (see Fig. 9), but caused no injury on the 14-day-old leaves. These irradiated mixtures also caused lower surface glazing and bleached banding of young expanding petunia leaves. Analysis of the diluted exhaust prior to irradiation showed approximately 2 p.p.m. of total hydrocarbon and 0·5 p.p.m. of nitrogen oxides. Thus plant damage which is indistinguishable from that caused by irradiated mixtures of oxides of nitrogen and hydrocarbon or that caused by polluted ambient air, can be produced quite easily from irradiated automobile exhaust.

Ozone-olefin Mixtures

Comparisons in plant response were made in dynamic air flow systems between irradiated and nonirradiated ozone-olefin reactions. Hydrocarbons and ozone were used at 1 p.p.m. to 2 p.p.m. and 0·5 to 1 p.p.m., respectively. Residence time in all instances was 40 min.

Nonirradiated mixtures of ozone and 1-pentene, 1-hexene, and 3-heptene caused typical oxidant injury on the 14-day-old primary leaves of pinto bean but did not injure the 8-day-old bean or petunia leaves. By contrast, when these mixtures were irradiated, the reaction products caused injury to petunia and 8-day-old bean leaves comparable with that caused by irradiated automobile exhaust and by mixtures of nitrogen dioxide plus olefin. No plant damage was obtained from ozone–*cis*-2-butene mixtures, either irradiated or nonirradiated, and this is in accordance with previous work (DARLEY, *et al.*, 1960). Plant damage has been obtained from *cis*-2-butene only when it is in the presence of photolyzed nitrogen oxides.

VOL. 4 1961

With the exception of 2-butene, oxidant-type injury was obtained from all of the nonirradiated ozone-olefin mixtures used in the experiments. Furthermore, irradiation of these mixtures of ozone and olefin caused damage on petunia and 8-day-old bean leaves. It is apparent that when certain products of ozone-olefin reactions are irradiated, phytotoxicants other than those formerly termed " oxidants " are formed (HAAGEN-SMIT, *et al.*, 1952).

Irradiated Aldehydes

Aldehydes are products of ozone-olefin reactions and they absorb radiation at the wave length emitted by the blacklite tubes (see Fig. 7). Therefore, the corresponding aldehydes (except valeraldehyde) of the ozone-olefin experiments were irradiated in static systems and the products passed over petunias and two ages of bean plants.

Phytotoxic materials were produced from the irradiated aldehydes, which could account for the additional injury obtained from irradiated ozone-olefin reactions as compared to those same reactions not irradiated. Furthermore, the phytotoxicants from the irradiated aldehydes affect the same plants and same ages of leaves as do the phytotoxicants from photolysis of nitrogen dioxide plus hydrocarbon mixtures, but do not affect the 14-day-old bean leaves (see Fig. 10) which are damaged typically by nonirradiated ozone-olefin mixtures.

Peroxyacid

Photooxidation of aldehydes is known to yield peroxyacid as a major product (MCDOWELL and FARMER, 1954). To explore this possibility, plants were fumigated

with peracetic acid vapor (at 0.5 p.p.m., as indicated by potassium iodide analysis). An atypical spotting occurred on 14-day-old bean leaves, but no damage occurred on 8-day-old beans.

Fumigation with hydrogen peroxide in very high concentrations confirmed earlier findings (Haagen-Smit, *et al.*, 1952) that this material could cause oxidant injury. In the present study, hydrogen peroxide caused typical oxidant injury of 14-day-old beans but caused only atypical injury on 8-day-old beans and petunias.

Thus it is evident that oxidant damage occurs from the irradiated olefin-nitrogen dioxide mixtures and from ozone-olefin reactions, but the phytotoxicants from the two systems are different as to species and age of tissues affected and longevity. The phytotoxicant from irradiated ozone-olefin reactions is, however, similar to irradiated olefin-nitrogen dioxide mixtures.

Pan

As noted in the foregoing, the one compound common to all the irradiated oxides of nitrogen mixtures was PAN.

Purified samples of PAN diluted with clean air (filtered through activated carbon) have been used in 16 experiments to fumigate petunias and two ages of pinto bean plants. The plant damage from this compound, in dilutions ranging from 5 p.p.m. for 1 hour to 0·1 p.p.m. for 5 hours, consistently caused leaf damage indistinguishable from that caused by the products of the photolysis of nitrogen dioxide plus hydrocarbon and the photolysis of mixtures of automobile exhaust, and from much of the damage from polluted ambient air. The higher concentrations of PAN caused severe glazing and bronzing of the entire lower surface of 8-day-old pinto bean leaves but caused no damage on 14-day-old bean leaves. Damage on young expanding petunia leaves was typically the bleached banding on the upper surface, usually accompanied by a somewhat larger area of glazing and bronzing of the lower leaf surface (see Fig. 11). Exposure for 5 hours to concentrations of 0·1 p.p.m. caused moderate damage on 8-day-old bean leaves (see Fig. 12) and severe injury on petunia leaves. The dilutions of PAN were mixed in the long-path cell, monitored with the infrared spectrometer, then passed across plants in the box. In one experiment, the diluted PAN was prepared one evening and allowed to stand in the long-path cell until the following morning (approximately 16 hours), then was passed over the test plants. The infrared spectrum showed that much (but not all) of the PAN had decomposed overnight. Nevertheless, there was still sufficient phytotoxicant to cause moderate damage on both the petunia and the young bean plants. The longevity of PAN is considerably greater than the phytotoxicant from ozone-olefin reactions (Arnold, 1959; Darley, *et al.*, 1958).

An improved method of dispensing PAN has been employed in more recent experiments. The sample of PAN was introduced (under vacuum) into a low-pressure oxygen tank, then carefully pressurized with nitrogen gas to 40 psi. The diluted PAN can be metered from this tank into a plant exposure box, located in natural sunlight at any rate necessary to maintain a constant calculated concentration of PAN. Plant symptoms obtained with this system of dispensing are identical with those previously described. In a preliminary test, there was no detectable decomposition of the dilute PAN (158 p.p.m. in the nitrogen atmosphere of the pressurized tank) over a 12-day period. With such stability of the material, extensive experiments may be con-

VOL.
4
1961

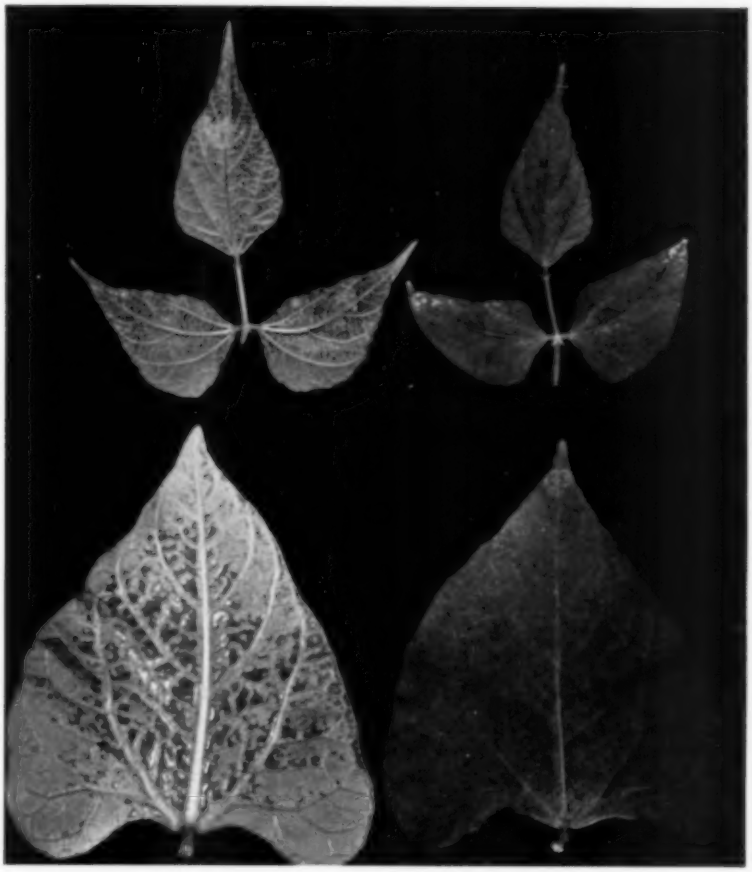

FIG. 9. Oxidant Glazing on Lower Surface of Trifoliate (Upper Left) and 8-Day-Old Primary (Lower Left) Leaves of Pinto Beans Caused by Irradiated Dilute Mixture of Exhaust from a Cruising and an Accelerating-Decelerating Automobile. Upper Surface of Corresponding Leaves on Right

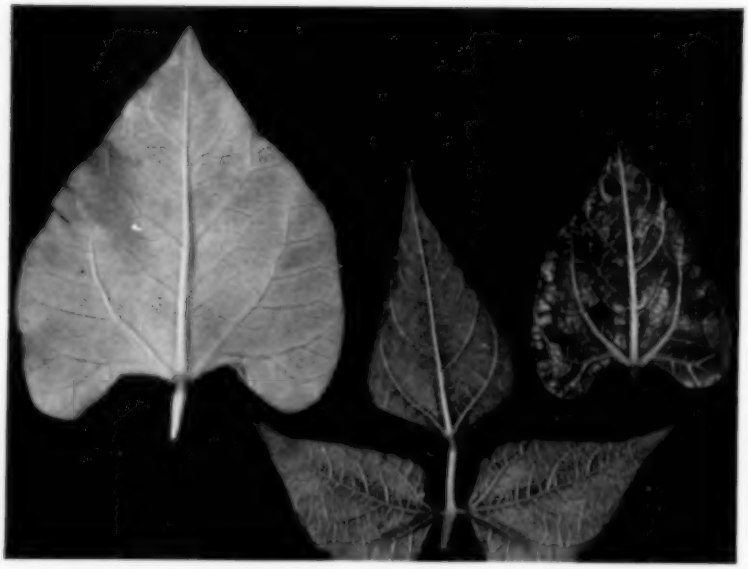

FIG. 10. Irradiated Propionaldehyde Caused Glazing on the Lower Surface of Trifoliate and 8-Day-Old Pinto Bean Leaves (Right), but Did Not Injure 14-Day-Old Leaves (Left)

VOL.
4
1961

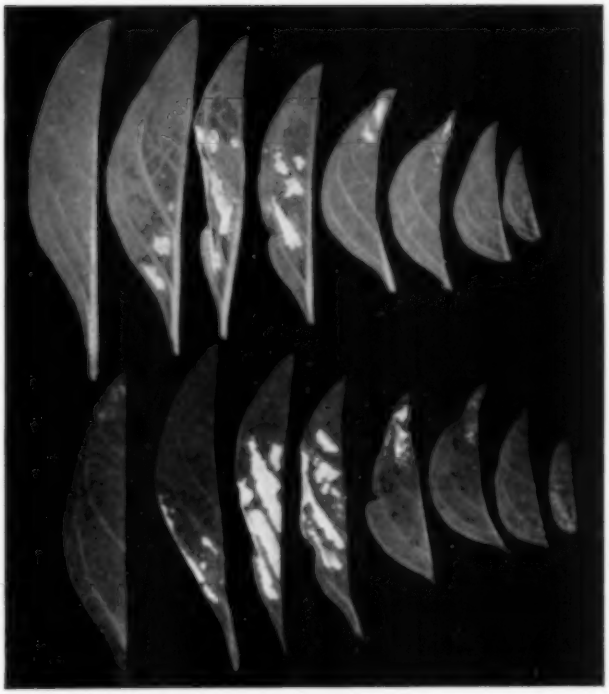

FIG. 11. PAN (0·1 ppm) Caused Glazing on Lower Surface of Expanding Petunia Leaves (Top) and Bleached or Collapsed Bands on Upper Leaf Surface (Bottom). No Injury Occured on Older or Very Young Leaves

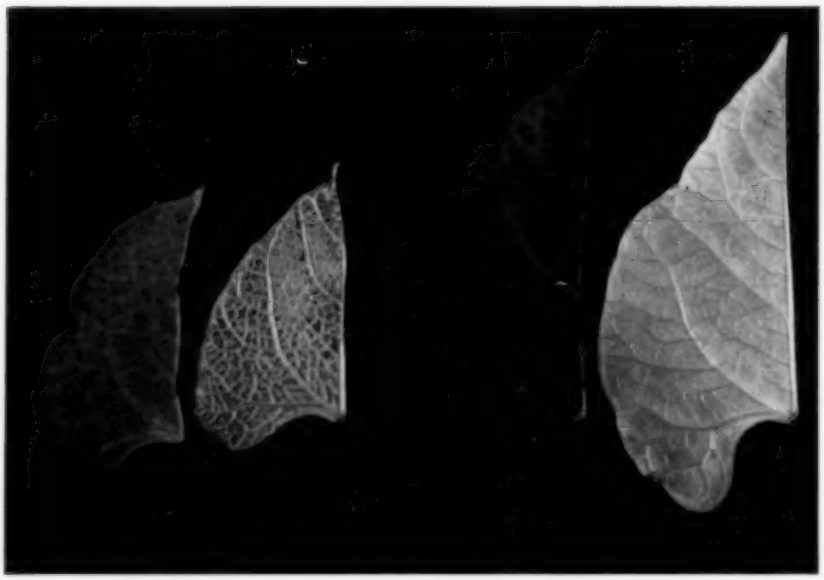

FIG. 12. PAN (0·14 ppm for 5 Hours) Caused Glazing of Lower Surface of 8-Day-Old Primary Leaf of Pinto Bean (Left), but Caused No Injury on 14-Day-Old Primary Leaf (Right)

ducted with a single tank of the material. It is also possible, with this system, to use calculated concentrations of PAN in the plant experiments which are much lower than those which can be detected by any of the available methods. An extensive study is planned of the response of a variety of plants to this material, both as to growth and as to visible injury. This will be greatly facilitated by the new method of dispensing PAN.

DISCUSSION

It is recognized that PAN is only one member of a homologous series of compounds, the other members of which may be more or less active than PAN in regard to eye irritation and plant damage. The infrared spectra of the products of the ethylene-nitrogen oxide photoreaction show no evidence of the presence of a formyl derivative, so it is believed that this one-carbon compound is not stable. The three-carbon compound may, on the other hand, be more stable than the acetyl compound, and plans are being made to prepare and purify this member of the series.

At the present time there is not sufficient evidence for ascertaining the relative importance of formaldehyde, acrolein, and PAN as eye irritants in photochemical air pollution because data on the concentrations of these three materials in polluted air are lacking. The limited data available indicate that these concentrations are approximately one order of magnitude lower than the concentrations necessary to produce significant irritation of a test panel. A number of factors may be suggested to explain this discrepancy: 1, the small size of the test panel compared to the population exposed to natural air pollution; 2, the short duration of the exposure of the test panel; 3, the simultaneous presence of several irritants in natural air pollution; and, 4, the exposure of the eyes to bright sunshine, which may increase their sensitivity. There remains the possibility that other irritants remain undiscovered. On the other hand, the importance of PAN as a plant toxicant seems established even by the limited studies so far completed. Prior to these studies, it was generally assumed that noxious properties of photochemical air pollution should be ascribed to various oxidized organic materials and that the role of the nitrogen oxides was simply that of a photoinitiator. With the recognition of PAN, which contains oxidized nitrogen, as an eye irritant and plant toxicant, the role of the nitrogen oxides assumes greater importance.

Acknowledgments—JOHN ENGLISH and EUGENE CARDIFF, of the University of California at Riverside, and JOHN LOCKE, of W. E. Scott and Associates, participated in the studies reported herein.

These studies were partly supported by the Smoke and Fumes Committee of the American Petroleum Institute. This support and the encouragement of the Research Advisory Committee are deeply appreciated.

A portion of the work reported herein was carried out while two of the authors (E. R. STEPHENS and W. E. SCOTT) were with The Franklin Institute Laboratories, Philadelphia, Pa.

REFERENCES

American Conference of Governmental Industrial Hygienists (1958) Threshold Limit Values for 1958. *A.M.A. Arch. Ind. Health* **18,** 178–82.

ARNOLD W. N. (1959) The Longevity of the Phytotoxicant Produced from Gaseous Ozone-Olefin Reactions. *Intern. J. Air Pollution* **2 [2],** 167–74.

DARLEY E. F., STEPHENS E. R., MIDDLETON J. T. and HANST P. L. (1958) Oxidant Plant Damage from Ozone-Olefin Reactions. *Proc. API* **38 [III],** 313–23; *Intern. J. Air Pollution* **1 [3],** 155–62 (1958).

VOL. 4 1961

Darley E. F., Middleton J. T. and Garber M. J. (1960) Plant Damage and Eye Irritation from Ozone-Hydrocarbon Reactions, *J. Agric. Food Chem.* **8**, 483–5.

Haagen-Smit A. J. (1952) Chemistry and Physiology of Los Angeles Smog. *Ind. Eng. Chem.* **44 [6]**, 1342–6.

Haagen-Smit A. J., Darley E. F., Zaitlin Milton, Hull Herbert and Noble W. M. (1952) Investigations on Injury to Plants from Air Pollution in the Los Angeles Area. *Plant Physiol.* **27 [1]**, 18–34.

Haagen-Smit A. J. and Fox M. M. (1956) Ozone Formation in Photochemical Oxidation of Organic Substances. *Ind. Eng. Chem.* **48 [9]**, 1484–7.

Harton E. E. Jr. and Bolze C. C. (1958) Eye Irritation from Solar Radiation of Organic Compounds and Nitrogen Dioxide. *Report No. 23*, Air Pollution Foundation, San Marino, Calif.

Heggestad H. E. and Middleton J. T. (1959) Ozone in High Concentrations as Cause of Tobacco Leaf Injury. *Science* **129 [3343]**, 208–10.

McDowell C. A. and Farmer J. B. (1954) The Kinetics of the Thermal and Photochemical Oxidation of Acetaldehyde, Fifth Symposium (International) on Combustion, Pittsburgh, Pa., Sept. 1954.

Middleton J. T., Darley E. F. and Brewer R. F. (1957) Damage to Vegetation from Polluted Atmospheres. *Proc. API* **37 [III]**, 184–91.

Noble W. M. (1955) Pattern of Damage Produced on Vegetation by Smog. *J. Agr. Food Chem.* **3 [4]**, 330–2.

Pictet A. and Khotinsky E. (1907) Über Acetyl Nitrate. *Ber.* **40**, 1163–6.

Richards B. L., Middleton J. T. and Hewitt W. H. (1958) Air Pollution with Relation to Agronomic Crops: V. Oxidant Stipple of Grape. *Agron. J.* **50**, 559–61.

Schuck E. A. (1957) Eye Irritation from Irradiated Auto Exhaust. *Report No. 18*, Air Pollution Foundation, San Marino, Calif.

Schuck E. A., Ford H. W. and Stephens E. R. (1958) Air Pollution Effects of Irradiated Automobile Exhaust as Related to Fuel Composition. *Report No. 26*, Air Pollution Foundation, San Marino, Calif.

Schuck E. A. and Doyle G. J. (1959) Photooxidation of Hydrocarbons in Mixtures Containing Oxides of Nitrogen and Sulfur Dioxide. *Report No. 29*, Air Pollution Foundation, San Marino, Calif.

Scott W. E., Stephens E. R., Hanst P. L. and Doerr R. C. (1957) Further Developments in the Chemistry of the Atmosphere. *Proc. API* **37 [III]**, 171–83.

Stephens E. R., Hanst P. L., Doerr R. C. and Scott W. E. (1956) Reactions of Nitrogen Dioxide and Organic Compounds in Air. *Ind. Eng. Chem.* **48, [9]**, 1498–1504.

Stephens E. R., Scott W. E., Hanst P. L. and Doerr R. C. (1956) Recent Developments in the Study of the Organic Chemistry of the Atmosphere. *Proc. API* **36 [III]**, 288–97; *J. Air Poll. Control Assoc.* **6**, 159–65.

Stephens E. R., Hanst P. L., Doerr R. C. and Scott W. E. (1959) Auto Exhaust: Composition and Photolysis Products. *J. Air Pollution Control Assoc.* **8 [4]**, 333–5.

Stephens E. R. and Schuck E. A. (1958) Air Pollution Effects of Irradiated Auto Exhaust as Related to Fuel Composition. *Chem. Eng. Progr.* **54 [11]**, 71–7.

Stephens E. R., Scott W. E., Hanst P. L. and Doerr R. C. (1959) Atmospheric Ozone-Olefin Reactions, paper presented at a meeting of the American Chemical Soc., Atlantic City, N. J., Sept. 1959.

Taylor O. C., Stephens E. R., Darley E. F. and Cardiff E. A. (1960) Effect of Air-borne Oxidants on Leaves of Pinto Bean and Petunia, *Proc. Am. Soc. Hort. Sci.* **75**, 435–44.

Int. J. Air and Water Poll. Pergamon Press 1961. Vol. 4, Nos. 1/2, pp. 101–105. Printed in Great Britain.

DIFFERENTIATING NEEDLE BLIGHTS OF WHITE PINE IN THE INTERPRETATION OF FUME DAMAGE*

GEORGE H. HEPTING and CHARLES R. BERRY
Division of Forest Disease Research,
Southeastern Forest Experiment Station,
U.S. Dept. Agriculture, Forest Service.
(*Received* 20 *June* 1960)

EASTERN white pine (*Pinus strobus*) is subject to an unusually large assortment of maladies, many of which could be, and have been, confused with fume damage. White pines, eastern and western, are regarded as sensitive to such pollutants as sulfur dioxide and fluorine. Recently HIRT of Syracuse (1959) put together a bibliography of diseases of eastern white pine. This included 24 references dating back to 1908 dealing with phases of the white pine needle blight complex. The titles of these papers indicate that needle fungi, root fungi, weather, air pollution, a virus, aphids, and other agents have been suspected, but few proven, as causing needle blights of this species. One of these papers, dealing with a prominent type of needle blight, was entitled " Needle Blight, Mystery Disease of White Pine "—a name that would still fit one of the most common blight types.

VOL. 4 1961

White pine typically bears three years' needles in summer and two in winter. However, very vigorous leaders or laterals may, by November of any given year, have only one year's needles still attached, and they may not extend all the way back to the first node. This habit on the part of many healthy trees to retain only the current year's foliage must be understood in interpreting needle shedding in connection with possible fume damage.

In the southern Appalachians there are two fungus needle blights that can be quite readily identified:

Bifusella blight

This is caused by the fungus *Bifusella linearis*. It occurs in local patches rather than over large areas, and is not noticeable on the current year's needles. Older needles can become blighted, the dead portions usually extending from the tip part way to the base, with the dead parts bearing large, black, long, raised fruiting-bodies of the fungus. It is easily identified.

Brown spot

This is caused by the fungus *Scirrhia acicola* that causes the well-known needle blight of longleaf and loblolly pines. White pines on localized areas have been found affected by this disease in recent years in the southern Appalachians. The current year's foliage may show tipburn symptoms early the first winter. Older needles become partly or entirely blighted, and a striking aspect of this disease on white pine is the copious shedding of affected foliage, usually in the spring of the second year. Small,

* Presented at 3rd. National Air Pollution Research Seminar, New Orleans, La., March 23, 1960.

black fruiting-bodies are evident on the needles by the time they shed, so this blight can usually be readily identified.

Besides the clear-cut, fungus-caused needle blights, there is a very general syndrome commonly referred to as white pine blight, involving to a greater or less degree browning of needle tips or whole needles, shortening of shoot growth, shortening and yellowing of needles, premature shedding of needles, general thinning of the crown, often death of the trees, but lack of any clear relation to a pathogen. Parts of this syndrome have been observed practically wherever eastern white pine grows, from Canada to Georgia, and through the Central and Lake States. The condition that is characterized mainly by perennially short shoot growth and yellow and short needles, with no pathogen evident, has been referred to as chlorotic dwarf. This condition is common with some planted trees from the time they are set out. At this point it should be emphasized that the terms white pine blight and chlorotic dwarf are simply symptom complexes and do not imply anything with regard to the causes.

The most widespread type of blighting, the so-called mystery disease, may occur only during certain years or may recur perennially on certain specific trees. It is characterized mainly by a browning of the distal parts of needles during the growing season. Henceforth, this will be referred to as emergence tipburn, because it occurs only during the period of needle growth and because the distal parts of the needles die. This is probably the commonest type of blighting observed over the East, and its cause, if it is a single entity, is not known. FAULL (1922) and his associates working in New England, and later LINZON (1958) working in Canada, have listed means by which they distinguished emergence tipburn from fume damage. TOOLE (1949) summarized studies made on this condition in the southern Appalachian region up to that time. He, like others, called attention to the marked tree-to-tree variation in blighting, the fact that large trees could be killed in a few years, and added that trees hit during successive years with tipburn alone could finally develop typical chlorotic dwarf symptoms in which the needles emerge yellow and stay short. For the characteristics of what we call emergence tipburn and for what appear to have been stack-gas effects in the Northeast, reference is made to the numerous publications of FAULL (1919) and the later work of LINZON (1958, 1960).

Because of chronic blighting of the foliage of white pine in recent years in east Tennessee, the U.S. Forest Services and Tennesee Valley Authority have renewed investigation of the white pine blight complex. One of the primary objectives has been to learn how to distinguish and separate the needle troubles occurring on white pine in the Southeast that can not now be attributed to a pathogen. The following are three that can be recognized as distinct entities:

Emergence tipburn

This is probably the same as the common " mystery " disease of the past, mentioned earlier, the cause of which has defied so many researchers. During the growing season, the distal parts of the needles become reddish-brown, then brown, and later grayish, after which the dead tips usually break off. Only the current year's needles are affected. A given tree is generally quite uniformly affected, and its needles may be dead just a short way back from the tips, or for most of their length. The affected needles are not shed prematurely. There is a marked tendency for the same trees to show this trouble during " blight " years, indicating genetic susceptibility, and for

neighboring trees to remain consistently free from it. The line of demarcation between the dead and living part of the needle is very sharp, and usually is a yellow-green band. During certain years, emergence tipburn may occur over large areas throughout the East, and in other years it is hard to find. It may recur perennially, and dominant trees have been known to die of it, but it is often not damaging in the southern Appalachians, and growth becomes normal between " blight " years. Dead root ends are common with this condition, and it is likely that the degree of recovery between attacks depends upon extent of root dying during attacks. If one can follow this condition from its onset during the growing season on specific trees, its identity can usually be established.

LINZON (1960) gives a good up-to-date account of this blight in Canada, and regards it as a physiogenic disturbance.

Post-emergence acute tipburn

This is a sudden browning of some or all of the foliage, often involving the entire length of the needles, that may occur at any time of year. Both current and old needles may be affected. Needles may shed, in quantity, shortly after the damage appears. This condition has been observed following accidental, very localized, heavy fumigation with chlorine, and experimental, confined fumigation with sulfur dioxide at levels beyond any known to occur in areas of white pine blight in Tennessee. It has also been observed occasionally on white pine near soft-coal-burning steam plants.

VOL.
4
1961

Post-emergence chronic tipburn

This condition may be a result of certain industrial stack gases. It is particularly similar to emergence tipburn in many respects, including the marked tree-to-tree variation from none to severe blighting, the often shortened and somewhat yellowish foliage, the marked reduction in shoot growth that accompanies severe blighting, and the frequent involvement of current year's needles. It differs, however, in that the needle browning may appear at any time of year rather than just during the growing season, and also in that the needles usually show a gradual dieback from the tips, with a gradient from brown at the tip to green at the base, with some mottling of the green parts, whereas in the case of emergence tipburn the line of separation of blighted and unblighted tissue is sharp.

If this condition is due to air pollution in east Tennessee—and that must be considered a possibility there and in some other areas—extensive analyses for sulphur from samples collected of current and older foliage on blighted trees from many localities near sources of coal smoke have failed to show elevated concentrations, and thus failed to indict sulfur dioxide. Analyses for fluorine on similar samples collected by TVA have failed to show concentrations of fluorine that appear at all likely to lead to blighting of foliage. Post-emergence chronic tipburn, when severe, affects trees systemically, with the foliage consistently short, often off-color, and with brown tips. The shoot growth becomes progressively shorter. Extensive root mortality accompanies this condition, involving not only the fine feeder roots, but also roots up to one-half inch or more in diameter.

Thirteen hundred isolations from root systems of such trees have failed to yield a single pathogen, and the occurrence of the trouble from creek bottoms to hilltops makes a relation to soil moisture unlikely. If post-emergence chronic tipburn is due

to air pollution, it must result either from gases not yet identified in connection with it, or to long-time effects of concentrations of sulfur dioxide or fluorine so low that their accumulation in toxic amounts has not been demonstrated in the analyses made so far.

TABLE 1. MEANS OF DISTINGUISHING FIVE NEEDLE BLIGHTS OF WHITE PINE THAT OCCUR IN THE SOUTHERN APPALACHIANS

Symptom	Disturbance				
	Bifusella linearis	*Scirrhia acicola*	Emergence tipburn	Post-emergence chronic tipburn	Post-emergence acute tipburn
Needles affected	Current	Current	Current	Any	Any
Time of obvious blighting	In spring when needles are 1 year old	In spring when needles are 1 year old	In summer when newly emerging	Any season	Any season
Margin *	Sharp	Sharp	Sharp	Indefinite	Usually sharp
Fruiting bodies of causal fungus	Large, black	Small, black	None	None	None
Mottling	None	Discrete spotting	None	Common	None
Needle shedding	Sometimes	Profuse in spring	None	Profuse with second-year needles	Sometimes
Onset	Sudden	Gradual	Sudden	Gradual	Sudden

* The point or area between the dead distal parts of needles and the living proximal parts.

In Table 1 an attempt has been made to provide means of identifying and separating needle blights of white pine in the southern Appalachians.

In addition to the white pine blights already mentioned, aphids clustering along new shoots have been reported to cause an irregular needle dieback, the length of the dead part varying among the needles of the same fascicle from none to most of a needle. In the case of one species of shoot aphid, attack thinned the crowns and made the new shoots very limp (HOFFMAN *et al.*, 1957). Root aphids of the genus *Prociphilus* have been suspected by TOOLE (1949) and by DAVISON (1950) as being capable of causing foliar blighting, and the root rot caused by *Fomes annosus* can cause crown thinning in the latest stages before death or windthrow. This latter disease, however, can be identified by the rot and the fungus sporophores, and should not be difficult to diagnose. Nematodes have also been getting some attention on white pine, and many species have been found in the soil around white pine roots. Another factor that can

add to the problem of identification when aerial surveys are being made for white pine blights is the tendency of the upper crowns of white pine to have very sparse foliage when heavy seed crops are produced.

The Canadians, who are doing interesting work with the white pine blights, the TVA, and the U.S. Forest Service, through a wide variety of investigations, including analytical work, culturing, grafting, transplanting, fertilizing, pruning, and the use of many other techniques, expect to get to the bottom of most of the elements that make up the white pine blight complex, particularly the two that we call emergence tipburn and post-emergence chronic tipburn. White pine has developed a sickly appearance and many trees have died in the vicinity of certain soft-coal-burning steam plants. It has proven to be difficult to assess the possible role of air pollution in such cases unless one can clearly differentiate the symptoms of fume damage from those of other troubles that so often occur in the same areas.

REFERENCES

DAVISON A. T. (1950) *Root aphids of the genus Prociphilus on pines in the Duke Forest.* Master's Thesis, Duke University, 17 pp.

FAULL J. H. (1919–1920) Needle blights of white pine. *Rpt. Dept. of Lands and Forests*, Toronto.

FAULL J. H. (1922) Some problems of forest pathology in Ontario—Needle blight of white pine. *J. Forestry* **20,** 67–70.

HIRT R. R. (1959) *Pinus strobus* L. A literature review and discussion of its fungous diseases in North America. State Univ. Col. of Forestry at Syracuse, New York, Tech. Pub. **82,** 90 pp.

HOFFMANN C. H., HEPTING G. H. and ROTH E. R. (1947) A twig droop of white pine caused by *Pineus*. *J. Econ. Ent.* **40**(2), 229–31.

LINZON S. N. (1958) The influence of smelter fumes on the growth of white pine in the Sudbury region. Ontario Dept. of Lands and Forests and Ontario Dept. of Mines, 45 pp.

LINZON S. N. (1960) The development of foliar symptoms and the possible cause and origin of white pine needle blight. *Canad. J. Bot.* **38,** 153–61.

TOOLE E. R. (1949) White pine blight in the Southeast. *J. Forestry* **47,** 378–82.

VOL. 4 1961

Int. J. Air and Water Poll. Pergamon Press 1961. Vol. 4, Nos. 1/2 pp. 106–114. Printed in Great Britain.

AEROBIC SLUDGE DIGESTION*†

N. JAWORSKI, G. W. LAWTON and G. A. ROHLICH
Hydraulic and Sanitary Laboratories, University of Wisconsin, Madison, Wisconsin

INTRODUCTION

MOST of the experimental studies which have been reported on aerobic digestion of domestic sewage sludges have been on mixed liquors with suspended solids concentrations of less than 10,000 p.p.m. Some work has been done on aerobic digestion (fermentation) of sludges at higher concentrations.

In 1950 COACKLEY (1955, 1958) carried out a series of experiments to determine the extent of aerobic digestion of sludge which had been previously subjected to anaerobic digestion. In one series, the anaerobically digested sludge was aerated without inoculation by aerobic organisms. Another series was inoculated with aerobic organisms found in a compost heap. The third series continued the anaerobic digestion of the sludge. The three series were carried on up to 71 days of digestion with temperatures of 18° C. and 37° C.

Although COACKLEY was primarily interested in the dewatering characteristics of the sludge, he also observed the reduction of solids and organic nitrogen. At a temperature of 18° C., the reduction of volatile solids after 48 days of digestion was not appreciable, even in the inoculated series. In the 37° C. non-inoculated series, the volatile solids were reduced from 2·98 per cent to 1·08 per cent after 47 days, while in the inoculated series, they were reduced from 2·66 per cent to 1·52 per cent. A decrease in organic nitrogen was also noted in the aerobic units which did not occur in the anaerobic series. The aerobic series produced a stable sludge which showed no signs of decomposition when left without aeration. Anaerobic digestion could not be initiated in this series even after the digesters were inoculated with anaerobic organisms.

MURPHY (1959) studied the effects of aeration on the filterability and the settleability of sewage sludges. He used primary and waste activated sludges, mixed at a ratio of 1 : 1 by volume, and aerated the sludges for various lengths of time at controlled temperatures. Most of his work was done at 15° C. He concluded that the reduction of volatile solids at 15° C. with digestion times up to six days was not appreciable.

AKERS (1959) of Iowa University investigated some of the factors that may influence the auto-oxidation (endogenous respiration) rate of biological sludge. Two primary factors were considered in his study:

(1) the effect of auto-oxidation rate on the mean sludge age (pounds of suspended volatile solids in the system divided by the pounds of suspended volatile solids into the system daily);
(2) the effect of separate aeration (aerobic digestion) of the mixed liquor without additional substrate being added during the aeration period.

* The work herein reported was supported by a grant from the Walker Process Equipment Company, Aurora, Illinois.

† Paper presented at the Conference on Biological Waste Treatment, Manhattan College, April 20–22, 1960.

In his study the average reduction in volatile solids in 8 days at 23° C. was greater than 20 per cent. The corresponding reductions in suspended volatile solids, BOD, and COD were 30, 60 and 35 per cent respectively.

His study also indicated that the rate of change of auto-oxidation is considerably less than the rate of change of the sludge age.

ECKENFELDER (1956) studied aerobic digestion using waste activated sludge from a conventional activated sludge plant. Four-liter digesters were aerated for a period of seven days with the temperature maintained at 25° C. At the end of the seven day period of aeration, his data showed a reduction in COD of 48·5 percent, a reduction in suspended volatile solids of 38·2 per cent, and a decrease in volatile solids content from 76·5 to 63·5 per cent. The soluble nitrogen increased from 46 p.p.m. to 94 p.p.m. in the 7 days of aeration.

The work reported herein was undertaken to study the effects of temperature, time, and loading rates on the aerobic fermentation of blends of primary and waste activated sludges. Both batch-type and incremental feeding (referred to as continuous feeding) studies were made. The sludges used were obtained from the east section of the Nine Springs Sewage Treatment Plant, at Madison, Wisconsin. This sludge is produced from a domestic waste comprised of approximately one-third pretreated meat packing waste and two-thirds domestic sewage.

EXPERIMENTAL APPARATUS

VOL. 4 1961

The digesters used in this study were 6-liter Erlenmeyer flasks with four inch diameter holes in the base. In operation, the flasks were inverted and placed in steel drums which served as constant temperature baths.

Air was supplied to the bottom of each digester by a glass tube inserted through a rubber stopper. These tubes produced air bubbles large enough to keep the digesters well-mixed in addition to supplying oxygen for the microbial population. The rate of air supplied to the digesters was measured by calibrated orifices and rated water manometers mounted on a nearby panel.

SKETCH OF AERATION APPARATUS

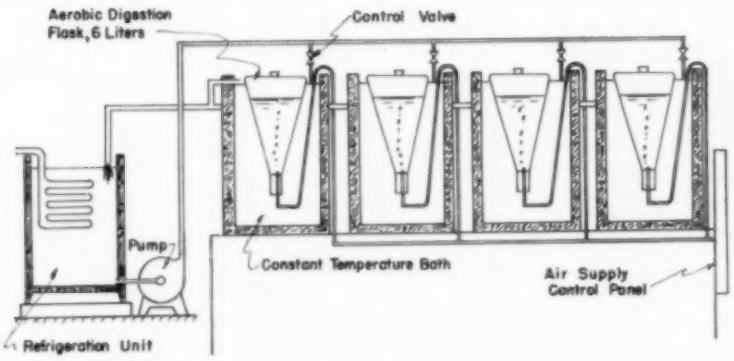

FIG. 1

The temperature was controlled separately in each bath by means of a 300 watt heating coil regulated by a precise temperature sensing element and relay. These controls held the temperature fluctuations in the baths to approximately plus or minus 0·5° C.

Cooling water from a refrigerated source was pumped into the baths by means of a 1/2 inch centrifugal pump and returned to the refrigerated tank by gravity. The flow to each bath was regulated separately, thus permitting more precise temperature control. A sketch of the aeration apparatus is shown in Fig. 1.

EXPERIMENTAL PROCEDURE

Batch Digestion Studies

Batch runs were made in which temperature, digestion time, and solids loading were varied. A starting volume of four liters of substrate was used in each of the digesters with 0·20 ft^3/m of air being supplied throughout the batch runs. Evaporation losses were made up with distilled water prior to daily sampling. The substrates were blends of primary and waste activated sludge.

Preliminary studies on a batch basis indicated that solids concentration and temperature were important variables. Aeration of sludges which had total solids concentrations of 0·75 and 3·06 per cent for six days at 20° C. gave COD reductions of 50 and 12 per cent respectively. At 0·75 per cent solids the reduction in volatile matter in six days ranged from 28 to 44 per cent for temperatures of 15° and 25° C. At a solids concentrations of 3·06 per cent reductions in volatile matter were considerably lower, being only 11 per cent at 15° C.

Continuous Digestion Studies

The feed used in the continuous digestion studies contained approximately 3·2 per cent total solids of which 70 to 80 per cent were volatile matter. This feed consisted of a 1,75 to 1·00 ratio (dry solids basis) of primary and waste activated sludges. The air rate was maintained at 0·20 ft^3/m per digester. The digesting volume was held at 4·00 liters throughout the study with evaporation losses being made up prior to daily sampling and feeding.

The detention time controlled the size of daily sample and loading rate. For example, with a 4000 ml. working volume and a 10-day detention time, a 400-ml. sample was withdrawn daily and the same volume of feed material added. With the feed being held constant at 3·2 per cent total solids (72·5 per cent volatile matter) the 10 day detention time fixed the volatile solids loading rate at 0·145 lbs/ft^3 of digester capacity per day.

Table I shows the detention times, sample sizes, loading rates, and temperatures used in the continuous digestion studies.

In the continuous feeding studies, digestion was carried on until equilibrium conditions were attained before analyses were made on a routine basis. The digestion was then continued for approximately one month with analytical data being obtained at intervals of one to three days. The data used in this report thus represent equilibrium conditions for each detention period considered. A total of eleven series of continuous aerobic digestions were conducted.

The effect of temperature and time of digestion on the volatile solids content of

TABLE 1

Detention Time days	Temperature (C°)	Volume of Sample (ml)	Loading Rate Volatile Solids (/ft³/day)
5	15	800	0·290
5	20	800	0·290
5	35	800	0·290
10	15	400	0·145
10	20	400	0·145
10	35	400	0·145
15	20	267	0·096
30	15	133	0·048
30	20	133	0·048
60	15	67	0·024
60	20	67	0·024

aerated sludge is shown in Fig. 2. The per cent reduction curves indicate that sharp increases in volatile solids removal take place as the detention time is extended up to about 12 days. Beyond that time the per cent reduction shows only moderate increases, indicating that for the temperatures considered the practical upper limit or detention time, as far as volatile solids reduction is concerned, is approximately 15 days. It is important to note that the loading rate varies inversely with the detention time in these studies, thus it appears that the maximum practical loading rates, based on per cent reduction in volatile solids, are approximately 0·1 lbs of volatile solids per cubic foot per day, again considering only volatile solids reduction.

VOL. 4 1961

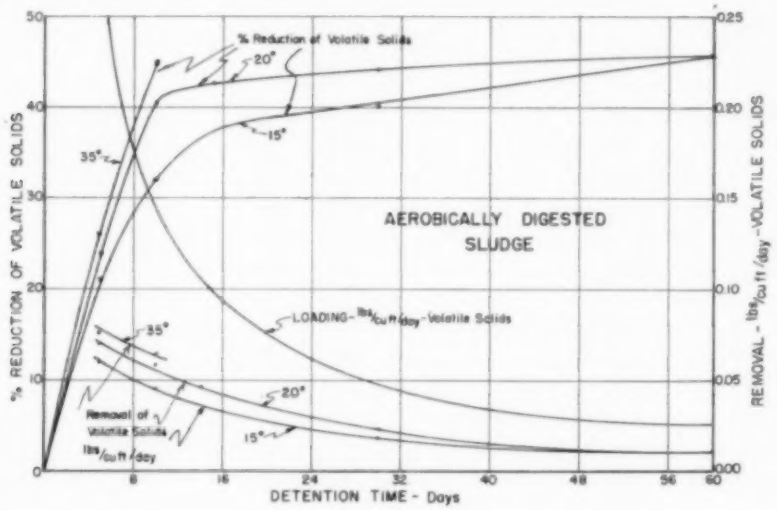

FIG. 2

Considering the volatile solids in terms of pounds removed per cubic foot of digester space per day it appears that short detention periods are definitely more practical. The efficiency of the digester, based on the pounds of volatile solids removal, increases as the loading rate increases, however other factors such as drainability, drying characteristics of the remaining solids, and supernatant characteristics must also be considered. The curves in this figure indicate that while temperature has an appreciable effect at short detention times, this effect decreases considerably as the time is lengthened (or the loading rate decreased). At an 8 day detention time the 35° C digester removed about 40 per cent more volatile solids per cubic foot than did the 15° C digester. On a percentage basis the removals range from 38 to 28 per cent respectively at the two temperatures.

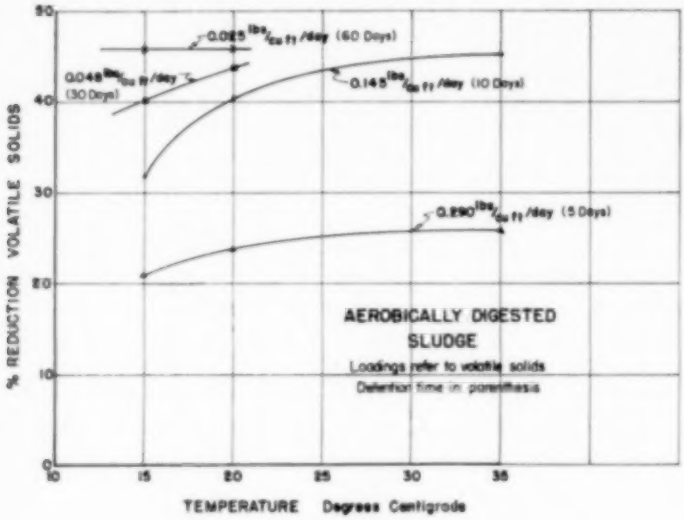

FIG. 3

Fig. 3 shows more clearly the effect of temperature on per cent reduction in volatile solids at various loading rates or detention times. For long detention times (60 days) temperature has little effect since digestion is essentially completed at all temperatures. For short detention times (five days) the effect of temperature also appears to be of minor importance, perhaps because of the heavy loadings to the digester. At intermediate detention times (and loadings) the temperature produces more noticeable effects on the volatile solids reduction, with the higher temperatures being more effective. Further studies at various loading rates for fixed detention periods would provide valuable supplementary data.

The effects of temperature and detention time on pH, alkalinity, and concentration of solids are presented in Fig. 4. The solids concentrations, total and volatile, show little change after 15 day detention periods at both 15° and 20° C. Alkalinity shows a gradual decrease for detention periods up to about 30 days at the temperatures studied. The alkalinity for the 60 day detention was at approximately the same level as for the 30 day detention period. The pH increased for detention periods up to about 10 days, to a maximum value of about 8·0, and then decreased gradually to values near 5·0.

These low pH values found at equilibrium in the long detention times are usually considered to be unsuitable for aerobic metabolism. However, in only one case did there appear to be appreciable build up of volatile solids in the digester after long aeration (65 days) following equilibrium conditions.

The effects of temperature and detention time on the concentration of ammonia,

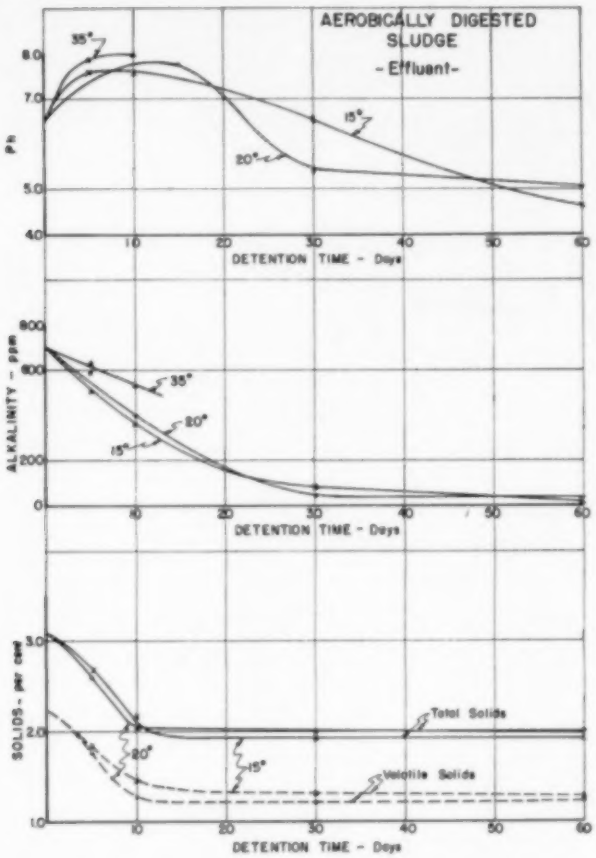

FIG. 4

nitrites, and nitrates are presented in Fig. 5. The curves in this figure indicate the usual relationship between ammonia, nitrites, and nitrates in aerobic fermentation. It is noted that more than 600 p.p.m. nitrate-nitrogen was formed at 60 days detention time, indicating that nitrification was proceeding uniformly even at the low pH levels present. (Summary data are given in Table 2.)

The drainability of the sludges was measured on gravity sand filters supported by filter paper in Buchner funnels. The volumes of filtrate were determined over periods of several hours. It was found that sludges digested for five days usually exhibited poorer drainability than undigested sludges, while sludges digested for 10 days or longer showed improved drainability. In general, for detention times of 10 days or more, 70 to 80 per cent of the original volume of the sludge appeared as filtrate within one

VOL. 4 1961

hour, as compared to about 40 per cent as filtrate in one hour from the untreated sludge. With detention times of 10 days or greater the effect of digestion temperature on drainability appeared to be of minor importance.

When digested sludges were dried for a period of four days, cracks appeared in the sludge cakes. No obnoxious odors developed during the drying process. The sludge cake, after one week of air drying was low in moisture content and held together firmly.

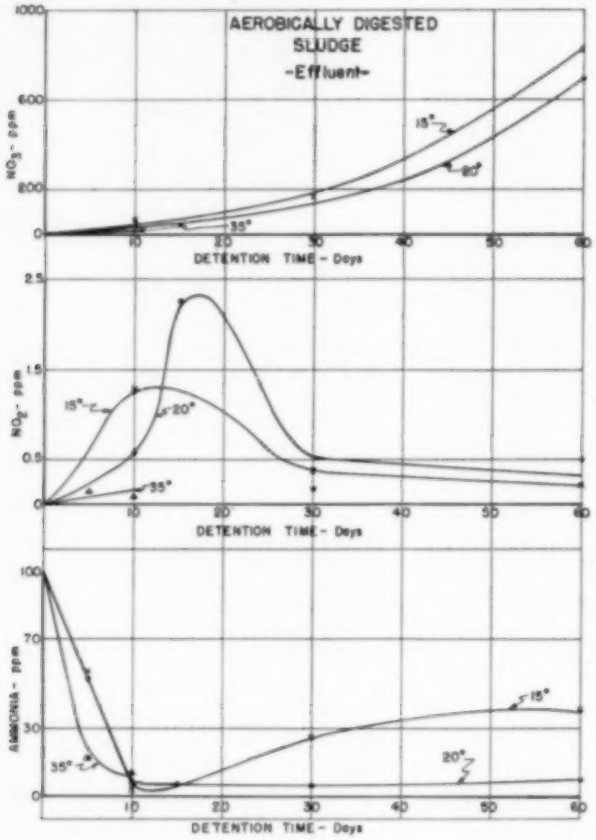

FIG. 5

Few of the digested sludges exhibited good settling characteristics. Sludges digested for short periods of time and at low temperatures showed poor settleability, perhaps due to the highly dispersed state of the undigested particles. Sludges that had been digested for 30 days showed formation of gas bubbles which caused the solids to float. In some cases the gas bubbles appeared in approximately one half hour, probably the result of denitrification of the sludge. The gasified sludges would not settle unless the gas bubbles were mechanically removed. Only the sludges digested for 60 days at 15° C and 20° C and those digested for 10 days at 35° C showed improved settling characteristics.

TABLE 2. SUMMARY DATA

Detention (days)	Temp. (° C)	V. Solids (% Red.)	ĥH	Alkalinity (p.p.m.)	NH_3 (p.p.m.)	NO_2 (p.p.m.)	NO_3 (p.p.m.)
5	15	21	7·6	510	54	tr	none
5	20	24	7·6	590	54	tr	none
5	35	26	7·9	630	14	0·18	none
10	15	32	7·6	380	3·2	1·28	64
10	20	41	7·6	390	4·9	0·59	60
10	35	45	8·0	540	10·0	0·08	none
15	20	43	7·8	560	7·0	2·27	29
30	15	40·5	6·6	81	4·0	0·36	170
30	20	44	5·4	31	28	0·19	275
60	15	46	4·6	23	38	0·23	835
60	20	46	5·1	35	7·0	0·51	700

The BOD values of the supernatant liquors were less than 100 p.p.m. in all samples analysed with the exception of one liquor from a digester having a 10 day detention time. The values ranged from 25 to 78 p.p.m. with the exception of the one value of 170 p.p.m. The COD values of the supernatant liquors analysed ranged from 360 to 670 p.p.m. for the various time and temperature conditions studied. (See Table 3.)

VOL. 4 1961

TABLE 3. SUPERNATANT CHARACTERISTICS

Detention (days)	Temperature (° C)	BOD (p.p.m.)	COD (p.p.m.)
5	35	76	670
10	15	170	—
10	20	55	—
10	35	30	360
15	20	25	440
30	15	78	—
30	20	37	—
60	20	25	460

At the end of the final series of the continuous digestion study, the digesters were adjusted to a pH of 7·2 with caustic soda and aerated without further feeding. The pH was maintained at 7·2 and aeration continued for 47 days. The volatile solids content of the sludges decreased from an average of about 62 per cent down to 55 per cent in those digesters where detention times previously had been 10, 15, and 60 days. In the digester which previously had a five day detention period the volatile solids content decreased from 70 per cent down to 47 per cent. It is likely that the former

sludges (10, 15, 60 day detention times) being more completely digested, had accumulated a greater amount of volatile matter which was more difficult to digest than had the sludge which originated from the five day detention period digester.

CONCLUSION

Data obtained from this study indicate that aerobic digestion of mixtures of raw and activated sludge is feasible. From a consideration of the results obtained it was concluded that:

1. Reduction of volatile solids is a function of detention time. However, beyond digestion periods of 15 days, only small increases in the reduction are obtained.
2. In general, greater reductions in volatile solids are obtained at higher temperatures of digestion.
3. In general, higher volatile solids removal is obtained at lower loading rates.
4. Settling characteristics of sludges digested for 30 days or less are generally poorer than those of the undigested sludges.
5. Sludges digested for periods greater than five days show satisfactory drainability characteristics.
6. Supernatant liquors from aerobic digesters exhibit relatively low BOD values when compared to anaerobic digester liquors.
7. Drying of aerobically digested sludges produces little odor.

REFERENCES

AKERS W. L. (1959) *The Effect of Sludge Age on the Auto-oxidation Rate of Long-term Aeration of Activated Sludge*. Unpublished Masters Thesis, University of Iowa.

COACKLEY F. (1955) Research on Sewage Sludge Carried Out in the C. E. Dept. of University College London. *J. Inst. Sew. Purif.*, 59–72 (1955).

COACKLEY P. (1958) Laboratory Scale Filtration Experiments and Their Application to Sewage Sludge Dewatering. *Biological Treatment of Sewage and Industrial Waste*, Vol. **2**, pp. 287–288. Reinhold, New York.

ECKENFELDER W. WESLEY (1956) Studies on the Oxidation Kinetics of Biological Sludges. *Sewage and Industrial Waste*, V. **28**, 983–989.

MURPHY K. L. (1959) *Sludge Conditioning by Aeration*. Unpublished Masters Thesis, University of Wisconsin.

Int. J. Air and Water Poll. Pergamon Press 1/2 pp. 115–138. Printed in Great Britain.

DEGRADATION OF NITROGEN-CONTAINING ORGANIC COMPOUNDS BY ACTIVATED SLUDGE*

J. M. SYMONS, R. E. MCKINNEY, R. M. SMITH and E. J. DONOVAN, JR.
Massachusetts Institute of Technology

INTRODUCTION

INTEREST in the biological degradability of nitrogen-containing organic compounds is twofold. First, if the nitrogen contained in the organic compound were available and sufficient for bacterial nutrient supplementation, no additional nitrogen would have to be added to promote unlimited bacterial growth. Second, as chemical and related industries continue to expand, the organic constituents of their waste streams become ever more varied. Some of these organics are nitrogen-containing; therefore, as industry attempts to reduce its pollutional load on receiving streams, it becomes important to know as much as possible about the biological degradability of nitrogen-containing organics. To deal effectively with this problem, the sanitary engineer must know how the type of nitrogen group, the number of groups, the position of the group on the organic molecule, and the structure of the organic molecule to which the nitrogen group is attached, will affect biological degradability.

VOL.
4
1961

LITERATURE SURVEY

A very brief literature review concerning the biological metabolism of the compounds used in this study will be given. An early mention of the availability of organic nitrogen was made by HELMERS, FRAME, GREENBERG, and SAWYER (1951). They presented the following table of organic nitrogen availability:

TABLE 1. AVAILABILITY OF ORGANIC NITROGEN IN VARIOUS WASTES

Waste	*Per Cent Nitrogen Available at 20° C*
Cotton Kiering	45
Rag-Rope	23
Brewery	72
Sewage (av.)	73

Later SAWYER (1956) in discussing his experiences at Sioux Falls, South Dakota stated that in biologically treating a combined domestic sewage and packing-house waste there was sufficient nitrogen release from the protein degradation to cause unusually severe problems of nitrification and denitrification.

Amino Nitrogen

Reports of alpha amino acid breakdown are widespread in the literature. Examples

* Paper presented at the Conference on Biological Waste Treatment. Manhattan College. April 20–22, 1960.

of the degradation of four alpha amino acids were given by TANG and HSUEH (1943) as follows:

Serine + $\frac{1}{2}O_2$ - - - - NH_3 + alpha-keto, beta hydroxy propionic acid
Aspartic Acid + $\frac{1}{2}O_2$ - - - NH_3 + alpha-keto succinic acid
Asparagine + $\frac{1}{2}O_2$ + H_2O - - $2NH_3$ + alpha-keto succinic acid
Glutamic Acid + $\frac{1}{2}O_2$ - - NH_3 + alpha-keto glutaric acid

Successful biological attack of the aromatic amine aniline by a pure culture of *Proactinomycetes* was demonstrated by MOORE (1949).

SAIAMOTO, UCHIDA and ICHINARA (1953) using Stanier's Method of Simultaneous Adaptation showed that o-aminobenzoic acid (anthranillic acid) was degraded through o-hydroxybenzoic acid (salicylic acid) and then to catechol. Catechol then splits into beta-keto adipic acid. Little appears in the literature concerning m-aminobenzoic, either with respect to its degradability or its method of breakdown. DURHAM (1956) using the Stanier Method with *Pseudomonas fluorescens* gave the metabolic pathway of p-aminobenzoic acid as: p-aminobenzoic acid to p-hydroxybenzoic acid to protacatechuic acid. The protocatechuic acid then breaks down to beta-keto adipic acid.

Nitro Nitrogen

KE, GEE, and DURHAM (1959) demonstrated, by Stanier's technique, the breakdown of o-nitrobenzoic acid to be through o-nitrosobenzoic and then to o-hydroxylamine benzoic acid. This they likened to the suggested reduction of nitrate nitrogen to ammonia nitrogen through hydroxylamine. They also showed that cells grown on o-nitrobenzoic acid were not adapted to o-aminobenzoic acid, o-hydroxybenzoic acid, or protocatechuic acid. The only mention of m-nitrobenzoic acid breakdown found in the literature was by CAIN (1957) who reported on an unsuccessful two-year attempt to culture bacteria on this substrate. DURHAM (1958) demonstrated by simultaneous adaptation that the first intermediate in the degradation of p-nitrobenzoic acid was p-aminobenzoic acid. Since he had already found the metabolic pathway of p-aminobenzoic acid, DURHAM (1956), the entire breakdown of p-nitrobenzoic acid was now defined. CAIN (1957) disagreed with this concept, however, as he found that bacteria grown on p-nitrobenzoic acid did not adapt to p-aminobenzoic acid. Little work has been done on the poly nitro benzoic acids.

Cyano Nitrogen

PAINTER and WARE (1955) isolated an organism, tentatively an *Actinomycetaceae*, from a trickling filter receiving sodium cyanide. This organism could convert the cyano nitrogen almost quantitatively to ammonia. More recently, NESBITT, KOHL and WAGNER, Jr. (1960) successfully treated 60 and 120 mg/l of cyanide as potassium cyanide by activated sludge. LUDZACK, SCHAFFER and BLOOMHUFF (1959) also reported on the metabolism of various organic cyanides (nitriles). Among others, they found that activated sludge units operated on acetonitrile and benzonitrile metabolized the nitrile satisfactorily. The nitrile concentrations studied were around 100 to 200 mg/l and the nitriles were mixed with settled sewage before treatment.

SELECTION OF COMPOUNDS

The compounds used in this study are given in Table 2.

TABLE 2. COMPOUNDS USED IN THIS STUDY

Class	*Compounds*
Complex Nitrogen Compound	Nutrient Broth
Amino Nitrogen Compounds	Alanine
	Propyl Amine
	Aniline
	o-amino Na benzoate
	m-amino Na benzoate
	p-amino Na benzoate
Nitro Nitrogen Compounds	o-nitro Na benzoate
	m-nitro Na benzoate
	p-nitro Na benzoate
	3,5-dinitro Na benzoate
	2,4,6-trinitro Na benzoate
Cyano Nitrogen	propionitrile
	benzonitrile

Note: Nitroso nitrogen compounds were commercially unavailable and therefore could not be studied.

VOL. 4 1961

Since there was some uncertainty as to the availability of the nitrogen in a complex organic material, a study was made using nutrient broth as the sole substrate for the activated sludge. Nutrient broth is a mixture of beef extract and peptone and is similar to a complex protein waste. On dilution, nutrient broth is nutritionally balanced and has an average COD/N ratio of 8·5/1 with 98 per cent of the nitrogen in the organic form.

To determine what effect the nature of the organic molecule to which the nitrogen group is attached has on degradability, the behaviour of alanine, propyl amine, and aniline was studied. These represented an alpha-amino acid, an alkyl amine, and an aromatic amine. To study the effect of position of the amino nitrogen group on an organic molecule, the o-, m-, and p-amino sodium benzoates were also investigated.

The study of the o-, m-, and p-nitro sodium benzoates was made to check the effect of position of the nitro nitrogen group on the molecule as well as to compare the results obtained with those obtained with the corresponding amino nitrogen compounds. This comparison will define the effect of the type of nitrogen group on metabolism. The two poly nitro compounds were investigated to determine the effect on the metabolism of the organic compound of having more than one nitro group in the molecule.

Two representative cyano nitrogen compounds were taken for study, one, propionitrile, to correspond to propyl amine and the other, benzonitrile, to correspond to aniline. It was felt that a study of the fourteen compounds listed above would give insight into the variables connected with the metabolism of nitrogen-containing organic compounds.

PROCEDURES

In general the procedures of this investigation followed those outlined below. The activated sludges were grown in 1·5-litre pilot plants. The aeration period was 23 hours. At the end of this time the air was shut off and settling allowed to occur for one hour. At the end of the settling period, 1·0 litre of supernatant liquor was withdrawn, 1·0 litre of Cambridge, Mass. tap water replaced, organics and buffer added, and aeration resumed. This cycle was repeated seven days a week for the duration of the study. No supplemental nitrogen was added to the systems.

The quantity of feed was based on C.O.D., the usual C.O.D. of the feed being 1000 mg/l. Control of the units was based on C.O.D. removal, MLSS (mixed liquor suspended solids), and pH. Occasionally, at the end of the aeration period, 25 ml of mixed liquor was passed through a weighed membrane filter which was then dried at 103° C and reweighed to determine the level of the MLSS. The membrane filtrate would then be analyzed for C.O.D. and all forms of inorganic nitrogen.

Investigation into the mechanism of operation of the systems was made on the Warburg Respirometer by two different types of tests. The first was a study of the possible metabolic intermediates occurring in the breakdown of the compound by the simultaneous adaptation method of Stanier's. Washed sludge, grown on the individual substrate, was placed in the Warburg Respirometer with low concentrations of several possible intermediates. The oxygen uptake was measured for six hours and at the end of that time the contents of each flask were passed through a membrane filter so that the filtrate could be analyzed for C.O.D. and the inorganic nitrogen forms. Acids were always fed as the sodium salts.

The second type of Warburg study was made by placing replicate samples of washed mixed liquor in the Respirometer flasks immediately after feeding. Then at various times during the next day a flask was removed from the Respirometer and its contents passed through a membrane filter. The filtrate was then analyzed for C.O.D. and all inorganic nitrogen forms. The change in C.O.D. and nitrogen was then correlated to the oxygen uptake to determine the mechanism of nitrogen release.

RESULTS

Complex Protein

Five systems were operated on a substrate of nutrient broth alone. The feed had an average C.O.D. of 1130 mg/l, an average organic nitrogen content of 131 mg/l, and an average ammonia content of 2·5 mg/l. The five units were all operated the same except for the sludge wasting. The units had respectively, 0, 100, 200, 400, and 600 ml of mixed liquor wasted every day just before the air was shut off at the end of the aeration period. The units were operated for 35 days. All five units operated well, giving good C.O.D. reduction throughout the test period. Only the 0- and 600-ml mixed liquor waste units will be discussed in detail as they represent the extreme conditions. In the 0-ml waste system the volatile suspended solids rose from 1100 mg/l to 4000 mg/l during the test period. At the same time the organic nitrogen in the sludge rose correspondingly so that the per cent nitrogen in the sludge remained steady at about 10 per cent. The volatile suspended solids in the 600-ml waste system held steady at about 500 mg/l during the entire run. Here again, although the data were a little erratic, the per cent nitrogen in the sludge averaged about 10 per cent for the

thirty-five days. The nature of the nitrogen forms in the effluents of these two systems, Fig. 1, are of interest. In both cases all or almost all of the nitrogen contained in the feed was released as inorganic nitrogen when the C.O.D. was removed. This nitrogen was then available for bacterial synthesis. The 10 to 15 mg/l of organic nitrogen recovered in the effluent was due mostly to suspended solids in the effluent as that determination was not made on membrane filtrate, but on the effluent as it

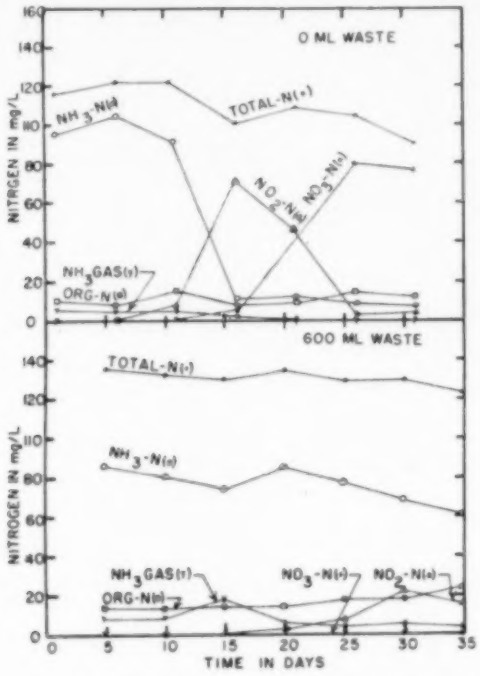

FIG. 1. Nitrogen in effluent substrate-nutrient broth.

came from the unit. In the 0-ml waste system the nitrogen was released as ammonia but after about the tenth day a nitrifying population developed and thereafter the ammonia was oxidized, first to nitrite, and then, about the 15th day, to nitrate. The ammonia gas lost to the system of about 7 mg/l decreased as the pH of the system dropped, due to the onset of nitrification. In the 600-ml waste unit the start of nitrification was delayed until the 20th day and only about 20 mg/l of nitrite were being produced by the end of the run with no nitrates being produced. The high amount of wasting kept the population of *Nitrosomonas* and *Nitrobacter* low. The resulting high pH from ammonia release allowed from 10 to 15 mg/l of ammonia gas to leave the system.

Amino Nitrogen. Simultaneous Adaptation Technique.

Alanine. The proposed metabolic pathway of alanine which was to be checked was: alanine yields on hydrolysis, acrylic acid and ammonia. Acrylic acid plus water gives lactic acid, which on the removal of two hydrogens produces pyruvic acid. The pyruvic acid then splits into formic and acetic acids for final metabolism. The

VOL. 4 1961

results of this study are shown in Fig. 2. Alanine, lactic acid, and acetic acid were all metabolized in a similar pattern. Formic acid might seem to be reduced in its metabolism, but since it is so much more oxidized than the other intermediates, its rate of oxygen uptake would be correspondingly lower.

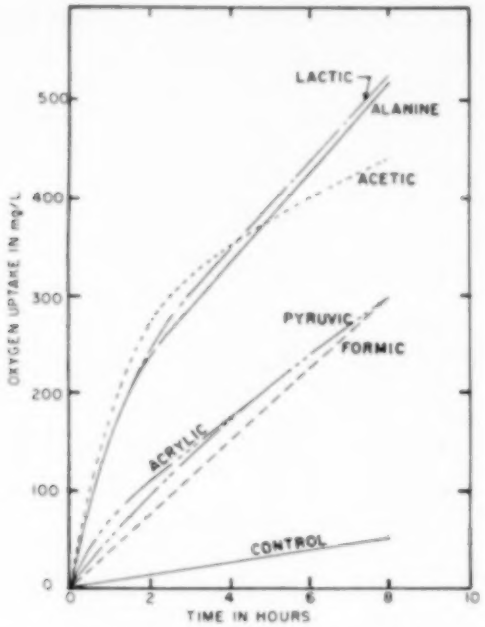

FIG. 2. Metabolism by activated sludge adapted to alanine.

Acrylic and pyruvic acids do not seem to fit into the pattern, however. This may mean that these steps are somehow by-passed during metabolism or that due to the increased chemical reactivity of these compounds due to the presence of a double bond they are altered in the external environment before passing across the cell wall. One difficulty with Stanier's Method is that internal cell reactions are to be investigated by supplying external substrates. These external substrates may not, in some cases, come into the cell in the proper form to act as true intermediates.

Propyl Amine. An activated sludge was easily developed on this compound. The most reasonable pathway for propyl amine was as follows: propyl amine on hydrolysis give propene which adds water to produce propanol. The propanol then loses two hydrogens to yield propionaldehyde which is further dehydrogenated and followed by water addition to form propionic acid. The propionic acid then follows the usual three carbon acid metabolism. The results of this study are shown in Fig. 3. Note that the compound propylamide was included to show that the amino group was removed before the acid step in the pathway. Also, propene was not included due to its volatility. Propyl amine, propanol, and propionic acid were all metabolized at the same initial rate indicating that they were all in the pathway. Propylamide was retarded in its initial oxygen uptake confirming an early removal of the amino

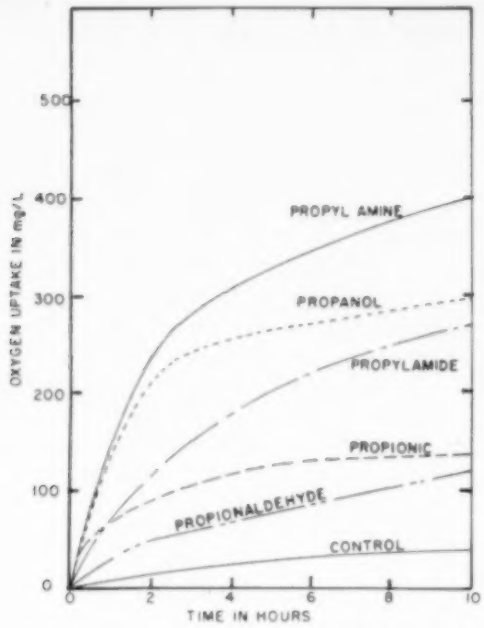

FIG. 3. Metabolism by activated sludge adapted to propyl amine.

VOL. 4 1961

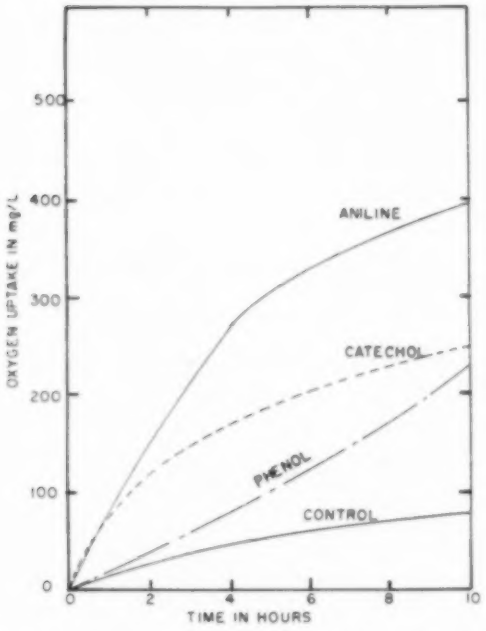

FIG. 4. Metabolism by activated sludge adapted to aniline.

nitrogen. Here, as above, some difficulty, possibly due to aldehyde reactivity, was experienced with a compound, propionaldehyde, which cannot be excluded as an intermediate.

Aniline. With the amino group attached to an aromatic compound instead of straight chain, different reactions might be expected. Therefore it was postulated that aniline might have the amino group hydrolysed off with water entering the reaction to yield phenol which would be further metabolized through the catechol system. To check this, a study was set up in which each compound was added at a concentration of 200 mg/l. The results of this study are shown in Fig. 4. Catechol was metabolized at the same initial rate as aniline, but phenol was definitely retarded. It was felt that the charge difference between aniline and phenol, or some toxicity was the cause of this retarded metabolism at a concentration of 200 mg/l. To confirm this, a test was made in which aniline-grown sludge was fed 200, 150, 100, 75, and 50 mg/l of phenol. Phenol was readily metabolized at 50 mg/l, thereby indicating its place in the scheme of metabolic breakdown. This illustrates another problem, electrical charge or compound toxicity, with STANIER'S Method of Simultaneous Adaptation.

Nitrogen Release Studies

Alanine, Propyl Amine, Aniline, o-, m-, p-amino Na benzoate. The results of the nitrogen release studies for these six compounds are shown in Figs. 5–10. The soluble C.O.D. and the measured and corrected net (gross-control) oxygen uptake

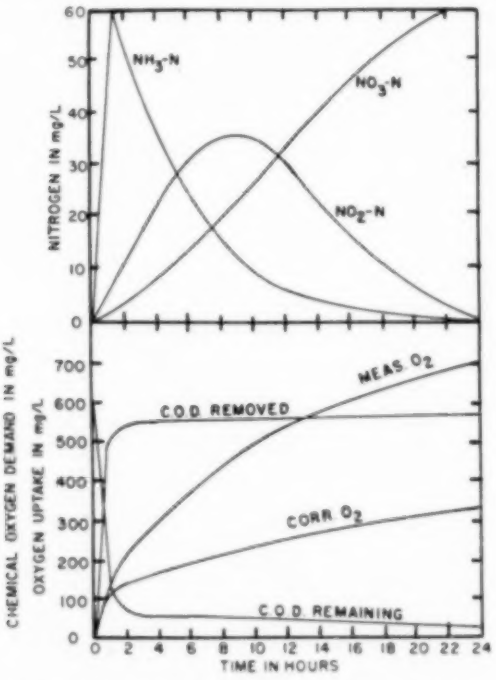

FIG. 5. Nitrogen release studies. Substrate-alanine.

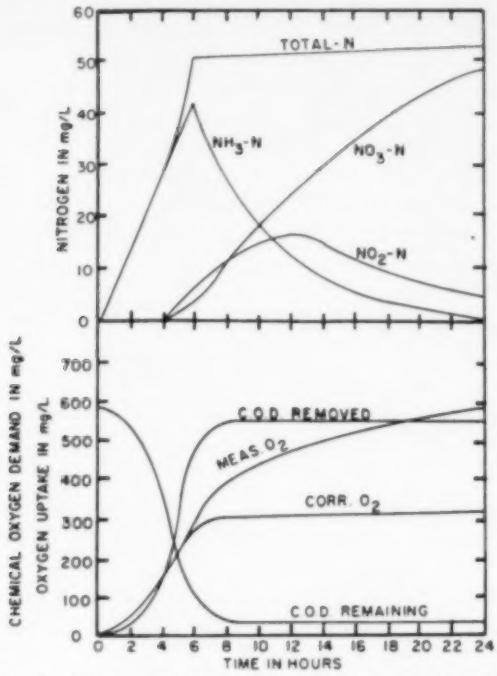

FIG. 6. Nitrogen release studies. Substrate-propyl amine.

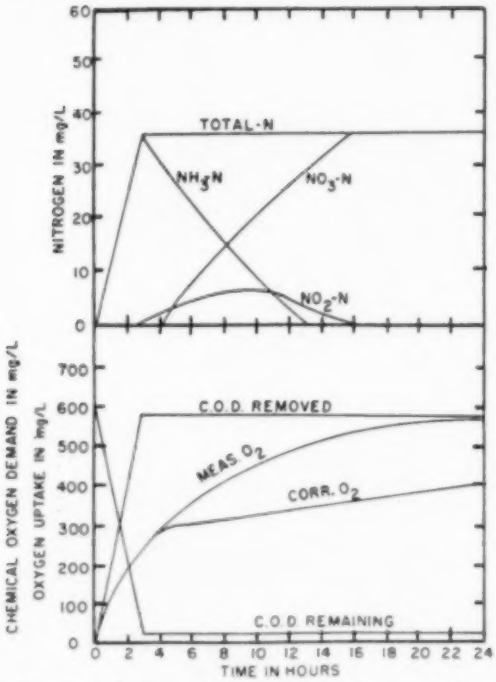

FIG. 7. Nitrogen release studies. Substrate-aniline.

VOL. 4 1961

are also plotted on the same figures to allow ready correlation with the nitrogen data. These results are all quite similar except for the m-amino Na benzoate which will be mentioned separately. The nitrogen release was complete just as the soluble C.O.D. was removed. At the same time the oxygen uptake curves began to bend over indicating the removal of food in solution. The nitrogen was released as ammonia nitrogen; later in some cases this ammonia was oxidized to nitrite and then to nitrate nitrogen, with a corresponding increase in oxygen uptake. This oxygen uptake has been corrected for, and the net oxygen uptake for substrate oxidation only has also been plotted to show the extent of oxygen uptake due to nitrification. It takes some

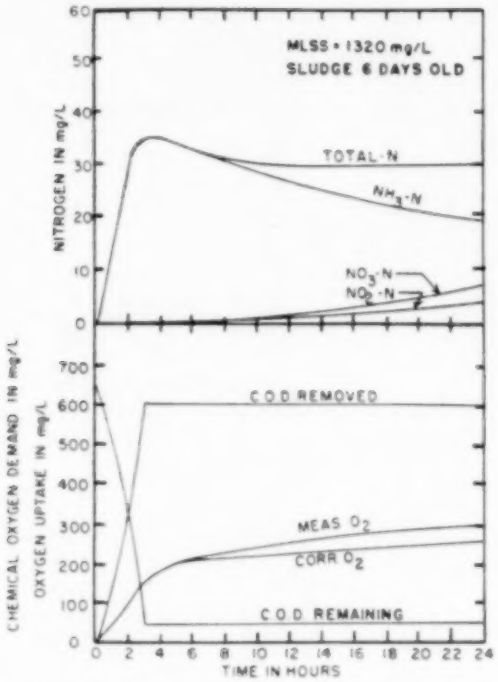

FIG. 8. Nitrogen release studies. Substrate-o-amino Na benzoate.

time for nitrifiers to develop in an activated sludge system; therefore if the nitrogen release studies are run soon enough after acclimation takes place, nitrification will not occur to any great extent. For example, in Figs. 8 and 10 the sludge was only six and eight days old, respectively; therefore nitrification was small. Fig. 11 shows the nitrogen release results for the o-amino Na benzoate sludge after 81 days of operation. A comparison of this " old " sludge with the " young " sludge shown in Fig. 8 demonstrates how nitrification has become well established as the sludge aged. The sludges grown on alanine, propyl amine, and aniline were old enough to have nitrification well established.

Great difficulty was experienced in growing the sludge on m-amino Na benzoate. Twice during the study the sludge was discovered not to be removing 1000 mg of C.O.D. per day, and the aeration period had to be extended and then slowly shortened

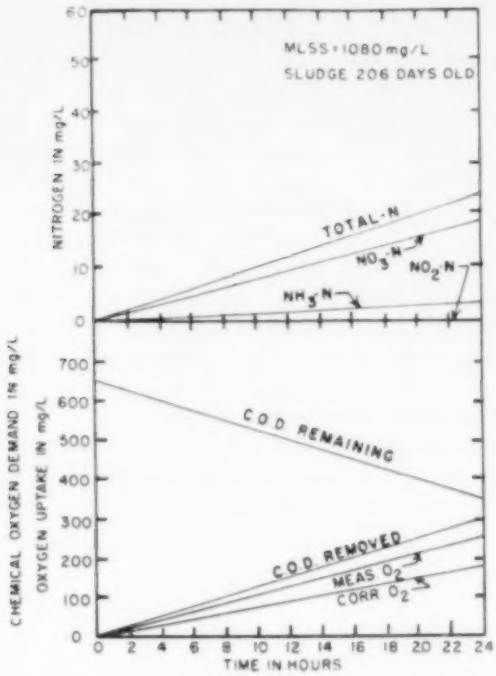

FIG. 9. Nitrogen release studies. Substrate-m-amino Na benzoate.

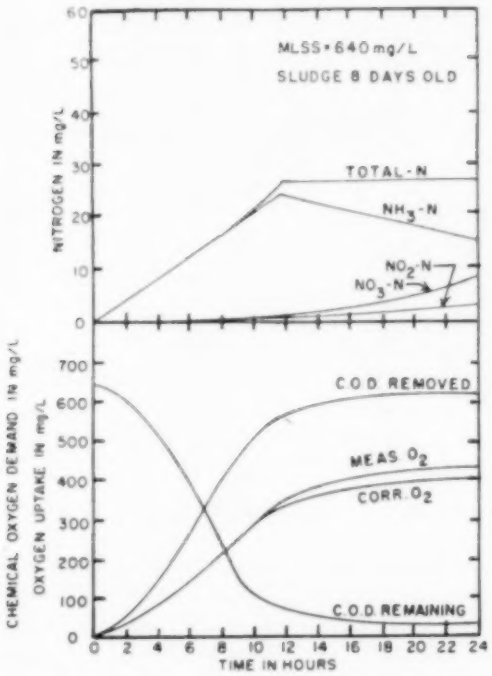

FIG. 10. Nitrogen release studies. Substrate-p-amino Na benzoate.

VOL. 4 1961

back to one day. Therefore, when the nitrogen release study, Fig. 9, was made, the sludge was 206 days old. Prior to the run, the sludge had been operating well for 30 days and the MLSS had slowly developed to 1580 mg/l. On the day of the test, however, so many solids were lost due to the triple wash of the sludge that the MLSS fell to 1080 mg/l. At this level the sludge was able only to metabolize 338 mg/l of the added C.O.D. It would be expected that the nitrogen would be released into solution as ammonia nitrogen as occurred with the o- and p-amino Na benzoate. The nitrogen probably was released as ammonia nitrogen during the oxidation of the organic matter, but this oxidation was so slow and the number of nitrifiers so high due to the age of the sludge that the ammonia released was immediately converted to nitrates. It is hard to obtain the true mechanism of metabolism with difficult to degrade organic materials such as m-amino Na benzoate.

Nitro Nitrogen. Simultaneous Adaptation Technique

o-nitro Na Benzoate. Since the report of KE, GEE, and DURHAM (1959) was not published at the time of these studies, it was thought that the breakdown pathway of o-nitro Na benzoate might be: o-nitrobenzoic acid to o-aminobenzoic acid to

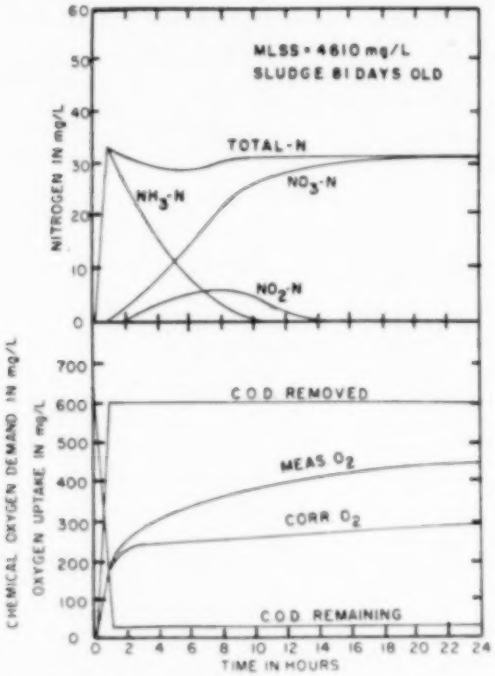

FIG. 11. Nitrogen release studies. Substrate-o-amino Na benzoate.

o-hydroxybenzoic acid to catechol to beta-keto adipic acid, and finally to succinic acid. In addition, protocatechuic acid was also studied. Each compound was added in such a concentration to exert a C.O.D. of 125 mg/l. The sludge was removed for testing 12 hours after feeding in an attempt to preserve the adaptive enzymes. The results of the study are shown in Fig. 12. Interpretation of these results is some-

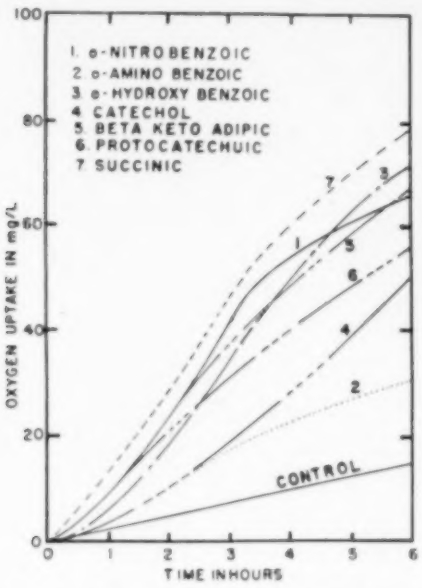

FIG. 12. Metabolism by activated sludge adapted to o-nitro Na benzoate uncorrected for nitrification.

VOL. 4 1961

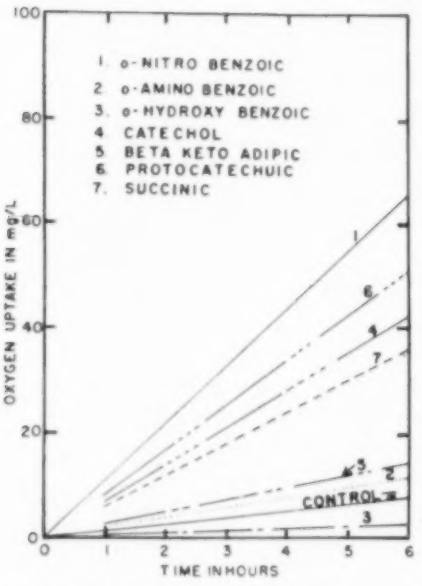

FIG. 13. Metabolism by activated sludge adapted to o-nitro Na benzoate corrected for nitrification.

what difficult due to the problem of nitrification which can cause oxygen uptake when there is no organic degradation occurring. In an effort to avoid this problem, the extent of nitrification at the end of the run was determined and the final values of oxygen uptake corrected. The corrected data are shown in Fig. 13. Since only one point, the final value, has been corrected, straight lines have been used to represent the progression of oxygen uptake for organic oxidation only. From these data it would appear that of the possible intermediates tested, only catechol, protocatechuic acid, and succinic acid seem to be in the pathway. This confirms the work of KE, *et al.* (1959) that o-nitrobenzoic acid is not degraded through o-aminobenzoic acid. In their article, KE, *et al.* (1959) did not suggest any intermediates to follow o-hydroxyl-

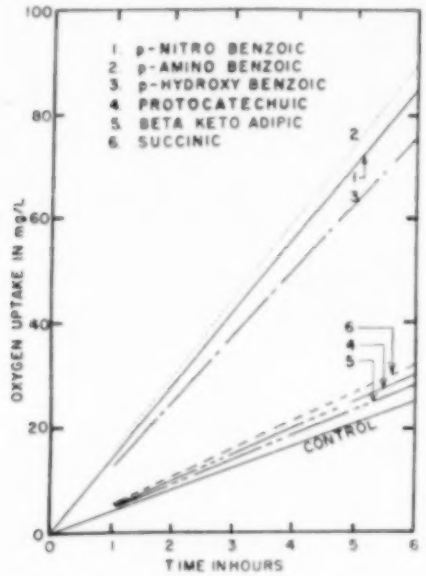

FIG. 14. Metabolism by activated sludge adapted to p-nitro Na benzoate corrected for nitrification.

amine benzoic acid. It may well be that catechol, protocatechuic acid, and succinic acid follow o-hydroxylamine benzoic acid in the pathway. It is also possible that o-aminobenzoic acid is in the pathway, but due to the difference in charge on the molecule, does not behave like a true intermediate when fed externally. KE, *et al.* (1959) did not find protocatechuic acid to be metabolized by o-nitrobenzoic acid-grown organisms, however. This pathway is still to be completely confirmed. The problem of nitrification adds still further complications to the use of Stanier's Method of Simultaneous Adaptation.

p-nitro Na benzoate. Based on DURHAM (1956, 1958) the probable metabolic pathway for the breakdown of p-nitro Na benzoate was: p-nitrobenzoic acid to p-aminobenzoic acid to p-hydroxybenzoic acid to protocatechuic acid to beta-keto adipic acid to succinic acid. The compounds were added, at a concentration of 125 mg/l of C.O.D., to washed sludge which had been fed only 12 hours previously.

The results of this study, corrected for nitrification (hence the straight lines) are shown in Fig. 14. These data show that the first two suggested intermediates are surely in the pathway, but the last three do not seem to fit into the scheme.

3,5-dinitro Na benzoate and 2,4,6-trinitro Na benzoate. Three attempts were made to adapt a sludge to the metabolism of 3,5-dinitro Na benzoate. The first, lasting 49 days, consisted of adding 500 mg/l of C.O.D. to the unit, starting with a small sludge inoculum, and adding anout 125 mg of sludge each day from a unit which was actively metabolizing p-nitro Na benzoate. After seven weeks of continual operation, no C.O.D. reduction was noted. A second unit was started with about 1300 mg/l of

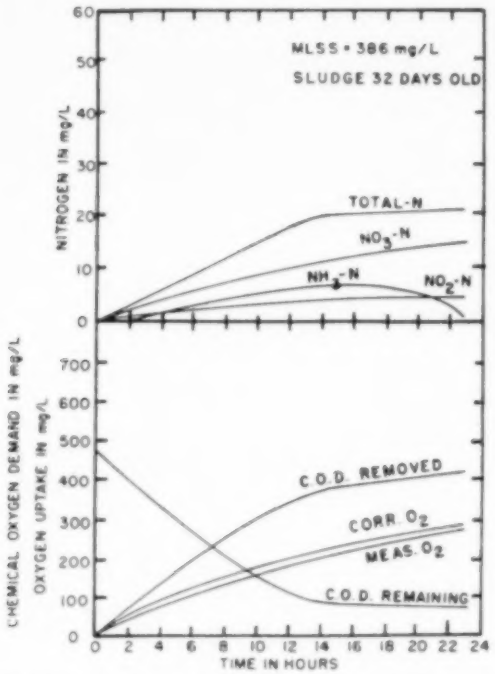

FIG. 15. Nitrogen release studies. Substrate-o-nitro Na benzoate.

sludge. This unit was fed a combination of equal parts of o-, m-, p-, and 3,5-dinitro Na benzoate daily. The total C.O.D. was 500 mg/l. After 21 days of operation the C.O.D. of the effluent showed the 3,5-dinitro Na benzoate to be undegraded. A third study consisted in continually aerating a high quantity of sludge, 1200 mg/l, with 500 mg/l of C.O.D. of 3,5-dinitro Na benzoate. After 54 days of operation, no C.O.D. reduction was noted.

An attempt to adapt a sludge to the metabolism of 2,4,6-trinitro Na benzoate by continually aerating a unit containing 500 mg/l of C.O.D. and daily seeding with about 125 mg of active p-nitro Na benzoate sludge was abandoned after 60 days, as no C.O.D. reduction was noted. Since neither the 3,5-dinitro Na benzoate nor the 2,4,6-trinitro Na benzoate was degradable, no simultaneous adaptation or nitrogen

VOL. 4 1961

release studies were made. The presence of more than one nitro group on the aromatic molecule makes metabolism very difficult, if not impossible.

Nitrogen Release Studies

o-, m-, and p-nitro Na benzoate. The results of the nitrogen release studies for o-nitro Na benzoate are shown in Fig. 15. This sludge was 32 days old, during which time the nitrifier population had developed enough to be converting much of the ammonia nitrogen released to solution to nitrites and nitrates. The possibility of the nitrogen being released as nitrate and then reduced to ammonia is slight in an oxidizing environment. The internal reduction of the nitro to the amino group,

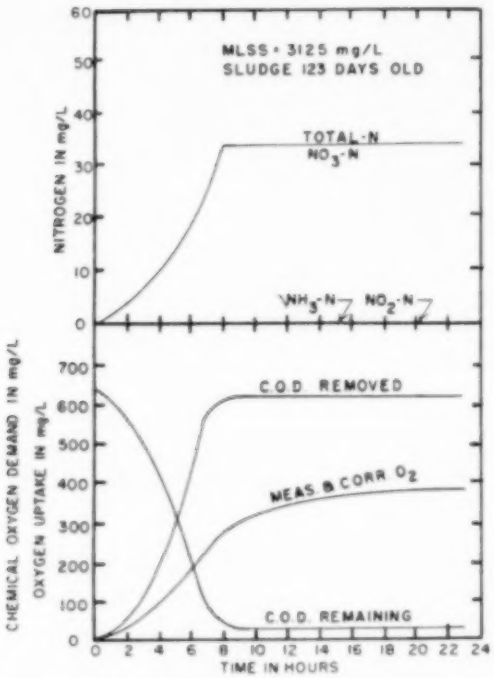

FIG. 16. Nitrogen release studies. Substrate-o-nitro Na benzoate.

followed by amino hydrolysis is a more reasonable reaction. This internal reduction supplies oxygen to the bacteria; therefore, in this case the corrected oxygen uptake is higher than the measured, taking this chemically-supplied oxygen into account.

The natural progression of partial to complete nitrification is shown by comparing Fig. 15, a 32-day old sludge, with Fig. 16, a 123-day old sludge. In the latter case, the nitrification reaction was so strong that no ammonia nitrogen appeared in solution at all, although it is surely produced. Interpreting Fig. 16 alone might lead to the erroneous conclusion that the nitrogen is removed from nitro-containing organic compounds as nitrate instead of ammonia nitrogen.

The nitrogen release studies from the m-nitro Na benzoate-adapted sludge are shown in Fig. 17. Because of the difficulty in growing a sludge which could readily

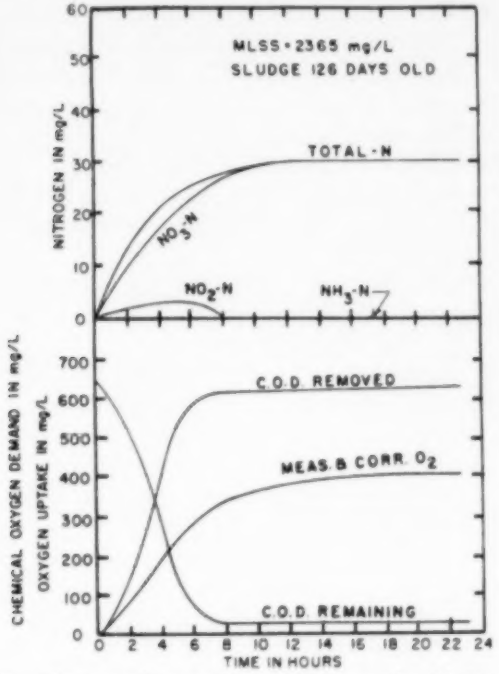

FIG. 17. Nitrogen release studies. Substrate-m-nitro Na benzoate.

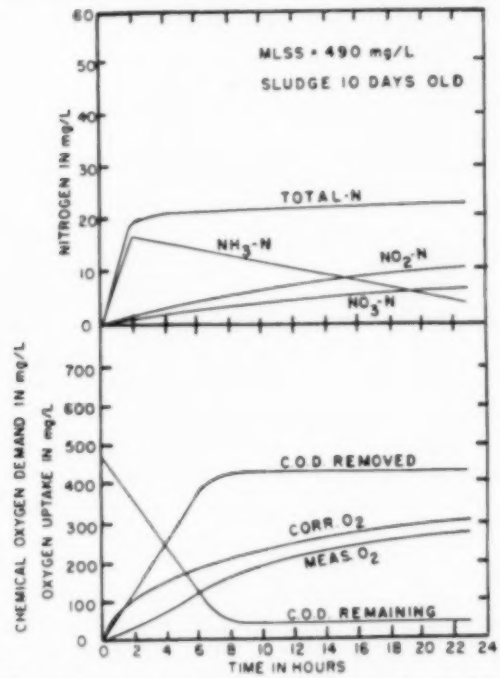

FIG. 18. Nitrogen release studies. Substrate-p-nitro Na benzoate.

VOL. 4 1961

metabolize 1000 mg of C.O.D. per day of this substrate, 62 days passed before the first 500 mg of C.O.D. was removed, the sludge was 126 days old when the nitrogen release studies were made. By this time nitrification was complete and the ammonia nitrogen which was probably released to solution during degradation was immediately oxidized to nitrates. Attempts to study a " young " sludge to demonstrate this ammonia release met with failure as a well-acclimated sludge could never be developed fast enough to prevent nitrification. Attempts to control nitrification with sludge wasting, a technique which was successful in the nutrient broth studies, Fig. 1, only impeded organic removal in this study.

Fig. 18 shows the nitrogen release results for the sludge grown on p-nitro Na benzoate. This sludge was started with seed sludge from a unit which was already metabolizing p-nitro Na benzoate; therefore, in only 10 days this sludge was ready for study. Since this sludge was so " young " nitrification was slight and the release of ammonia nitrogen was clearly shown. The only odd feature of this study was the apparent release of all of the nitrogen before the complete removal of soluble C.O.D. A later study after 133 days of operation showed that this was an unusual condition and that after the sludge was well established the complete release of nitrogen corresponded to the complete removal of soluble C.O.D.

Cyano Nitrogen. Simultaneous Adaptation Technique

Propionitrile. There were two possibilities for the mechanism of metabolism of propionitrile. One is the hydrolysis of the cyano group to form propionamide, the other is the reduction of the cyano group to form propyl amine. If the first case were true, the next step would be propionic acid. If the second case were true, the next step would be propanol, then propionaldehyde, and then to propionic acid. A Warburg Respirometer run was made to test which pathway was the true one. The results of this test are shown in Fig. 19. The rapid uptake of propionamide and propionic acid and the retarded uptake of propylamine and propanol indicated that the pathway of metabolism was the hydrolysis to the amide, followed by the hydrolysis of the amino group off with propionic acid resulting.

Benzonitrile. If the same scheme held for benzonitrile as for propionitrile metabolism would proceed to benzalamide and hence to benzoic acid instead of to benzalamine, then to benzyl alcohol, then to benzaldehyde, and finally to benzoic acid. Neither benzalamide nor benzalamine was commercially available, but the other compounds were tested in the Warburg Respirometer. The results of this study are presented in Fig. 20. Benzoic acid was metabolized as rapidly as benzonitrile while benzyl alcohol showed a definite adaptive type of curve. This would confirm the first scheme of metabolism, hydrolysis to the amide and then hydrolysis of the amino group off, with the production of the acid. Benzaldehyde showed a very rapid rate of oxygen uptake, almost as fast as benzonitrile. This compound is closely related to the benzonitrile.

DISCUSSION

Two factors hold true for all of the degradable nitrogen-containing organic compounds studied in this investigation. They are : (1) During degradation, the nitrogen contained in the molecule is released to solution and (2) the nitrogen is released as

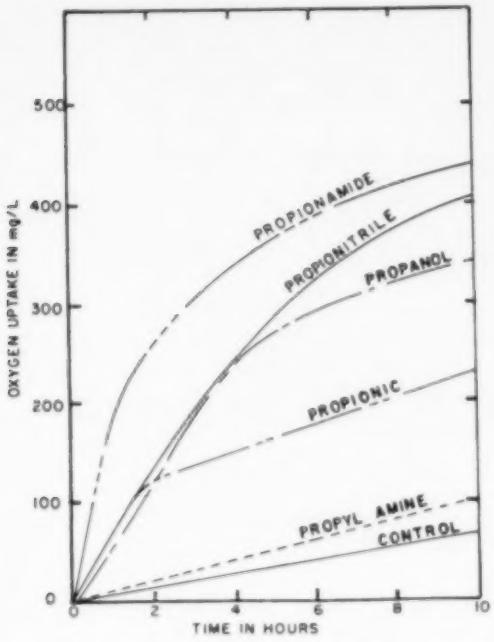

FIG. 19. Metabolism by activated sludge adapted to propionitrile.

VOL. 4 1961

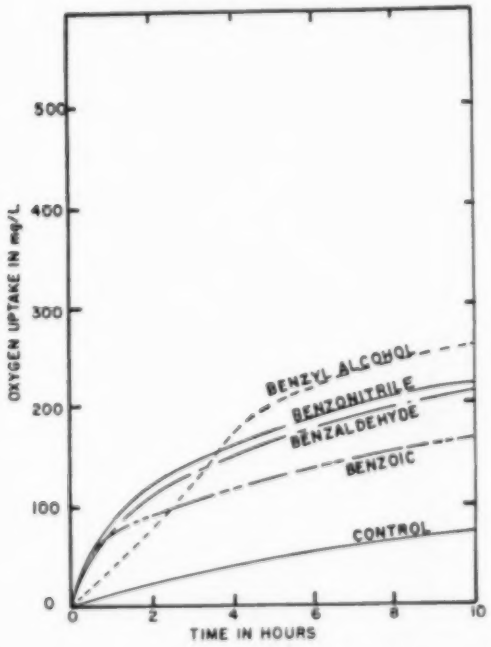

FIG. 20. Metabolism by activated sludge adapted to benzonitrile.

ammonia nitrogen. This means that if an activated sludge unit is to be operated on a nitrogen-containing industrial waste, and the waste is biologically degradable, the nitrogen in the molecule can be utilized for bacterial nutrient supplementation. In fact, the nitrogen in most nitrogen-containing organics is so plentiful, see Table 3,

Table 3. C.O.D. to N ratios of degradable compounds used in this study

Compound	*C.O.D./N*
Nutrient Broth	About 8·5/1
Alanine	7·1/1
Propylamine	10·3/1
Aniline	16/1
mono amino benzoic acids	16/1
mono nitro benzoic acids	17·7/1
propionitrile	13·3/1
benzonitrile	22·3/1

that some non-nitrogen-containing organics may be mixed with the nitrogen-containing waste without fear of nitrogen deficiency. The results of this investigation also show that the same over-all mechanism of biological nitrogen removal, conversion to an amino group and hydrolysis from the molecule, occurs regardless of the form

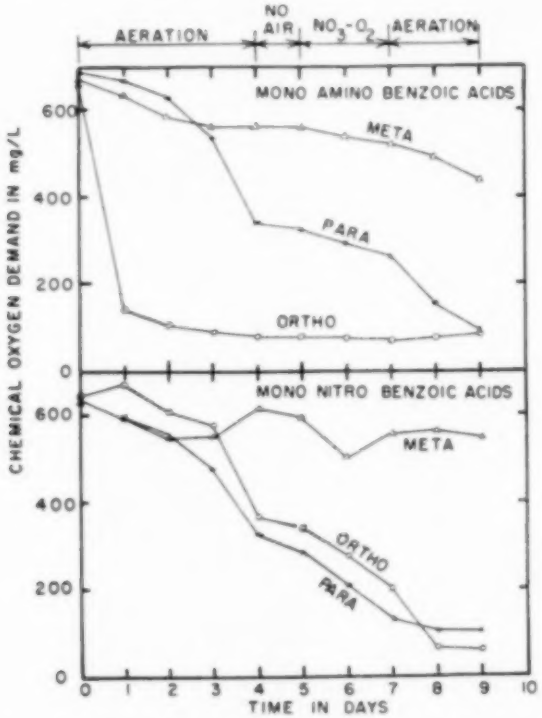

Fig. 21. Effect of nitrogen group position on metabolism.

of the nitrogen group as it is attached to the organic molecule. This is not to say the metabolic intermediates are the same in all cases, just that the nitrogen group is removed as the amino group.

In order to determine the relative effect both of position and type of nitrogen group on activated sludge metabolism, the following test was made. Sludge was developed on sodium benzoate, passed through a Waring Blender and divided equally into six pilot plants. The MLSS in the six units ranged between 1324 mg/l and 1364 mg/l.

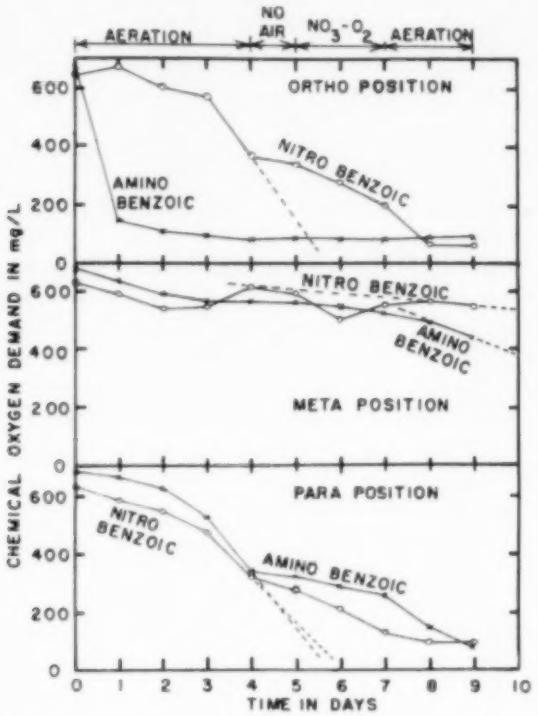

FIG. 22. Effect of nature of nitrogen group on metabolism.

To each of these units one of the following substrates was added, o-, m-, p-amino Na benzoate, o-, m-, p-nitro Na benzoate. The initial C.O.D. concentrations were between 630 and 690 mg/l at time zero. Each day for the next nine days the soluble C.O.D. was determined in each unit. At first no nitrogen was added to any of the units. This study would then show the relative rates of metabolism of these six compounds under nearly identical environmental conditions. Unfortunately, at the end of the fourth day the air compressor failed. The units were without any oxygen for 24 hours; then, in an effort to remedy the problem, they had nitrate oxygen supplied and were stirred on a flocculator for another 48 hours until aeration was restored for the last two days of the test. The results of this test are shown in Fig. 21 and 22.

In Fig. 21 it is seen that in the case of the mono amino Na benzoates, the ortho position was metabolized first, then the para position and finally the meta position. With the mono nitro Na benzoates, however, the ortho and para position compounds

VOL. 4 1961

were metabolized almost at the same rate, with the meta position compound again being the slowest. This may be explained on the basis of the nature of the groups themselves. The amino group is a small positively-charged group, while the nitro is a large negatively-charged group. The acid end of the molecule is, on ionization, negatively charged. In the compound o-amino Na benzoate the small amino group will be attracted to the carboxylate anion. This attraction would not be significant with the amino group in the para position. This attraction may well be the reason that the ortho compound was metabolized in one day while the para compound took much longer to be degraded.

When the nitro group is attached to the molecule the situation is quite different. If the closeness of the nitrogen group to the carboxylate anion affects biological degradability as it seems to, based on the o-amino Na benzoate data, the repulsion between the large nitro group and the carboxylate anion, when the nitro group is in the ortho position may well reduce the biological activity of the molecule due to spacial arrangement. This would explain why the o-nitro Na benzoate, which would be expected to go quite readily being an ortho compound was reduced in its activity. Meta position substitution is very hard to react, both chemically and biologically; therefore, it was not surprising that these compounds reacted slowly.

Fig. 22 shows the relative rates of the ortho, meta, and para positioned groups, comparing in each case the amino and nitro group. In the case of the ortho and meta positions, the amino group was more readily attacked than the nitro group. This was probably the case in the para position also, except that the interruption of aeration strongly affected the rate of p-amino Na benzoate metabolism. The projected curves (dotted lines) of Fig. 22 show the p-amino Na benzoate unit reached the 100 mg/L C.O.D. level about 0·3 day before the p-nitro Na benzoate unit reached the same level. In any event, the difference in group had the least effect in the para position, possibly because the group was so far from the carboxylate anion as to exert little influence on the spacial arrangement of the molecule, thereby exerting little influence on the biological degradability of the compound. Spacial arrangement seems to have an important effect on bacterial metabolism. Based on the projected curves in Fig. 22, Table 4 gives the relative rates of compound degradation.

TABLE 4. TIME TO REACH 100 mg/l LEVEL OF C.O.D. BASED ON PROJECTED CURVES

Compound	*Time To Be Degraded, in Days*
o-amino Na benzoate	2·8
p-amino Na benzoate	5·2
o-nitro Na benzoate	5·2
p-nitro Na benzoate	5·5
m-amino Na benzoate	16·5
m-nitro Na benzoate	46

CONCLUSIONS

Based on the results of this investigation, the following conclusions may be drawn:

1. Nutrient Broth, alanine, propyl amine, aniline, o-, m-, and p-amino Na benzoate,

o-, m-, and p-nitro Na benzoate, propionitrile, and benzonitrile were all found to be biologically degradable by activated sludge.

2. 3,5-dinitro Na benzoate and 2,4,6-trinito Na benzoate were not biologically degradable by activated sludge.

3. The nitrogen-containing organic compounds which were biologically degradable released their nitrogen into solution during metabolism. Once in solution, this nitrogen could be used for synthesis.

4. The mechanism removal of nitrogen from the organic molecule was the same regardless of the original form of the nitrogen group. The nitrogen group was converted to an amino group, if necessary, and was then hydrolysed from the molecule as ammonia nitrogen.

5. Both the form, position, and number of nitrogen groups has an important influence on the ease of biological degradability of an organic compound containing nitrogen.

6. Metabolism of alanine by activated sludge appears to be by hydrolysis to lactic acid which is oxidized through pyruvic acid to formic acid and acetic acid prior to complete oxidation.

7. Metabolism of propyl amine by activated sludge appears to be by hydrolysis of the amino group followed by oxidation of the propanol which was formed.

8. Metabolism of aniline by activated sludge appears to be by hydrolysis to phenol and by oxidation through catechol.

9. Metabolism of p-nitro Na benzoate by activated sludge appears to be by reduction of the nitro group to form p-aminobenzoic acid which is then converted to p-hydrobenzoic acid. Beyond this point the pathway was not defined.

10. Metabolism of propionitrile by activated sludge appears to be by hydrolysis to form the amide and then to propionic acid which is oxidized.

11. Metabolism of benzonitrile by activated sludge appears to be by hydrolysis to benzoic acid which is then oxidized.

12. Care must be taken in the interpretation of results from Stanier's Method of Simultaneous Adaptation because of problems with nitrification, toxicity, and chemical reactivity of the suspected intermediate. Also compounds which are formed as intermediates intracellularly may have difficulty diffusing across the cell wall when fed externally due to differences in charge.

Acknowledgments—This research was supported in part by research grants from the National Institutes of Health, United States Public Health Service.

VOL. 4 1961

REFERENCES

CAIN, R. B. (1957) " The Microbial Metabolism of Nitro Aromatic Compounds," *J. Gen. Microbiol.* **19,** 1–14.

DURHAM, N. N. (1956) Bacterial Oxidation of p-Aminobenzoic Acid by *Pseudomonas fluorescens*, *J. Bacteriol.* **72,** 333–6.

DURHAM, N. N. (1958) Bacterial Oxidation of p-Nitrobenzoic Acid by *Pseudomonas fluorescens*, *Canad. J. of Microbiol.* **4,** 141–8.

HELMERS, E. N., FRAME, J. D., GREENBERG, A. E., and SAWYER, C. N. (1951) Nutritional Requirements in the Biological Stabilization of Industrial Wastes, II. Treatment with Domestic Sewage. *Sewage and Industrial Wastes* **23,** 884–99.

KE, Y-H, GEE, L. L. and DURHAM, N. N. (1959) Mechanism Involved in the Metabolism of Nitrophenyl carboxylic Acid Compounds by Microorganisms, *J. Bacteriol.* **77,** 593–8.

Ludzack, F. J., Schaffer, R. B., and Bloomhuff, R. N. (1959) Experimental Treatment of Organic Cyanides by Conventional Sewage Disposal Processes. *Proceedings of the Fourteenth Industrial Waste Conference*, Purdue University.

Moore, F. W. (1949) The Utilization of Pyridine by Microorganisms. *J. Gen. Microbiol.* **3**, 143–7.

Nesbitt, J. B., Kohl, H. R., and Wagner, Jr., E. L. (1960) The Aerobic Metabolism of Potassium Cyanide. *J. Sanit. Engnr. Div.* **86**, 1–14.

Painter, H. A. and Ware, G. C. (1955) Bacterial Utilization of Cyanide. *Nature, Lond.* **175**, 900.

Sakamoto, Y., Uchida, M., Ichihara, K. (1953) The Bacterial Decomposition of Indole, I. Studies on its Metabolis Pathway by Successive Adaptation. *Med. J. Osaka University* **3**, 477–86. *Chemical Abstracts* **47**, 7585f.

Sawyer, C. N. (1956) Bacterial Nutrition and Synthesis. *Biological Treatment of Sewage and Industrial Wastes* **1**, 3–17. Reinhold Publishing Corp., New York.

Tang, P. S. and Hsueh, T. Y. (1943) Studies on the Kinetics of Cell Respiration, IX. Acceleration of Pyruvate Oxidation in *Escherichia* coli by Certain Amino Acids, Ammonia, and 4 Carbon Dicarboxylic Acids. *Arch. Biochem.* **2**, 15–21.

Int. J. Air and Water Poll. Pergamon Press 1961. Vol. 4, Nos. 1/2 p. 139. Printed in Great Britain.

Book Reviews

Levels of radioactivity in the environment. A new monthly publication entitled " Radiation Health Data " has been initiated by the United States Public Health Service, the first issue being dated April 1960. This tabulates measurements made in the United States of radiation levels in air, water and milk. The latest and most detailed figures reported are those for November 1959.

Fission products in the atmosphere are monitored by the measurement of beta activity in samples collected at 44 stations widely spaced throughout the United States. A special survey is also made from a chain of Latin American and U.S. sites along the 80th Meridian. In addition to fission products, radon and thoron measurements are reported from Cincinnati.

It is intended that each third report of the series should contain interpretative statements as well as data. The price of the publication is 50 cents per single issue and $3.00 for a 6-month subscription, from the Office of Technical Services, U.S. Department of Commerce, Washington 25, D.C.

G. B. C.

VOL.
4
1961

PAPERS TO BE PUBLISHED IN FUTURE ISSUES

P. STOCKS: A study of polycyclic hydrocarbons and trace elements in smoke in Merseyside and other northern localities of England and Wales.

ROBERT R. AUSTIN: A new atmosphere irradiation chamber.

DONALD F. ADAMS: A quantitive study of the limed filter paper technique for fluoric air pollution studies.

JAMES HALITSKY: Single camera measurement of smoke plumes.

FRANCIS POOLER, Jr.: A prediction model of mean urban pollution for use with standard wind roses.

P. A. E. CROSSE, D. H. LUCAS and W. L. SNOWSHILL: The measurement of dust nuisance emitted by chimneys.

A. GOETZ: On the nature of the synergistic action of aerosols.

F. ROSENBERG, N. DONDERO and H. HEUKELEKIAN: Bacterial indicators of pollution in household well waters.

A. D. OSBORNE, E. F. DARLEY and J. N. PITTS, Jr.: On the stability of acrolein towards photo-oxidation.

A. TURK, J. MORROW, P. F. LEVY and P. WEISSMAN: Adsorption sampling—II. Collection of ethylene on brominated carbon.

Int. J. Air and Water Poll. Pergamon Press 1961. Vol. 4, Nos. 3/4, pp. 141–153. Printed in Great Britain.

A STUDY OF POLYCYCLIC HYDROCARBONS AND TRACE ELEMENTS IN SMOKE IN MERSEYSIDE AND OTHER NORTHERN LOCALITIES*

P. STOCKS,† B. T. COMMINS‡ and K. V. AUBREY §

(*Received* 30 *August* 1960)

Abstract—(1) Smoke samples collected continuously for one or more years by filters in Merseyside conurbation and elsewhere in northern England and Wales were analysed for 7 polycyclic hydrocarbons and 13 trace elements. The locations included seaside and riverside, small and large towns, a smokeless zone, the Mersey Tunnel, bus and motor car garages, an office and a steelworks.

(2) The amount of coronene in smoke varied little in town or country but the higher levels in tunnel smoke and in the motor garage were such as to suggest its usefulness for measurement of air pollution by motor traffic.

(3) In country places amounts of smoke and of the hydrocarbons were 2½ times as great in the autumn–winter half of the year as in the spring-summer half, but in Merseyside, whilst the seasonal ratio for total smoke was similar, for the hydrocarbons it was about 5 to 1. Indoor office air was less polluted than that outside in winter, the hydrocarbons showing a seasonal ratio about 4 to 1.

(4) Trace element concentrations in air were all higher in urban than in country places, but only for antimony, vanadium and molybdenum was the excess relatively greater than for total ash. Mersey tunnel air contained very much greater amounts of lead than did the entering air, and in a motor garage the air contained more lead and vanadium than the air outside. In the smokeless zone trace elements were present in smaller amount than at the town centre. In the rolling-mill shed and melting-shop of the steelworks, concentrations of all the elements, particularly of copper, were largely increased.

VOL. 4 1961

INTRODUCTION

SOME detailed studies of air pollution in English cities have been made in Leicester (D.S.I.R. 1945), London (GORE and SHADDICK, 1958) and Sheffield (PEMBERTON *et al.*, 1959). The data in this paper do not constitute a systematic study of spatial distribution, but were obtained in the course of an investigation during 1954–58 of the relations between air pollution and mortality in districts located in an area extending from Anglesey to Tyneside, and preliminary reports on parts of this work have been made (STOCKS, 1955, 1958a, 1958b, 1959; STOCKS and CAMPBELL, 1955). Instruments for collecting smoke samples continuously, the filter papers being changed at suitable intervals, were installed by the Fuel Research Station of the D.S.I.R. for periods of one to three years at 41 locations in all, of which 26 were chosen with a view to getting representative samples of the atmosphere in districts where mortality rates from cancer and respiratory diseases could be calculated. The remaining 15 were in abnormal situations of special interest such as seaside and riverside sites, the Mersey Tunnel, bus and motor garages, an office interior, a smokeless zone and a steelworks, or at

* Supported by grants from the British Empire Cancer Campaign and Medical Research Council.

† Colwyn Bay, North Wales.

‡ Medical Research Council Air Pollution Research Unit, St. Bartholomew's Hospital, London.

§ Warren Spring Laboratory, Department of Scientific and Industrial Research, Stevenage, Hertfordshire.

alternative places in the conurbations, and the present paper deals in the main with these. A few of the representative districts have been introduced also for comparative purposes and for examination of seasonal and time factors. Relations with disease incidence are not here involved; they can only be studied in the 26 districts, and that has been done in another paper (STOCKS, 1960).

METHODS OF ANALYSIS

Polycyclic Aromatic Hydrocarbons

The smoke containing polycyclic hydrocarbons was collected by drawing air at rates up to 500 ft^3/week by means of an electric pump through Whatman No. 1 filter papers held in 4 inch diameter brass filter holders. A gas meter in series with the pump recorded the amount of air drawn through the filter.

After collecting the smoke for one year the papers from each site were pooled, cut into small pieces and extracted for three hours with 200 ml of purified cyclohexane using a soxhlet apparatus. The extract was then distilled at atmospheric pressure to a bulk of about 50 ml before being evaporated to small bulk by means of a small electric blower at about 30° C. The reduced extract was then either made up to 5 or 10 ml with cyclohexane in a standard flask or reduced to about 2 ml, and this or a 2 ml aliquot of the extracts in standard flasks transferred to an alumina column. The actual fraction taken for analysis depended on the amount and nature of the smoke extracted. The amount analysed was carefully controlled to prevent the alumina column being saturated and also to ensure that enough material was used for an accurate determination. The alumina (Peter Spence 100/200 mesh) was deactivated by shaking it with 5 per cent w/w of distilled water. This prepared material was mixed to a slurry with cyclohexane and poured into a glass chromatographic tube 0·5 inches wide to form a column of alumina 3 in. long; a plug of cyclohexane washed glass wool was used to support the alumina. The chromatographic column was developed with cyclohexane throughout, and about thirty 2·7 ml fractions collected. Each of these was examined using a Beckman D.K.2 spectrophotometer according to a previously published technique (COMMINS, 1958a). From the spectral data obtained the amounts of the following hydrocarbons were accurately determined: 3 : 4 benzpyrene, 1 : 12 benzperylene, pyrene, fluoranthene, 1 : 2 benzpyrene, coronene and anthanthrene. Phenanthrene and anthracene were also determined but the amounts were such that they could not be measured accurately.

The wavelengths used for determination of all the hydrocarbons except coronene, anthanthrene and phenanthrene have been published previously. The wavelengths used for coronene were 336·0–339·0–342·0 mμ, for anthanthrene 427·0–429·5–432·0 mμ, and for phenanthrene 291·25–293·25–295·25 mμ.

The techniques used for the determination of the hydrocarbons quoted in this paper are different from those used previously in other surveys (STOCKS and CAMPBELL, 1955; COMMINS, 1958b). The main features of the new method are:

(1) Use of narrow base lines instead of wide bases for spectral determination of hydrocarbons; this has the advantage of reducing the interference caused by other hydrocarbons and unknown substances also present.

(2) Use of cyclohexane only for extraction of hydrocarbons and their chromatographic separation; this eliminates transference losses from acetone and benzene to cyclohexane solution.

(3) Spectral examination of each chromatographic fraction; previously spectral analysis was applied to bulked fractions and this caused considerable errors due to the overlapping of hydrocarbons.

(4) Use of the large peak at 384·5 mμ for the determination of 3 : 4 benzpyrene where possible, and use of the small peak at 403·0 mμ in fractions containing 1 : 12 benzperylene also. Previous techniques relied only on the use of the small peak for 3 : 4 benzpyrene; this produces errors due to the interference by background absorption caused by 11 : 12 benzfluoranthene (known to be present) and by some unknown hydrocarbons.

Trace Elements

The thirteen trace elements studied were: antimony, arsenic, beryllium, chromium, cobalt, copper, lead, manganese, molybdenum, nickel, titanium, vanadium and zinc. They were determined by the spectrographic analysis of the ashes of the filter papers carrying the collected samples. The ashing was carried out at a temperature not exceeding 500° C.

A few mg of each ash were mixed with an exactly equal amount of a spectroscopic buffer which consisted of 70 per cent calcium carbonate, 30 per cent barium carbonate and small amounts of gold and bismuth as chlorides to act as spectroscopic internal standards. Portions of the buffered sample, each of 2 mg, were packed into small cavities in high purity graphite rods of 6·5 mm diameter. The spectra of the samples were excited with a d.c. arc. The first 30 seconds of the arcing, at 5 amps, was recorded simultaneously on two spectrographs; a further 60 seconds of arcing, when the current was raised to 8 amps, was recorded on one of the instruments only. As far as possible the more refractory elements were measured in the spectra obtained with 90 seconds of arcing, and the volatile elements in the spectra of the first 30 seconds of arcing.

The optical densities of the spectrum lines were measured with a non-recording microphotometer, and were converted to arbitrary intensity units by suitable calibration of the developed photographic image. The ratio of intensity of the spectrum line of an element and its internal standard was then referred to a calibration curve, and the concentration of the element evaluated from this ratio. The standards used to obtain the calibration curve were compounded from " Specpure " chemicals and had a basic composition similar to that of a coal-ash. Each contained a variety of trace elements at concentrations which involved a ratio of about 2 to 1 between adjacent standards.

The filter papers used for collecting the smoke samples contained certain amounts of many of the elements under consideration, and these quantities were incorporated in the smoke ashes which were analysed. This contamination of the analysed sample was most serious in 1956 when the filter papers were relatively lightly loaded with collected smoke. As a consequence no figures could be quoted for copper and chromium, and those for titanium were only approximate: reliable corrections could be applied for the remaining elements. During 1957 and 1958 some six times as much smoke sample was collected on each filter paper and, in addition, a selected type of paper was utilised for all collections. As a result it was found necessary to make corrections for three elements only, chromium, cobalt and copper, and these corrections rarely exceeded one tenth of the total weight of the element present.

VOL. 4 1961

ANNUAL SMOKE AND HYDROCARBON VALUES

Concentrations in Air

Table 1 gives the average annual amounts of smoke and seven hydrocarbons in the air at 22 places. The hydrocarbon figures in μg per 1000 m^3 were obtained by dividing ascertained amounts of each substance in aggregated filter deposits by the known volume of air which had passed through. The smoke figures in mg/1000 m^3 were estimated from a photometric measure of the blackness of those portions of the filter papers through which the air had passed, the readings being converted to mg of smoke by a standard calibration curve. The calibration applies to the mixture of domestic smoke with a little industrial and traffic smoke usually found in the air of British towns, but it is unlikely to be correct for special locations where traffic or industrial smoke

Table 1. Average annual amounts of smoke and 7 polycyclic hydrocarbons per 1000 cubic metres of air at 22 localities in Lancashire, West Riding of Yorkshire and Tyneside in 1958

Location of filter (see Table 2 for details)	Total smoke (mg)	Hydrocarbons (μg/1000 m^3)						
		3 : 4 Benz-pyrene	1 : 12 Benz-perylene	Pyrene	Fluor-anthene	1 : 2 Benz-pyrene	Coro-nene	Anth-anthrene
Merseyside Conurbation								
St. George's Dock	262	31	26	7	23	22	6	6
Roe Street	271	34	30	10	12	19	7	6
Edge Lane	331	38	41	18	24	26	8	9
Inside Bus Depot	*346*	*49*	*43*	*19*	*26*	*32*	*8*	*11*
Inside Motor Garage	*427*	*45*	*48*	*16*	*22*	*30*	*12*	*14*
Mersey Tunnel								
Mid-point	(*710*)	*37*	*81*	*22*	*19*	*22*	*50*	*9*
Road junction	(*1588*)	*53*	*137*	*44*	*37*	*36*	*75*	*16*
In Other Conurbations								
Elland	150	15	14	5	7	9	3	3
Keighley	291	32	32	10	18	22	6	7
Leeds	421	42	40	14	21	26	9	9
Gateshead	399	62	50	29	40	37	8	13
Newcastle-on-Tyne								
(Wharncliffe St.)	505	75	73	37	58	46	10	20
(Shields Rd.)	622	69	63	35	49	41	11	19
Salford (Regent Rd.)	562	108	62	38	49	52	12	16
(Smokeless Zone)	385	43	46	27	37	30	9	10
Small Country Towns								
Wetherby	98	11	11	7	10	8	2	2
Ripon	135	15	12	6	10	9	3	3
Larger Towns								
Lancaster	276	20	14	9	14	14	5	6
Darwen	288	36	35	17	25	25	6	8
Warrington	308	34	33	12	18	22	7	8
Burnley	311	32	30	4	8	21	6	7
York	177	24	21	14	20	16	4	5

predominate. For this reason the smoke figures for the Mersey Tunnel are shown in parentheses, but the hydrocarbon values are not affected by this source of error.

In Merseyside the St. George's Dock instrument was placed near the riverside at the main air inlet for ventilating the tunnel. Roe Street was near the city centre, ¾ mile east of the river. Edge Lane was 2¼ miles further east but still in a densely populated area and here another filter was placed inside a large bus depot and a third inside a motor car garage a short distance away. In the tunnel one filter was placed at the middle point and another at the junction between two outlets to Liverpool controlled by traffic lights, where high pollution is caused by vehicles accelerating after stopping.

In West Yorkshire conurbation Elland and Keighley are towns with 20 and 57 thousand people respectively near the western limits, the city of Leeds being near the eastern limits. In Tyneside conurbation Gateshead and Wharncliffe Street locations were chosen as representative and Shields Road as exemplifying the eastern part of Newcastle. In Salford a filter was placed in a smokeless zone near the western edge for comparison with the town centre. Wetherby is a small township in a rural district to the north-east of Leeds, and Ripon is a country town further north. The five larger towns are arranged in ascending order of their population (shown in Table 2).

When the garage and tunnel locations are excluded the smoke density ranges from 98 to 622 mg/1000 m^3, and the hydrocarbon figures follow in similar proportions. The Tyneside locations show no important differences in hydrocarbon levels. In Salford the concentrations were all somewhat lower in the smokeless zone. The small country towns had lower figures, and amongst the larger towns York showed low levels considering its size.

VOL. 4 1961

Air in the motor car garage had rather more smoke with corresponding increases for most of the hydrocarbons. Comparing the air in the tunnel with that entering at St. George's Dock, the ratios were as follows at the mid-point and junction: 3 : 4 benzpyrene 1·19, 1·71; 1 : 12 benzperylene 3·12, 5·27; pyrene 3·14, 6·29; fluoranthene 0·83, 1·61; 1 : 2 benzpyrene 1·00, 1·64; coronene 8·33, 12·50; anthanthrene 1·50, 2·67. At the mid-point there was a moderate increase in anthanthrene, whilst 1 : 12 benzperylene and pyrene were greatly, and coronene very greatly, increased. Since, in comparison with most of the other hydrocarbons, coronene is a stable substance, occurring in domestic smoke in almost constant low proportion, as shown below, it may prove useful as an index of air pollution caused by motor traffic. At the point of highest pollution the amounts of all the hydrocarbons were increased further, coronene being 12 times and 1 : 12 benzperylene and pyrene 5 or 6 times as plentiful as in the entering air. Smoke figures quoted for the tunnel, which depend on photometric measurement, are over-estimations of true values since vehicular smoke tends to be much blacker than ordinary smoke.

Proportions of hydrocarbons in smoke

Table 2 shows the average amounts of the 7 hydrocarbons per million parts of smoke at the same places, obtained by dividing the measured concentrations in air by the corresponding photometric estimates of the total smoke. When the four " inside " locations are excluded coronene values show no more variability (18–24) than might be explained by experimental error, and anthanthrene content is fairly constant, but the other hydrocarbon figures are very variable. In Liverpool the proportion of most

of the hydrocarbons in the smoke is lowest near the river; and in Newcastle-on-Tyne the smoke on the seaward side contained smaller amounts of all the hydrocarbons than at the centre. In the smokeless zone of Salford 3 : 4 benzpyrene alone shows any pronounced difference. Size of town seems to bear little relation to the amounts of the hydrocarbons per unit of smoke; Wetherby figures were surprisingly high, as were those of York in comparison with Liverpool. The Mersey Tunnel figures are all too low for the reason stated, but they cannot be accurately corrected since experiments in

Table 2. Average annual amounts of 7 polycyclic hydrocarbons per million parts of suspended matter (smoke) in 1958 at 22 localities in Lancashire, West Riding of Yorkshire and Tyneside

Location of filter	3 : 4 Benz-pyrene	1 : 12 Benz-perylene	Pyrene	Fluor-anthene	1 : 2 Benz-pyrene	Coro-nene	Anth-anthrene
Merseyside Conurbation							
St. George's Dock (riverside)	117	99	28	88	85	23	24
Roe Street (¾ m. E. of river)	127	110	36	44	69	24	23
Edge Lane (2¼ m. E. of river)	115	123	53	72	78	23	26
Inside Bus Depot	*142*	*126*	*55*	*74*	*93*	*25*	*32*
Inside Motor Garage	*104*	*113*	*38*	*52*	*69*	*29*	*32*
Mersey Tunnel							
Mid-point	(*52*)	(*113*)	(*31*)	(*33*)	(*32*)	(*71*)	(*13*)
Road junction	(*33*)	(*86*)	(*27*)	(*23*)	(*23*)	(*47*)	(*10*)
In Other Conurbations							
Elland (14 m. W. of Leeds)	108	96	32	49	63	21	20
Keighley (16 m. WSW. of Leeds)	109	108	34	61	74	22	23
Leeds (Vicar Lane)	100	95	34	49	61	22	22
Gateshead (Boro' offices)	156	125	73	101	92	21	33
Newcastle-on-Tyne							
(Wharncliffe St.)	149	145	74	115	90	20	40
(Shields Rd.)	111	101	57	79	66	18	30
Salford (Regent Road)	189	108	66	87	91	21	29
(Smokeless zone)	111	119	69	96	78	24	25
*Small Country Towns**							
Wetherby	115	114	69	105	80	24	23
Ripon (9·5)	109	89	48	72	66	21	23
*Larger towns**							
Lancaster (24·2)	71	49	34	51	49	20	21
Darwen (30·8)	125	123	60	85	87	19	28
Warrington (80·7)	111	108	40	58	72	22	24
Burnley (84·9)	105	95	14	24	69	20	21
York (105·3)	137	121	78	110	92	24	26

* Figures in parentheses are 1951 census populations in thousands.

the tunnel have shown that the ratio of the weight of smoke assessed by blackness to the true weight was not constant. Actual figures from six weekly samples at the tunnel junction showed a variation between 1·2 and 2·8, with a mean 1·8, in the ratio.

SEASONAL CHANGES IN AMOUNTS OF SMOKE AND HYDROCARBONS

Table 3 compares the mean concentrations in air in half-year autumn–winter (W) and spring–summer (S) periods, starting from mid-October 1954, at 10 places in respect of smoke and 4 polycyclic hydrocarbons. The smoke densities changed little from year to year in either of the periods. In contrast with the other hydrocarbons 3 : 4 benzpyrene figures showed a downward trend during 1955–58 in all the localities, but since the significance of this is doubtful only the averages of the W and S periods are given in the table. The average W/S ratios in the country townships, larger towns and Merseyside excluding Hoylake were as follows: Total smoke 2·4, 2·8, 2·6; 3 : 4 benzpyrene 2·9, 6·0, 4·8; 1 : 12 benzperylene 2·7, 5·3, 5·3; pyrene 2·6, 5·0, 5·3; fluoranthene 2·5, 4·6, 6·2. This shows that although the relative seasonal effect on

TABLE 3. AVERAGE AMOUNTS OF SMOKE AND HYDROCARBONS PER 1000 CUBIC METRES OF AIR AT 10 PLACES IN NORTH WALES, CHESHIRE AND LANCASHIRE DURING AUTUMN–WINTER (W) AND SPRING–SUMMER (S) PERIODS.*

Locality	Period	Total smoke (mg)		3 : 4 Benzpyrene (μg)		1 : 12 Benz-perylene (μg)		Pyrene (μg)		Fluor-anthene (μg)	
		W	S	W	S	W	S	W	S	W	S
Country townships											
Tattenhall	1954–7	101	59	23	9	10	4	9	3	15	5
Llangefni	1954–7	68	25	17	6	8	3	4	2	6	4
Larger towns											
Flint	1954–7	240	80	60	11	31	5	18	3	28	5
Chester	1954–7	393	109	51	12	36	8	14	4	24	7
Wrexham	1954–7	361	138	91	18	37	8	21	5	28	8
Industrial town											
St. Helens	1954–7	527	195	148	37	72	19	47	6	68	12
Merseyside											
Hoylake (seaside)	1954–6	160	66	50	13	14	4	10	3	14	5
Birkenhead	1954–7	400	179	108	29	61	14	37	6	53	8
Bootle	1954–7	501	172	152	34	72	14	47	6	66	10
Liverpool (Princes Road)	1954–7	560	225	166	33	95	18	40	6	61	12

* See note below Table 4.

total smoke was only slightly greater in town than country the effect on amounts of individual hydrocarbons was twice as great in the urbanised areas as in the small country townships. In the latter places with little industrial smoke the winter increases are due to more domestic smoke and relatively they are about the same for the hydrocarbons as for total smoke. In larger towns the summer smoke is mainly from non-domestic sources and this part changes little with season, but in winter more domestic smoke is mixed with it with a resulting increase in the amounts of the hydrocarbons.

Table 4 compares the W and S concentrations in 1956–57 in 7 towns around Merseyside, ranked according to their populations, and at 7 outdoor locations and 5 special sites within the conurbation. The outdoor locations in Merseyside are arranged

VOL. 4 1961

according to proximity to the sea and estuary, and the W figures increase up to 1 mile east and then decline at 3 miles east of the river, as also do the S values if Birkenhead is ignored. The W/S ratios for smoke were 3·6 at the seaside, 2·1 at Birkenhead and around 3 elsewhere. At the seaside hydrocarbons almost disappeared in summer, giving very high W/S ratios. On the Birkenhead side of the river the hydrocarbon ratios were 5 to 6, and on the east bank the W/S ratios for 3 : 4 benzpyrene, pyrene, 1 : 12 benzperylene and fluoranthene were 11, 7, 9 and 10 respectively, at ¾–1 mile east of the river they were 14, 14, 7, 7 and at 7 miles to the east they were 12, 16, 3 and 12. The autumn–winter increase was much more pronounced, therefore, in respect of the hydrocarbons than for total smoke, implying that smoke in Merseyside contains more of these substances in winter than in summer.

At Princes Road, Liverpool, instruments were placed outside and inside a large office to ascertain the amount of air-pollution to which open-air workers are exposed

Table 4. Average amounts of smoke and 4 polycyclic hydrocarbons per 1000 cubic metres of air at 19 locations in Merseyside and neighbouring towns during Autumn–Winter (W) and Spring–Summer (S) periods of 1956–57.†

Location of filter	Relation to (*a*) Liverpool or (*b*) River Mersey	Total smoke (mgm) W	S	3 : 4 Benz-pyrene (μgm) W	S	1 : 12 Benz-perylene (μgm) W	S	Pyrene (μgm) W	S	Fluor-anthene (μgm) W	S
Outside Merseyside	(*a*)										
Ruthin (pop. 3·6) •	25 m. to S.W.	130	68	13	2	15	2	5	1	8	2
Flint (14·3)	12 m. to S.S.W.	234	77	39	4	33	4	20	2	22	4
Ormskirk (20·6)	12 m. to N.N.E.	310	125	43	6	42	11	19	1	29	1
Wrexham (31·0)	25 m. to S.	343	144	41	4	36	6	18	3	23	4
Chester (48·2)	15 m. to S.S.E.	278	104	30	4	28	7	17	2	22	4
Warrington (80·7)	18 m. to E.	573	200	92	10	60	9	34	2	55	6
St. Helens (110·3)	11 m. to E.N.E.	513	183	100	21	77	17	47	3	73	5
In the Conurbation	(*b*)										
West Kirby (seaside)	7 m. to W.	169	47	6	1	19	1	10	0	18	1
St. George's Dock	E. riverside	410	157	45	4	38	4	14	2	20	2
Birkenhead	¼ m. to W.	428	200	69	9	68	11	32	4	41	6
Roe Street (Dale St.)	¾ m. to E.	500	179	62	2	68	8	31	2	44	7
Bootle	¾ m. to E.	508	161	79	11	79	13	39	3	49	8
Princes Road	1 m. to E.	624	215	142	27	117	22	49	4	80	11
Inside Office	do.	*507*	*162*	*104*	*23*	*64*	*12*	*20*	*5*	*25*	*6*
Edge Lane	3 m. to E.	604	207	95	8	82	25	48	3	61	5
In Bus Depot	do.	*605*	*231*	*130*	*21*	*62*	*24*	*40*	*1*	*40*	*5*
In Motor Garage	do.	*700*	*281*	*111*	*27*	*96*	*25*	*81*	*1*	*83*	*5*
Mersey Tunnel											
Mid-point	Under river	(*1044*)	(*749*)	*97*	*25*	*72*	*64*	*38*	*8*	*41*	*29*
Road junction	do.	(*2027*)	(*1811*)	*88*	*65*	*146*	*92*	*63*	*18*	*68*	*19*

• 1951 Census populations in thousands.

† *Note*. The rates for hydrocarbons have been adjusted for changes in analytical technique introduced for 1958, and some may differ in consequence from rates published previously, but seasonal and geographical comparisons for any one hydrocarbon are unaffected by this. All rates in tables of this paper are comparable with one another.

compared with indoor workers in a centrally heated building. The absolute outdoor excess of 3 : 4 benzpyrene was 38 in autumn–winter and only 4 in spring–summer; for 1 : 12 benzperylene the differences were 53 and 12, for pyrene 29 and nil, and for fluoranthene 65 and 5. In the W period, inside air was considerably less polluted than that outside, but nevertheless the amounts of hydrocarbons were about 4 times as great as in the S period inside the office.

The concentrations of hydrocarbons inside the motor garage and the bus depot were not significantly different from concentrations outside during the winter period. During the summer the results showed an excess of 3 : 4 benzpyrene inside the garage and the depot, indicating that the vehicles were producing a small amount of benzpyrene. The inside concentrations were not large, however, and were similar to those of 3 : 4 benzpyrene found inside diesel bus garages in London (COMMINS *et al.*, 1957). Concentrations in those garages during the summer varied between 3 and 29 μg/1000 m^3 compared with values from 3 to 27 μg/1000 m^3 in the outside air.

In the Mersey Tunnel the autumn–winter (W) and spring–summer (S) concentrations were increased as shown by Table 5. The total of the 4 hydrocarbons was enhanced at each measuring point by rather more in the W than in the S period. The right-hand part of the table shows how the total was made up in the air entering the

TABLE 5. INCREASES IN HYDROCARBONS IN MERSEY TUNNEL AIR IN TWO HALVES OF THE YEAR

	Initial amounts at inlets		Increase (μg/1000m^3)				Expressed as percent of total					
			Mid-tunnel		Junction		Inlet air		Increases at Midpoint		Junction	
	W	S	W	S	W	S	W	S	W	S	W	S
3 : 4 benzpyrene	45	4	52	21	43	61	38	33	40	18	17	34
1 : 12 benzperylene	38	4	34	60	108	88	33	33	26	53	44	48
Pyrene	14	2	24	6	49	16	12	17	18	5	20	9
Fluoranthene	20	2	21	27	48	17	17	17	16	24	19	9
Total of 4	117	12	131	114	248	182	100	100	100	100	100	100

tunnel and at the two points. In the W period the added hydrocarbons at the mid-point contained relatively more pyrene and less 1 : 12 benzperylene than in the entering air, but at the junction it contained relatively more of each of these and less 3 : 4 benzpyrene. In the S period the added hydrocarbons at the mid-point contained relatively more 1 : 12 benzperylene and fluoranthene and less of the other two than in the inlet air, and at the junction they contained relatively more 1 : 12 benzperylene, and less pyrene and fluoranthene. Although the absolute concentration of each of the four hydrocarbons was greatly increased in the tunnel, as shown by the left hand part of the table, it appears that 1 : 12 benzperylene was increased by the motor traffic in relatively greater degree than the others.

AMOUNTS OF TRACE ELEMENTS IN AIR

Tables 6 and 7 give the amounts of various trace elements per 1000 m^3 of air at 16 representative and 9 special locations, the copper and chromium measurements not

VOL. 4 1961

being available for all of these. At a large steelworks by the river Dee instruments were placed in four situations to ascertain the effects of the various processes on the atmosphere in terms of trace element concentrations, the research laboratory site being in the administrative building at some distance from the workshops and providing a control measure of the normal air in the district. The control for Mersey Tunnel is provided by the air entering the ventilation shaft at St. George's Dock.

TABLE 6. AVERAGE ANNUAL AMOUNTS OF TOTAL ASH, LEAD, ZINC, COPPER, TITANIUM, ARSENIC AND MANGANESE PER 1000 CUBIC METRES OF AIR AT 25 LOCALITIES IN LANCASHIRE, WEST RIDING OF YORKSHIRE AND NORTH WALES IN 1956–58

Location of filter	Year	mg/1000m³		μg/1000m³				
		Total ash	Lead	Zinc	Copper	Titanium	Arsenic	Manganese
Merseyside Conurbation *								
St. George's Dock	1957	24·5	0·55	250	74	9	40	28
Roe Street	1957	19·5	1·19	260	46	54	45	18
Edge Lane	1957	17·0	0·60	325	50	44	31	17
In Bus Depot	1957	*17·5*	*0·61*	*260*	*47*	*68*	*40*	*18*
In Motor Garage	1957	*10·5*	*1·29*	*175*	*41*	*30*	*37*	*18*
Mersey Tunnel								
Mid point	1957	*54·5*	*7·30*	*325*	*120*	*19*	*36*	*53*
Road Junction	1957	*120·5*	*20·45*	*600*	*205*	*38*	*66*	*104*
Birkenhead	1956	13·0	0·60	240		20	68	35
Bootle	1956	22·0	0·58	490		50	130	50
Princes Road	1956	15·0	0·57	280		60	94	34
Hoylake (seaside)	1956	5·0	0·26	130		20	33	22
In Other Conurbations								
Elland	1958	7·2	0·42	285	50	16	32	12
Keighley	1958	13·0	0·71	140	44	42	41	43
Leeds	1958	37·1	1·30	370	96	180	60	130
Salford (Regent Road)	1958	21·0	1·43	335	252	75	74	43
(Smokeless zone)	1958	12·4	0·95	245	42	38	42	28
Steelworks †								
Research laboratory	1958	12·8	0·26	185	23	36	17	31
Near Blast furnace	1958	51·7	0·33	955	320	59	50	160
In Rolling mill shed	1958	*192·0*	*0·65*	*850*	*930*	*106*	*400*	*455*
In Melting shop	1958	*375·0*	*11·05*	*9950*	*2850*	*265*	*800*	*2750*
Rural Situattons								
Conway Valley	1957	4·0	0·08	48	7	11	5	5
Ruthin	1957	8·5	0·47	73	14	33	13	10
Wetherby	1958	6·6	0·35	205	38	17	27	13
Industrial Towns								
St. Helens (glass)	1956	15·0	0·44	330		40	160	32
Warrington (chemical)	1957	24·0	0·75	440	53	84	51	50

* See Table 2 for details.

† These figures are comparable one with another but not with other locations.

TABLE 7. AVERAGE ANNUAL AMOUNTS OF NICKEL, ANTIMONY, VANADIUM, CHROMIUM, MOLYBDENUM, COBALT AND BERYLIUM PER 1000 CUBIC METRES OF AIR AT 25 LOCALITIES IN LANCASHIRE, WEST RIDING OF YORKSHIRE AND NORTH WALES IN 1956–58

Location of filter	Year	μg/1000m³						
		Nickel	Anti-mony	Vana-dium	Chro-mium	Molyb-denum	Cobalt	Beryl-lium
Merseyside Conurbation *								
St. George's Dock	1957	19·0	15·5	53·5	5·4	3·15	2·20	0·58
Roe Street	1957	55·5	20·0	18·0	6·7	2·95	2·65	0·42
Edge Lane	1957	96·0	11·0	13·0	4·7	2·45	1·80	0·38
In Bus Depot	1957	*13·9*	*10·0*	*23·5*	*5·1*	*3·25*	*1·46*	*0·54*
In Motor Garage	1957	*7·8*	*10·1*	*23·5*	*2·9*	*2·45*	*0·95*	*0·31*
Mersey Tunnel.								
Mid-point	1957	*15·5*	*14·5*	*27·0*	*7·5*	*1·90*	*4·85*	*0·71*
Road junction	1957	*30·5*	*21·5*	*48·0*	*14·5*	*3·40*	*4·35*	*1·60*
Birkenhead	1956	10·0	12·0	31·0		2·00	1·60	0·60
Bootle	1956	23·0	20·0	42·0		1·80	2·00	1·00
Princes Road	1956	11·0	16·0	30·0		2·70	1·40	1·00
Hoylake (seaside)	1956	2·0	3·6	7·9		0·40	1·00	0·40
In Other Conurbations								
Elland	1958	205·0	8·6	1·1	2·1	1·25	2·30	0·19
Keighley	1958	32·5	12·8	3·7	4·1	2·50	2·05	0·31
Leeds	1958	23·0	16·0	15·0	21·5	6·10	4·25	0·84
Salford (Regent Road)	1958	32·0	18·5	14·2	7·0	5·60	2·60	0·67
(Smokeless zone)	1958	16·5	15·5	13·6	5·2	3·75	2·50	0·43
Steelworks †								
Research laboratory	1958	6·5	5·9	2·9	3·2	0·57	1·20	0·18
Near Blast furnace	1958	22·0	15·5	5·5	9·5	1·00	1·50	0·04
In Rolling mill shed	1958	*36·0*	*67·0*	*59·0*	*29·0*	*4·00*	*9·15*	*1·00*
In Melting shop	1958	*99·0*	*130·0*	*50·0*	*38·0*	*7·00*	*12·00*	*2·00*
Rural Situations								
Conway Valley	1957	1·3	0·9	1·2	0·9	0·29	0·25	0·06
Ruthin	1957	1·8	3·3	1·2	1·6	0·60	0·74	0·15
Wetherby	1958	74·5	5·3	1·5	2·7	1·29	0·85	0·14
Industrial Towns								
St. Helens (glass)	1956	24·0	250·0	18·0		3·20	1·60	0·90
Warrington (chemical)	1957	37·0	21·5	12·0	4·4	5·00	2·90	0·81

* See Table 2 for details.
† See note under Table 6.

Abnormally high concentrations in outdoor locations occurred for copper in the winter period at Salford, for arsenic in the summer period at St. Helens, for nickel at Elland, for antimony at St. Helens and for chromium at Leeds. At the steel works the amount of total ash was enhanced 4-fold near the blast furnace, 15-fold in the rolling mill shed and 29-fold in the melting shop, and compared with this 4–15–29 sequence individual elements showed the following: lead 2–2–42, zinc 5–5–54, copper 14–40–124, titanium 2–3–7, arsenic 3–24–47, manganese 5–15–89, nickel 4–10–15, antimony 3–11–22, vanadium 2–20–17, chromium 3–9–119, cobalt 1–8–10. Both near

VOL. 4 1961

the blast-furnace and in the rolling-mill shed the proportional increase in copper concentration was notably greater than that of total ash; and in the melting-shop lead, zinc, copper, arsenic, manganese and chromium were all more than 40 times as plentiful as in the normal air whereas the concentration of total ash was enhanced by a factor of 29.

Table 8 summarizes two aspects of the data, comparing the average levels in 4 non-urban situations (Conway Valley, Ruthin, Wetherby, Hoylake), in 4 large industrial towns (Salford, Leeds, St. Helens, Warrington) and 4 locations in Merseyside (Roe Street, Edge Lane, Bootle, Princes Road), and expressing the values at five sites of a special character in terms of their respective controls. Comparison between the urban

Table 8. Effects of urban and other conditions on amounts of trace elements present in the atmosphere

Element	Average amounts in air (μg/1000m^3)			Expressed as ratios to controls				
	Semi-rural	Industrial towns	Conurbation	Bus depot	Motor garage	Mersey tunnel		Smokeless zone
						Mid	Junction	
Lead	290	980	735	1·0	2·1	13·3	37·2	0·7
Zinc	114	369	339	0·8	0·5	1·3	2·4	0·7
Copper*	(20)	(134)	(48)	0·9	0·8	1·6	2·8	0·2
Titanium	20	95	52	1·5	0·7	2·2	4·4	0·5
Arsenic	20	86	75	1·3	1·2	0·9	1·6	0·6
Manganese	13	64	30	1·1	1·0	1·9	3·7	0·7
Nickel	20	29	46	0·2	0·1	0·8	1·6	0·5
Antimony	3·3	(76)	17	0·9	0·9	0·9	1·4	0·8
Vanadium	3·0	14·8	26	1·8	1·8	0·5	0·9	1·0
Chromium*	(1·7)	(11·0)	(5·7)	1·1	0·6	1·4	2·7	0·7
Molybdenum	0·6	5·0	2·5	1·3	1·0	0·6	1·1	0·7
Cobalt	0·7	2·8	2·0	0·8	0·5	2·2	2·0	1·0
Beryllium	0·2	0·8	0·7	1·4	0·8	1·2	2·8	0·6
	(mg/1000m^3)							
Total ash	6·0	24·3	18·4	1·0	0·6	2·2	4·9	0·6

* Averages in first three columns are based on 3, 3 and 2, locations only, none being available for Hoylake, St. Helens, Bootle and Princes Road.

and rural values shows that in general the element concentrations in the towns were raised in about the same proportion as the total ash, except antimony, vanadium and molybdenum which showed larger urban excess.

Comparing the indoor locations with their controls, the bus depot air had increases in titanium and vanadium of 1·5 : 1 or more and in the motor garage lead and vanadium were in excess, but many of the elements were present in lower concentration inside than out. Mersey tunnel air contained very much greater amounts of lead than did the air entering the tunnel; next in order of enhancement came titanium, manganese, copper, beryllium, chromium and zinc, but the increases were not as great as those for total ash. Vanadium and molybdenum showed no increase in concentration in the tunnel sites. In the smokeless zone of Salford the concentrations of most

elements were lower than those measured at the town centre, the decrease being most appreciable (5 : 1) for copper.

Acknowledgement—In a previous paper by one of us (STOCKS, 1958b) acknowledgements were made to the many people who had helped and were continuing to help in this co-operative study. Our thanks are due also to the Directors of John Summers' steelworks for allowing instruments to operate there during 1958, and to Dr. P. J. LAWTHER, M.R.C. Air Pollution Research Unit at St. Bartholomew's Hospital and Dr. E. T. WILKINS, Warren Spring Laboratory of the D.S.I.R. for their help and advice.

REFERENCES

D.S.I.R. (1945) Atmospheric Pollution in Leicester; A Scientific Survey. H.M.S.O., London.

COMMINS B. T. (1958a) *Analyst* **83**, 386.

(1958b) *Int. J. Air Poll.* **1**, 14.

COMMINS B. T., WALLER R. E. and LAWTHER P. J. (1957) *Brit. J. Indust. Med.* **14**, 232.

GORE A. T. and SHADDOCK C. W. (1958) *Brit. J. Prev. Soc. Med.* **12** (2), 104.

PEMBERTON J., CLIFTON M., DONOGHUE J. K., KERRIDGE D. and MOULDS W. (1959) *Int. J. Air Poll.* **2**, 175.

STOCKS P. (1955) *J. Fac. Radiol.* **6**, 166; (1958a) Supplement to Ann. Rep. of Brit. Empire Cancer Campaign for 1957; (1958b) *Int. J. Air Poll.* **1**, 1; (1959) *Brit. Med. J.* **1**, 74; (1960) *Brit. J. of Cancer* **14**, 397.

STOCKS P. and CAMPBELL J. M. (1955) *Brit. Med. J.* **2**, 923.

VOL.
4
1961

Int. J. Air and Water Poll. Pergamon Press 1961. Vol. 4, Nos. 3/4, pp. 154–167. Printed in Great Britain.

ACUTE EFFECT OF SULPHUR DIOXIDE ON THE RATE OF CILIARY BEAT IN THE TRACHEA OF RABBIT, *IN VIVO* AND *IN VITRO*, WITH STUDIES ON THE ABSORPTIONAL CAPACITY OF THE NASAL CAVITY

TORE DALHAMN and LARS STRANDBERG
The Karolinska Institute, Institute of Hygiene, and the
Department of General Hygiene, National Institute of
Public Health, Stockholm, Sweden
(*Received* 25 *April* 1960)

INTRODUCTION

THE reasons for the acute, deleterious effects of smog are extremely complicated, since smog contains a large number of different substances and both chemical and physical processes occur. It has been discussed whether one of the contributory causes might not be the adsorption of gaseous pollutions by the particulate elements. Depending on the size of the particles, these penetrate down and are retained to a greater or a lesser extent at different depths in the respiratory tracts, whereupon the toxic influence of the gases can make itself felt. The physical qualities of the gases, and perhaps above all their solubility in water, are clearly also of essential importance for their toxicity (LA BELLE *et al.*, 1955). This argument has been put forward regarding, *inter alia*, sulphur dioxide, which might be adsorbed on carbon particles, whereupon these latter, after being inhaled, could give off the adsorbed sulphur dioxide (Committee on Atmospheric Pollution 1953: MEETHAM, 1954). PATTLE and BURGESS (1957) consider that this is a case of a simple additional effect, but it has long been known from industry that the corrosive effect of a constant concentration of sulphur dioxide varies tremendously as between the presence and absence of particulate elements. Similarly, the effect of sulphur dioxide increases in the presence of moisture (HARRISON, 1957).

The acute effects of inhalation of low concentrations of sulphur dioxide have been studied by AMDUR *et al.* (1953), among others, who published a work in which they demonstrated that inhalation of 1–8 p.p.m. sulphur dioxide during a period of 10 minutes caused increases in the respiration and pulse rates in man. Individuals who had their daily work in an atmosphere of ca. 10 p.p.m. sulphur dioxide or more showed, however, no change either in the respiration or the pulse rate. The results of these experiments have, however, since been called into question by LAWTHER (1955), who was unable to determine any change in either the tidal volume or the respiration and pulse rates after 10 minutes' inhalation of 5 and 10 p.p.m. sulphur dioxide. In a later work, AMDUR (1957) has investigated in guinea pigs the effect on the pulmonary flow resistance that occurs after the inhalation of sulphuric acid mist and sulphur dioxide, as well as that of an inert aerosol of sodium chloride mixed with these other substances. The mixture of sulphur dioxide and sulphuric acid mist gave a result that showed the increase in pulmonary flow resistance as being greater than could be accounted for by simple additivity. This was also the case when sulphur dioxide was mixed with the sodium chloride aerosol.

A factor of essential importance for the discussion and understanding of the toxicity of different gases and particulate elements is their absorption in the respiratory tracts. One of the physiological effects of the nasal cavity is, as is well known, the warming and moistening of the inhaled air. In the inhalation of polluted air there takes place a certain filtration and an absorption of pollutants. There is a great deal of literature describing the capacity of particles of different sizes to penetrate in the respiratory tract, but the literature on the gas absorption capacity of the nasal cavity, on the other hand, seems to be very sparse.

This absorptional capacity is dependent on a great many chemical and physical qualities on the part of the gases in question, but the most important, perhaps, is their degree of solubility in water. The secretion in the nose and bronchi consists, in fact, of roughly 2·5–3 per cent mucin, 1–2 per cent salts, and 95–97 per cent water (PROETZ, 1953). LEHMANN (1908) carried out a number of experiments on the absorption of different gases in the respiratory tract. In this connection he used four different methods, and his subjects have been both human beings and animals. The concentrations of sulphur dioxide used by LEHMANN in certain experiments on human beings were, (*a*) around 130 p.p.m. and (*b*) around 240 p.p.m., during a period of 30 minutes. The air analyses were carried out on a mixture of inspired and expired air, and an absorption of 70 per cent and 65 per cent respectively was determined for the concentrations of sulphur dioxide employed. It was noted particularly that strong reaction symptoms in the nasal mucosa, in the form of powerful secretion and a feeling of irritation, lasted a remarkably long time after exposure had ceased.

VOL. 4 1961

In the experiments on animals, rabbits were used, and the concentrations were considerably higher, namely around 400 p.p.m. to around 6000 p.p.m. The animals inhaled the gas either through a tracheal cannula or through a tube set in the nose. The gas absorption in both cases was 46 per cent.

GADASKINA (1947) investigated the absorption capacity for sulphur dioxide in the upper respiratory tract of rabbits, and she found that with concentrations varying between about 200 p.p.m. and 6000 p.p.m. the mean figure for the total absorption was 63 per cent (range 46–81 per cent), while the absorption in the case of tracheotomized animals sank to 42 per cent (range 21–55 per cent).

Among other investigations on the effect of sulphur dioxide on the respiratory tracts can be mentioned CRALLEY'S (1942) and DALHAMN'S (1956). CRALLEY investigated the effect of, *inter alia*, sulphur dioxide on the ciliary activity in the trachea of rabbits *in vitro*. He found that 50 p.p.m. sulphur dioxide stopped the ciliary activity in 60 seconds. Corresponding investigations on live material have been performed by DALHAMN, using his own method. By blowing moistened and heated gas over the trachea, which was laid open with a longitudinal slit, it was shown that the ciliary activity of rats stopped about 5 minutes after exposure to 12 p.p.m. sulphur dioxide, and after about 60 seconds in the case of exposure to 50 p.p.m.

Investigations have also been carried out with a view to throwing light on the effect of long-term inhalation of sulphur dioxide, and one of the things that has been demonstrated is that serious epithelial damage can occur in the respiratory tract after exposure even to low concentrations (DALHAMN and RHODIN, 1956). Since, however, the writers of the present article have not been concerned with this problem, no more detailed account of the literature in this field would seem to be necessary here.

EXPERIMENTS

This article contains a detailed examination, of certain toxicologic problems regarding the acute effects of sulphur dioxide on the respiratory tract. Special interest has been devoted to the reactions of the ciliary epithelium, and to the absorption of sulphur dioxide in the respiratory tracts. The reactions of the ciliary epithelium have been observed both with the animals themselves inhaling the sulphur dioxide and with the gas being applied to the trachea *in vitro*.

METHODS OF ANALYSIS

When analysing the sulphur dioxide content, either the current iodometric titration method was used alone, as described by JACOBS (1953) among others, or, in the case of certain absorption experiments, together with the conductimetric method.

With the titrimetric method, the sulphur dioxide is absorbed in iodine solution in a peligot tube that also contains equivalent amounts of thiosulphate.

After absorption, by mixing the iodine solution and the thiosulphate and by titrating back with iodine, the concentration of sulphur dioxide can be determined.

Samples were taken by connecting to the exposure chamber a sampler as illustrated in Fig. 1. The gas mixture is taken through the peligot tube, which contains 25 ml iodine solution and 25 ml thiosulphate, via a gas pump to a rotameter. The sampling was performed by the gas mixture being sucked through the peligot tube at a speed of 2·00 litres per minute for five minutes, i.e. 10 litres in all. The pressure and the temperature were recorded and corrected to N.T.P. The reagents, which were mixed daily from a standard solution of 0·1 N iodine solution and 0·1 N thiosulphate solution, was around 0·01 N. To begin with, three analyses were made for each experiment, namely an initial value, a value during the exposure, and, finally, an analysis after the exposure had been concluded. With the large amounts used (100–300 p.p.m.), however, it was found that the variations between the three values in this connection were quite negligible, so that most often two, and sometimes only one determination of the concentration was made. In this latter case, the one determination was always made during exposure. A series of ten initial values showed a mean of 185 p.p.m. sulphur dioxide, and after 45 minutes the corresponding figure was 191 p.p.m.

In order to assess the reliability of the method with low contents of sulphur dioxide, two control series were made. The first was a series of ten blanks, i.e. samples in which no absorption of sulphur dioxide in iodine solution had taken place. This series gives an idea of the error of titration (pipetting error, individual variations in readings, etc.). The mean figure was 0·90 ml iodine solution: $\sigma = 0{\cdot}02$ ml. This means a 2·3 per cent error for the mean figure in this series, but this can obviously not be generalised to apply to other fields of titration. The other control series comprised ten samples taken immediately after each other, i.e. about every tenth minute from the exposure chamber. These samples give a value for the total error in the taking of the sample, including error of titration, error in the determination of volume, and any other sources of error that may exist. The mean figure was 2·65 ml iodine solution corresponding to 8·6 p.p.m. sulphur dioxide: $\sigma = 0{\cdot}05$ ml. With these low concentrations a qualitative test has also as a rule been made after the exposure. Here the gas was led down either into a fuchsin solution or into an iodine solution, both of which are decolourized in the presence of sulphur dioxide. With the iodine test a stream of air was at the same time led through another tube with iodine solution and the differences in colour between the non-treated solution, the iodine solution exposed to the air, and the solution exposed to the sulphur dioxide were observed.

In all cases where the analyses showed the presence of even small amounts of sulphur dioxide either the fuchsin solution was decolourized, or the iodine solution that was exposed to the sulphur dioxide was decolourized, while that which was exposed to the air did, in fact, lighten, but was not decolourized.

With certain adsorption experiments not only iodometric titration but also a conductimetric method of analysis was used to determine the sulphur dioxide concentrations.

Apart from the general sources of error connected with this method of measurement (variation in the temperature of the liquid, pollution with other conductive substances, neutralisation of the hydrogen ions through the alkali, in the glass, changes in ion activity with large concentrations, etc.) there are certain special sources of error that can arise during the determination of low concentrations

of sulphur dioxide. Low concentrations of other gases which react with water and form ions could give rise to errors. Of particular interest in this connection is carbon dioxide. The size of the carbon dioxide error in these experiments was determined by the measurement of the absorption liquid both before and after the elimination of the carbon dioxide by heating the liquid to 100° C for a few minutes. Adjusted to p.p.m. sulphur dioxide, the carbon dioxide error was 1–1·5 p.p.m. As regards the other sources of error, it can be mentioned that a temperature variation of 1° at the determination of the conductive ability gives an error in the region of 2 per cent. In the present case the measurements were always made at a constant, controlled temperature, 25° C, the absorption solutions were subjected to a routine purity check before each experiment and used glass chambers were inspected and carefully washed out in glass-distilled water, etc. The cell constant for the measuring cell was determined at regular intervals against standardized potassium chloride solution. In addition to this, two measurement cells were used simultaneously in a large number of cases, in order to avoid occasional errors in the measurement cell. A check that conductivity was determined within a suitable area of concentration was made by taking measurements on a dilution series 1–1, 1–10, 1–100, and, in certain cases, 1–1000, on the solutions obtained from the absorption chamber. The sulphur dioxide content of air mixtures of known concentration down to 5 p.p.m. were also determined. With these low concentrations variations from the expected concentration lay around 1–2 p.p.m. The errors predominating at these low concentrations stem more from the difficulty of determining conductivity with sufficient precision, and preventing pollution from influencing the determination in different ways, than from any difficulty in obtaining an exact gas dosage. With greater concentrations of sulphur dioxide, on the other hand, the error of measurement consists for the greater part of a gas dosage error and the error that can arise as a result of changes in the ion activity in higher concentrations. This latter type of error can be controlled to a certain degree by making a dilution series of the solution from the absorption chamber.

VOL. 4 1961

METHODS OF EXPOSURE

In order to *record the ciliary activity in vivo* the method described by DALHAMN (1960) was used. Briefly this involves, after the tracheotomization of the animal, the fastening of a rubber bellows round the trachea, and the airtight connection of the bellows to a microscope with vertical light. In this way the ciliary activity in the trachea can be observed and recorded with the use of a moving picture camera. With this method, the animals breathe through their normal channels of respiration. After the animals had been prepared in this way they were exposed to the required concentration of sulphur dioxide: recordings of the ciliary activity were then made.

A special exposure chamber was constructed, the appearance of which can be seen in Figs. 1 and 2. In a spherical plastic container, with a capacity of about 100 litres,

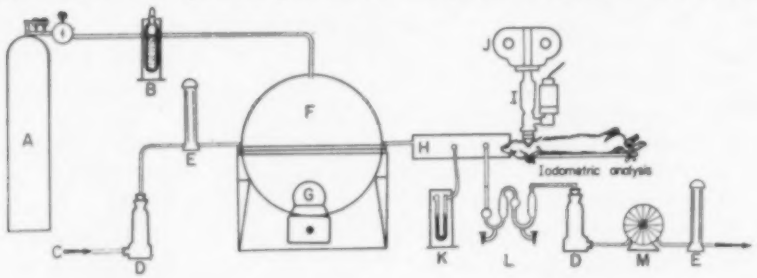

A Cylinder with about 12% SO_2
B Capillary manometer
C Compressed air
D Drying tower
E Rotameter
F Mixing vessel
G Fan
H Sedimentation chamber
I Microscope
J High speed camera
F Manometer
L Peligot-tube
M Pump

FIG. 1

roughly 12 per cent sulphur dioxide was mixed with air. The supply of sulphur dioxide was controlled with the aid of a capillary manometer, and the air stream was controlled with a rotameter. From this container the gas mixture was led into a smaller chamber. Along both sides of this there are terminals for a thermal precipitator, for a millipore filter holder, and for gas analyses. The end of this smaller chamber has a hole suitable for the head of a rabbit. The outlet terminus, for the analyses mentioned above, is in the immediate neighbourhood of the animal's nostrils. The seal around the head of the rabbit was accomplished with the aid of a plastic cuff.

The apparatus for the exposure of the trachea of rabbits *in vitro* was much the same as that previously used for the trachea of rats (DALHAMN, 1956). The latter experiments, however, were made *in vivo*.

The trachea, opened longitudinally and removed from the animal, was placed in a chamber, where the relative humidity was about 100 per cent and the temperature around 37° C.

The exposure to sulphur dioxide took place in the following manner. The gas-air mixture was obtained in the same manner as with the previous exposures to sulphur dioxide. From the mixing chamber the gas was drawn into a wash bottle with a minute amount of water, and the wash bottle was placed in the moistened chamber. In this way the gas coming from the wash bottle was both moistened and warmed. From the wash bottle the gas was conducted at a speed of 20–30 cm per second over the trachea with the aid of a plastic mouthpiece, from which also gas samples were taken for the determination of concentration. A control of the method of exposure was made by blowing only air over the trachea for 15 minutes, while at the same time observing the ciliary movements. After this, sulphur dioxide was drawn over the trachea in a similar way for a period of 30 minutes.

The absorption in the respiratory tracts of rabbits was studied in two different ways. The principle difference was that with method (A) the absorptional capacity of the nose or the mouth was studied, while with method (B) an idea was obtained of the absorptional capacity of the entire respiratory channel.

A. The trachea of the rabbit was dissected free, after which an airtight cannula was set in the cranial part. The animal was then allowed to breathe through the caudal part of the trachea. The nostrils, or, alternatively, the mouth, were sealed off, after which the head of the animal was placed in the exposure chamber described previously. From the cranial part of the trachea, air with a percentage of sulphur dioxide was then continuously sucked with a speed of 1 litre per minute for 45 minutes, and the sulphur dioxide content of the air sucked out was iodometrically determined every 15 minutes with the method previously described.

B. Nembutal was applied through a plastic tube placed in one of the rabbit's ear veins. After this the trachea was carefully freed immediately below the thyroid, and a minute opening between two rings of cartilage made on the ventral side. Through this opening a cannula ca. 1·5 mm thick and 2·5 cm long was introduced, the other end of the cannula having previously been joined to a plastic tube. The cannula was fixed in the surrounding throat musculature with a few sutures. Before the wound was closed a check was made that breathing through the nose could take place unhindered, and that air could freely pass through the cannula in both directions.

The rabbit thus prepared was placed in an exposure chamber containing about 185 litres and fitted with two fans in order to permit a quick mixing of the air-plus-sulphur-

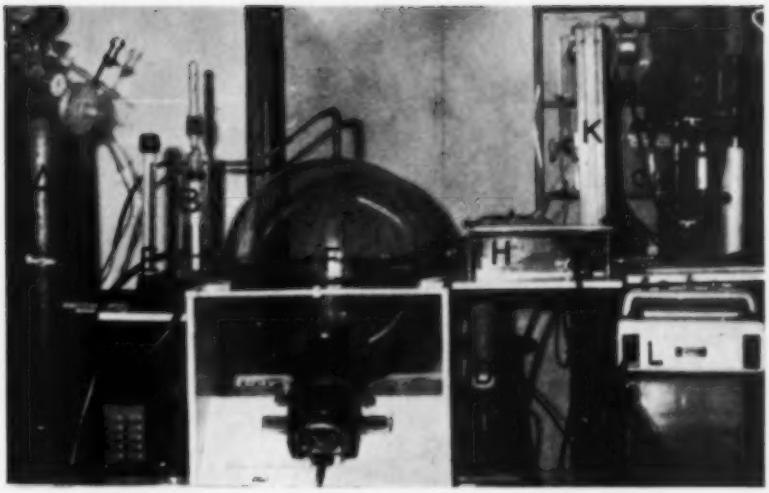

FIG. 2. A. Cylinder with about 12% SO_2. B. Capillary manometer. D. Drying tower. E. Rotameter. F. Mixing vessel. G. Fan. H. Sedimentation chamber. I. Microscope. J. High-speed camera. K. Manometer. L. Thermo-electric temperature indicator.

VOL.
4
1961

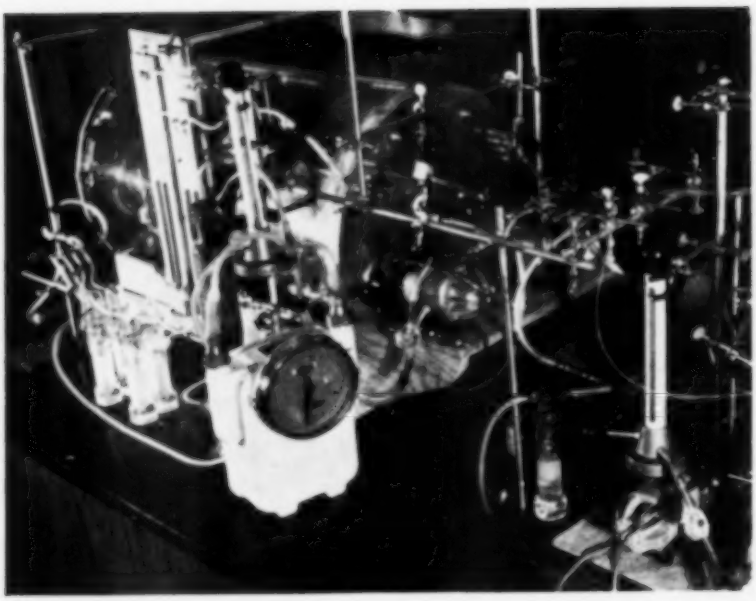

FIG. 4

dioxide that was later applied (Figs. 3 and 4). The temperature and mixture of the air in the exposure chamber were continually recorded in every experiment, and it was found that these did not undergo any essential changes during the actual exposure. The tubes from the ear vein and the tracheal cannula were conducted airtight from the exposure chamber, which made it possible to control the anaesthetic and take samples from the trachea without opening the exposure chamber while the experiment was going on. The chamber was continually supplied with air with a sulphur dioxide content of known concentration. As soon as the required concentration in the chamber had been reached, air with sulphur dioxide of the concentration being studied was supplied in a maintenance dose of 10 litres per minute. Only when the maintenance dose had been provided for some minutes was the taking of samples from the trachea

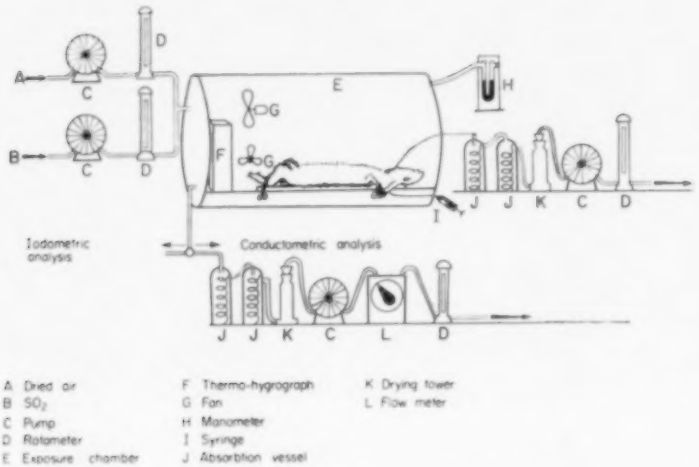

A Dried air
B SO_2
C Pump
D Rotameter
E Exposure chamber
F Thermo-hygrograph
G Fan
H Manometer
I Syringe
J Absorbtion vessel
K Drying tower
L Flow meter

FIG. 3

and the exposure chamber started. The time between the starting of the sulphur dioxide supply and the start of sample-taking was as a rule 15–20 minutes. The concentration of sulphur dioxide in the exposure chamber was determined both iodometrically and conductimetrically, while the concentration in the tracheal air was determined only conductimetrically.

RESULTS

To begin with, using the *in vivo* method described above, a preliminary investigation was made into how the ciliary beat mechanism in the trachea reacted to different concentrations of sulphur dioxide. The results seem to suggest that no effect is to be expected under 100 p.p.m., whereas around 300 p.p.m. and over, always leads to the cessation of ciliary activity during exposure. The region between 100–300 p.p.m would seem to be critical.

With a view to studying more closely the affect of different concentrations, three concentrations were chosen cn the basis of the test series, namely around 100 p.p.m., around 200 p.p.m. and, finally, around 300 p.p.m. Each series comprised 10 animals,

VOL. 4 1961

which were exposed for 45 minutes, with the recording of the ciliary activity every 15 minutes in those cases where it had not ceased.

The results of these experiments are seen in Tables 1, 2, and 3. After 15 minutes of exposure the ciliary activity had stopped in 5 cases when the concentration of sulphur dioxide was 200 p.p.m. and in 8 cases when it was 300 p.p.m. On the other hand, with 100 p.p.m. no visible effect could be observed. After 30 minutes exposure no further

TABLE 1. THE EFFECT OF ca. 100 p.p.m. SO_2 ON THE CILIARY ACTIVITY

So_2 (p.p.m.)	Stopped after minutes	Rate of ciliary activity in beats per minute		Rectal temp.	Rate of ciliary activity in beats per minute		Rectal temp.	Rate of ciliary activity in beats per minute		Rectal temp.	Rate of ciliary activity in beats per minute		Rectal temp.
		Initial value	Mean value		After 15 min.	Mean value		After 30 min.	Mean value		After 45 min.	Mean value	
74	—	1256 1222 1263	1247	37·8	1414 1450 1450	1438	37·6	1219 1109 1109	1146	37·6	1347 1322 1385	1351	37·6
85	—	1544 1544 1584	1557	37·6	1437 1451 1414	1434	37·6	1200 1165 1179	1181	37·7	1414 1509 1451	1458	37·7
85	—	1238 1200 1303	1247	36·4	965 988 967	973	36·6	820 797 818	812	36·6	1226 1007 1125	1119	36·6
89	—	1020 1042 1022	1028	37·1	1334 1289 1320	1314	37·3	1320 1320 1278	1306	37·2	1238 1278 1217	1244	36·9
92	—	1257 1226 1277	1253	37·4	1048 1039 1039	1042	37·4	971 938 943	951	37·6	990 986 961	979	37·6
95	—	1286 1286 1257	1276	37·4	1257 1286 1200	1248	37·4	992 1000 1029	1007	37·1	950 900 910	920	37·1
100	—	1179 1222 1100	1167	37·5	966 973 900	946	37·6	900 898 1000	933	37·5	947 931 947	942	37·5
103	—	1725 1706 1751	1727	38·3	1191 1191 1179	1187	38·2	900 921 943	921	38·0	834 880 879	864	37·8
128	—	1222 1238 1252	1237	39·2	1238 1238 1263	1246	38·4	1257 1263 1238	1253	38·4	1226 1201 1200	1209	38·4
134	—	906 906 906	906	37·1	943 880 925	916	37·1	898 906 900	901	37·3	850 810 800	820	37·3
Mean (99)			1265	37·6		1175	37·5		1041	37·5		1091	37·4

changes had taken place, but after 45 minutes the ciliary activity stopped in a further case, both at 200 p.p.m. and at 300 p.p.m. Thus in the group exposed to 200 p.p.m. there remained, after 45 minutes exposure, four animals with registrable ciliary activity, and in the 300 p.p.m. group, only one animal.

As regards the 100 p.p.m. group, the mean figure for the initial value was 1265 beats per minute; after 15 minutes exposure was 1175 beats per minute, after 30 minutes 1041 beats per minute, and finally, after 45 minutes, 1091 beats per minute. If a statistical analysis is made of this material it is seen that the variation between the rabbits was 143 beats per minute, and the error of method, i.e. the error in the calculation of the films, 33 beats per minute. These values are in very close agreement with the figures given in a previous publication (DALHAMN, 1960). The inter-animal variation was 176 beats per minute, and the error of method, 40 beats per minute. It

was also found that the effect of exposure to sulphur dioxide may be a moderate decrease of the rate of beat. This can be fixed at a low level of significance, namely $0{\cdot}05^{x} > P > 0{\cdot}01$.

The temperature of the tissues has an important effect on the rate of ciliary beat, as has been pointed out in several publications. The rectal temperature in the group exposed to 100 p.p.m. varied very little; the mean figures for the quarter hour intervals

TABLE 2. THE EFFECT OF ca. 200 p.pm. SO_2 ON THE CILIARY ACTIVITY

SO_2 (p.p.m.)	Stopped after minutes	Rate of ciliary activity in beats per minute		Rectal temp.	Rate of ciliary activity in beats per minute		Rectal temp.	Rate of ciliary activity in beats per minute		Rectal temp.	Rate of ciliary activity in beats per minute		Rectal temp.
		Initial value	Mean value		After 15 min.	Mean value		After 30 min.	Mean value		After 45 min.	Mean Value	
175	—	1125 1189 1109	1141	37·2	843 818 840	834	37·2	825 808 786	806	37·2	754 740 754	749	37·2
196	7	1324 1217 1257	1266	38·0	—			—			—		
196	An inconsiderable part beat after 45 min. Could not be filmed	1200 1222 1256	1226	37·0	—			—			—		
199	20	1059 1088 1126	1091	36·0	—			—			—		
208	14	1375 1437 1437	1416	38·3	—			—			—		
219	Inconsiderable after 45 min. Could not be filmed	1150 1140 1200	1163	38·7	958 946 943	950	38·6	915 900 920	912	38·6	—		
223	—	1109 1079 1090	1093	38·5	1109 1109 1131	1116	38·8	943 1015	977 973	38·7	1091 1100 1076	1089	38·7
228	—	1257 1259 1313	1276	36·0	1305 1302 1322	1310	36·2	990 1019 985	998	36·1	900 860 919	893	36·1
229	—	1150 1200 1175	1175	37·5	850 910 940	883	37·6	850 805 875	843	37·6	875 800 820	832	37·5
239	4	1165 1131 1165	1154	36·2	—			—			—		
Mean (210)	—	—	1200	37·3	—	1019	37·7	—	907	37·6	—	891	37·4

were 37·6, 37·5, 37·5, 37·4. A drop in the rectal temperature cannot thus be responsible for the observed drop in rate of beat.

If, however, one inspects the individual values in the table, it is seen that the initial value for animal No. 8 is very high, 1727 beats per minute, and no similar rate was obtained on any other occasion. If this animal is disregarded, and the significance calculated on the remaining animals, no significant effect of the sulphur dioxide exposure is obtained ($P > 0{\cdot}2$). We have, however, considered it proper to give an account of the material in its entirety.

The initial value for the 10 animals in the 200 p.p.m. group was 1200 beats per minute. The variation between the animals was 98 beats per minute, and the error of

VOL. 4 1961

method 34 beats per minute. The mean figure for the rectal temperature was 37·3 (range 36·0–38·7).

The initial value for the group exposed to 300 p.p.m. sulphur dioxide was 1077 beats per minute. The inter-animal variation was calculated at 60 beats per minute, and the error of method at 59 beats per minute. The mean figure for the rectal temperature was 37·1 (range 38·8–35·4).

TABLE 3. THE EFFECT OF ca. 300 p.p.m. SO_2 ON THE CILIARY ACTIVITY

SO_2 (p.p.m.)	Stopped after minutes	Rate of ciliary activity in beats per minute		Rectal temp.	Rate of ciliary activity in beats per minute		Rectal temp.	Rate of ciliary activity in beats per minute		Rectal temp.	Rate of ciliary activity in beats per minute		Rectal temp.
		Initial value	Mean value		After 15 min.	Mean value		After 30 min.	Mean value		After 45 min.	Mean value	
267	Inconsiderable after 45 min. Could not be filmed	1106 1042 1042	1063	35·4	825 838 811	825	35·4	842 811 860	838	35·4	—		
277	15	1050 950 1100	1033	37·1	—			—			—		
286	15	975 950 1050	992	37·2	—			—			—		
290	20	1048 1025 1015	1029	36·7	—			—			—		
322	17	1200 1200 1100	1167	36·0	—			—			—		
330		1100 1158 1178	1145	37·0	1190 1164 1164	1173	37·4	1421 1018 1067	1169	37·3	967 1042 1068	1026	37·3
330	9	900 1000 1100	1000	37·5	—			—			—		
342	1	1100 1050 1150	1100	37·6	—			—			—		
348	14	1164 1164 1229	1185	37·0	—			—			—		
350	15	1045 1135 980	1053	38·8	—			—			—		
Mean (314)		1077		37·1									

The results of the experiments with the trachea *in vitro* are seen in Table 4, which shows that no effect could be observed from concentrations of less than around 7 p.p.m. sulphur dioxide. With higher concentrations a cessation of ciliary activity was observed in all cases. The time when this effect took place varied within wide limits. A correlation calculation between the sulphur dioxide concentration and the time of the occurrence of the effect suggests, however, that there is a correlation here of a high degree of significance ($t = 4{\cdot}79^{xxx}$).

The results of the absorption studies are seen in Tables 5–8. The highest relative absorption was obtained with samples taken via the tracheal cannula from spontaneously breathing rabbits, Tables 5 and 6.

Somewhat lower values for absorption were obtained with the continuous suction of

TABLE 4. THE EFFECT OF VARYING SULPHUR DIOXIDE CONCENTRATIONS ON THE CILIARY MOVEMENT OF THE TRACHEA, *in vitro*

SO_2 (p.p.m.)	Effect on ciliary movement	SO_2 (p.p.m.)	Effect on ciliary movement
4	A small part stopped The greater part did not stop	9 13	Stopped after 28 min. „ „ 9 „
4	Did not stop	14	„ „ 10 „
5	„ „ „	15	„ „ 10 „
5	„ „ „	17	„ „ 14 „
6	„ „ „	18	„ „ 5 „
6	„ „ „	27	„ „ 6 „
7	„ „ „	27	„ „ 7 „
7	Stopped after 25 min.	28	„ „ 6 „
7	„ „ 9 „	33	„ „ 4 „
9	„ „ 13 „		

TABLE 5. ABSORPTION OF SULPHUR DIOXIDE IN THE RESPIRATORY TRACT WITH EXPOSURE TO ABOUT 100 p.p.m.
(Spontaneous breathing, method B)

Rabbit No.	Inhaled sulphur dioxide (p.p.m.)	Sulphur dioxide from tracheal air (p.p.m.)
1	102	3
2	66	2
3	110	2
4	121	2
5	128	2
6	117	2
7	111	2
8	116	2
9	111	2
10	102	2
Mean	108	2

VOL. 4 1961

air from the trachea via the nasal cavity (Table 7) and the relatively lowest values, finally, in those cases where the samples were taken continuously from the trachea via the cavity of the mouth (Table 8). The concentration of sulphur dioxide in the trachea lies around 5–10 per cent of the original concentration, and no very manifest variation seems to have occurred during the 45 minutes in which the experiment was taking place. During one of the exposures for 300 p.p.m. sulphur dioxide, an animal died about 10 minutes after the experiment had started. The initial value in the trachea was 34 p.p.m. after 15 minutes the concentration had increased to 138 p.p.m. and after 30 minutes it exceeded 200 p.p.m.

TABLE 6. ABSORPTION OF SULPHUR DIOXIDE IN THE RESPIRATORY TRACT WITH EXPOSURE TO ABOUT 250 p.p.m.
(Spontaneous breathing, method B)

Rabbit No.	Inhaled sulhur dioxide (p.p.m.)	Sulphur dioxide from tracheal air (p.p.m.)
1	338	2
2	208	2
3	233	2
4	238	2
5	202	3
6	218	3
7	222	3
8	243	3
9	255	3
10	257	2
Mean	241	2·5

DISCUSSION

In the present investigation, the main object of study was the acute effect of sulphur dioxide. Three groups of rabbits, with ten animals in each, were made to inhale 100, 200, and 300 p.p.m. sulphur dioxide for a period of 45 minutes, while at the same time the ciliary beat in the trachea was recorded. It was determined that at 100 p.p.m. the ciliary movements were not affected. At 300 p.p.m., on the other hand, the ciliary movements ceased practically completely after 45 minutes. These results might appear surprising in view of the fact that it has been demonstrated in previous investigations, with direct exposure on the trachea of rats *in vitro*, that ciliary movement is very sensitive to exposure to sulphur dioxide. In those investigations it was, thus, shown that

the ciliary movements ceased after ca. 2 minutes exposure to about 25 p.p.m. The explanation for this discrepancy could be sought either in rabbit trachea having a considerably smaller sensitivity to sulphur dioxide than that of rats, or in considerably lower concentrations of sulphur dioxide being obtained in the trachea with experiments *in vivo*, owing to absorption in the nasal cavity and the pharynx.

TABLE 7. ABSORPTION OF SULPHUR DIOXIDE IN THE NASAL CAVITY WITH EXPOSURE TO 100, 200 and 300 p.p.m.
(The air was sucked through the nasal cavity)

Rabbit No.	Inhaled sulphur dioxide (p.p.m.)	Sulphur dioxide concentrations in p.p.m. after passing through nasal cavity			
		At the commencement of exposure	After 15 min.	After 30 min.	After 45 min.
1	104	6	4	4	4
2	106	7	4	5	5
3	119	5	4	3	3
4	119	5	6	11	14
5	121	5	4	4	6
1	161	4	4	6	6
2	178	4	9	8	7
3	180	4	4	4	7
4	200	7	5	4	6
5	206	11	11	12	15
1	290	15	23	22	14
2	293	30	20	26	25
3	299	16	25	27	39
4	304	14	16	12	27
5	318	45	49	42	49

TABLE 8. ABSORPTION OF SULPHUR DIOXIDE IN THE MOUTH AND PHARYNX AT EXPOSURE TO 200 p.p.m.

Rabbit No.	Inhaled sulphur dioxide (p.p.m.)	Concentration of sulphur dioxide after passing through the mouth and pharynx			
		At the commencement of exposure	After 15 min.	After 30 min.	After 45 min.
5	175	11	13	19	17
3	180	10	9	11	16
1	190	6	8	8	11
4	196	12	13	15	20
2	213	25	26	18	13

VOL. 4 1961

By carrying out direct exposure experiments on rabbit trachea *in vitro* it has been possible to demonstrate that there is no important difference in sensitivity in this respect, as between the trachea of rabbits and rats. With concentrations as low as around 10 p.p.m. sulphur dioxide the ciliary movements ceased in the trachea of both types of animal.

The other possibility of explaining the discrepancy between, on the one hand, the absence of ciliary reaction at the inhalation of 100 p.p.m., and on the other, the high degree of sensitivity to sulphur dioxide demonstrated in the mucosa, is that the greater part of the sulphur dioxide was absorbed before it reached the trachea. An investigation of the absorption was therefore made, two different methods of exposure being used. It was found that the absorption of sulphur dioxide in the upper respiratory tracts of rabbits was very great in the case of the concentrations studied. With the *in vivo* experiments in which an effect on the ciliary activity was recorded, i.e. with the inhalation of about 300 p.p.m. sulphur dioxide, it was determined that the concentration of sulphur dioxide in the trachea was of about the same extent as that which gave rise to corresponding effects in the *in vitro* experiments.

The experiments show that only a small part of the gas manages to penetrate down into the trachea via the absorption mechanism in the rabbit's nasal cavity, which is extremely effective, at least in the case of sulphur dioxide. This is the case even with sulphur dioxide concentrations in the inhaled air many times greater than the contents recorded in smog. Even if absorption is different in man, as is probable, from that in rabbits, it still seems that the experiments made do not support the idea that the effects of smog are the result of an acute inhibition of the ciliary movements owing to a pure sulphur dioxide action.

The idea of a synergism between the different components of smog has been put forward from a number of quarters. The gaseous components, it is suggested, are absorbed by particles of different kinds, and these are then variously retained on inhalation, depending on their size, in the respiratory tracts of different animals. In previous experiments, it has been shown that long-term exposure to sulphur dioxide in low concentrations (about 10 p.p.m.) gives rise to local damage to the mucosa in the respiratory tracts of rats. To what extent this damage occurred as a result of ciliary inhibition appearing later, or whether there were other contributory factors as well, cannot be determined. It can thus not be excluded, on the basis of the experiments made to date, that sulphur dioxide in even lower concentrations than those found in smog, can give rise to other local damage to the mucosa, and affect the secretion. It is thus not possible at the moment to take up a position on the question of the role played by sulphur dioxide in smog from the point of view of human pathology. Among other things needed here are further studies on the question of synergistic effects.

SUMMARY

The writers have studied the effect of acute sulphur dioxide exposure on the ciliary movements in the trachea. Both live rabbits and isolated trachea were used. For the recordings, a previously published method involving, *inter alia*, the filming of the ciliary movement was used. The experiments in which the animals inhaled the sulphur dioxide show that no certain effect on the ciliary movement could be recorded

at concentrations below about 200 p.p.m. Experiments which involved blowing the sulphur dioxide directly on to the trachea *in vitro* show, however, that about 10 p.p.m. of sulphur dioxide is enough to stop the ciliary movements. This discrepancy can be explained by the absorption by the rabbits' nasal cavities of large quantities of sulphur dioxide. The two series of experiments, differing in principle, show clearly that this is the case. About 90–95 per cent of the sulphur dioxide concentrations used (100–300 p.p.m.) were absorbed.

As regards the effect of the sulphur dioxide in smog, the writers draw the conclusion that it is unlikely that any acute inhibition of the ciliary movements takes place as an effect of sulphur dioxide alone. In order to make clearer the role played by sulphur dioxide in smog from the point of view of human pathology, further studies are required, *inter alia*, of synergistic effects.

REFERENCES

AMDUR M. O., MELVIN W. W. and DRINKER P. M. (1953) Effects of inhalation of sulphur dioxide by man. *Lancet* **265**, II, 758–62.

AMDUR M. O. (1957) The respiratory response of guinea pigs to sulphur dioxide. *Am. Indust. Hyg. Ass. Quart.* **18**, 149–55.

COMMITTEE ON ATMOSPHERIC POLLUTION (1953) Beaver report. HMSO, London.

CRALLEY L. (1942) The effects of irritant gases upon the rate of ciliary activity. *J. Indust. Hyg. and Tox.* **24**, 193–8.

DALHAMN T. and RHODIN J. (1956) Mucous flow and ciliary activity in the trachea of rats exposed to pulmonary irritant gas. *Brit. J. Indust. Hyg.* **13**, 110–13.

DALHAMN T. (1956) Mucous flow and ciliary activity in the trachea of healthy rats and rats exposed to respiratory irritant gases. *Act. Phys. Scand.* **36**, Supp. 123, 1–161.

DALHAMN T. (1960) The determination *in vivo* of the rate of ciliary beat in the trachea; a methodological, experimental study on animals. *Act. Phys. Scand.* **49**, 242–50.

GADASKINA I. D. 1946 Adsorption of sulphur dioxide in the respiratory passages. FARMAKOL. *i* TOKSIKOL. No. 1, **9**, quoted in *Am. Chem. Soc. Abstracts*, 1308, **41**, 1947.

HARRISON J. W. E. (1958) Public health aspects of air pollution. *Ass. Food and Drug Officials* **22**, 116–26.

JACOBS M. B. (1953) *Analytical Chem. Industr. Poisons, Hazards and Solvents*, London.

LABELLE CH. W., LONG J. E. and CHRISTOFANO E. E. (1955) Synergistic Effects of Aerosols. *Arch. Indust. Health* **11**, 297–304.

LAWTHER P. J. (1955) Effects of inhalation of sulphur dioxide on respiration and pulse-rate in normal subjects. *Lancet* **269**, II, 745–8.

LEHMANN K. L. (1908) Neue Untersuchungen über die quantitative Absorption einiger giftigen Gase von Tier und Mensch durch den Respiratius Traktus und seiner Teile. *Arch. für Hyg.* **67**, 57–98.

MEETHAM A. R. (1954) Natural removal of atmospheric pollution during fog. *Quart. J. Roy. Med. Soc.* **80**, 96–9.

MINISTRY OF HEALTH (1959) Mortality during the London fog of December 1952. Reports on Public Health and Medical Subjects, no. 95, 1–61. HMSO, London.

PATTLE R. E. and BURGESS F. (1957) Toxic effects of mixtures of sulphur dioxide and smoke with air. *J. Path. Bact.* **73**, 411–19.

PROETZ A. W. (1953) Essays on the Applied Physiology of the Nose. Annals Publishing Comp. Saint Louis, U.S.A., 1–452.

VOL. 4 1961

Int. J. Air and Water Poll. Pergamon Press 1961. Vol. 4, Nos. 3/4, pp. 168–184. Printed in Great Britain.

ON THE NATURE OF THE SYNERGISTIC ACTION OF AEROSOLS

ALEXANDER GOETZ
California Institute of Technology, Pasadena, California
(*Received* 1 *April* 1960)

Abstract—The paper gives a theoretical treatment of the kinetic aspects of free gas molecules and their interaction with the surface of air-borne particles. It aims at a physical interpretation of aerosol synergism in general, and in particular of the intensification of toxic (or irritant) gas traces by certain aerosol types.

Aerosols can act as intensifiers of the physiological reaction if their substance has a sorptive affinity for the toxic gas component large enough to produce an accumulation on the particle surface, but smaller than the affinity of the tissue surface which they contact in order to effect a transfer of the molecules thereon. If the particle affinity substantially exceeds that of the tissue, an attenuation of the effect should occur.

The theoretical functions derived from these assumptions are applied qualitatively to the data reported by LABELLE, *et. al.* (1955) for 27 gas-aerosol combinations, and quantitatively to those by AMDUR (1960) on the effect of NaCl aerosols in the presence of HCHO, and good agreement is obtained.

Within the margin of experimental error the data can be described quite accurately by the theoretical functions and no conflict is apparent.

1. INTRODUCTION

THE existence of a synergistic effect of air-borne particulate matter (aerosols) on toxic gaseous trace components has been suggested by several authors (VORWALD, 1952; MAGILL, 1949; DAUTREBRANDE and CAPPS, 1950). There have also been reports to the contrary which question whether the presence of aerosols could affect appreciably the physiological effects of toxic or irritant gas traces in the atmosphere (GORDIEYEFF, 1956). Since 1956 more systematic investigations have been made which leave no doubt that under certain conditions strong synergistic effects can be produced.

From a practical point of view, this raises the serious question of the general validity of the tolerance limits set for various atmospheric pollutants, should their toxicity be dependent on the nature, concentration and even the size distribution of the coexisting aerosol.

The following is an attempt to interpret these effects semi-quantitatively by the kinetics of gas molecules and their interaction at particle surfaces. This attempt appears to be justified since for the first time sufficiently well defined quantitative data are available which permit a comparison with theoretical postulates.

2. BASIC ASSUMPTIONS

The basic assumptions of the interpretation (GOETZ, 1958) concern the mechanism initiating the more or less complex chain reaction leading to the physiological irritation signal as recorded by the observer. The nature of the reaction as such is irrelevant in this discussion. These assumptions may be formulated as follows:

(1) The condition of prime importance is the permanent transfer of the toxic or irritant molecules, denoted by T, from the air-borne state on to the exposed tissue surface by irreversible collision.

In terms of the dynamics of sorption phenomena (DE BOER, 1953) this results in a practically infinite residence time of the molecule on the surface and its incorporation into it because of the affinity of the surface for T.

(2) The recorded irritation signal, Σ, is assumed as a first approximation to be proportional to its cause. It reflects the topical concentration of T occurring during a short time interval on any small fraction of the exposed tissue surface. The nature of the ensuing reaction is unknown, and so the functional form of Σ is not predictable, but could be determined empirically for each type of T and Σ.

(3) The aerosols whose synergistic effect is considered are assumed to be physiologically neutral themselves. The particle surface is assumed to have an affinity for T which results in the accumulation of T thereon, and the particle acts as a carrier of a large number of T-molecules.

(4) The synergistic effect resulting from irreversible collision of the particle with the surface depends on the different affinities which the particle and the tissue surface have for T. It can be expected that the particle types with a *high* affinity for specific T-molecules can *attenuate* the response, provided the concentration of the aerosol is large enough to decrease the concentration of the gaseous fraction of T substantially. On the other hand, if the tissue has a larger affinity for T than the particle surface, T will be transferred and produce an increase in concentration of T on the tissue, thereby causing an *intensification* of the response.

It can also be seen that the effect must be restricted to relatively low concentrations of T, and must depend on the concentration and size of the air-borne particles.

Before deriving quantitative relations we shall discuss the first systematic data on the interaction between various types of T and aerosols, namely those of LABELLE *et al.* (1955) because they appear to justify at least qualitatively the principal assumptions.

VOL. 4 1961

3. THE RESULTS OF LABELLE *ET AL.*

The experiments determined the survival time of test animal (mice) exposed to toxic gases with and without the addition of aerosols. Three different toxic gases were used: two aldehydes (formaldehyde and acrolein), and nitric acid vapor. Their concentrations were the same in the presence and absence of the aerosol and were such as to cause, in the absence of aerosols, about the same survival period of the animals (of the order of 10^2 min).

As aerosols, nine different substances were used: four liquids (tri-ethylene-glycol, ethylene-glycol, glycerol, mineral oil), one electrolyte (sodium chloride), and four solid sorptive materials (two commercial types of diatomaceous earth—Dicalite and Celite—silica gel, and an absorptive clay).

The mass median diameter d of the particles ranged from 1·8 to 3·3 microns, i.e. the upper end of the size range likely to reach, at least partially, the lower parts of the respiratory system (ALTSHULLER *et al.*, 1957).

The mass concentration C_p varied over the fairly wide range from 5×10^{-5} to 2×10^{-3} g/litre, i.e. a concentration more than 100 times larger than occurring in normal atmospheric aerosol pollution, though still insufficient to affect the animals in the absence of T.

Of prime importance is the finding that the survival time can be either substantially increased or decreased for the same type and concentration of T by different aerosols:

furthermore, that the same aerosol acts as an attenuator for one, and as an intensifier for another vapor.

The results lend themselves to the following analytical presentation:

The total particle surface area per unit volume A_p is given by

$$A_p = \frac{6C_p}{\rho d} \tag{1}$$

TABLE 1. DATA—LABELLE *et al.*

	Tri-Ethylene Glycol	Ethylene Glycol	Glycerol	Mineral Oil	Silica gel	Clay	Dicalite	Celite	NaCl	Control	
ρ (g cm^{-3})	1·1	1·1	1·3	0·8	1·4	2·5	2·1	2·1	2·1		
d (10^{-4} cm)	1·8	2·0	2·0	2·1	2·7	3·3	3·3	2·9	2·6		
					Formaldehyde						
A_P (cm^2)	67	79	29·6	50	4·9	7·0	3·65	3·55	25·3	147	
t_A (min)	71	(168)	114	72	(145)	(157)	118	102	114	—	
α	+0·775	(−0·177)	+0·78	+1·02	(+0·20)	(−0·71)	+5·5	+8·72	+0·91		
					Acrolein						
A_P (cm^2)	11·5	13·6	5·1	8·5	0·79	1·16	0·61	0·59	4·25	87	
t_A (min)	(73)	(106)	(94)	69	65	(78)	(91)	(99)	0·71	—	
α	(+1·39)	(−1·62)	(−1·37)	+2·47	+31·7	(+0·86)	(−8·2)	−23·8	+4·22		
					Nitric Acid						
t_A (min)	142	151	(103)	72	177	198	254	188	220	118	
α	−1·74	−2·06	(+3·9)	+4·5	−63	−59	−189	−100	−20·2	—	

In ( ) data of no statistical significance.

where C_p is the aerosol concentration per unit volume, ρ the density of the particles and d their median diameter.

The relative synergistic effect α' of an aerosol can be defined as

$$\alpha' = 1 - \frac{t_A}{t} \tag{2a}$$

where t and t_A are the animal lifetimes on exposure to T in the absence and in the presence of aerosol respectively. A *negative* value of α' represents an attenuating, and a *positive* value an intensifying synergism.

The specific effectiveness, or synergistic potential, α of an aerosol is defined as the ratio of α' to the particle surface area:

$$\alpha = \frac{\alpha'}{A_p} = \frac{\rho d}{6C_p}\left[1 - \frac{t_A}{t}\right] \tag{2b}$$

α is thus a direct, although arbitrary, measure of the degree to which the total particle surface contributes to the intensification or attenuation of the toxic vapor.

Table I presents values of A_p and α derived from the data (LABELLE, 1955) for C_p and d, together with the assumed bulk densities.

C_p was systematically larger (by about 5 times) for formaldehyde than for the other two T-types, and a larger A_p value has to be used for them. Obviously $A\rho$ is correct only for the liquid aerosols, and reasonably so for sodium chloride. For the other solids, however, it may be much too small, since any contribution by their internal surface to the accumulation of T cannot be accounted for. If A_p is actually greater than the value given by Eq. (1), the value of α given by Eq. (2b) will be too large. Consequently, the majority of the α values for porous aerosols exceed substantially those for sodium chloride and the liquid aerosols. LABELLE graded the tests into three classes of statistical significance according to the mean deviation of t_A. In Table I the data of " no significance " are bracketed.

VOL. 4 1961

TABLE 2. SYNERGISTIC POTENTIAL OF VARIOUS AEROSOL TYPES

	Formaldehyde	Acrolein	Nitric Acid
Intensifying Action	*Celite* Dicalite *Mineral Oil* NaCl *Glycerol* *Triethylene Glycol*	Silica gel NaCl Mineral Oil	Mineral Oil
Attenuating Action	none	(Celite) (Dicalite)	*Dicalite* *Celite* *Silica gel* *Clay* *NaCl* *Ethylene Glycol* *Triethylene Glycol*

In italics: " highly significant " data. In ( ) data of no statistical significance if $\alpha > 5$.

In Table 2 the aerosol types are arranged in order of their specific effectiveness for the three *T*-types. The " highly significant " results are in italics, and those of " no significance " are omitted if $\alpha' < 5$ and bracketed if $\alpha > 5$.

The following relationships for the 27 vapor-aerosol combinations are apparent:

(*a*) The intensifying effect of the aerosol—regardless of type, with one exception—disappears and reverts to an attenuation with decreasing volatility of *T*. The exception is mineral oil, which for each *T* also has the largest value of α' among the aerosols composed of liquid particles, i.e. of those with well-defined A_p.

(*b*) The porous particles, notably both types of diatomaceous earth (well known for their large capillary volume and surface), act in a strikingly different manner. For formaldehyde, the *T*-type with the highest volatility, they act as intensifiers; whilst they are the most potent attenuators for nitric acid vapour. Silica gel (possibly because of its much lower porosity) changes from the intensifying to the attenuating role for nitric acid. The action of clay is insignificant except for nitric acid vapour.

(*c*) The glycols and glycerol show a very limited synergistic capacity, acting as weak intensifiers for formaldehyde and as the poorest attenuators for nitric acid.

These results support the basic assumptions 3 and 4 made above, as can be seen from the following discussion:

Mineral oil, which acts as intensifier for all three *T*-types, may be taken as representative of the interaction between aerosol and *T*. It is unlikely to interact chemically with any of the *T*-types, but is apparently capable of adsorbing (without dissolving) the *T*-molecules so that they will readily be transferred on subsequent contact with the tissue surface. In this respect the oil droplets seem to act very similarly to aerosolized latex particles (GOETZ and TSUNEISHI, 1959).

The action of the porous particles seems to be determined by the potential reversibility of the accumulation process for *T* in the pore structure. If the vapor pressure of *T* is large, the subsequent yield will be quite substantial and rapidly attained because of the large pore volume. Therefore, they are potent intensifiers for formaldehyde. When the low vapour pressure renders the initial capillary condensation of *T* virtually irreversible they act as effective attenuators.

It is noteworthy in this respect that the silica gel, characterized by an extremely fine pore structure, acts as intensifier for a relatively large *T*-molecule like acrolein, while the diatomaceous earths, with their coarse capillaries, are attenuators. For less volatile *T*-molecules the gel (and also the clay) acts in a similar manner to the diatomaceous earths but is definitely less effective (Table 2).

It is uncertain whether sodium chloride occurred in the tests as hydrated or crystalline particles (ORR *et al.*, 1958) while air-borne. The A_p values are likely, however, to be about as representative as those of the liquid aerosols, and its α value appears comparable with the latter. It is thus an intensifier for the aldehydes, almost equal in effect to mineral oil. This indicates the absence of a chemical interaction. Sodium chloride is also the most effective non-porous attenuator for nitric acid vapor, because of such interaction.

From the above discussion it can be seen that there are no significant discrepancies between the test results and the principle pattern of the synergistic mechanism.

LABELLE's investigation, although valuable in an exploratory sense, lacks information on the quantitative variation of the synergistic effect with the concentration of $T(C_T)$, and the concentration of aerosol (C_p).

Such data have been obtained by AMDUR (1960) for sodium chloride and certain T-types over a range of C_T and C_p values. The extent of the concentration ranges, together with the fact that the investigated physiological signal (respiratory response in guinea-pigs) can be used as a measure of Σ over a wide range, warrant a more quantitative interpretation. Therefore the discussion of the basic assumptions put forward in section 2 will be developed further.

4. THEORETICAL CONSIDERATIONS

We have attempted to derive, using elementary methods, the quantitative physical relationships which govern the interaction between tissue surface, T-molecule, and aerosol particles.

The tissue surface unit may be represented by a hollow spherical cavity, diameter D, having an inner surface area $A_c\ (=\pi D^2)$ and a volume capacity $V_c\ (=0{\cdot}52D^3)$.

For illustrative purposes a cavity diameter of 10^{-1} cm. in rough analogy with the dimensions of the lower respiratatory channels, will be assumed, giving values of

$$A_c = 3{\cdot}14 \times 10^{-2}\ \text{cm}^2, \quad \text{and} \quad V_c = 5{\cdot}2 \times 10^{-4}\ \text{cm}^3.$$

The number of T-molecules in the cavity, at atmospheric pressure and 0°C, for a T-concentration of 1 p.p.m. (i.e. $C_T = 10^{-6}$ cm^3 per cm^3) is

$$N_T = 0{\cdot}52\bar{N}C_T D^3 = 1{\cdot}4 \times 10^{10} \tag{3}$$

where $\bar{N}$ is the number of molecules per cm$^3 = 2{\cdot}7 \times 10^{19}$.

The area occupied by each T-molecule after its transfer on to the surface A_T is approximately 15Å^2 (i.e. $A_T = 1{\cdot}5 \times 10^{-5}$ cm^2). The maximum average surface concentration on A_c, after every T-molecule in the cavity has collided irreversibly thereon, is thus

$$K_T = \frac{N_T A_T}{A_c} = 0{\cdot}167\ \bar{N}C_T D A_T = 6{\cdot}7 \times 10^{-4} \sim 0{\cdot}067\% \tag{4}$$

K_T increases linearly with C_T and with the diameter of the cavity, and represents in this illustration a surface coverage of less than 0·1% of A_c. These quantities, however, are changed drastically in the presence of air-borne particles with which the T-molecules can associate reversibly.

For simplicity a monodisperse aerosol of particle diameter $d = 0{\cdot}3\mu$, specific gravity $\rho = 1$, and concentration $C_p = 1$ mg . m$^{-3} = 10^{-9}$ g . cm^{-3}, may be assumed. The number of particles in V_c is then

$$N_p = C_p\ .\ D\ .\ d^{-3} = 37 \tag{5}$$

representing a total surface area of

$$A_p = \pi C_p D^3 d^{-1} = 1 \times 10^{-7}\ \text{cm}^2 \tag{6}$$

The fraction of the entire cavity surface which receives a concentration great in excess of K_T by the transfer of T-molecules from the particles is

$$n' = \frac{A_p}{A_c} = C_p\ .\ D\ .\ d^{-1} = 3{\cdot}4 \times 10^{-6} \tag{7}$$

i.e. n' increases with C_p and D, and decreases with d.

VOL. 4 1961

The number of T-molecules bound to the particle surface A_p for each complete monolayer is

$$N'_T = \frac{A_p}{A_T} = \pi C_p D^2 (dA_T)^{-1} = 6{\cdot}7 \times 10^7 \tag{8}$$

and the ratio of bound to free molecules is

$$F_T = \frac{N'_T}{N_T} = \frac{A_p}{A_T N_T} = 6C_p (NC_T dA_T)^{-1} = 5 \times 10^{-3} \sim 0{\cdot}5\% \tag{8a}$$

Hence, in contrast to n', F_T *increases* with C_p/C_T, *decreases* with d, and is independent of the cavity dimensions (D).

If, in analogy to the free T-molecules, all particles in the cavity have been deposited on the cavity surface A_c, and if conditions favour the transfer of all the T-molecules from the particles to the surface fraction n', then the resulting surface concentration can be defined as

$$K'_T = \frac{N'_T A_T}{n' A_c} = \frac{DC_p}{n'd} \rightleftharpoons 1 \tag{9}$$

$K'_T = 1$ if each particle is covered by one complete monolayer from which all the T-molecules are transferred to the cavity surface, i.e. if equations (7) and (8) are valid. In this case K'_T would be about 1500 times greater than the average concentration produced by the free molecules over the whole area K_T, although only 0·5% of the T-molecules is actually carried by the aerosol particles. It can be seen that K'_T will be less (or greater) than unity if less (or more) than the equivalent of a monolayer is associated with the particles—or when the transfer affects a larger (or smaller) area than that represented geometrically by A_p.

The model outlined above is an oversimplification and must be modified in several respects to give a more realistic picture.

(*a*) For given values of C_p, D, A_T, and d, the number of T-molecules bound to the particle surface N'_T must vary with the concentration and partial pressure of T in the cavity, since the absorbed T-molecules must be in equilibrium with those in the free state. The nature of the equilibrium depends on the characteristics of the absorption isotherm for the particular T-aerosol combination. The general behaviour of such isotherms is a more or less steep rise of N'_T for low values of C_T, and an asymptotic approach to a saturation value $\bar{N}'_T$ as C_T increases, so that N'_T becomes virtually invariable for high concentrations of T. The initial variation of N'_T with concentration can be represented, to a first approximation (DE BOER, *ibid*), by

$$\frac{N'_T}{\bar{N}'_T} = \theta = \frac{kN_T}{1 + kN_T} \tag{10}$$

$N'_T = \bar{N}'_T$ when θ, the saturation coefficient, is unity. This is realized when $kN_T \gg 1$. k is a constant which determines the "steepness" of the isotherm, i.e. the rate at which N'_T approaches saturation with increasing C_T.

We have, from Eqs (3), (9) and (10),

$$K'_T = \frac{DC_p \theta}{n'd} = \frac{DC_p}{n'd} \frac{\eta C_T}{1 + C_T} \tag{10a}$$

where $\eta = 0{\cdot}52k\bar{N}D^3$.

(*b*) The number of free *T*-molecules, and hence K_T, is diminished by those which become associated with the particles. However, this correction can be omitted, except for strong attenuation, where $N_T > N'_T$ (since $A_p \ll A_c$).

(*c*) The sorptive capacity of A_p for *T*-molecules is not adequately defined by A_p/A_T (Eq. 8), nor are the areas on the cavity surface exposed to transfer of *T* from the particles necessarily equal to A_p. These uncertainties, together with that of the possibility of multilayers, are accounted for by replacing n' in Eq. (7) by $n = Cn'$, where C is an empirical proportionality factor of the order of unity. Since n and n' do not vary with the concentration of particles and of *T* (if θ approaches unity), it should be possible to determine n experimentally from K'_T by varying d.

(*d*) The free *T*-molecules and the particles in the cavity will not reach the surface instantly, but gradually at an exponentially declining rate. Hence, it may be argued that for a more accurate representation of the irritation signal, a factor should be applied to each K_T and K'_T value which reflects the respective surface collision probabilities, i.e. the respective mobilities of the *T*-molecules and the particles. However, this effect appears to be of second order significance because of the small cavity dimensions involved, and because the rate of air replacement (due to inhalation) should be sufficient to establish a steady state in the cavity. Then a constant large fraction, though not the total of $N\mu$ and N_T, will be transferred to A_c. This would alter K_T and K_T' only to the extent that the effective value of D would be less than that derived from the geometrical dimensions.

The overall concentration causing the irritation signal Σ, derived from Eqs. (4) and (10), is

$$\bar{K} = K_T + K'_T = D\left[\frac{\bar{N}A_T C_T}{6} + \frac{C_p \eta C_T}{nd(H\eta C_T)}\right] \tag{11}$$

This relation should describe in principle the intensification by synergistic aerosols.

Fig. 1 illustrates the variation of $\bar{K}$ with C_T, derived by substituting arbitrary values into Eq. (11), in the absence ($C_p = 0$) and in the presence of a synergistic aerosol, for three different concentrations ($C_p = 1, 3, 10$). The dashed lines are for $\theta = 1$, i.e. for the case of the invariance of N'_T with N_T.

If the intensity, Σ, of the physiological response reflects the variation of $\bar{K}$, then the following experimentally verifiable predictions can be made:

1. In the *absence* of aerosols Σ should increase with C_T according to an empirically determinable relation $\Sigma(C_T)$ from which $\Sigma(\bar{K})$ can be derived to a fair approximation.
2. In the *presence* of aerosols Σ should increase:

(*a*) with C_p for constant C_T, provided the latter does not exceed certain limits which increase with C_p.

(*b*) with C_T for constant C_p. For large values of C_T the magnitude of the increase would be expected to decrease gradually to the vanishing point of the synergistic effect, and the vanishing point should increase with C_p. In terms of Eq. 11 the effect disappears as the second term becomes small compared with the first term.

(*c*) with decrease in the particle size of an intensifying agent, provided both C_p and C_T remain constant.

VOL. 4 1961

3. The difference between the irration signals obtained in the *presence* and *absence* of a synergistic aerosol in the same C_T range [i.e. $\Sigma(\bar{K}) - \Sigma(K_T) = \Sigma(K'_T)$] should increase for small C_T values until $\theta = 1$ and then be constant and *independent* of C_T.

These relations imply that a synergistic intensification is restricted to small concentrations of T and to a relatively narrow range therein. This may explain the fact that

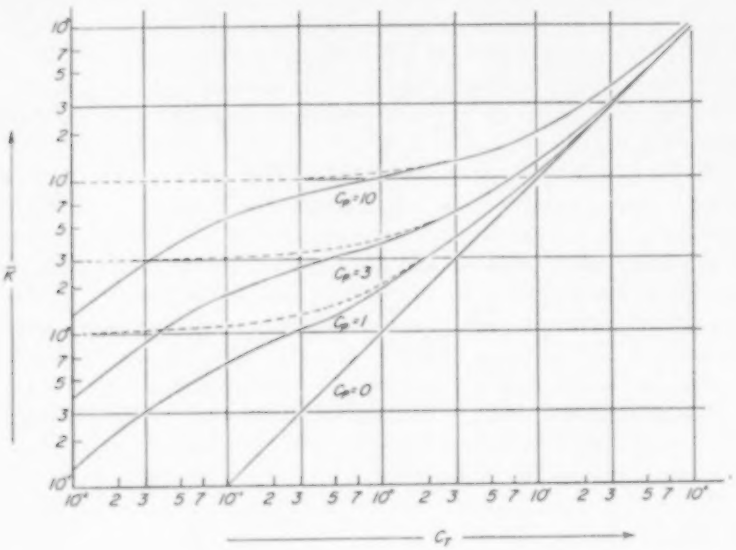

FIG. 1. Graphic representation of the basic function (Eq. 11) in arbitrary units [$A_T \cdot \bar{N}/6 =$; $(n \cdot d)^{-1} =$; $D = 1$], indicating the variation of $(\bar{K})$ with (C_T) in the absence ($C_p = 0$), and the presence of 3 different concentrations ($C_p = 1$, 3, 10) of a synergistic aerosol. The dashed curves represent ($\theta = 1$; i.e. $\eta C_T \gg 1$), the full drawn curves ($\theta = 0{\cdot}13$; $\eta = 0{\cdot}15/C_T$).

such effects have often escaped discovery. Neither would an unlimited increase in intensification be expected by increasing C_p or by a corresponding decrease of d, because both variations tend to increase the coagulation rate of the particles with a resulting limitation for A_p and thus of their adsorptive capacity.

5. DISCUSSION OF AMDUR'S RESULTS

The results obtained by AMDUR (1960) from the exposure of guinea-pigs to two types of T (formaldehyde and formic acid) in the presence and absence of a sodium chloride aerosol have been reported in a previous paper, hence discussion of the experimental and evaluation procedures is unnecessary.

However, the physical state of the aerosol appears to require further definition because the theoretical aspects indicate the large influence of the *size* as well as of the *state* of the particles. Consequently an effort was made in this laboratory to investigate both using the same type of nebulizer (DAUTREBANDE, 1958) under the conditions prevailing in AMDUR's work.

A 1% sodium chloride solution was used. The mean residence time of about 1 min (at $50\% \leqslant rh \leqslant 60\%$) was realized by passing the aerosol into a chamber of suitable size prior to its entry into an aerosol spectrometer (GOETZ, 1957) at a rate of 2 liter/min. The amount of particle deposit analysed was equivalent to an original air

FIG. 2. Size distribution of an NaCl aerosol produced from a 1% solution in a Dautrebande nebulizer after 1 min residence at 50–60% relative humidity, as determined by the aerosol spectrometer; δ represents the kinetic (Stokes') diameter; $C \cdot S'$ is the particle frequency in terms of light scattering power.

volume of about 60 liters. The size distribution of the aerosol, determined by applying a light scattering method (PREINING *et al.*, 1959 and GOETZ 1958) to the particle deposit, is shown in Fig. 2. It shows a distinct lower limit for a Stokes* diameter $\delta = 0{\cdot}18\mu$ which for a sodium chloride crystal ($\rho_c = 2{\cdot}17$) would correspond to a geometrical diameter $d = \delta/\sqrt{\rho_c} = 0{\cdot}123\mu$, and for a saturated sodium chloride *solution* ($\rho L > 1{\cdot}39$) to $d = 0{\cdot}152\mu$ respectively.

There is a definite range [$0{\cdot}225\mu \leqslant \delta \leqslant 0{\cdot}525\mu$] wherein particles occur with equal frequency. The latter decreases to a negligible value for $\delta > 0{\cdot}7\mu$. If an average size is taken at $\delta = 0{\cdot}4\mu$ a geometrical diameter range of $0{\cdot}27 \leqslant d \leqslant 0{\cdot}35$ results, according to whether the aerosol represents crystals or saturated droplets. This alternative depends upon the previous history of the aerosol and the relative humidity at the time interval prior to inhalation.

VOL. 4 1961

From the tests it is clear that for the humidities used ($50\% \leqslant rh \leqslant 60\%$) the sodium chloride is in a crystalline state. Upon entering the more humid atmosphere of the respiratory system a crystal will undergo a significant increase in diameter, with a corresponding decrease in mobility. The drastic change in surface properties is expected to alter the nature of the bond of the previously adsorbed *T*-molecules, provided the *T*-type is water soluble—as is the case for HCHO. This must change the transfer conditions of *T* to the tissue surface upon contact with the particle.

In view of this situation it appears realistic to use the previously assumed particle diameter $d = 3 \times 10^{-5}$ cm prior to inhalation. This value is much larger at the time it contacts the tissue surface and yields its previously adsorbed *T*-molecules. This would be indicated by a much larger value of A_p in Eq. 6.

In order to make a qualitative comparison between theoretical postulates and experiment, the following procedure was used:

The physiological signal Σ was defined throughout as the relative respiratory resistance:

$$\Sigma = \left(\frac{F}{E} - 1\right) \times 100$$

where *E* is the resistance of each animal group *prior* to exposure, and *F after* one hour's exposure to the agents. Σ is expressed as the percentage variation of the respiratory reaction with the change of C_T or C_p.

* δ is the diameter of spherical particles which fall with the same velocity as the actual particles and for which Stokes drag law is assumed to be valid. The *geometrical diameter* can thus differ substantially from δ.

The quantitative relationship of Σ to C_T—and thereby to K_T—for HCHO in the absence of the aerosol is a linear function in log-coordinates over the range

$$5 \times 10^{-7} \leqslant C_T \leqslant 10^{-5},$$

i.e. over an almost 50-fold concentration range of T. The same relationship holds for the application of T by tracheal cannula. The data for F, E and C_T (taken from Tables 1 and 3 of AMDUR's papers) are reproduced together with the reported uncertainty margins in Fig. 3a.

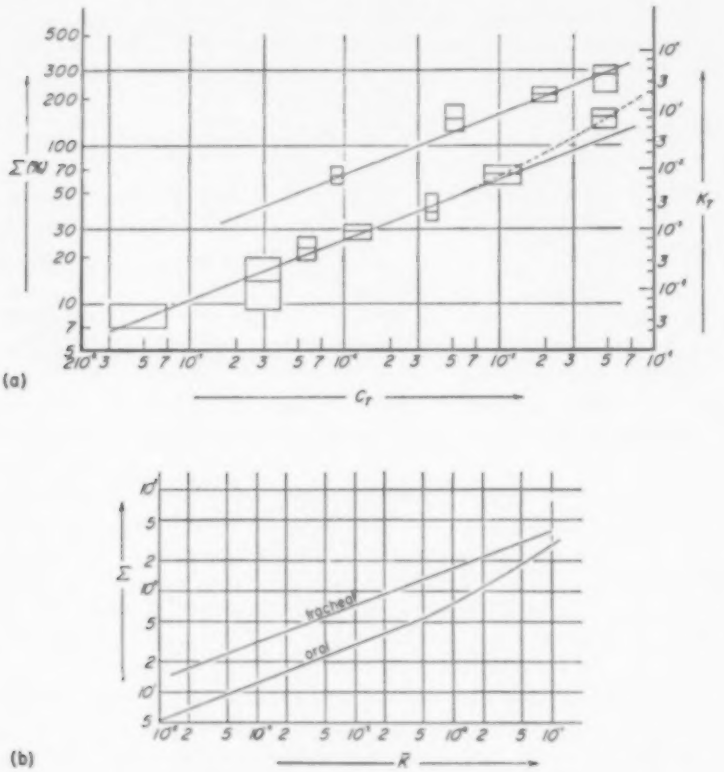

FIG. 3(*a*). Assumed interpolation function of the variation of the relative respiratory response, Σ, with the HCHO concentration, C_T, in the absence of NaCl as derived from AMDUR's data. The lower function represents Σ for oral, the upper for tracheal application. The rectangles indicate the margin of possible error. The right ordinate represents $\bar{K}$, derived from the linear interpolation according to (Eq. 12*b*).

(*b*). The relation between Σ and $\bar{K}$ as derived from (3*a*) for oral and tracheal application.

The interpolation is thus defined by:

$$\Sigma = A \,.\, C_T^{\,b} \ldots \text{resp:} \quad \Sigma = \bar{A} \,.\, C_T^{\,b} \tag{12a}$$

where $A = 4{\cdot}24 \times 10^{3}$; $\bar{A} = 1{\cdot}17 \times 10^{4}$; $b = 3{\cdot}75 \times 10^{-1}$. A and $\bar{A}$ refer to the normal and tracheal application respectively.*

* Thus with oral application only about 38% of T reached the lower respiratory realm.

From equations (4) and (12a) we have:

$$\Sigma = A\left(\frac{K_T}{\omega}\right)^b \ldots \quad K_T = \left(\frac{\Sigma}{\phi}\right)^{\frac{1}{b}} \tag{12b}$$

where $\omega = 0{\cdot}167\bar{N}\,.\,D\,.\,A_T = 6{\cdot}74 \times 10^{8}$ and $\phi = \dfrac{\bar{A}}{\omega b} = 1{\cdot}02 \times 10^{9}$.

A reduction of the log Σ-scale by a factor of b and its shift by a factor of ϕ will thus convert the Σ-values to the corresponding values of K_T and $\bar{K}$.

The right ordinate axis in Fig. 3a represents the K_T-values corresponding to the values of Σ shown on the left ordinate. Eq. 12b appears to be valid over the entire range of C_T used in tracheal application, but becomes incorrect for normal application when $C_T > 10^{-5}$. An empirical extrapolation was used for the latter concentration range (Fig. 3a), and it proved convenient to convert values of Σ into corresponding $\bar{K}$ values graphically by means of the relation shown in Fig. 3b.

Combination of Eqs. 11 and 12b gives a general expression

$$(\Sigma/\phi)^{\frac{1}{b}} = \bar{K} = \left[\omega C_T + \beta\, C_p\, \frac{(\eta\,.\,C_T)}{1+\eta C_T}\right] \tag{13}$$

which for suitable values of the constants ϕ, b, ω, β and η, should describe all variations of Σ with C_T and C_p.

VOL. 4 1961

The choice of values for these constants, however, is not wholly arbitrary. ϕ and b are fixed by the experimental conditions, and ω contains only two arbitrary quantities, D and A_T. The former is equivalent to a scale factor, in common with β, and thus does not affect $\bar{K}(C_p, C_T)$, while the value assumed for $A_T(1{\cdot}5 \times 10^{-15}\ \text{cm}^2)$ is unlikely to vary significantly. The values of β and η are much more arbitrary than those of ϕ, ω and b.

The constant $\beta\left(=\dfrac{D}{nd}\right)$ represents both, the ratio of cavity to particle diameter and the surface concentration n. Since $n = Cn'$, β contains such unknown factors as the possibility of multilayer adsorption and the magnitude of the effective transfer areas on the tissue (see Section 4*c*). Since β is determined by the best fit of Eq. 13 with experimental values, it can be used as a measure of $C\left(=\dfrac{n}{n'}\right)$, provided approximate values of D and d are known. For the previously assumed values of

$$D = 10^{-1}\ \text{cm}, \quad d = 3\,.\,10^{-5}\ \text{cm} \quad \text{and} \quad n' = 3{\cdot}4 \times 10^{-6},$$

the corresponding value of β is $10^{9}/C$.

Equation 13 can be converted to give

$$\beta = \frac{\bar{K} - \omega C_T}{\theta C_p} \tag{14a}$$

Hence β can be evaluated to a fair approximation from any set of correlated experimental data for C_p, C_T and Σ, provided C_T is large enough to ' saturate ' the particles, i.e. θ approaches unity (Eq. 10). Under these conditions the values of β obtained from different C_T or C_p values should be approximately the same.

The second empirical constant, η, characterizes the adsorption isotherm for the T-aerosol components. It can be derived by the following procedure: Two corresponding values Σ, Σ' and C_T, C'_T for the same C_p are selected from the experimental data so that Σ', C'_T represent the *saturated* ($\theta = 1$), and Σ, C_T a definitely *unsaturated* state ($\theta < 1$). Converting Σ, Σ' to corresponding values K, K', it follows from Eq. 13 that

$$\frac{K - \omega C_T}{K' - \omega C'_T} = \theta = \frac{\eta C_T}{1 + \eta C_T} \quad \text{or:} \quad \eta = \frac{\theta}{C_T(1-\theta)} \tag{14b}$$

Obviously η is derived independently from β.

This procedure was applied to AMDUR's data for HCHO in order to demonstrate the degree of validity of the theoretical relation (Eq. 13). A criterion is the degree of the fit of the experimental data for all variations of C_p and C_T under the same conditions and with identical values for β and η.

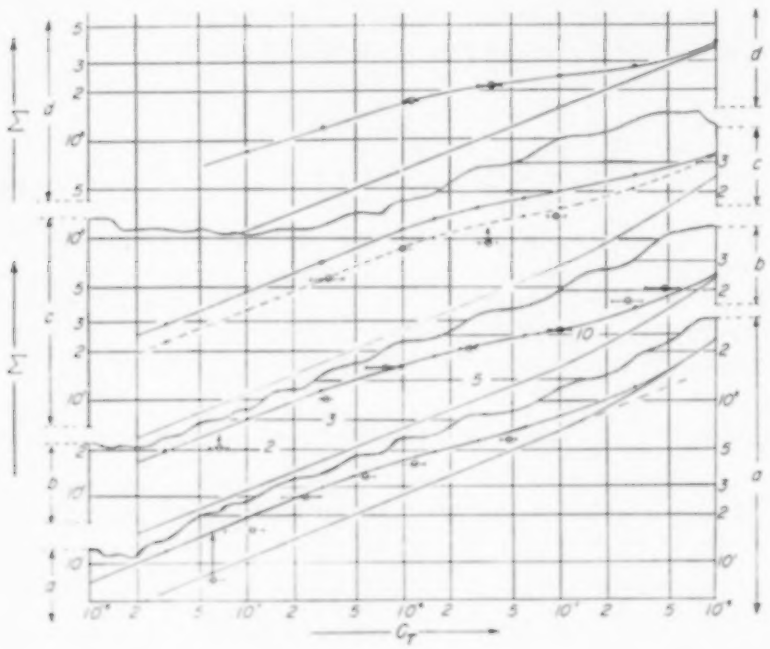

FIG. 4. Comparison of all of AMDUR's data for HCHO with the theoretical function (Eq. 13) for 3 aerosol concentrations (a): $C_p = 3$ mg m^{-3}; (b): $C_p = 10$ mg m^{-3}; (c): $C_p = 30$ mg m^{-3}; (d): tracheal application $C_p = 10$ mg m^{-3}.

The dashed curve in (c) refers to a mean particle diameter ($d = 0{\cdot}5\mu$) instead of ($d = 0{\cdot}3\mu$) in all other curves. All diagrams refer to the same abscissa, but their ordinates are shifted relative to another to avoid congestion. AMDUR's data are marked as circles, the calculated values as dots.

Fig. 4 shows a plot of Σ vs C_T in log-coordinates. AMDUR's data are indicated by circles, with a horizontal line indicating the margin of uncertainty for C_p. An analogous indication for the margin of Σ was omitted because of difficulty in its determination—a rough estimate, however, indicated that this margin is at least as large as that for C_T. Each set of curves represents the postulated function (Eq. 13),

the indicated values being derived by calculation and $\Sigma(K_T)$ for comparison. For clarity the curves for different C_p values were separated from one another by vertical shift.

The chosen values for the empirical constants were $\beta = 1{\cdot}65 \times 10^6$ and $\eta = 6{\cdot}7 \times 10^5$, and are the same for all curves relating to *oral* application (Fig. 4a, b, c). The fit for $C_p = 3 \times 10^{-8}$ (30 mg . m^{-3}) is obviously inadequate, but could be improved (dashed curve) by using a value for β (denoted β') of $1{\cdot}0 \times 10^6$. This is not unexpected in view of the abnormal density of the aerosol, and the resulting coagulation which leads to a larger mean d-value (d'), from $d' = \frac{d \cdot \beta}{\beta'}$ follows that the assumed mean diameter should have been increased from $d = 3 \times 10^{-5}$ cm to about $d' = 5 \times 10^{-5}$ cm.

However, the *tracheal* application (Fig. 4d) requires a value for $\bar{\beta}$ of $2{\cdot}24 \times 10^6$, i.e. 35% higher than the β value which fits the *oral* application data for the same C_p (10 mg . m^{-3}). This is possibly indicative of a lesser hydration state upon contact with the tissue surface.

The value of η was the same throughout—an obvious requirement, for it is independent of the mode of application.

In view of the unavoidable quantitative uncertainties, inherent in animal experiments, the agreement obtained with the theoretical function appears to support the basic assumptions made concerning the mechanism, despite the fact of a possibly systematic deviation for $C_T < 3 \times 10^{-7}$. AMDUR describes no significance to values of $C_T < 10^{-7}$. All the other data seem to lie within the estimated uncertainty margin.

VOL. 4 1961

The discrepancy between AMDUR's data and Eq. 13 can be examined in greater detail by using a linear scale for Σ. Fig. 5 shows such a plot of Σ vs C_T for $C_p =$ 10 mg . m^{-3}, both with and without aerosol. The deviations appear surprisingly small in view of the varying C_p values within the same test series (AMDUR's Tables 6 and 8). These variations were not compensated for, hence the curves in Fig. 4 and 5 are based on approximate values ($C_p = 3$, 10, 30 mg . m^{-3}). The fluctuations in C_p contribute, no doubt, substantially to the discrepancies between the experimental data and the theoretical function.

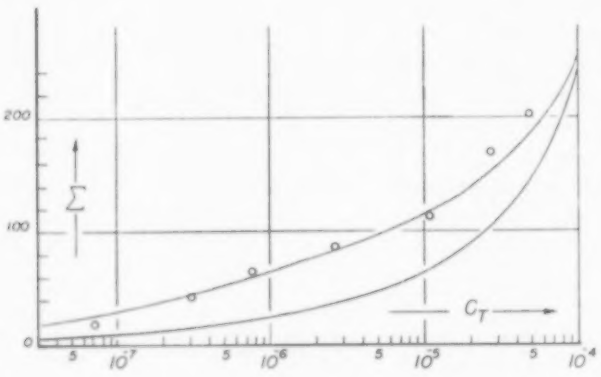

FIG. 5. Comparison of experimental data for ($C_p = 10$ mg m^{-3}) with theoretical functions $\Sigma(K_T)$, $\Sigma(\bar{K})$ on a linear Σ-scale vs. (lg C_T).

As mentioned above, the value of β derived from the best fit for the experimental data permits an estimate of n, since $n = \frac{D}{d \cdot \beta} = Cn'$ (Eq. 7). For assumed values of $D = 10^{-1}$ cm, $d = 3 \times 10^{-5}$ cm and $n' = 3{\cdot}4 \times 10^{-6}$, C becomes 6×10^{2}, indicating that the tissue area affected by the transfer of T is about 600 times larger than A_p, the geometrically defined particle surface (Eq. 6). It is certain that hydration of the salt particles occurs during transit through the respiratory channels, causing an increase in the particle surface of at least $\frac{A_L}{A_c}$ ($= 4{\cdot}4$), thus decreasing C to about $1{\cdot}3 \times 10^{2}$ or, more likely, even less. Furthermore, if the particle carried more T-molecules than the equivalent of a monolayer, which is almost certain in view of the solubility of HCHO, C would be reduced in proportion to the range of 20–60. This value of C can be explained either by the spreading of T on the surface after collision, or by the inadequacy of the assumed numerical values—most likely by both.

The corresponding data for the exposure to formic acid—though less detailed—show a basically similar pattern to that for formaldehyde. In the absence of the sodium chloride aerosol $\log \Sigma$ increases linearly with C_T, though at a lesser rate, and an intensification is produced in the presence of the aerosol. The intensifying effect however, appears to vanish at a C_T value as low as 3×10^{-5}. It must be realized that HCOOH (B.P. = 100·7° C) differs so drastically from HCHO (B.P. = −21° C) with regard to volatility, that a close analogy of the adsorptive affinities of the two substances is not at all to be expected.

More data, especially with non-hygroscopic aerosol materials (paraffin oil or latex) of well defined d are needed to clarify further the quantitative aspects of such problems.

NOMENCLATURE

Particle definitions:

d	geometrical diameter
δ	kinetic (Stokes') diameter
ρ	density
C_p	mass-concentration (g . m^{-3})
A_p	(total) surface area
N_p	number of particles in cavity
$N_{\dot{T}}$	number of T-molecules sorbed on A_p per monolayer

Cavity definitions:

D	diameter of (spherical) cavity
A_c	surface area ,, ,,
V_c	volume ,, ,,

T-gas definitions

$\bar{N}$	number of molecules per cm^3 at 1 atm
A_T	surface occupied by one T-molecule
C_T	volume concentration
N_T	number of T-molecules in cavity
$N_{\dot{T}}$	,, ,, ,, ,, sorbed on particles

K_T surface concentration resulting from N_T
$K_{\dot{T}}$ „ „ „ „ $N_{\dot{T}}$
$\bar{K}$ $= K_T + K_{\dot{T}}$
ω $= K_T/C_T$
k, η constants of adsorption isotherm
θ saturation coefficient of isotherm

(T) *gas-particle cavity definitions:*
$n' = A_p/A_c$ ratio between effective surfaces of particles and cavity
$C = n/n'$ empirical factor indicating ratio between actual surface concentration (n) and that resulting from monolayer under geometrically defined conditions (n')
$\beta = D(n \,.\, d)^{-1}$

Physiological response:
t, t_A animal life time without and with aerosol
D, F resistance of animal group *prior* and *after* exposure
$\Sigma, \bar{\Sigma}$ $= [(F/E) - 1] \,.\, 10^2$ . . . relative respiratory response to oral, tracheal application
$A, \bar{A}, b$ constants derived empirically from animal response
α synergistic potential of aerosol

Acknowledgements—The above work has been part of the activities sponsored under the U.S. Public Health Service Research Grant, No. RG-6743, " Synergistic Properties of Aerosols ". The author is particularly indebted to Mr. HEBER STEVENSON for his experimental work in reproducing as closely as possible the NaCl aerosols used by Dr. AMDUR. Without repeated discussions and exchange of detailed data with Dr. AMDUR and Dr. LABELLE this work would not have been possible.

BIBLIOGRAPHY

VORWALD A. J. (1952) *Effects of Inert Dusts in Air Pollution.* Proc. of the U.S. Technical Conference on Air Pollution, p. 485, McGraw-Hill, New York.

MAGILL P. L. (1949) Los Angeles Smog Problem, *Ind. Eng. Chem.* **41,** 2476–2486.

DAUTREBANDE L. and CAPPS R. (1950) Studies on Aerosols: IX Enhancement of Irritating Effects of Various Substances on the Eye, Nose, and Throat by Particulate Matter and Liquid Aerosols in Connection with Pollution of the Atmosphere. *Arch. Int. Pharmacodyn* **82,** 505–528.

GORDIEYEFF V. A. (1956) Adsorption of Gases and Vapors on Aerosol Particulates. *Amer. Ind. Hyg. Assoc. Quart.* **17,** No. 4, 411–417.

GOETZ, A. (1957) *Zur Physik der Luftkolloide im Submikronenbereich,* Physikertag Heidelberg Hauptvorträge 1957 (Physik Verlag, Mosbach Baden, 1958) pp. 170–184.

GOETZ A. (1958) *Study of the Properties of Aerosols, with Particular Reference to the Nature of the Air-Particle Interface.* Final Report USPHS Research Contract SAph-69557, The Robert A. Taft San. Eng. Center, Tech. Report No. A58–10.

DE BOER J. H. (1953) *The Dynamical Character of Adsorption* Chap. 3. Clarendon Press, Oxford.

LABELLE Ch. W., LONG J. E. and CHRISTOFANO E. E. (1955) Synergistic Effects of Aerosols. *A.M.A. Arch. Ind. Health* **11,** 297–304.

ALTSHULLER B., YARMUS L., PALMES E. D. and NELSON N. (1957) Aerosol Deposition in the Human Respiratory Track. *A.M.A. Arch. Ind. Health* **15,** No. 4, 293–303.

ORR C. JR., HURD F. K., HENDRIX W. P. and JUNGE C. (1958) The Behaviour of Condensation Nuclei under Changing Humidity, *J. Met.* **15,** 240–242.

AMDUR M. O. (1960) The Response of Guinea Pigs to Inhalation of Formaldehyde and Formic Acid Alone and with a Sodium Chloride Aerosol, *Int. J. Air Poll.* **3,** 201–220.

GOETZ A. and TSUNEISHI N. (1959) Bacteriological Test for Air-borne Irritants. *Ind. Eng. Chem.* **51,** 772.

GOETZ A. and TSUNEISHI N. A Bacteriological Irritation Analogue for Aerosols. *A.M.A. Arch. Ind. Health* **20,** 167–180.

DE BOER, J. H. ibid. Chap. 5.

DAUTREBANDE L., BECKMANN H. and WALKENHORST W. (1958) New Studies on Aerosols. III. Production of solid, small-sized, aerosols. *Arch. Int. Pharmacodyn, et de Thérapie* **116,** 170–187.

GOETZ A. (1957) An Instrument for the Quantitative Separation and Size-Classification of Air-Borne Particulate Matter Down to 0·2 Micron. Rev. Geofisica Pura E Applicata, Proc. II. *Int. Symp. Condensation Nuclei*, Basel-Locarno, **36,** 49–69.

PREINING O., STEVENSON H. J. R. and GOETZ A. Analysis of Aerosol Spectra. Proceedings of the 52nd Annual Meeting APCA, June 1959, Los Angeles.

GOETZ A. and PREINING O. (1959) The Aerosol Spectrometer and its Application to Nuclear Condensation Studies. *Amer. Geophysical Union.* Physics of precipitation, Monogr. 5, 164–182, 1960.

Int. J. Air and Water Poll. Pergamon Press 1961. Vol. 4, Nos. 3/4, pp. 185–198. Printed in Great Britain.

SINGLE-CAMERA MEASUREMENT OF SMOKE PLUMES

JAMES HALITSKY
Engineering Research Division, New York University, New York 53, N. Y.
(*Received in final form*, 9 *September* 1960)

Abstract—Smoke plumes are useful for determining diffusion characteristics of the atmosphere. Photographic techniques for recording instantaneous plume shapes usually require two cameras operated simultaneously and arranged either stereoscopically at one side of the plume or one below and the other to the side. While theoretically accurate, the two camera system is not flexible for unpredictable wind shifts, it requires a timing interconnection and the mathematical data reduction process is complicated.

The author proposes a system wherein a single camera is placed on the ground to the side of the plume and a wind direction recorder replaces the other camera. This system, which uses a simple commercially available camera and permits wide latitude in selection of a camera site (although optimum locations exist), has simple perspective corrections and good accuracy.

This paper describes the plume properties of interest to meteorologists, the requirements of a single-camera system, the perspective corrections and the error to be expected due to azimuthal wind fluctuations about the mean wind.

VOL.
4
1961

INTRODUCTION

OBSERVATIONS of smoke plumes from chimneys have been used at various times to verify predictions of plume rise due to emission velocity and buoyancy. It is not clear in much of the published data what corrections, if any, have been used for distortions arising from visual perspective. Recently, GIFFORD (1959) suggested that direct observation of smoke plumes would be convenient for evaluation of atmospheric diffusion coefficients, since concentration measurements would be unnecessary. DAVIDSON and HALITSKY (1958) used this technique to determine diffusion coefficients as well as to estimate ground concentrations.

The accuracy of measurements taken from a photograph of a smoke plume depends upon two conditions: the edge of the plume must be clearly defined, and the angular relationship of camera axis and mean wind must be known. The first condition may be met satisfactorily, at least for distances from the source up to several thousand feet, by using a non-evaporating oil fog whose white color shows up quite clearly against a blue sky. Possibly colored smokes may improve the contrast for other sky conditions. Professional photographers will undoubtedly be of assistance in this aspect. The more serious factor, however, is the perspective distortion.

When a plane figure is photographed, the image will be geometrically similar only if the planes of the figure and the film are parallel. A smoke plume at any instant of time is a sinuous three-dimensional figure whose azimuthal orientation is only approximately known. Also, topographical limitations usually restrict the choice of a camera location. Thus the co-ordinates of most points in the plume as measured from the photograph will rarely be correct. Of course, elaborate stereoscopic techniques may be devised to overcome this difficulty, but simplicity is a virtue in these cases and it may be well to examine the errors inherent in the single-camera technique,

together with procedures for their minimization without compromising flexibility and speed.

The error analysis presented herein has been developed from the perspective corrections derived during the afore-mentioned investigation.

EXPERIMENTAL PROCEDURE

The success of the single-camera technique will depend in part on the ease with which the data for correcting the photographs may be obtained. It would be very helpful if one could take candid snaps at random from any convenient location and be assured that correction equations would suffice to recover the true dimensions. Unfortunately, the less control one uses in taking the photographs the more complicated the equations become. Also, the basic uncertainty in the wind direction at any instant introduces an error which varies at a greater than linear rate with lateral plume displacement from the mean. One must also consider that the mean wind direction assumed in the correction may not be the one in an individual photograph; a sufficient number of photographs should be taken to provide a statistically significant average.

Thus, a balance must be achieved between the desirability of photographic control to simplify corrections and the undesirability of a lengthy set-up during which time the wind may shift. The method used by the author is one compromise of possible interest to others. It was developed in conjunction with the correction theory and its motivation will be clearer if the assumptions in the theory are explained first.

The method of data correction assumes that the instantaneous plume lies in a vertical plane which passes through the source in the direction of the mean wind. If the instantaneous plume did behave in this manner, the computed co-ordinates would be exact. The lateral wind fluctuations, however, carry the plume outside this plane. It is theoretically possible to determine the instantaneous azimuth angle of each puff from a bivane trace if the timing were extremely precise. Each puff would thus require individual correction. However, a more practical approach is to assume each puff to lie in the vertical plane containing the mean wind and to estimate the error by the method described in the last section of this paper.

The assumption of a vertical plume plane simplifies the corrections considerably at the expense of maintaining a vertical film plane. This is a minor concession and is accomplished by mounting the camera on a tripod with provision for levelling. A horizontal angle indicator is useful but not required. The information necessary for analysis consists of camera and projector constants, location of camera with respect to plume source, and mean wind direction. With maps and a wind direction recorder, this information may be obtained after test.

It is apparent from the above that with this method it is unnecessary to record any data during the test except the time each photograph is taken. Immediately prior to the test, the mean wind direction is observed and drawn on a map of the area which includes the plume source. One of several previously located camera sites is selected which gives approximately the appropriate plume angle with the camera axis. The photographer then drives to that site and sets up the camera so that the camera axis is horizontal and the source appears in the field of view. The customary aperture, speed and distance adjustments are made and the set-up is ready. The smoke generation begins and ends according to a schedule and the photographs are taken at regular intervals during the run.

PHOTOGRAPHIC DATA REDUCTION

List of Symbols

A plume dimension appears in four planes: film, screen, imaginary full-size and mean wind full-size. The first three planes are parallel. Corresponding dimensions in these planes are given the same letter in lower case, lower case primed and upper case respectively. The corresponding mean wind dimension is given another letter entirely. However, all four are grouped for definition.

a, a', A	horizontal distance from edge of frame to plume source
D	horizontal distance from camera to plume source
E	fractional error resulting from omission of β correction
E'	fractional error resulting from omission of ϕ correction
F	quantity defined by Equation 5
f_c	focal length of camera
f_p	focal length of projector
G	quantity defined by Equation 6
K	enlargement factor defined by Equation 3
m'	horizontal distance from projector to screen
v, v', V, T	vertical plume thickness
v_0'	inclined plume thickness
w, w', W	frame width
x, x', X, L	horizontal plume length
x_0'	inclined plume length
Δz, $\Delta z'$, ΔZ, ΔH	plume rise above source
ΔZ_h	quantity defined by Equation 8
Z	height of plume source above camera
α	horizontal angle between camera axis and camera-source line
β	horizontal angle between film plane and mean wind plane
γ	horizontal angle from North to camera-source line
ϵ	horizontal angle from North to mean wind
λ	horizontal angle between camera axis and line joining camera and any point in plume
θ	elevation angle of point in plume from horizontal line through source
ϕ	horizontal deviation of instantaneous wind from the mean wind
ψ	vertical expansion angle of a plume segment from the source

The plume co-ordinates which are of interest to the meteorologist are the plume rise above source, vertical thickness, local angle of expansion and angle of elevation of the instantaneous plume at a given downwind distance. The correction equations for all these quantities contain two angles which are characteristic of a given test run. These are α and β shown in Fig. 1. They are related by the expression

$$\beta = \alpha + 90^\circ - \epsilon + \gamma \tag{1}$$

where ϵ is obtained from the wind direction recorder, and γ is obtained from a map.

The angle α need not be measured in the field since it may be obtained from the

VOL. 4 1961

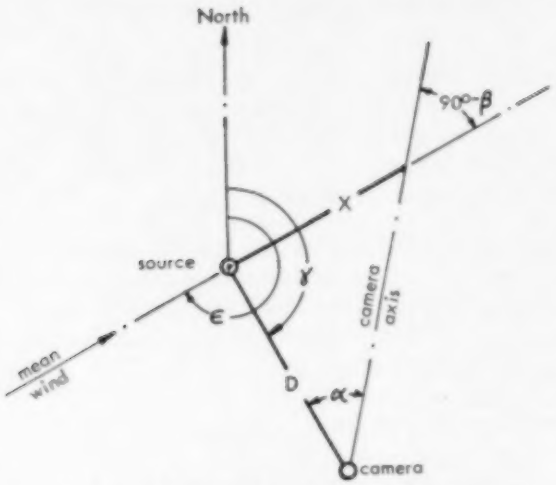

FIG. 1. Azimuthal orientation of mean wind and camera.

projected image. Fig. 2 shows schematically the source, instantaneous plume, camera, projector and screen, in plan and elevation views. The source appears a distance a from the edge of the film frame whose total width is w. By geometry and trigonometry, then,

$$\tan\alpha=\left(\frac{w}{2}-a\right)\frac{1}{f_c}=\frac{w'}{m'}\,\frac{f_p}{f_c}\left(\frac{1}{2}-\frac{a'}{w'}\right). \tag{2}$$

When $\beta=0$, the planes of screen, film and mean wind are parallel. In this special case, dimensions measured on the screen will be directly proportional to full size dimensions. The constant of proportionality is

$$K=Mf_p/m'f_c. \tag{3}$$

Thus, from Figs. 2 and 3, the true dimensions of the plume become

$$\left.\begin{aligned}
&\text{length:} && X=Kx'\\
&\text{rise above source:} && \Delta Z=K\,\Delta z'\\
&\text{vertical thickness:} && V=Kv'\\
&\text{local expansion angle of plume segment from source:} && \tan\psi=V\cos^2\theta/X\\
& && \quad=v'\cos^2\theta/x'\\
&\text{elevation angle from horizontal line through source:} && \tan\theta=\Delta Z/X\\
& && \quad=\Delta z'/x'
\end{aligned}\right\} \tag{4}$$

In the expression for $\tan\psi$ the factor $\cos^2\theta$ may be eliminated if X and V are measured along and normal to the line joining the source and the center of the plume

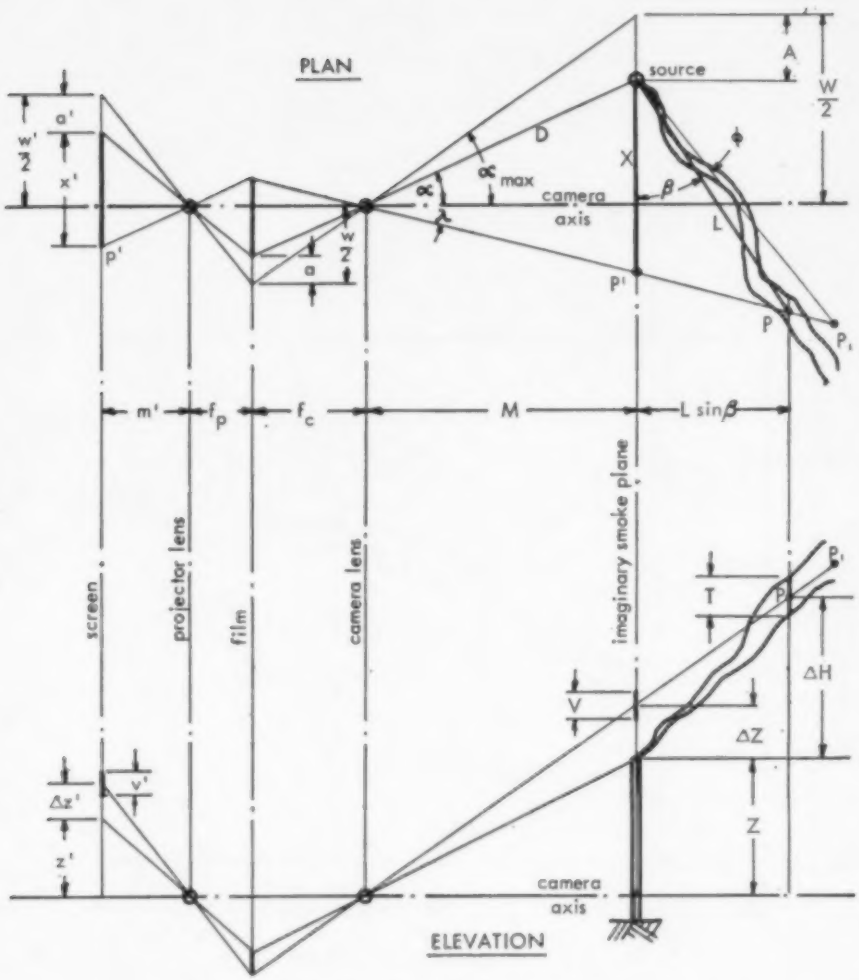

FIG. 2. Geometry of plume, film and projected image.

segment. When measured in this manner, the coordinates will be termed V_0 and X_0. Then $\tan \psi = v_0'/x_0'$.

When β is other than zero, the scaled-up screen dimensions represent a projection of the true plume on an imaginary plane parallel to the film plane. The coordinates X, ΔZ and V are only components of the true dimensions L, ΔH and T. To find the latter quantities, we may make use of the plan view of Fig. 2. By trigonometry,

$$\frac{X}{L} = \frac{\sin(90-\beta-\lambda)}{\sin(90+\lambda)} = \sin\beta(\cot\beta - \tan\lambda)$$

and

$$\tan\lambda = X/M - \tan\alpha,$$

VOL. 4 1961

from which,

$$L = \frac{X}{\cos\beta + \sin\beta \tan\alpha - X \sin\beta / M}.$$

Introducing the new quantities F and G, defined as follows:

$$F = \cos\beta + \sin\beta \tan\alpha \tag{5}$$

$$G = X \sin\beta / MF, \tag{6}$$

we obtain

$$L = X/F(1 - G). \tag{7}$$

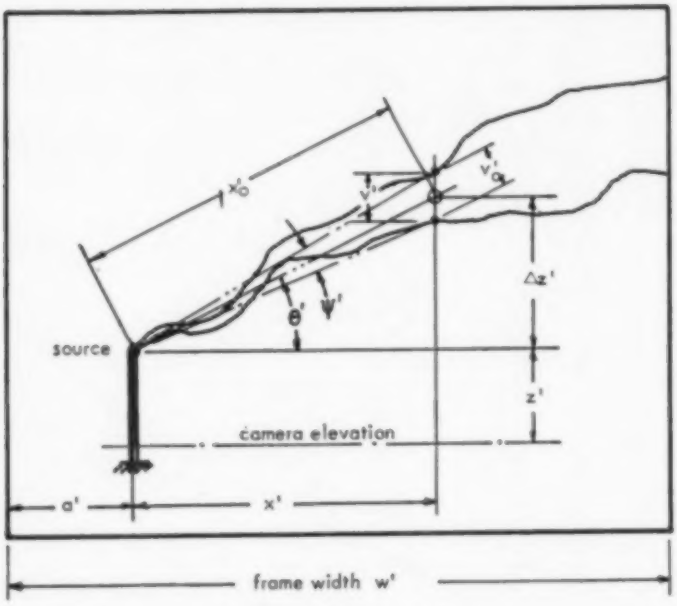

FIG. 3. Projected image of plume.

Now, from the elevation view of Fig. 2, we find

$$\frac{Z + \Delta H}{Z + \Delta Z} = \frac{M + L \sin\beta}{M}$$

which, when combined with (5), (6) and (7) yields

$$\Delta H = (\Delta Z + ZG)/(1 - G).$$

The plume corrections assume a simpler form if we let

$$\Delta Z_h = \Delta Z + ZG. \tag{8}$$

Then

$$\Delta H = \Delta Z_h/(1 - G). \tag{9}$$

The plume thickness is obtained by subtracting the height of the top of the plume from that of the bottom. Thus:

$$T = V/(1 - G). \tag{10}$$

The tangent of the local expansion angle ψ becomes, from (7) and (10),

$$\begin{aligned} \tan \psi &= T \cos^2 \theta / L = (V \cos^2 \theta / X)F \\ &= (V_0/X_0)F. \end{aligned} \tag{11}$$

The tangent of the elevation angle θ becomes, from (7) and (9),

$$\begin{aligned} \tan \theta &= \Delta H/L \\ &= (\Delta Z_h/X)F. \end{aligned} \tag{12}$$

Equations (5) through (12) provide the correction factors by which the dimensions of the plume obtained from the screen by Equations (4) may be transformed into true dimensions in the vertical plane containing the plume centerline. These are summarized in Table 1.

VOL. 4 1961

TABLE 1. CORRECTION FACTORS FOR PLUME COORDINATES IN THE VERTICAL CENTERPLANE OF THE MEAN WIND

Length from source:	$L = X/F(1 - G)$	(7)
Rise above source:	$\Delta H = \Delta Z_h/(1 - G)$	(9)
Vertical thickness:	$T = V/(1 - G)$	(10)
Tangent of local expansion angle:	$\tan \psi = (V_o/X_o)F$	(11)
Tangent of elevation angle of point in plume:	$\tan \theta = (\Delta Z_h/X)F$	(12)

Auxiliary Formulae:

$$\beta = \alpha + 90^\circ - \epsilon + \gamma \qquad \text{(See Fig. 1)} \tag{1}$$

= positive when plume moves away from observer

$$\tan \alpha = \frac{w'}{m'} \frac{f_p}{f_c}\left(\frac{1}{2} - \frac{a'}{w'}\right) \qquad \text{(See Fig. 2)} \tag{2}$$

$$K = Mf_p/m'f_c \tag{3}$$

$$F = \cos \beta + \sin \beta \tan \alpha \tag{5}$$

$$G = X \sin \beta / MF \tag{6}$$

$$\Delta Z_h = \Delta Z + ZG \tag{8}$$

EVALUATION OF ERRORS

Error Caused by Omission of the β Correction

A numerical evaluation of the error caused by omission of the β corrections developed in the preceding section may be of interest. A practical case is described in App. 1, where the plume source was 300 ft. above camera elevation and the camera was 4180 ft. from the tower.

The first correction is for the tilt of the horizontal reference line through the smoke source. This affects the measurement of plume rise and elevation angle, although it cancels out in measurement of plume thickness and local expansion angle.

The inclination of the horizontal reference line may be found from Equations (8) and (9). Setting $\Delta H = 0$,

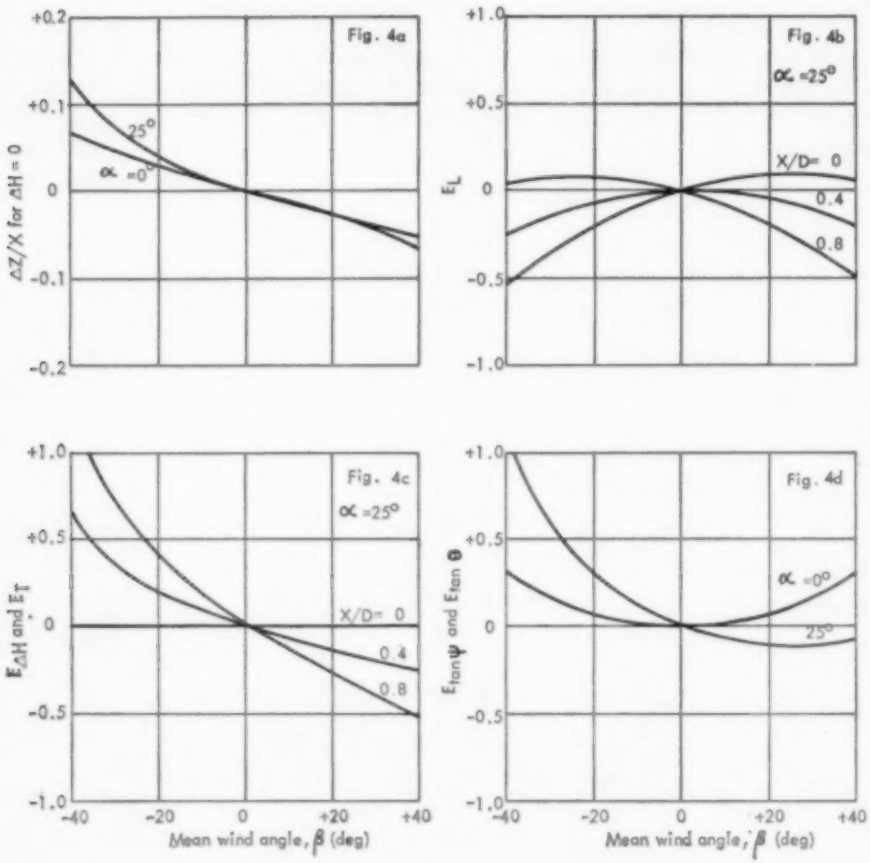

FIG. 4. Errors due to omission of β correction.
(*a*) Inclination of horizontal reference line.
(*b*) Error in plume length.
(*c*) Error in plume rise and vertical thickness.
(*d*) Error in local expansion angle and elevation angle.

$$\Delta Z = -ZG = [-Z \sin \beta / MF]X$$
$$= [-Z \sin \beta / D \cos (\alpha - \beta)]X$$
$$\sim [-Z \tan \beta / D]X \quad \text{for small } \alpha.$$

Substituting actual values of Z and D,

$$\Delta Z/X = -330 \tan \beta / 4180 = -\cdot 079 \tan \beta$$

and the inclination of the reference line through the source is approximately $\pm 1{\cdot}7°$ at $\beta = \mp 20°$ and $\pm 3{\cdot}8°$ at $\beta = \mp 40°$.

When the tower is at the center of the film frame, $\alpha = 0$ and the above approximation holds. The effect of α on the inclination is not large for $-20° < \beta < +40°$ but is significant for $\beta < -20°$. The exact values of $\Delta Z/X$ for $\alpha = 0°$ and $25°$ are shown in Fig. 4a.

After correction for reference line inclination, the fractional errors in the five plume parameters may be found from Equations (7) to (12) as follows:

$$E = \text{uncorrected/corrected} - 1.$$

Length from source $E_L = F(1 - G) - 1$

Rise above source $E_{\Delta H} = -G$

Vertical thickness: $E_T = -G$

Tangent of local expansion angle: $E_{\tan \psi} = 1/F - 1$

Tangent of elevation angle: $E_{\tan \theta} = 1/F - 1$, where

$$F = \cos \beta + \sin \beta \tan \alpha$$
$$G = X \sin \beta / MF = [\sin \beta / \cos (\alpha - \beta)]\,(X/D).$$

VOL. 4 1961

Figs. 4b, c and d show these errors graphically for $\alpha = 25°$. The errors in the linear coordinates are quite large, especially at large distances from the tower. However, the errors in the angular coordinates are small for values of β approximately equal to α.

Error Due to Lateral Wind Fluctuations

The atmospheric characteristics of interest to the meteorologist are the local expansion angle ψ and the distribution of elevation angle θ of individual smoke puffs. The errors in both these quantities have the same form if measurements of vertical distance are taken from the corrected horizontal reference line. Thus, the following analysis will be valid for both.

Let ϕ represent the azimuthal deviation of the instantaneous wind from the mean wind (Fig. 2). A point p' in the projected image would represent not P of the mean wind but P_1 of the instantaneous wind. The true coordinates of the instantaneous plume would then be given by Equations (7) through (12) with β replaced by $\beta + \phi$.

The angular expansion of the instantaneous plume ψ is defined by Equations (5) and (11). Thus,

$$\tan \psi_\beta = (V_0/X_0)(\cos \beta + \sin \beta \tan \alpha)$$

and

$$\tan \psi_{\beta+\phi} = (V_0/X_0)\,[\cos (\beta + \phi) + \sin (\beta + \phi) \tan \alpha].$$

The fractional error is then

$$E'_{\tan \psi} = \frac{\tan \psi_\beta}{\tan \psi_{\beta+\phi}} - 1 = \frac{\cos \beta + \sin \beta \tan \alpha}{\cos (\beta + \phi) + \sin (\beta + \phi) \tan \alpha} - 1.$$

By trigonometric substitution this reduces to

$$E'_{\tan\phi} = \frac{1}{\cos\phi + \sin\phi \tan(\alpha - \beta)} - 1. \tag{17}$$

Fig. 5 is a graph of the above function with $(\alpha - \beta)$ as a parameter. When $(\alpha - \beta) = 0$, positive and negative fluctuations produce equal positive errors. From $\phi = -20°$ to $+20°$, the error varies from 0 to 6 per cent, but wider fluctuations have much greater

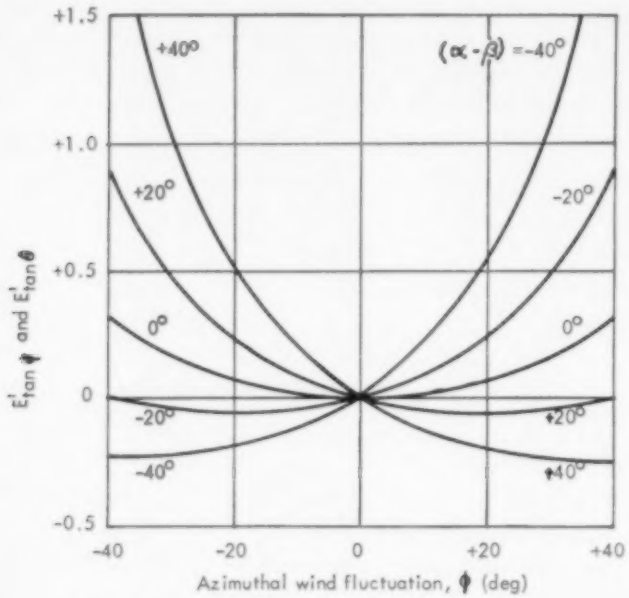

FIG. 5. Error due to azimuthal wind fluctuation ϕ.

errors, viz., 30 per cent at $\phi = \pm 40°$. When $(\alpha - \beta) \neq 0$, the error is not symmetrical and the average of errors for symmetrical ϕ fluctuations is higher than for the $(\alpha - \beta) = 0$ condition. For example, at $\phi = \pm 20°$, the average error is $(\cdot 06 + \cdot 06)/2 = \cdot 06$ when $(\alpha - \beta) = 0$ and is $(\cdot 22 - \cdot 06)/2 = \cdot 08$ at $(\alpha - \beta) = 20°$.

The azimuthal distribution of ϕ may be approximated by the normal curve

$$f = (1/\sigma\sqrt{2\pi}) \exp[-\phi^2/2\sigma^2] \tag{18}$$

where f = frequency density, σ = standard deviation.

If the error equation (17) is multiplied by the frequency distribution (18) and the product integrated over the width of the plume, a weighted error will be obtained which will be representative of the arithmetic average of random observations. For the case of $(\alpha - \beta) = 0$,

$$\text{Weighted } E' = 2\int_0^{\phi} (\sec\phi - 1) \exp[-\phi^2/2\sigma^2]\, d\phi / \sigma\sqrt{2\pi}.$$

Now, expressing the angle ϕ as a multiple n of the standard deviation, we obtain

$$\phi = n\sigma, \quad d\phi = \sigma\, dn, \quad -\phi^2/2\sigma^2 = -n^2/2$$

and

$$\text{Weighted } E' = \sqrt{2/\pi} \int_0^{n_1} (\sec n\sigma - 1) \exp[-n^2/2]\, dn \tag{19}$$

The upper limit n_1 must be given a practical value, since sec $n\sigma$ approaches ∞ as $n\sigma$ approaches $\pi/2$. Experience shows that an angular dispersion of $\pm 3\sigma$ will include most of the observations. Therefore $n_1 = 3$. The integration has been performed graphically for $\sigma = 10°$, 15° and 20°, yielding values of the weighted error = ·015, ·036, and ·070 respectively.

The experiments of App. 1 produced the frequency distribution shown in Fig. 6 ($\sigma = 14{\cdot}8°$). A weighted error for the actual distribution was calculated by using

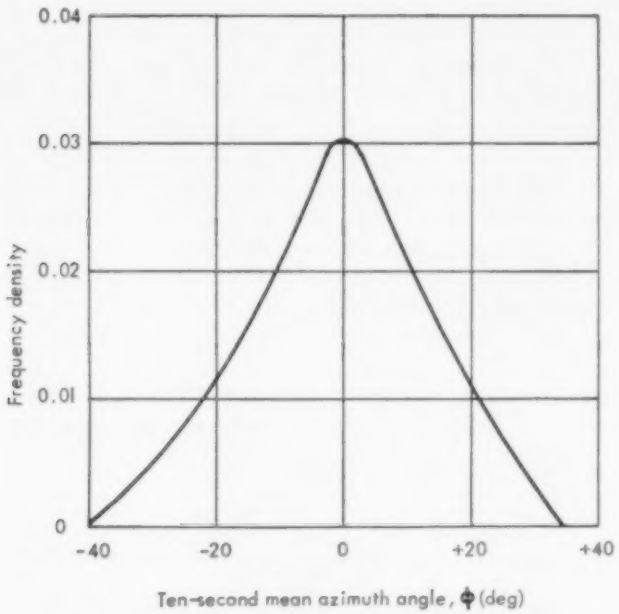

FIG. 6. Azimuthal wind frequency distribution at Buchanan.

Equation 17 and Fig. 6. Fig. 7 shows the variation of weighted error with $\alpha - \beta$. The slight asymmetry is due to the frequency distribution. We note that the weighted error has a minimum value of 3 per cent at $\alpha - \beta = 0$ and is less than 10 per cent for the range of $\alpha - \beta = \pm 35°$. The value of the weighted error at $\alpha - \beta = 0$ checks well with the value obtained using the normal curve up to $\pm 3\sigma$.

Effect of Camera Location and Orientation

Although the previous equations have been derived without restricting the camera location and orientation, care in selection of a camera site and camera angle can reduce errors and in some cases eliminate part of the β correction.

For instance, to minimize error due to azimuthal fluctuations about the mean wind,

VOL. 4 1961

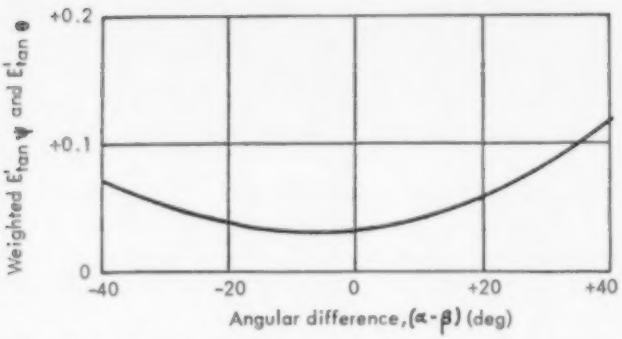

FIG. 7. Weighted error due to azimuthal wind fluctuation ϕ for test set-up of App. 1.

it is advisable to make $\alpha=\beta$. This condition is obtained by placing the camera on a line through the source perpendicular to the mean wind (see Equation 1 and Fig. 1 with $\epsilon-\gamma=90°$). The camera may then be rotated to place the source anywhere in the field of view. The optimum location for accuracy is at the midpoint since $\alpha=\beta=0$ and all mean wind corrections become unity. There are two drawbacks to this procedure. First, it may not be possible to find a suitable camera location on this line, which must be determined immediately prior to test. Second, the plume will occupy only half of the frame. Since the weighted error due to ϕ is not very sensitive to $\alpha-\beta$ (see Fig. 7) some displacement of the camera from the aforementioned perpendicular is acceptable. However, if the camera were to be rotated to place the source at one end of the frame in order to photograph a longer plume, α and β increase and the β corrections become significant.

An interesting compromise appears if the camera location and orientation satisfy the condition $\alpha=\beta/2$. After correcting for reference line inclination, this value of α yields $F=1$ and $E_{\tan\phi}=E_{\tan\theta}=0$. Thus, the plume angles can be measured

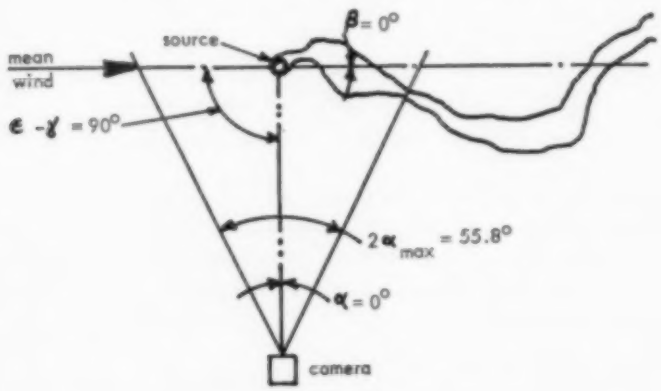

a) Condition $\alpha=\beta=0°$

FIG. 8 (a). Camera positions for minimum error.

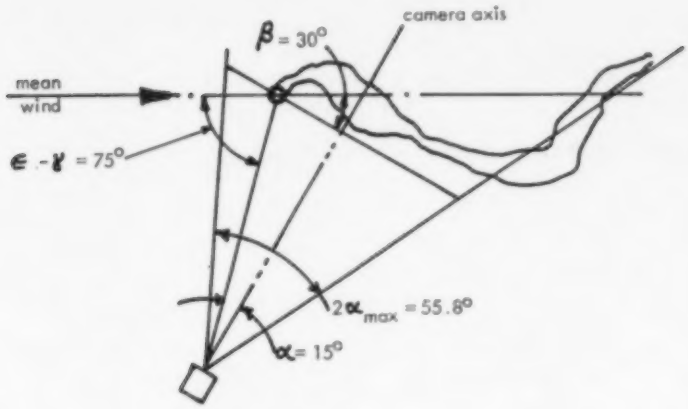

b) Condition $\alpha = \beta/2 = 15°$

FIG. 8 (b). Camera positions for minimum error.

directly on the screen without error. This condition is met when $\epsilon - \gamma = 90° - \alpha$ (see Equation 1), which places the camera off the perpendicular by α degrees. The camera may then be rotated in azimuth until the source is α degrees from the centerline in the field of view. In the example of App. 1, α may take any value from $-27{\cdot}9°$ to $+27{\cdot}9°$, the positive values producing the longer plumes.

Figs. 8a and b illustrate the arrangement for greatest accuracy with $\alpha = \beta = 0$, and for a practical compromise with $\alpha = \beta/2 = 15°$.

Acknowledgement—The experimental technique and method of data reduction described herein were developed as part of a meteorological project directed by Dr. BEN DAVIDSON and carried out by the New York University Engineering Research Division under sponsorship of the Consolidated Edison Co. of N. Y., Inc.

REFERENCES

DAVIDSON B. and HALITSKY J. (1958) A method of estimating instantaneous ground concentration from tower bivane data. *J. Air Poll. Cont. Assoc.* **7**, No. 4, pp. 316–319.

GIFFORD F. (1959) Smoke plumes as quantitative air pollution indices. *Int. J. Air Poll.* **2**, No. 1, pp. 42–50.

APPENDIX 1

EXPERIMENTAL CONSTANTS FOR THE TESTS DESCRIBED BY DAVIDSON AND HALITSKY (1958)

Camera Location

Site: Consolidated Edison Nuclear Generating Station at Buchanan, N.Y.

D = Distance from camera to source = 4180 ft.

Z = Height of plume source above camera = 330 ft.

Camera and Projector	*Camera*	*Projector*
Frame width, w, in.	1·45	—
Focal length f_e or f_p, in.	1·37	4·93
Maximum half angle, $\alpha_{max} = \tan^{-1} w/2f$	27·9°	

Scale factor for Conversion of Projected Image

From Eq. (3), $K = Mf_p/m'f_c = D\cos\alpha f_p/m'f_c$.

For a desired scale of 2400 : 1, the projection distance was:

$$m' = 4180 \times 4{\cdot}93 \cos\alpha/2400 \times 1{\cdot}37 = 6{\cdot}27\cos\alpha \text{ ft.}$$

For a common value of $\alpha = 25°$,

$$m' = 6{\cdot}27 \times {\cdot}906 = 5{\cdot}92 \text{ ft.}$$

Maximum uncorrected plume length from this camera location,

$$X = D(\sin\alpha + \sin\alpha_{max}) = 4180({\cdot}423 + {\cdot}469) = 3730 \text{ ft.}$$

$$x' = 3730/2400 = 1{\cdot}57 \text{ ft. on screen.}$$

Int. J. Air and Water Poll. Pergamon Press 1961. Vol. 4, Nos. 3/4, pp. 199–211. Printed in Great Britain.

A PREDICTION MODEL OF MEAN URBAN POLLUTION FOR USE WITH STANDARD WIND ROSES

FRANCIS POOLER, Jr.
U.S. Weather Bureau Research Station, Air Pollution Engineering Research Program,
Robert A. Taft Sanitary Engineering Center, Cincinnati, Ohio
(*Received* 6 *September* 1960)

Abstract—AN empirical diffusion equation was used with published summaries of wind direction and speed frequencies obtained at the Nashville Weather Bureau station to compute patterns of mean monthly relative concentrations. The patterns consisted of the relative concentration contributions from grid points at 1-mile intervals to the central grid point. An estimate of SO_2 emissions for each square mile of the Nashville area was combined with these relative concentration patterns, using an electronic computer, to obtain patterns of mean monthly SO_2 concentrations. Computations were made for five principal space-heating months.

A network of 123 lead peroxide candle measurement sites provided patterns of observed SO_2 concentrations. While the absolute magnitude of the concentrations predicted could not be verified, due to cumulative uncertainties in the source inventory, and in the interpretation of the candle measurements, the error of prediction is considered to be less than a factor of two. Predicted and observed patterns were generally similar, with a superimposed topographic effect on observed concentrations. Hillside locations facing towards the sources showed generally higher than predicted values, and valley locations sheltered from the sources by intervening terrain, lower values.

Relative monthly emission rates determined from a comparison of predicted and observed values for the area showed a close linear relationship to monthly degree-day totals, for the five months considered. A drop-off from the linear trend could be noted for non-heating and transitional months.

VOL.
4
1961

INTRODUCTION

CONSIDERABLE attention in recent years has been given to describing exposures of receptors to emissions from known single sources. Very little information has been assembled pertaining to the distribution, strength, and temporal variations of the multiple sources responsible for exposures of receptors in urban areas. Consequently, while the possibility of computing exposures as being the sum of the effects of numerous individual sources exists, little such work has been undertaken except by considering the multiple urban sources as a uniform horizontal plane source (LUCAS, 1958). Urban exposures have been described principally by means of direct air quality measurements, or through empirical relationships expressing these measurements in terms of indices of meteorological processes (MARKEE, 1959; D.S.I.R., 1945; DAVIDSON, 1942). For both planning and control purposes, a direct means to compute concentrations is desirable, since measuring the effects of proposed alterations of existing source patterns is impossible.

As part of an air pollution study in Nashville, Tennessee (ZEIDBERG *et al.*, 1960), a relatively dense array of sampling locations was set up. A preliminary inventory of sulphur dioxide emissions was made to permit computation of concentration patterns for comparison with the measured data. A comparison of 24-hour values from the Nashville study is to be reported elsewhere (TURNER, 1960); the work here reported is intended to test the success with which monthly mean concentrations may be computed.

SOURCE INVENTORY

The source inventory was made by Dr. Harold J. Paulus, of the University of Minnesota, and consisted of an estimate of the SO_2 emissions in arbitrary units, for each square mile of the Nashville area. Since the preponderant source of SO_2 is the burning of coal, it is convenient to express the inventory units in terms of the number of tons of coal burned per day. By extrapolation of estimates of the state-wide trend of coal consumption in recent years, together with an estimate of the coal consumption by the Nashville area (KENLINE, 1957), and considering the total number of arbitrary units of the source inventory, one inventory unit is calculated to be equivalent to $1\frac{1}{3}$ tons of coal per day, for an annual average. Since there are several factors to be considered in converting an inventory of emissions into measured concentrations, they will not be discussed separately, but will be considered together in the comparison of calculated and observed concentrations. The inventory was intended to represent the pattern of relative emission rates for a typical heating-season day; consequently the pattern should be altered for different heating requirements. This was taken into consideration only to the extent that no attempt was made to calculate concentration patterns for marginal or non-heating months, even though sampling measurements are available for such months.

The inventory was plotted on a rectangular grid, the grid points corresponding to the centers of the one-mile square source areas. Each source square, with an exception to be noted, was then considered as a poin ource located at an appropriate grid point.

DIFFUSION MODEL

The vertical variance, σ^2, of the distribution of effluent from a point source was assumed expressible as

$$\sigma^2 = 2Lu^{\alpha}t^{\beta} = 2Lu^{\alpha-\beta}x^{\beta} \tag{1}$$

where u is a representative surface layer wind speed, t is travel time, and x, travel distance, and the coefficient L and the exponents α and β are constants to be determined.

The relative concentration at ground level from a continuous point source at height h, assuming a Gaussian distribution with variance σ^2 in the vertical, reflection from the surface, and mass continuity, and assuming uniform horizontal distribution over a sector of angle $\pi/8$ is given by

$$\frac{\chi}{Q} = \frac{2\exp\left[-\frac{h^2}{2\sigma^2}\right]}{(2\pi)^{0.5}(1/8\pi x)u\sigma} \tag{2}$$

where χ is concentration in parts per unit volume, and Q is emission rate in parts per unit time.

Substituting from Equation (1),

$$\frac{\chi}{Q} = \frac{8\exp\left[-\frac{h^2u^{\beta-\alpha}}{4Lx^{\beta}}\right]}{\pi^{1.5}L^{0.5}u^{1+0.5(\alpha-\beta)}x^{1+0.5\beta}} \tag{3}$$

The relationship expressed by Equation (1), and the choice of numerical values to be used were based on several considerations. Horizontal flow past surface obstacles will generate turbulent motions, particularly over the rough surface of an urban area. The speed of flow near the surface is itself in part a reflection of existing turbulent exchange of horizontal momentum, however, particularly in the areas of appreciable topographic variation, so that surface winds are both a cause and an effect of vertical diffusion. The scale of wind-generated turbulence should be determined by the size of the obstacles to the flow which act as generating elements. The scale of the " wind-creating " turbulence, being associated with thermal convective cells and larger-scale processes, should be at least an order of magnitude larger. The intensity of the turbulence, defined as the ratio of the mean speed of the turbulent elements to the mean transport speed should be quite high and invariate for wind-generated turbulence, because there are so many obstacles to the flow in an urban area. The intensity of the larger-scale turbulence should be much more variable, with a considerably reduced average value.

The implication of this view of turbulence over urban areas is that, for short travel times under any conditions, the rate of diffusion should be determined by wind speed only; with increased travel times, a direct dependence on wind speed will be increasingly obscured by a generally larger component due to other causes. There will be some relationship between wind speed and this larger component, however, so that a virtual relationship between wind speed and rate of diffusion should be found for all travel times. In terms of the exponent α of Equation (1), for short travel times, or in the absence of any turbulence except that generated by the surface wind, α should have a value of unity, from dimensional considerations. For long travel times, with high values of the intensity of the large-scale turbulence, there would exist essentially no dependence of diffusion rate on the wind-generated turbulence, so that α would be zero. In general, however, because of the relationship between the magnitude of the larger-scale turbulence and low-level wind speeds, an effective value of the exponent α should decrease to a lower limit determined by the correlation between large-scale turbulence and wind speed.

The value of the exponent β will depend on the travel time in relation to the scale of turbulence. For very short travel times, β would have a value of two; for travel times increasing to many times the (time) scale of turbulence, and with homogeneous turbulence, β would decrease to unity. For most real pollutants, there should be some depletion by surface deposition. The vertical mass transfer by convection, when present, would provide a much greater depletion. The influence of both these effects on surface concentrations could be represented by increasing the exponent β over its " pure diffusion " value.

Finally, cognizance must be taken of the results of empirical investigations relating concentrations to meteorological parameters. Several investigations have shown that urban concentrations can be related to wind speed by an inverse power law relationship, with a wind speed exponent of 0·5 being derived or assumed in dealing with relationships combining data for all times of the day. If a simple form of Equation (3), such that the exponential term will be always near unity, is considered an appropriate formulation for general area sources, the empirical results imply that the wind speed exponent in the denominator of Equation (3), viz. $1+0{\cdot}5(\alpha-\beta)$, will be 0·5, i.e., that $(\alpha-\beta)$ will be $-1{\cdot}0$. From limited and unpublished investigations of

VOL. 4 1961

relationships of Cincinnati and Louisville data, a slightly higher power law exponent was obtained. Since both these cities are in more hilly terrain (than Leicester and New York, say), this difference should be expected, because of a higher expected. correlation between wind speed and larger-scale turbulence. A value for the difference $(\alpha - \beta)$ of $-0{\cdot}9$ was adopted for the period of record to be considered at Nashville.

Somewhat greater weight should be given to conditions associated with higher concentrations than with low, in representing mean effective diffusion rates. Relative concentrations for travel distances up to several miles should be described. To represent such diffusion conditions, it was considered that the exponent α should be in the range 0·5 to 0·8, and the exponent β, 1·3 to 1·6. With the restriction imposed by the difference $(\alpha - \beta)$ noted above, α would be 0·5 to 0·7, and β, 1·4 to 1·6. The middle value of each range was then selected as being the most likely value, or $\alpha = 0{\cdot}6$, and $\beta = 1{\cdot}5$. The choice of values for other locations, or other seasons, would generally be different, in accordance with the preceding discussion.

The value of the coefficient L was obtained by assuming, with the above values for α and β, that with a wind of 5 m/s, the mean plume would have a depth (taken as 2σ) of about 60 m at a travel distance of 1 km, or $L = 0{\cdot}06$ m$^{1{\cdot}4}$ sec $^{-0{\cdot}9}$. The value of 60 m was based primarily on observations by the author of visible smoke plumes from a variety of sources. As was true of the exponents α and β, a different mean value of the coefficient L would be chosen for different seasons and locations.

Expressing distances in miles, s, choosing an effective mean value of 30 m for h, and substituting numerical values for the constants in Equation (3), we have

$$\frac{\chi}{Q} = \frac{1{\cdot}435 \times 10^{-5} \exp\left[-\dfrac{0{\cdot}0581\, u^{0{\cdot}9}}{s^{1{\cdot}5}}\right]}{u^{0{\cdot}55}\, s^{1{\cdot}75}} = g_{u,s}. \tag{4}$$

Choosing a representative wind speed for each Beaufort wind speed class (Table I), the relative concentration for winds of a given speed class as a function of distance $(g_{u,s})$ can be calculated. The mean relative concentration at distance s and direction θ from a single source, $(\chi/Q)_{s,\theta}$ is given by

$$\left(\frac{\chi}{Q}\right)_{s,\theta} = \sum_{u} f_{u,\theta}\, g_{u,s}, \tag{5}$$

where $f_{u,\theta}$ is the fractional frequency of winds of speed u and direction θ.

Equation (5) was used to provide relative concentrations along the center lines of the wind direction sectors. Concentrations at intermediate directions were obtained by

TABLE I. WIND SPEEDS CHOSEN FOR BEAUFORT SPEED CLASSES

Wind speed (m.p.h.)	0–3	4–7	8–12	13–18	19–24	25–31
Representative speed (m/s)	0·9	2·5	4·5	6·9	9·6	12·5

linear interpolation between adjacent directions. More sophisticated interpolation formulae, which can be developed by assuming a more realistic instantaneous horizontal plume distribution, and assuming a continuous function for the probability

of winds from an infinitesimal sector width, are not justified in view of the uncertainties of the necessary assumptions, and in view of the approximations represented by the observations themselves.

The contribution from the source square centered at the grid origin was calculated by assuming the source to be a circular area source of uniform emission strength, and of area one square mile. The concentration at the center of the circle is independent of wind direction and is given by

$$\left(\frac{\chi}{Q}\right) = \int \frac{2\exp\left[-\frac{h^2}{2\sigma^2}\right]}{A(2\pi)^{0.5}u\sigma}\,dx = \frac{0{\cdot}889\times10^{-6}}{u^{0.35}}\int_0^{908}\frac{\exp\left[-\frac{3750u^{0.9}}{x^{1.5}}\right]}{x^{0.75}}\,dx = g_{u,0} \qquad (6)$$

A is the number of square meters per square mile, and the integration limit, 908 m, is the radius of a one square mile circle. The mean concentration is the summation of the concentration for each wind speed ($g_{u,0}$) times the fractional frequency of winds of that speed (f_u),

$$\left(\frac{\chi}{Q}\right)_0 = \sum_u f_u g_{u,0} \qquad (7)$$

The wind speed and direction frequencies used in Equations (5) and (7) were monthly summaries of hourly observations taken at the Nashville Airport, Berry Field (U.S. WEATHER BUREAU). These data were examined for odd-even bias, which, if sufficient,

VOL. 4 1961

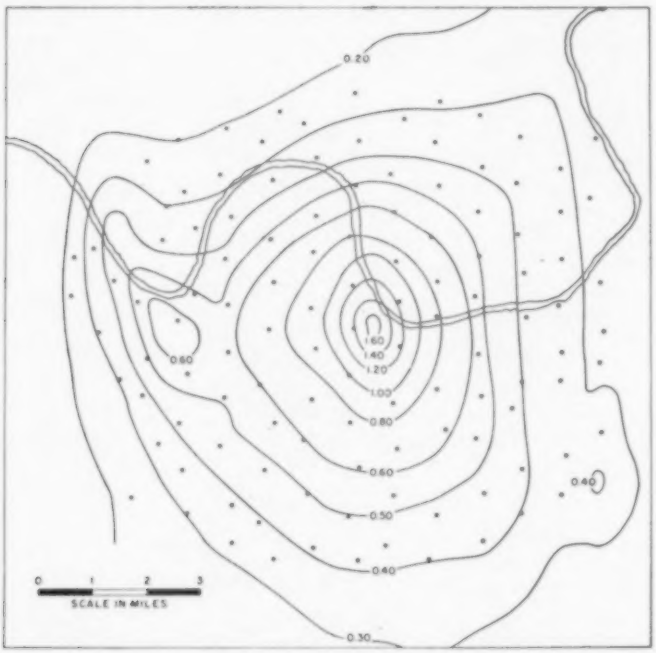

FIG. 1. Nashville Sampling Station Network, and Calculated Mean SO_2 Concentrations, in Inventory Units. Sec m $3{\cdot}10^4$, for December, 1958.

was removed by equalizing the total number of observations from odd and even directions and adjusting the number of observations for the speed classes from each direction to yield the de-biased total frequency from that direction. Hours of reported calm were then assigned to the 16 directions in the 0–3 m.p.h. classification in proportion to the de-biased frequencies of winds of 0–7 m.p.h.

A " diffusion " grid was then plotted, showing the relative concentrations from grid points at one-mile intervals to the point at the grid origin.

The calculated value of concentration for a point was obtained by centering the " diffusion " grid on the point of the source grid for which concentration was to be calculated, multiplying the pairs of numbers at the grid points and summing the products. Hand calculations were made for a number of points for purposes of comparison, but the bulk of calculating work was accomplished by programing the calculations for an IBM 650 computer. The values obtained from the computer were then plotted on a map of the Nashville area and isopleths of calculated concentration drawn. The resultant patterns for the various months calculated did not differ appreciably from each other. The pattern for each month resembled a smoothed source inventory map. An example for December, 1958, is shown in Fig. 1.

MEASURING NETWORK

Observed mean monthly SO_2 concentrations were obtained from a network (Fig. 1) of 123 sampling sites. Lead peroxide candles were exposed in louvred shelters for monthly periods, then analyzed chemically to determine the amount of sulphate formed. The principal reaction is presumed to be $PbO_2 + SO_2 \rightarrow PbSO_4$, although any

FIG. 2. Mean Daily Sulphation Rate of PbO_2 Candles, in mg SO^3 dm^{-2} da^{-1}, Nashville, November, 1958–March, 1959.

SO_3 or $SO_4^=$ should add to the sulphate determination (TABOR, 1959). The analytic results were expressed as milligrams of SO_3 per square decimeter per day.

Observed patterns for the five principal heating months, November, 1958 through March, 1959, were drawn. Except for a proportional variation at all sites, the patterns for all months are quite similar, so that the pattern of 5-month average concentrations was drawn (Fig. 2), thereby eliminating some of the apparently random month-to-month variations at individual stations. The observed pattern shows similarity to the predicted pattern, but with more irregularities and distortions.

CONVERSION OF RELATIVE CONCENTRATIONS TO UNITS OF MEASUREMENT

To convert the calculated relative concentration values to the measurement units, a conversion factor, C, was calculated, given by

$$C = 1{\cdot}065\,\frac{mpr}{n} \tag{8}$$

where m is the ratio of the average coal consumption rate during a given month to the annual average consumption rate;

p is the percentage (by weight) of sulphur in the coal;

r is the proportion emitted to the atmosphere as SO_2;

n is the volumetric SO_2 concentration, in p.p.h.m., corresponding to a sulphation rate of 1 mg dm^{-2} da^{-1}.

The numerical coefficient, 1·065, was calculated for a temperature of 44·2° F, and a pressure of 995 mb, which are approximately the heating season average values for Nashville. It includes the factor, $1\frac{1}{3}$ tons per day per inventory unit, previously derived. The factor C, when multiplied by relative concentrations times 10^4, yields the sulphation rate in mg dm^{-2} da^{-1}. The proportion r and the conversion factor n are defined above in terms of SO_2. It would be more correct to define both in terms of the sulphur oxides (including combined forms) which may react with the lead peroxide candles; discussion in terms of SO_2 alone is primarily a matter of convenience.

TABLE 2. ESTIMATES FOR CALCULATING CONVERSION FACTOR $C = 1{\cdot}065\,\frac{mpr}{n}$

Parameter	" Best Estimate "	Probable Error Ratio †
p *	2·5	1·20
r §	0·75	1·15
n ‡	4·00	1·50
Constant	1·065	1·20
C/m	0·499	1·65

† A probable error ratio, analogous to the usual linear probable error, is here used because the parameters are multiplied, not added. For the parameter n, for instance, it is assumed that the probability is 0·50 that the true value of n is within a factor of 1·50 of 4·00, i.e., between 2·67 and 6·00.

* From analyses of coal from SELVIG and GIBSON (1956).

§ Estimated.

‡ From FORAN *et al.* (1958): D.S.I.R. (1945); MEADE and PASQUILL (1958); and limited analyses of Nashville data.

VOL. 4 1961

Estimates of p, r, and n can be made (Table 2) and a value of m for each month can be obtained from a consideration of all months' data, as will be done below. The combined uncertainty from all these parameters is too great to permit a reliable calculation of the conversion factor C, and therefore an empirical conversion factor was determined for each month from a comparison of observed and calculated concentrations. For each sampling site, a calculated concentration was determined by interpolation from the isopleths drawn (e.g., Fig. 1). A graph was plotted of observed vs. calculated concentrations, and a linear regression line computed by the least squares method (Fig. 3). If there were no bias in either the calculated or observed values, the slope of the regression line would be the empirical conversion factor desired, and the intercept with the ordinate would represent the average exotic contribution—exotic here meaning from sources not included in the inventory. Evidence of some bias, and its probable effect, will be discussed below.

Conversion factors for additional months could be obtained by the same rather lengthy procedure as was done for the five principal heating months, but it is probable that the change of relative emission patterns would invalidate such computations. A simpler method was therefore devised and is believed to provide results which are of comparable validity to those that might be obtained by the more involved procedure.

A simple nondirectional monthly diffusion index was obtained from Equations (5) and (7). A proportionality constant, equal to the sum of concentrations at six

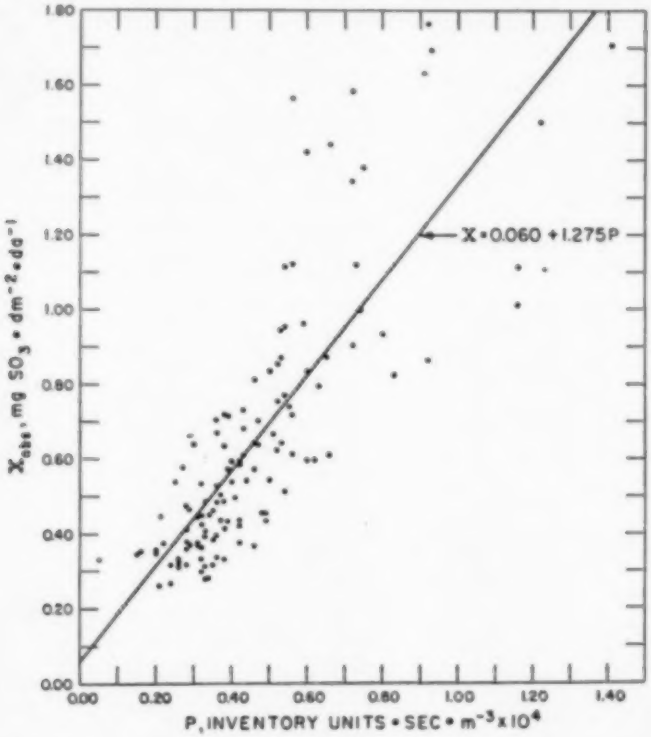

FIG. 3. Observed vs. Predicted Mean SO_3 Concentrations. Nashville, December, 1958.

TABLE 3a. COMPUTATION OF MONTHLY PROPORTIONALITY FACTOR F

Month	0_s	I_d	C_r	F
Nov., 1958	750	307	0·812	3·01
Dec., 1958	1094	299	1·275	2·87
Jan., 1959	1035	285	1·326	2·74
Feb., 1959	864	292	1·091	2·71
Mar., 1959	719	248	0·968	3·00
Mean	—	—	—	2·87

TABLE 3b. ESTIMATES OF CONVERSION FACTOR, C_a, FOR ADDITIONAL MONTHS

Month	0_s	I_d	F	C_a
Sept., 1958	135	391	2·87	0·12
Oct., 1958	414	429	2·87	0·34
Apr., 1959	351	246	2·87	0·50
May, 1959	118	332	2·87	0·12

0_s = sum of mean daily sulphation rates, in 10^{-2} Mg SO_3 dm^{-2} da^{-1}, for stations 59, 60, 61, 69, 70, and 71.

I_d = monthly diffusion index value = $\sum_u f_u (g_{u,0} + 2g_{u,4}) \times 10^6$.

C_r = empirically determined conversion factor from regression equation.

$F = 0_s / I_d C_r$.

$C_a = 0_s / I_d F$.

VOL. 4 1961

selected stations in the region of highest concentrations divided by the index value times the regression line slope value, was computed for each of the five heating months, and the five numbers averaged to obtain a single constant (Table 3a). The conversion factor for each of several additional months was then estimated as being equal to the 6-station total concentration divided by the product of the proportionality constant and the diffusion index value for that month (Table 3b).

Assuming that the conversion factor for each of the remaining summer months is that computed for September, the relative monthly emissions for a complete year are known, and therefore the parameter m in Equation (8) can be computed (Table 4). Values for months in different years should differ somewhat from the values for the particular year computed, aside from any new sources or changes in types of fuel consumed by existing sources, because of differing heating requirements. The indicated annual variation of emissions is undoubtedly larger than would be found in most urban areas. One of the criteria by which Nashville was selected as a study area was that there be a large annual variation of " pollution ".

Since the parameter m is defined as the ratio of the daily average consumption (or emissions) during a given month to the annual daily average, the ratio C/m will be the same for all months and is simply the average of the 12 monthly values of C, or 0·576. This value is about 15 per cent greater than the " best estimate " value calculated (Table 2). The agreement may be closer if the effect of sampling bias, discussed in the following section, is considered, and if the small contributions to SO_2 emissions from sources other than the burning of coal are included.

This apparent agreement may be fortuitous, however. If all calculated concentra-

TABLE 4. VALUES OF m, RATIO OF MONTHLY AVERAGE DAILY SO_2 EMISSION RATE TO ANNUAL DAILY AVERAGE RATE, NASHVILLE

Month	m	Month	m
Jan.	2·30	July	0·21
Feb.	1·90	Aug.	0·21
Mar.	1·68	Sept.	0·21
Apr.	0·86	Oct.	0·58
May	0·22	Nov.	1·41
June	0·21	Dec.	2·21

tions were in error because of a wrong choice of the mean diffusion coefficient, and a compensating error of estimate were made in computing the conversion factor, the results would be in agreement, but in error. Therefore, the over-all accuracy of the diffusion equation cannot be determined to any greater precision than that to which the conversion factor can be calculated.

DISCUSSION AND CONCLUSIONS

For each of the five principal heating months, the observed concentrations were expressed as percentages of the values predicted from the regression equation for that month. These percentages were plotted and isopleths drawn to provide a comparison of the patterns of calculated with observed concentrations. The percentage isopleths for all months showed very similar patterns, and so the results were combined for all five months by calculating and plotting an average percentage, the average of the five monthly percentages, for each station (Fig. 4).

The more elevated locations, particularly where the slope of the land is down toward the effective sources for that location, showed higher than predicted concentrations. In low areas, concentrations were generally lower than predicted, particularly if higher terrain separates the location from the effective sources. Concentrations were quite consistently below predicted values along the Cumberland River. From limited comparisons of sulphation rates of the lead peroxide candles with mean volumetric sulphur dioxide concentrations, it appears that higher wind speeds increase the sulphation rate. Some of the association between topography and relative concentrations should be a consequence of an association between topography and wind speed, but it is felt that the greater part of the apparent relationship is a real topographic effect on concentrations themselves.

The indicated topographic effect is physically plausible, although it would be extremely troublesome to represent mathematically. It also, in this case, introduces a difficulty in determining an empirical conversion factor. Some correlation exists between calculated and relative concentrations (Figs. 1 and 4) such that low values of both tend to occur together. Because of this bias, the numerical coefficients obtained by regression analyses should be interpreted with caution. To provide an indication of the significance of this bias, another regression line was computed, using only data from stations at ground elevations of between 450 and 550 ft MSL that were not separated from the principal contributing sources by terrain exceeding 550 ft in elevation. Slightly less than half the sampling sites were retained in this selection, which represents an approximation to the level plain over which mathematical

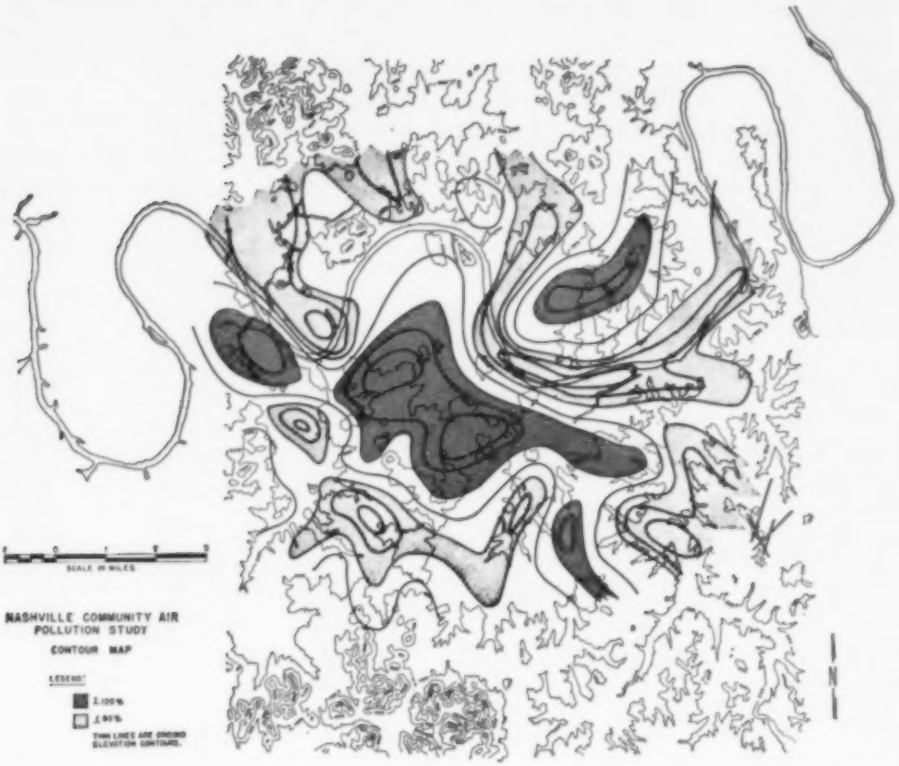

FIG. 4. Observed SO_2 Concentrations as Percent of Predicted. Nashville, November, 1953–March, 1959.

diffusion conventionally takes place. For December, the ordinate intercept was increased from 0·060 to 0·151, and the slope constant slightly decreased from 1·275 to 1·186, by using the selected data. There is apparently additional bias in the data, for the exotic component, based on the distribution of observed values (Fig. 3) and on the locations at which the minimum values occurred, is about 0·30 mg, or twice the value determined from the supposedly de-biased sampling data. The value of the empirical conversion factor (the slope) appears to be a relatively stable statistic; about the same proportionate change was also found for other months examined. The slope constants based on data from all stations were adopted as representing the empirical conversion factors for different months since a more reliable statistic should be expected from the larger number of data. The values adopted appear slightly to overestimate the conversion factors because of sampling bias.

The monthly conversion factors should be proportional to mean monthly emission rates, and hence to fuel consumption. Fuel consumption, in turn, should be dependent on space-heating needs. Within limits, then, a linear relationship between the monthly conversion factors and space-heating needs (expressible as degree-day totals) should exist. For the five principal heating months, a good linear relationship was found

VOL. 4 1961

(Fig. 5), providing an internal check on the consistency of the model as used. The slight departures from the linear trend suggest that the dependence of concentrations on wind speed has been over-emphasized by the model, i.e., in Equation (1) *et seq.*, the exponent α should be slightly decreased, or β, increased.

The linear trend of emissions with degree-days is not sustained through the transitional months. It is likely that the autumn increase and the spring decrease of emissions is more a reflection of the number of sources operating than of the emission

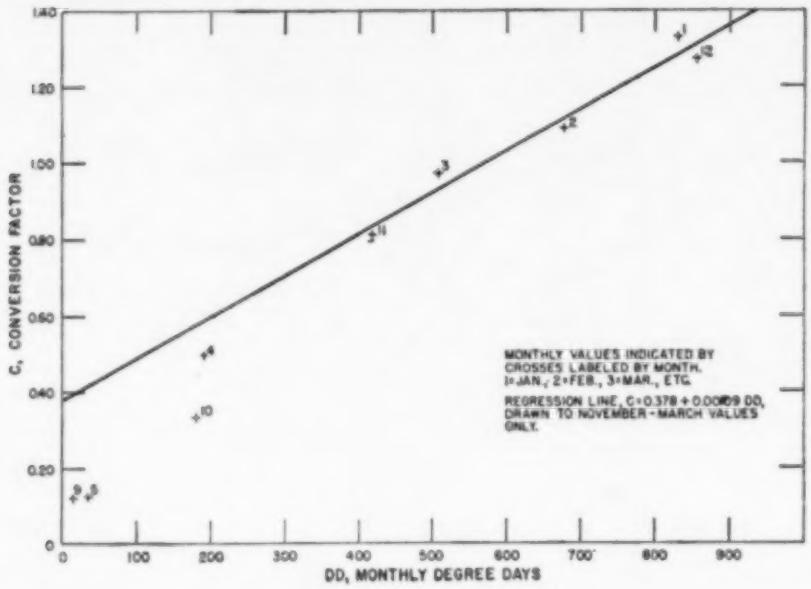

FIG. 5. Conversion Factor, Computed to Observed Concentrations vs. 30-Day Degree Day Totals. Nashville, September, 1958–May, 1959.

rates of operative sources; the relative emission rate for no heating requirements from the regression line (Fig. 5) is evidently not the minimum emission rate for the area, but is perhaps the minimum emission rate with all sources operating.

A number of adjustments are possible that would result in closer agreement between computed and observed concentrations. Such adjustments are not necessarily better assumptions, however. The source inventory is of a preliminary nature and should be expected to be in error in a few important particulars. The diffusion equation cannot adequately describe spatial variations of diffusion, nor can the simple utilization of the equation take into account spatial variations of transport. Also, the influence of nearby sources is greatly oversimplified by the assumed source distributions. Some divergence of observed, from computed concentrations, is therefore to be expected; the divergence indicated is of insufficient magnitude to make a recomputation of relative concentrations feasible, in view of the many sources of possible error. For computing concentrations in the Nashville area, the regression equations for the five months analyzed provide values that are satisfactorily close to observed values. One-half of the observed concentrations were between 80 and 125 per cent of predicted values; less than 1/20 of the observed values differed from predicted by more than a

factor of 2, with many of these being apparently erroneous data. A subjective modification of computed concentrations to take into account topographic effects would permit even closer estimates of actual concentrations to be made.

Acknowledgements—The computer work was programed and supervised by Mr. C. E. ZIMMER. His interest and help are sincerely appreciated.

REFERENCES

DAVIDSON W. F. (1942) Monthly Weather Review 70, No. 10, 225.

D.S.I.R. (1945) *Atmospheric Pollution in Leicester*. HMSO, London.

FORAN M. R., GIBBONS E. V., and WELLINGTON J. R. (1958) *Chemistry in Canada* **10**, No. 5, 33.

KENLINE P. A. (1957) *Appraisal of Air Pollution in Tennessee*. U.S. Public Health Service, Cincinnati, Ohio.

LUCAS D. H. (1958) The Atmospheric Pollution of Cities. *Int. J. Air Poll.* **1**, 1/2, 71–86.

MARKEE E. H., Jr. (1959) *J. Amer. Industr. Hyg. Assoc.* **20**, No. 1, 50.

MEADE P. J. and PASQUILL F. (1958) A Study of the Average Distribution of Pollution around Staythorpe. *Int. J. Air Poll.* **1**, 1/2, 60–70.

SELVIG W. A. and GIBSON F. H. (1956) Analyses of Ash from United States Coals. *Bureau of Mines Bull.* 567. GPO, Washington.

TABOR E. C. (1959) Personal Communication.

TURNER D. B. (1960) A Diffusion Model for an Urban Area. (In preparation.)

U.S. WEATHER BUREAU. Local Climatological Data and Supplement. (Issued Monthly), Asheville, N.C.

ZEIDBERG L. D., SCHUENEMAN J. J., HUMPHREY P. A. and PRINDLE R. A. (1960) Air Pollution and Health: General Description of a Study in Nashville, Tennessee. Paper presented at the Air Pollution Control Association meeting, May 1960, Cincinnati, Ohio.

VOL. 4 1961

Int. J. Air and Water Poll. Pergamon Press 1961. Vol. 4, Nos. 3/4, pp. 212–224. Printed in Great Britain.

THE MEASUREMENT OF DUST NUISANCE EMITTED BY CHIMNEYS

P. A. E. Crosse, D. H. Lucas and W. L. Snowsill
Central Electricity Research Laboratories
(*Received* 25 *November* 1960)

Abstract—The causes of dust pollution are studied and it is argued that vertical surfaces are far more likely to be polluted than horizontal surfaces and that optical obscuration of surfaces is a better indication of nuisance than weight of dust. A new type of instrument has been designed on this basis to measure the dust emitted from a chimney in units which are related to the likelihood of dust nuisance at ground level. The new design of instrument is shown to be more responsive to coarse dust than to fine. The final measurement is carried out by optical methods but the instrument is designed so that the errors which often occur with optical measurements are avoided. The instrument has had periods of test in power stations, it has ample sensitivity and also can cover a very wide range of signal levels. It will facilitate the control of dust emission from industrial chimneys.

1. INTRODUCTION

All coal burning furnaces and, to a lesser extent, oil burning furnaces, carry considerable quantities of ash, some of which is finely-divided and is likely to be lifted by the velocity of the furnace gases, and emitted from the chimney, to the detriment of the neighbourhood. When the coal itself is finely divided, as in pulverised fuel furnaces, the problem is, of course, intensified. For all large furnaces, and for all furnaces burning pulverised fuel, it is now mandatory to instal dust collecting plant, so that the pollution of the neighbourhood is minimized.

Modern plant is capable of such high efficiency in combustion and electrostatic precipitation that when it is suitably designed and maintained in perfect order there is no likelihood of offence being caused. However, if there is some degree of failure in the plant there is a possibility of objectionable emission. It is therefore desirable to monitor the flue gases leaving a chimney, so that a record is obtained which either gives proof of satisfactory operation or gives warning of failure. It is also desirable to monitor effluent gases to ensure that the plant maintains the expected standard of performance and justifies the capital and running costs involved.

Before designing a monitoring instrument, it is essential to analyse the nature of nuisance by dust, so that the best form of instrument is obtained. It is convenient to divide dust into three categories and each makes its own contribution to air pollution. The first category has a size range greater than 100 microns, falls rapidly to the ground unless the atmosphere is unusually turbulent, and causes a particularly obvious and crude form of nuisance. This kind of dust is relatively easy to remove from flue gases and is ceasing to be a form of pollution which is in any way excusable. At the other end of the scale is dust with a diameter less than 10 microns. Its motion in the atmosphere is determined for practical purposes entirely by air movements and not by the falling speed of the particle. This kind of dust is objectionable in that it produces visible and persistent plumes, in that it obscures sunshine which would otherwise reach the ground, and that it drifts into houses and produces, in time, general dinginess of appearance. The measurement of this category of dust can in principle be carried

out by instruments which measure the optical density of the flue gases before they leave the chimney and recently, with improvements in the design of these instruments, can be measured successfully in practice (LUCAS, 1961).

The intermediate category of dust is partly affected by air movements in the atmosphere and partly by its own falling speed. It contributes little to the visibility of plumes and the obscuration of sunshine, but it can contribute markedly to pollution at ground level, though its behaviour is somewhat more complicated than the behaviour of extremely coarse particles. It cannot be satisfactorily measured by the optical density type of instrument mentioned above since it is effectively masked by finer dust.

The instrument described in this paper has been designed to cope with this category of dust, but also responds well to coarse grit if for any reason this should still be emitted. The measurement of pollution by dust at ground level is generally at present only carried out by the standard deposit gauge. This gives a useful result where very coarse dust and low wind speeds are involved. Its efficiency becomes virtually zero for all other conditions. It is based on the assumption that nuisance is caused by the dust falling on a horizontal area. This is probably only true of a small and decreasing proportion of cases of dust pollution. It must be pointed out that a typical free falling speed for a dust particle is 20 cm/sec and a typical wind velocity is 300 cm/sec. Dust therefore moves almost in a horizontal line and is far more likely to affect vertical surfaces than horizontal. Thus, complaints of pollution are caused by dust which settles on drying washing, obscures the surfaces of houses and trees, or enters open windows. Even when dust settles on horizontal surfaces it rarely remains there but is blown along until it is intercepted by a vertical feature such as a gutter or house. Conversely when dust is observed to lie on a horizontal surface such as a window sill it has been caught initially by the window itself and has subsequently fallen on the sill. Further, when dust lies on horizontal surfaces inside houses, the amount which enters is a function of the area of open window. This area is of course vertical.

VOL. 4 1961

The pollution of some outdoor object takes place in two stages. In the first stage, the dust has to reach the surface of the object by settlement or impingement. In the second place, it obscures some of the light which is normally reflected from the object. The likelihood that a dust particle will settle or impinge is a complicated function of the particle's size and density, the velocity of the air stream in which it finds itself, and the size and nature of the object. If we consider the amount of dust which would pass through the outline of the object if the object were removed, the fraction of this amount of dust which in fact reaches the surface of the object is roughly proportional to the free falling speed of the particle in air, until this fraction approaches unity. (The free falling speed of a particle in air is approximately proportional to the square of its diameter.) It follows that on a weight-for-weight basis, coarse particles are more likely to cause complaint than fine ones. This is to some extent offset by the fact that after the particles have settled the obscuration is a function of the surface area of the settled particles, and in this respect fine particles are more serious. When one considers the nett result of these two functions it can be shown that the nuisance value of dust increases proportionately with particle size. It is perhaps worth pointing out that on a similar basis the response of an instrument which measures the optical density of the flue gas is inversely proportional to particle size.

The dusty air at ground level which causes nuisance differs from the dusty gas in the chimney in velocity and in dilution, and both factors in principle can be computed.

If the nuisance value of the dusty gas in the duct can be measured, then the likelihood of nuisance in the neighbourhood of a power station or other source of emission can be calculated. The most convenient definition of nuisance value, both from the point of view of measurement in the duct and measurement at ground level, is the percentage obscuration caused on unit area by the dust which impinges on unit vertical area in one minute.

An instrument* has been designed in accordance with this definition and is described below. Besides observing this basic principle to design the instrument, the essential principles of good instrument design have also been followed, so that the accuracy of the instrument is maintained, even though there are variations in supply voltage, cleanliness of the optical system, ambient temperature and the ageing of components. The instrumental features are described in more detail in a paper published in *J. Sci. Instr.*, Jan, 1961.

A gauge has been designed by the authors to measure the nuisance caused by dust at a particular point at ground level, based on the same arguments as the present instrument. It is hoped in the near future to publish a description of this gauge. The correlation of the results obtained by the gauge with the measurements made by the instrument will be an interesting exercise for the future.

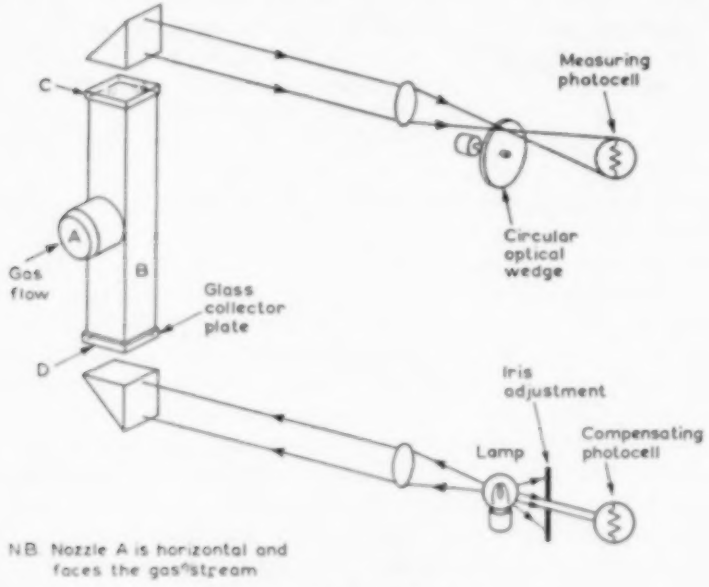

Fig. 1. Diagrammatic view of optical system.

2. DESCRIPTION OF THE INSTRUMENT

The instrument consists of three units, the collecting and measuring unit, control unit and recorder. The collecting and measuring unit is attached to the side of a horizontal duct leading to the stack, with the sampling head inside. The instrument sampling head is shown in Fig. 1. A small horizontal duct, A, faces into the gas stream. This leads into a vertical duct, B, of equal cross sectional area which is closed at the top and bottom by glass plates, C and D. The flue gas does not enter the duct A since

* Covered by British Patent Applications Nos. 6121/58 and 31283/59.

there is no outlet, but is deflected around it, carrying the very fine dust with it. The coarser particles are carried by inertia into B, and settle in a random manner on the lower glass plate, D. The duct B is sufficiently long compared with its width to prevent turbulent gas movements reaching the glass plates, and the settled dust is therefore undisturbed. The mechanism of the dust sampling is discussed in Appendix I.

Parallel light from a lamp on the outside of the duct is directed by means of a system of lenses and prisms through the plate D and back to the outside of the duct. Here, the light is focussed on to a cadmium sulphide photoconductor, after passing through an annular optical wedge. The wedge has a linear density variation from 0 to 2 and can be rotated by means of a reversible electric motor so that the obscuration of the light beam can be varied. Light from the same lamp bulb also falls directly on to a second similar photoconductor, after passing through an iris diaphragm. The light falling on the two photoconductors allows a current to pass in each when a voltage is applied across them.

The optical wedge is used to make the current in the measuring photoconductor equal to the current in the other, first, before dust collects and secondly, after dust has collected for a predetermined time. The amount of wedge movement required after the dust has collected is a measure of the collected dust.

The instrument normally collects dust for 15 minutes and then draws a line on the recorder chart proportional to the optical obscuration produced by the collected dust. However, experience in power stations has shown that at periods of peak load and when a fault exists, dust burdens more than 100 times the normal dust burden may be encountered. In order to cope with these exceptional circumstances, the instrument has been designed so that if enough dust has collected to give a full-scale reading the instrument immediately records a full-scale signal without waiting for the normal timing period to elapse. Thus, under conditions of heavy dust emission the instrument may record ten lines in the 15-minute period instead of one, and this extends the full-scale reading of the instrument by a factor of ten.

Under conditions where the usual rate of dust emission is exceptionally high, the overall sensitivity of the instrument may be reduced by fitting a cone to the sampling head, which has an entrance area which is a convenient fraction of the cross-sectional area of the horizontal duct.

VOL. 4 1961

3. PRINCIPLE OF THE LIGHT INTENSITY MEASUREMENT

In order to measure the optical obscuration produced by the dust, the instrument in fact makes two measurements. It measures the light reaching the photocell at the beginning of the collecting period and it measures the light reaching the photocell at the end of the collecting period, and it is the difference between these two measurements which is recorded. It follows that any variations which affect the two readings equally are automatically cancelled out. Thus, the ageing of the lamp or photocell, changes of sensitivity due to changes of ambient temperature, the progressive dirtying of the optical system, and long-term changes in supply voltage do not produce errors in the measurement. Changes which take place during a particular measurement produce an error in that single measurement but do not affect subsequent measurements. Such changes are minimized by using the second photocell differentially. However, there is no attempt made to match the two photocells accurately.

4. CALIBRATION

The instrument was calibrated by setting it up with the sampling duct facing into an 8 inch diameter horizontal pipe from which air was flowing at a velocity which could be varied from 0–80 ft/sec. Weighed quantities of dust of various grades were introduced into the pipe through a funnel 15 diameters upstream from the instrument. Fig. 2 shows the linear response with dust concentration. Fig. 3, curve 3, shows the results obtained when dust samples separated according to the terminal velocity of

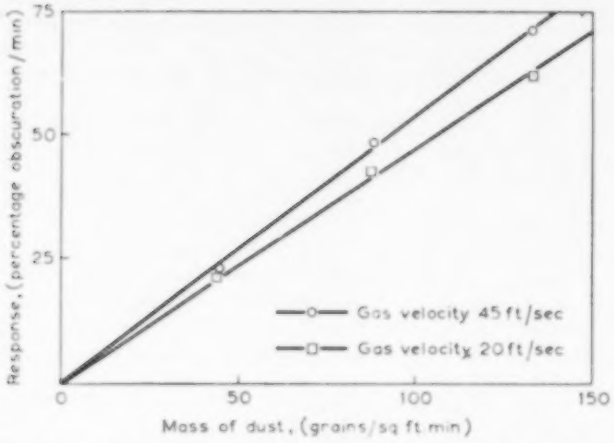

Fig. 2. Variation in response of instrument with mass of dust at different gas velocities.

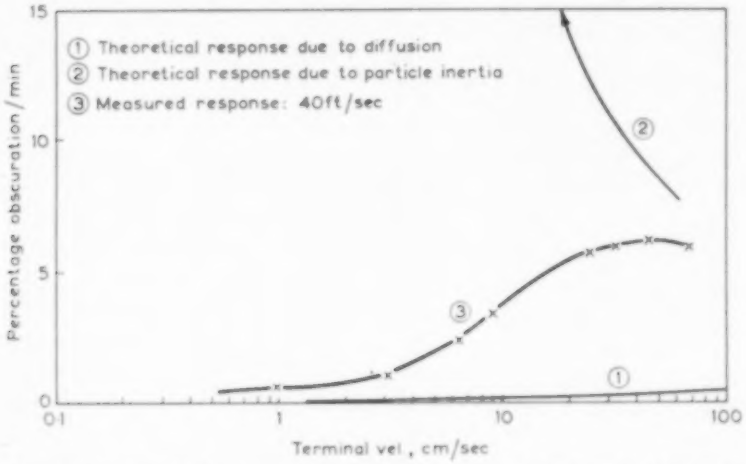

Fig. 3. Theoretical and actual response of instrument assuming dust rate of 10 grains ft^3/min passing collecting head. (Assuming density 1·2).

the particles are used,* and illustrates the increasing sensitivity of the instrument as the dust coarseness increases.

5. INTERPRETATION OF INSTRUMENT READINGS

The sensitivity of the instrument has been fixed arbitrarily so that a 70 per cent scale reading implies that a vertical surface exposed in the duct will become 7 per cent obscured in one minute. (On a circular chart the upper 30 per cent of the scale is very congested in time and is not used).

If the surface in the sampling head is obscured at 5 per cent per min it will be 53 per cent obscured after 15 minutes and not 75 per cent, due to the mutual interference of particles. Nevertheless the instrument will read 75 per cent because the optical

* A particle with a terminal velocity of n cms/sec is described as an n vel particle.

obscuration of the wedge varies logarithmically and exactly compensates (see Appendix II). This is desirable since when the dust particles produce nuisance they will be greatly diluted and the amount of mutual interference will be negligible.

It is essential to be able to relate the readings of the instrument (in percentage obscuration per minute) to the likelihood of nuisance. In the last resort this can only be done by experience or by the application of a reliable theory of plume rise and dust dispersion. This is not being attempted in the present paper. However, it is desirable to fix levels provisionally so that a standard exists which can be tested by experience. The assumptions made below are necessarily crude and the figures which result are only stated to give the order of magnitude which appears likely.

5.1. MAXIMUM PERMISSIBLE LEVELS

The following assumptions have been made.

(1) A surface begins to appear dirty when 0·5 per cent is covered (CAREY, 1959).

(2) The dust moves with the plume and the worst effects at ground level correspond to the dust being spaced over a plume cross-sectional area of $0{\cdot}5\ e\pi h^2$ where h is the chimney height. This expression is derived from O. G. Sutton's formula for gaseous diffusion and corresponds to the situation of maximum ground level concentration.

(3) The instrument test surface is typical of an area A of flue duct cross-section carrying dust to the chimney.

(4) That a particular area is not subjected to a particular plume for more than 5 hours at a time (300 minutes).

(5) That the dust which impinges on a vertical area either sticks to it or, alternatively, if it does not stick it falls on to a horizontal area of equal size.

(6) That there are 'n' similar ducts carrying dust from the power station.

It follows that the condition for no nuisance to be caused is

$$n\,\frac{RA \times 300}{0{\cdot}5\ e\pi h^2} < 0{\cdot}5$$

where R is the instrument reading in percentage obscuration per minute.

$$\text{i.e.} \qquad R < 0{\cdot}007\,\frac{h^2}{nA}$$

If the dust emitted is so coarse that it rapidly leaves the plume, nuisance is more likely to be caused than the calculation suggests, and special values will be needed if dust is coarser than 100 vel $\approx 200\mu$.

On the other hand, when weather conditions minimize the chance of nuisance, less stringent values may be applicable.

5.2. THE EFFECT OF DURATION OF HIGH EMISSION

The likelihood of nuisance depends not only on the nature of the emission but also on the time for which it persists. Much higher rates of emission can be tolerated if they persist for a short time.

On the assumption that the steady emission from a station is at half the level necessary to cause nuisance, it is of interest to consider the levels which would be

VOL. 4 1961

permissible for one relatively short period. This will be evaluated for the case $h = 250$ ft., $A = 50$ sq. ft., $n = 1$.

For other cases the levels quoted below should be multiplied by

$$(h/250)^2 \times (50/A) \times (1/n).$$

Permissible Level	*Time of Persistence*
27% obscuration per minute	1 hr
50% obscuration per minute	½ hr
94% obscuration per minute	¼ hr
270% obscuration per minute	5 min
1350% obscuration per minute	1 min

The maximum continuous level is 9%/min.

It would be unnecessarily stringent to have an alarm sounded when the level reached 10 per cent per minute, for instance, because emission could proceed at this level for several hours without causing nuisance. It is suggested that if a nuisance is likely to be caused in 15 minutes, that is, when the level is 94 per cent per minute, an alarm should be sounded. Although the instrument normally operates only once in 15 minutes, if the dust emission level reached 94 per cent per minute the instrument would react in 70 seconds.

Some of the assumptions made above are pessimistic and it is expected that experience will show that a multiple of the readings given above will be allowable.

5.3. COMPARISON WITH DUST SAMPLING TESTS

The instrument was not designed to give a reading in grains per ft.^{3} However, since this is a familiar unit it will be of interest to relate the instrument reading to grains per ft^3 in certain cases. Strictly, it can only be related to grains per ft^2 per second (actual)

Table 1.

Vels	Typical Dust			Fine Case	
	%	Response	Product	%	Product
>40	2	6·3%/min	12·6	1	6·3
40–20	6	5·25%/min	31·5	1	5·25
20–10	10	4·2%/min	42·0	1	4·2
10–5	10	2·8%/min	28·0	1	2·8
5–2	7	1·05%/min	7·3	1	1·05
<2	65	0·28%/min	18·0	95	26·6
			139·4		46·2
Mean response 139·4 ÷ 100				46·2 ÷ 100	

Columns 2 and 5 give typical gradings of coarse and fine dust respectively. Column 3 gives the response of the instrument to 10 grains/ft.^{3}/min of dust of the stated grading; taken from Fig. 3.

and then only when the dust grading is known. Fig. 3 (curve 3) gives the response of the instrument plotted against dust grading for 10 grains per ft² per minute (actual). Using this result, a conversion constant can be worked out for any grading. Table 1 gives a comparison between a typical case and a case of fine dust, i.e. 10 grains/ft² min corresponds to 1·4% obscuration/min for average dust and 0·46% obscuration/min for fine dust.

This implies that 1% obscuration/min ≈ 0·003 grains ft³ (actual) for average dust when the duct velocity is 40 ft/sec.

1% obscuration/min ≈ 0·009 grains ft³ (actual) for fine dust when the duct velocity is 40 ft/sec.

It is of interest to consider whether the response of the instrument could have been calculated from existing theories of dust sampling. This has been done in Appendix I. It is quite clear that DAVIES (1954) theory for aspirated nozzles does not apply when extrapolated to zero aspiration rate except for very coarse particles. The same is true of BADZIOCH'S work and indeed he makes this point explicitly.

It is clear that the sampling nozzle of the instrument has a zone of intense turbulence at the entrance. Particles penetrate this partly by inertia and partly by diffusion and the relative importance of the two varies with the terminal velocity of each particle. A complete theory would, of course, need to assess both effects simultaneously.

6. EXPERIENCE IN POWER STATIONS

A number of instruments have been installed in power stations, primarily to test and improve the serviceability of the instrument but, in addition, a limited amount of

VOL. 4 1961

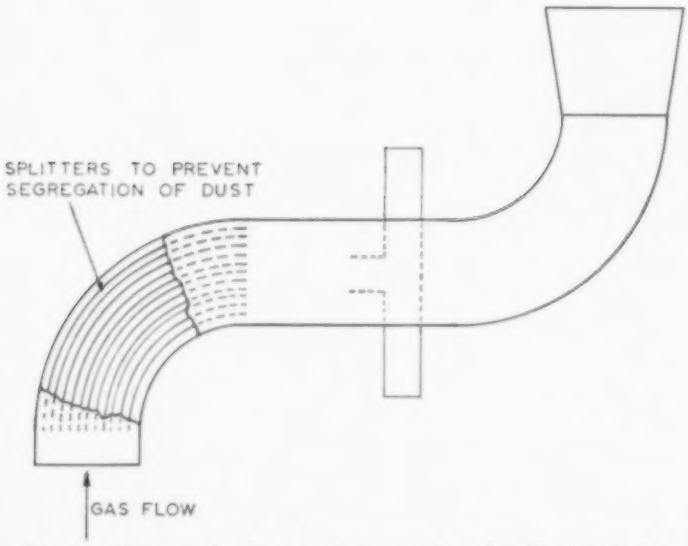

CENTRAL ELECTRICITY RESEARCH LABORATORIES

FIG. 4. Adaptor to be fitted to Instrument Sampling Head when Gas Flow is vertically up. (The adaptor is inverted for gas flow vertically down).

information on power station performance has also been obtained. It was found necessary to redesign a number of minor points. For instance, an improved pen and ink reservoir has been provided and a number of materials for use as gaskets to seal the instrument from the flue gases have been tried out. It has been found that silicone rubber is generally satisfactory but is not completely immune from attack by sulphuric acid. Klingerit gaskets are satisfactory if they are resilient enough to fit the glass. The glass collecting surface is now made of Technoplate, an armoured glass, instead of ordinary glass, which was liable to crack. The use of transistor-type photocells was discontinued because they were far too sensitive to the changes of temperature which occur from station to station and from time to time. The cadmium sulphide photocells give satisfactory performance over a range of temperatures from 0° C to 65° C.

One of the most alarming discoveries of the experimental period was that dust burdens on occasion were very much higher than had been expected, and in addition to the built-in ability of the instrument to record more rapidly under these conditions, it is necessary to make use of reducing cones. As a result of this experience, the present design of instrument is approximately half as sensitive as the original design.

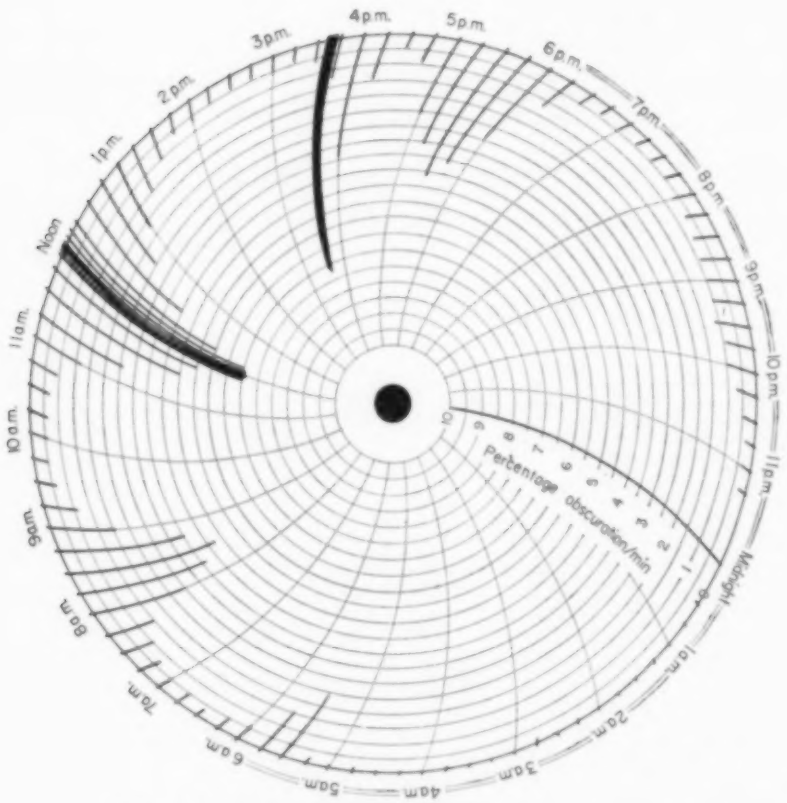

Fig. 5. Composite chart showing type of record obtained.

In many cases the instrument can be installed in a horizontal duct, but in other cases it is only convenient to use a vertical duct with the gas flowing either upwards, as in the chimney, or downwards, as in the duct leading to the I.D. fan. In these cases, a modification to the sampling head as shown in Fig. 4 has been found to work satisfactorily without apparently changing the calibration of the instrument.

On a number of occasions the instrument has been used to assess the effect of different modifications of power station operation on dust emission. In this limited experience a change of boiler load appears to have the most dramatic effect on dust emission and an increase from 85 per cent full load to full load can increase the nuisance value of the dust emitted by a factor as much as 10.

A change in the coarseness of grinding also has a marked effect and at one power station when the mill classifier was by-passed the reading of the instrument increased by a factor of 2. It is of interest to record that the reading of an optical density type instrument did not change appreciably at the same time.

Although the instrument was designed primarily to measure dust emission, tests have been carried out at two oil burning stations to discover whether it would satisfactorily record the emission of acid smuts. It was found to be most successful and is being used to give immediate information of the dependence of acid smut emission on various operational changes in the power station. As a precaution, small heaters were added to the sampling head to minimize the risk of acid attack under these conditions.

A composite chart has been prepared (Fig. 5) to illustrate the kind of record provided by the instrument. It shows the normal rise in emission as the load on the station reaches a peak at 8.30 a.m.; the effect of a fault in the classifying of the pulverised fuel at noon and the temporary breakdown of a precipitator at 3.40 p.m.

Acknowledgements—This paper is published by permission of Dr. J. S. FORREST, Director of Central Electricity Research Laboratories.

Acknowledgement is made of the assistance of our colleagues at Research Laboratories and at a number of C.E.G.B. power stations, particularly Earley Power Station, where the first prototype was tested out.

VOL. 4 1961

APPENDIX I: DEPENDENCE OF THE INSTRUMENT ON DUST GRADING

When sampling dust using a normal sampling probe, the ratio of the concentration of dust in the sample, C_s, to that in the air flow, C_a, is given by DAVIES (1954)

$$\frac{C_s}{C_a} = \frac{V_a}{V_s} - \tfrac{1}{2}\left(\frac{V_a}{V_s} - 1\right)\frac{1}{(P+\frac{1}{2})} \tag{1}$$

where V_a is the air velocity in the duct
V_s is the air velocity in the sampling cyclone
and P is a particle parameter.

$$P = \frac{d^2\rho V_a}{9\mu D} \tag{2}$$

where d is the particle diameter
ρ is the particle density
μ is the air viscosity
D is the diameter of the collecting orifice.

The terminal velocity of a particle, V, is given by

$$V = \frac{gd^2\rho}{18\mu} \tag{3}$$

where g is the acceleration due to gravity, so that we rewrite P in terms of the terminal velocity

$$P = \frac{2V V_a}{gD}$$

Hence from (1),

$$\frac{C_s}{C_a} = \frac{V_a}{V_s} - \tfrac{1}{2}\left(\frac{V_a}{V_s} - 1\right)\Big/\left(\frac{2V V_a}{gD} + \tfrac{1}{2}\right)$$

The amount sampled per unit area per sec is given by

$$C_s V_s = C_a V_a \left(1 - \frac{\left(1 - \frac{V_s}{V_a}\right)gD}{(4V V_a + gD)}\right)$$

In the case of the collector box in the instrument,

$$V_s = 0$$

Hence the amount sampled will be

$$C_a V_a \left(1 - \frac{gD}{4V V_a + gD}\right)$$

$$= C_a V_a \left(\frac{4V V_a}{4V V_a + gD}\right)$$

$$= C_a V_a \left[\frac{1}{1 + gD/(4V V_a)}\right]$$

In the case of a normal sampling cyclone,

$$V_a = V_s$$

and consequently

$$C_a V_a = C_s V_s$$

Thus the factor

$$\left[\frac{1}{1 + gD/(4V V_a)}\right]$$

is an efficiency factor. Given a dust rate of W grammes per second per unit area the instrument would collect

$$w = W\left[\frac{1}{1 + gD/(4V V_a)}\right] \text{ grams/sec per unit area.}$$

Assuming that all the particles that enter the collecting box obscure the test plate, we can estimate the obscuration produced by a weight w of dust of a given size d.

The number of particles will be

$$\frac{6w}{\rho\pi d^3}$$

and the obscuration produced will be proportional to the area of the particles, that is,

$$\frac{6w}{\rho\pi d^3} \times \frac{\pi d^2}{4} = \frac{1{\cdot}5w}{\rho d}$$

Since $V = \frac{gd^2\rho}{18\mu}$, the obscuration produced

$$= 1{\cdot}5\ W\left[\frac{1}{1+gD/(4V\ V_a)}\right] \times \sqrt{\frac{g}{18\mu\ V\rho}}$$

Hence % obscuration/sec $= 150\ W\left(\frac{1}{1+gD/(4V\ V_a)}\right)\sqrt{\frac{g}{18\mu\ V\rho}}$ (plotted as Curve 2, Fig. 3).

The analysis given above will only apply if no dust leaves the collector box after it once enters. Particles <10 vel will have an increasing tendency to come to rest in the region of turbulence in the mouth of the collector box, and will have an increasing likelihood of escaping by diffusion. Under these diffusion dominated conditions it is unlikely that the concentration of dust inside the collector box would be greater than the concentration in the flue duct. If we make the assumption that the two concentrations are equal and that dust reaches the glass plate by settlement from the dusty gas. Then if the concentration is Z grams/cm³ of dust of diameter d, the number of particles

$$= \frac{6Z}{\rho\pi d^3} \text{ per cm}^3$$

The number which fall towards the glass plate $= \frac{6ZV}{\rho\pi d^3}$ per cm²/sec. The obscuring area of the fallen dust is $\frac{6ZV}{\rho\pi d^3} \times \frac{\pi d^2}{4} = \frac{1{\cdot}5\ ZV}{\rho d}$.

But $$d = \sqrt{\frac{18\mu V}{g\rho}}\ .$$

Hence the obscuration produced $= 150\ Z\sqrt{\frac{gV}{18\mu\rho}}$ % per second.

But $$Z = \frac{W}{V_a}\ .$$

Hence % obscuration per second $= 150\ \frac{W}{V_a}\sqrt{\frac{gV}{\rho 18\mu}}$ (plotted as Curve 1).

The two curves are shown plotted in Fig. 3 and compared with the measured result. It is apparent that the first analysis given is valid for the coarsest particles, but the second analysis has more and more validity as the particle size falls. A true analysis must consider simultaneously the effects of inertia and diffusion on the particle.

VOL. 4 1961

APPENDIX II: CALCULATION OF RESPONSE OF RECORDER AND COUNTER

As the optical wedge is turned from density 0 to density 2 it emits 216 pulses. Hence $d = P/108$ where d is density at any point P pulses from density 0. i.e.

$$\log_{10} \frac{I_0}{I} = \frac{P}{108} \; ; \; I = I_0 \, . \, 10^{-(P/108)}$$

Where I_0 is the initial and I the final light intensity. If dust with a total cross sectional area a is deposited on area A, the fraction of light transmitted will be

$$e^{-(a/A)} \quad \text{or} \quad 10^{-(a/A)\log_{10} e}$$

With clean glass $I = I_0 \, . \, 10^{-(P_1/108)}$

With dirty glass $I = I_0 \, . \, 10^{-(P_2/108)} \, . \, 10^{-(a/A)\log_{10} e} = I_0 \, . \, 10^{-(P_2/108)-(a/A)\log_{10} e}$

Since I is maintained constant

$$\frac{-P_1}{108} = \frac{-P_2}{108} - \frac{a}{A} \log_{10} e$$

Hence $\dfrac{a}{A} = \dfrac{P_1 - P_2}{108 \log_{10} e}$.

Hence the response of the instrument is linear with a. If

$$P_1 - P_2 = 1, \frac{a}{A} = \frac{1}{108 \log_{10} e} = \frac{1}{108 \times \cdot 4343} = 2{\cdot}13 \; \% \, .$$

Hence 1 pulse recorded on the counter corresponds to an obscuration of 2·13%.

The chart is calibrated such that 10 divisions correspond to 1% obscuration/min. Hence the number of pulses in one counting period of 15 minutes to give 10 divisions deflection must be

$$\frac{1\% \times 15}{2{\cdot}13\%} = 7 \, .$$

The movement of the pen per pulse is adjusted so that 7 pulses give a deflection of 10 divisions.

REFERENCES

Badzioch S. (1960) Correction for Anisokinetic Sampling of Gas-Borne Dust Particles. *J. Inst. Fuel* XXXIII, p. 106.

Carey W. F. (1959) Atmospheric Deposits in Britain: a Study of Dinginess. *Int. J. Air Poll.*, **2**, (1), 1–26.

Davies C. N. (1954) *Dust is Dangerous.* Faber and Faber., London.

Lucas D. H. (1961) *The Purification of Gases—A Manual of Modern Practice*, Chapter 13. Newnes, London.

Int. J. Air and Water Poll. Pergamon Press 1961. Vol. 4, Nos. 3/4, pp. 225–236. Printed in Great Britain.

THE IMPROVEMENT OF EFFICIENCY OF FIBROUS DIELECTRIC FILTERS BY APPLICATION OF AN EXTERNAL ELECTRIC FIELD

VÍTĚZSLAV HAVLÍČEK
Prague

Abstract—When an external electric field is applied to a fibrous dielectric air filter both the filter and aerosol are polarized. The dependence of the particulate collection efficiency of the filter is considered for different orientations of the electric field with respect to the direction of air flow. The electric field exerts its greatest influence when parallel with the flow and high filtration efficiencies may then be obtained at relatively high flow rates.

A method based on the Weierstrass' Sigma, Zeta and ℘ functions is used to derive equations for the magnitude of the forces exerted between the aerosol particles and the fibres of the filter.

INTRODUCTION

WHEN an external electric field is applied to a dielectric fibrous filter through which an aerosol is passing both particles and sheet are polarized and attractive forces are generated which add to the collection efficiency due to other mechanisms. In this paper the fibres are considered to be arranged randomly in parallel planes normal to the gas stream but the conclusions derived for this type of distribution are also valid to some extent for a randomly oriented system of fibres.

The angle between the general direction of the electric field and the gas flow influences the collection efficiency and we consider the two extreme cases; firstly, where the field and flow are perpendicular and secondly where they are parallel.

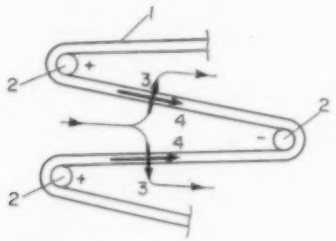

FIG. 1. Cross-section through the filter. Field and flow perpendicular.

Fig. 1 corresponds to the first case. (1) and (2) are cross-sections through the filter sheet and rod electrodes. The gas flows in the direction (3), normal to the main field direction (4). The idealized structure of the fibrous material is shown in Fig. 2 where the numbers (1) to (4) have the same meaning as in Fig. 1. The maxima of the field gradients are shown marked on the fibres by the number 5 so that the electric polarization forces have the greatest influence on the collection of particles at these points. It is, however, at these points that the gas velocity round the fibre is a maximum so that re-entrainment of particles may take place and the effect of the electric forces is reduced, if not destroyed, at the higher velocities.

VOL. 4 1961

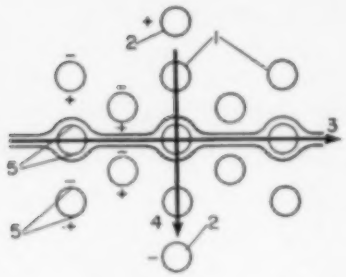

FIG. 2. Idealized structure of the fibrous filter. Field and flow perpendicular.

Re-orientation of the electric field to obtain coincidence of gradient maxima with velocity minima will reduce the possibility of re-entrainment and provide conditions for the full assertion of the electric forces. This is the second extreme case, in which the electric field and gas flow are parallel, and is shown in Figs. 3 and 4 where the numbers 1–5 have the same meaning as in Figs. 1 and 2. The electrodes now consist of two plane parallel wire meshes of negligible resistance to air flow.

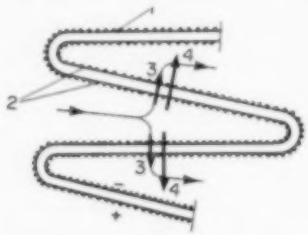

FIG. 3. Cross-section through the filter. Field and flow parallel.

A greater mean value of the electric gradient is now attainable because a more even field can be applied between the mesh electrodes than between the rods and since, as will be shown later, the electric forces in the channels of the sheet increase approximately as the second power of the gradient, the efficiency of the mesh arrangement is thereby increased.

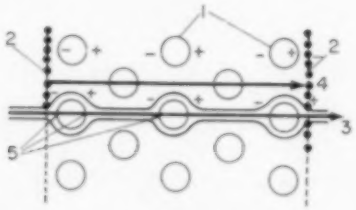

FIG. 4. Idealized structure of the fibrous filter. Field and flow parallel.

EXPERIMENTS

The preceding considerations were put to a preliminary test by measurements of collection efficiencies and pressure drop. The experimental layout is shown in Fig. 5.

The aerosol was generated by atomising an aqueous 1% solution of potassium

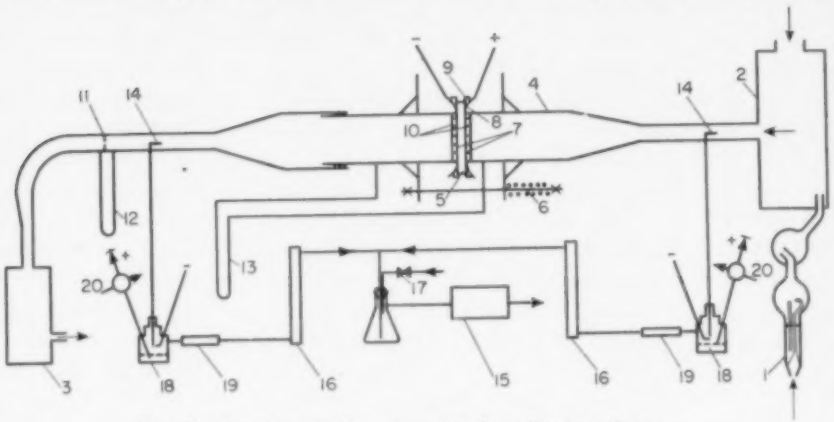

FIG. 5. Arrangement for measuring the collection efficiency.

dichromate from the nebulizer 1, evaporating the droplets and diluting in a mixing chamber 2. The particulate loading was 3×10^{-9} g/cm³. The parameters of the distribution of the aerosol particles found by microscopical methods are shown in the first three columns of Table 1. ϕ_i denotes the middle value of the particle diameters and k the percentage number of particles. Both are for the diameter interval $\Delta\phi i$.

TABLE 1

$\Delta\phi_i$ (μ)	ϕ_i (μ)	k_i (%)	$^1O_{fi}$ (%)	$^2O_{fi}$ (%)
0·5	0·75	61·8	42	63
0·4	1·2	30·3	50	71
0·7	1·75	6·9	65	83
0·7	2·45	—	77	90
1·4	3·5	0·7	90	97
1·4	4·9	0·3	98	99

After leaving the chamber the aerosol, exhausted by the vacuum cleaner 3, entered the P.V.C. test pipeline 4, containing the filter pad in the form of a disk 17 cm diameter and consisting of basaltic fibres of about 3 μ diameter. The thickness of the pad was 2 cm before packing, whilst for the test the compression was adjusted by three springs (6) to 11·75 g/cm² under which conditions the pad was 1 cm thick and the density was 0·16 g/cm³. Electrodes (7) cut from fine wire net, were placed on the faces of the disk, the edges of the mesh in contact with metal rings (8) covered with P.V.C. insulating rings (9) so that the influence of sharp edges on the decrease of the value of the electric strength (about 27 kV/cm, D.C.) of the fibrous pad was suppressed; the applied voltage during test was 10 kV/cm, D.C. The faces of the disk were reinforced by the P.V.C. insulating grid (10). The aerosol velocity was measured

VOL. 4 1961

by the orifice plate (11) and manometer (12) and the pressure drop across the filter by manometer (13). To determine the collection efficiency, that is to determine the concentration of particles in front of and behind the filter, two isokinetic sampling taps (14) were branched off and samples of aerosol drawn off by the oil pump (15). The flow in the taps was measured by flowmeters (16) and adjusted by air inlets (17). The dichromate particles of both neat and filtered clouds were sampled with 99·7 per cent efficiency and were dissolved in two electric impingers (18) which were joined to charcoal ozone-absorbers (19). The potential applied to the electrodes of the impingers was 10 kV d.c. and the electrode current was measured by micro-ammeters (20). The weights of diluted particles in the liquid impingers after addition of sulphuric acid and diphenylcarbazide of phthalic acid were estimated by the colorimetric method: its sensitivity was about 10^{-9} g/25 cm³ water.

The results are shown in Fig. 6 where the values of efficiencies and pressure drops are plotted against the weights of particles sampled in a series of time intervals, and are reduced to unit face area of the filter sheet. At the beginning of the measurements the fourth digit of the efficiency value was not determinable but efficiency was always greater than 99·9 per cent; later, as it became possible to weigh the larger amounts of effluent more accurately, efficiencies of 99·98 per cent were measured. The velocity at the filter face was 20 cm/sec as opposed to the usual 5–10 cm/sec. The increase of pressure drop from an initial 14·9 mm w.g. is also shown in Fig. 6 plotted against the dust loading. If no electric field was applied, the efficiency dropped to 55 per cent.

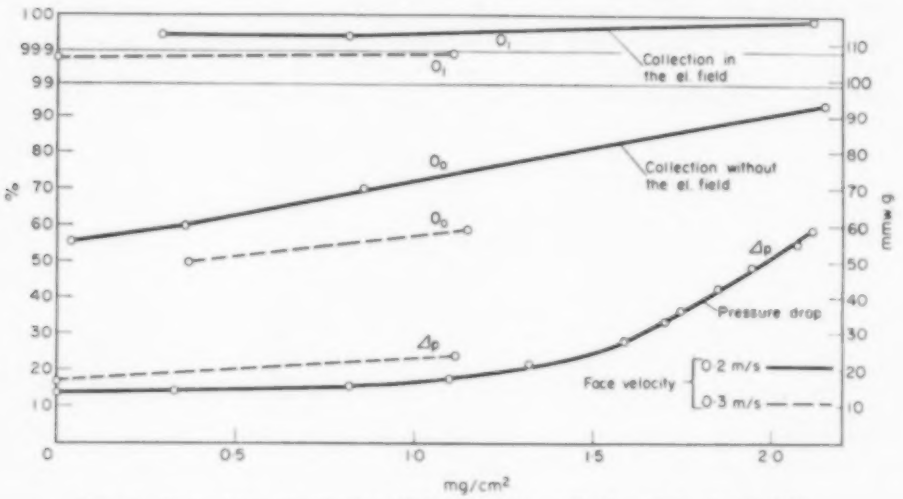

FIG. 6. Dependence of collection efficiency on the application of the electric field.

For the approximate comparison of vertical and parallel fluxes, the partial collection efficiencies of the known filter arrangement with vertical fluxes are plotted in columns 4 and 5 of Table 1. ${}^{1}0_{fi}$ and ${}^{2}0_{fi}$ respectively mean partial efficiency related to the weight of the particle, with and without the application of the electric field. The total collection efficiencies given by the equation

$$ {}^{1,2,}0_{(\%)} = \frac{\sum_a^b k_{i(\%)} \cdot \phi^0_{i(\mu)} \cdot {}^{1,2,}0_{fi(\%)}}{\sum_a^b k_{i(\%)} \cdot \phi^3_{i(\mu)}} $$

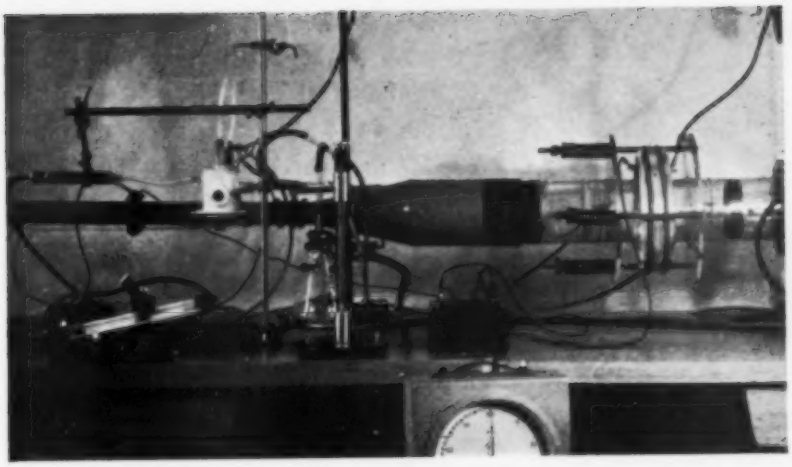

FIG. 5a

VOL.
4
1961

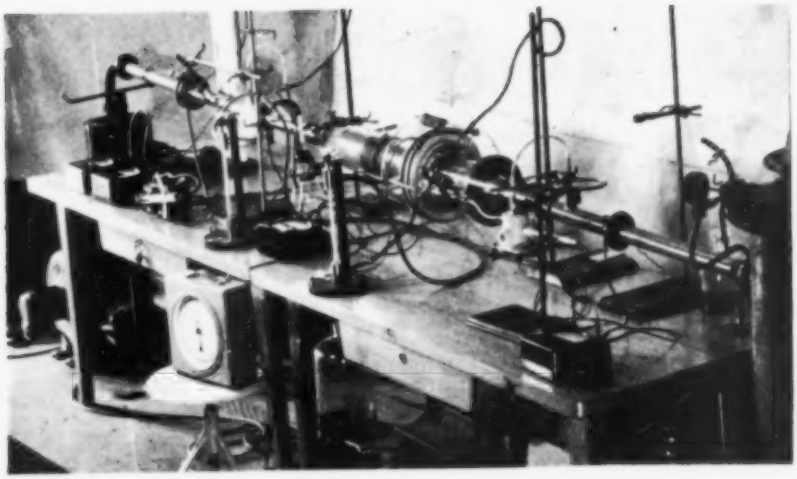

FIG. 5b

Photographs of the measuring equipment

as the number of intervals $i = a\,b$, in our case $1 \div 6$, are 68 per cent and 82 per cent respectively (velocity at the filter face about 5 cm/s). These values are analogous to the measured values 55 per cent and 99·98 per cent for parallel fluxes (velocity at the filter face 20 cm/s). It was possible to use the above equation by the free assumption that the aerosol we have used, with a known particle distribution related to the number of particles, did not differ greatly from the aerosol used in the other case (1), with the particle distribution unknown to the author. In the equation, the known distribution related to the number of particles is transformed in the distribution related to the weight of the particles; this is because of defficiencies relative to the particles' weight. The particles are assumed to be spherical.

From this comparison the significance of employing the same direction of gas flow and electric field is obvious.

THEORY

The values of forces $\vec{F}$, in the channels of the dielectric fibrous medium exerted between the aerosol particle and the system of fibres, when both polarized by an external field, will now be derived from the general equation (BECKER, 1941).

$$\vec{F} = \frac{\phi^3}{16} \frac{\epsilon_p - 1}{\epsilon_p + 2} \nabla |\vec{E}|^2 + q\vec{E}, \tag{1}$$

ϕ denotes the diameter of the particle assumed to be spherical, ϵ_p its dielectric constant, $\vec{E}$ the vector of the field intensity at the place of the particle's position and q the electric charge on the particle besides the dipole charge due to the polarization. We shall assume $q = 0$. To deduce the concrete terms for $\vec{F}$ we proceed as follows: In the idealized structure of the fibrous medium the cylindrical fibres are assumed to be parallel and their lengths infinite, so that the polarized structure can be substituted approximately by a double grid of dipole line-sources. The distribution of the intensity $\vec{E}$ in this grid is derived from the known potential distribution in a double grid of lines with unipolar charges (OBERHETTINGER-MAGNUS, 1949), given by

$$c - c' \operatorname{Log} \vartheta_1(z), \tag{2}$$

where c and c' are constants and ϑ_1 the quasi doubly-periodic Theta-function of the complex variable z which depends on the position of the particle in the channel. The procedure to get the final results can be simplified by use of the Weierstrass Sigma-function $\sigma(z)$ instead of $\vartheta_1(z)$, respecting the distinctions between them. Both are related together by

$$\vartheta_1(z) = c'' \sigma(z) e^{c''' z^2},$$

where c'' and c''' are other constants. Then

$$\operatorname{Log} \vartheta_1(z) = \operatorname{Log} c'' + \operatorname{Log} \sigma(z) + c''' z^2,$$

so that in the first derivative of the last term the difference between $\operatorname{Log} \vartheta_1(z)$ and $\operatorname{Log} \sigma(z)$ will partly go over into the constants, which are determined according to the boundary conditions of the applied electric field. In the second derivative, the difference disappears entirely.

The first derivative of $\operatorname{Log} \sigma(z)$ taken in the direction of the applied field corresponds again to the potential distribution of the double grid but with dipole line-sources, which

VOL. 4 1961

is a good approximate substitute for a grid formed by cylindrical fibres polarized by the field between two parallel plane electrodes placed parallel to the fibres:

$$\frac{d \operatorname{Log} \sigma(z)}{dz} = \frac{\sigma'(z)}{\sigma(z)} = \zeta(z),$$

where $\zeta(z)$ is the Weierstrass Zeta-function. The complete complex potential ω, as the superposition of the potential $E_0 z$, of an imaginary field E_0, which is correlated to the potential impressed on the electrodes, and of the grid potential $C \cdot \zeta(z)$, is then

$$E_0 z + C\zeta(z). \tag{3}$$

After finding the real values of $\zeta(z)$, constant C and E_0, the value of the conjugate field intensity distribution in the double grid of the dipole line-sources is the negative derivative of (3):

$$\vec{E}^* = -\frac{d\omega}{dz} = \frac{d[-E_0 z - C\zeta(z)]}{dz}$$

containing the negative derivative of $\zeta(z)$, which is the elliptic doubly-periodic Weierstrass function $\mathfrak{p}$:

$$-\zeta'(z) = \mathfrak{p}(z).$$

The square $|\vec{E}|^2$ as the product $\vec{E}\vec{E}^*$ will be obtained transforming the term for $\vec{E}^*$ into the polar coordinates r, ϕ, where the value $\vec{E}$ adjacent to $\vec{E}^*$ is given at once.

By substituting the components of the gradient of $|\vec{E}|^2$ given by the partial derivatives $\partial |\vec{E}|^2/\partial r$, $\partial |\vec{E}|^2/\partial \phi$ in (1) we have the equations for the radial and azimuthal components of force as the final solution. Next the outlined procedures are carried out.

POTENTIAL DISTRIBUTION IN A DOUBLE GRID WITH DIPOLE LINE SOURCES

(*a*) Determination of $\zeta(z)$.
This function is defined by the series

$$\left.\begin{aligned} \zeta(z) &= \frac{1}{z} - \frac{a_2}{3} z^3 - \frac{a_3}{5} z^5 - \ldots - \frac{a_\nu}{2\nu - 1} z^{2\nu-1} - \ldots, \\ \text{where} \qquad \frac{a_\nu}{2\nu - 1} &= \sum{}' \frac{1}{w^{2\nu}} \\ \text{and} \qquad w &= 2m\kappa + 2n\kappa'; \ \operatorname{Im}\left(\frac{\kappa'}{\kappa}\right) > 0. \end{aligned}\right\} \tag{4}$$

w are roots of the function $\sigma(z)$, 2κ, $2\kappa'$ its primitive periods and m, n, the integers. From Fig. 7, which is the intersection of the lines grid with a vertical plane, and equivalent to the Argand diagram

$$2\kappa = p, \quad 2\kappa' = p\left(\cos\frac{\pi}{3} + i \sin\frac{\pi}{3}\right) = pe^{i\pi/3}. \tag{5}$$

Σ' denotes the summation over all integer values of m, n, simultaneous zero values of m and n, excepted. It is sufficient to choose the numbers m, n, corresponding to the apices from 0 to 5 of those from all regular hexagons which form the grid (Fig. 7).

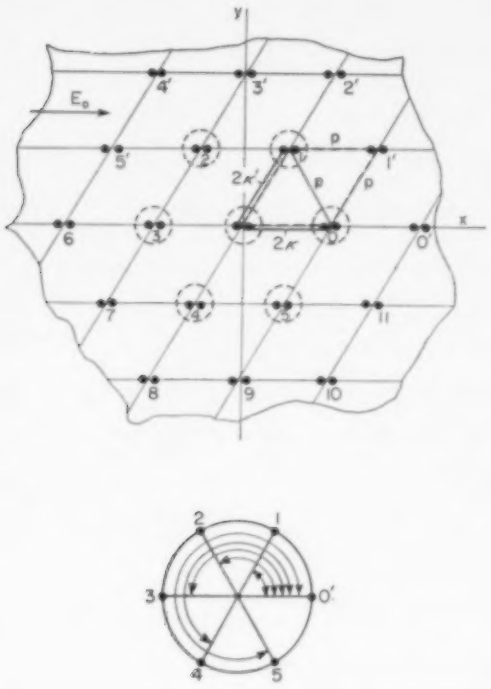

FIG. 7. Cross-section through the double grid of lines.

The centre of the hexagon corresponds to the term $\frac{1}{z}$ of the series (4). The values of m, n, w and of the coefficient $\frac{a_\nu}{2\nu-1}$ obtained from (4), are in Table 2.

TABLE 2

Apex	m	n	w
0	1	0	p
1	0	1	$pe^{i\cdot\pi/3}$
2	−1	1	$pe^{i\cdot 2\pi/3}$
3	−1	0	$-p$
4	0	−1	$pe^{i\cdot 4\pi/3}$
5	1	−1	$pe^{i\cdot 5\pi/3}$

$\frac{a_2}{3}$	$\frac{a_3}{5}$	$\frac{a_4}{7}$	$\frac{a_5}{9}$	$\frac{a_6}{11}$
0	$6\frac{1}{p^6}$ +...†	0	0	$6\frac{1}{p^{12}}$ +...

† neglected members corresponding to the next hexagons

VOL. 4 1961

Substituting them in series the (4) gives:

$$\zeta(z) = \frac{1}{z} - \frac{6}{p^6} z^5 - \frac{6}{p^{12}} z^{11} - \dots . \tag{6}$$

(*b*) Determination of the constant C:

For the potential on the surface of the fibre it is sufficient to take the term $\frac{1}{z}$ only because of rapid convergency of (6). For $p = 4R$, where R denotes the radius of the fibre, the error is 1·5 per cent. For this reason the term for a complex potential on the surface of a single cylindrical fibre is used for the evaluation of C.

$$E_0 z - E_0 \frac{\epsilon_f - 1}{\epsilon_f + 1} R^2 \frac{1}{z},$$

where ϵ_f is the dielectric constant of the fibre. The function $\zeta(z)$ corresponds to the member $\left|\frac{1}{z}\right| \cos\phi$ of the term for the real potential of a charged single cylinder. In polar coordinates it is

$$\left(E_0 r - E_0 \frac{\epsilon_f - 1}{\epsilon_f + 1} R^2 \frac{1}{r}\right) \cos\phi.$$

Thus

$$\omega = E_0 z + C\zeta(z) = E_0 z - E_0 \frac{\epsilon_f - 1}{\epsilon_f + 1} R^2 \zeta(z) \tag{7}$$

(*c*) Determination of the value of the imaginary field E_0:

Because of the fixed potential difference V on the electrodes but not because of their fixed charge, it is not possible to superimpose the field of the grid with the external field $E_0' = V/L$ between the plane electrodes at a distance L, created in the absence of the grid. Thus E_0 must be determined according to the fixed value of V. Substituting

$$L = np = |z|, \tag{8}$$

gives

$$E_0 np - E_0 \frac{\epsilon_f - 1}{\epsilon_f + 1} R^2 n\eta, \tag{9}$$

where η is a number the function $\zeta(z)$ always adds for each next period of z. In (8) ζ vanishes because the difference on the electrodes

$$\zeta(z_1) - \zeta(z_2) = n\eta.$$

From (8) and (9)

$$E_0 = \frac{V}{L\left(1 - \frac{\epsilon_f - 1}{\epsilon_f + 1} R^2 \frac{\eta}{p}\right)} \tag{10}$$

As concerning the value of η we have,

$$\zeta(e^{2\pi i/6} z) = \frac{1}{e^{2\pi i/6} z} + \dots , \tag{11}$$

where the right side is the first term in the expansion close to the origin of the coordinate system. Hence, the expansion of

$$e^{2\pi i/6} z \,.\, \zeta\left(e^{2\pi i/6} z\right) \tag{12}$$

begins with the same term $\frac{1}{z}$ as $\zeta(z)$ does and the two functions, (11) and (12) have the same residues at the pole as at the origin. From the quasi-periodicity of the two functions then it follows that they have the same residues at all poles and are therefore identical.

If now z increases to $z+\kappa$, we have

$$e^{2\pi i/6}\,\zeta\,[e^{2\pi i/6}(z+\kappa)] = \zeta(z+\kappa)\,.$$

The right side of this equation is equal to

$$\zeta(z)+\eta.$$

On the left side, after multiplication, we have

$$e^{2\pi i/6}\alpha = \kappa'\,, \tag{13}$$

and since the argument changes by α', the function changes by η', which means the left hand side of the equation changes by $e^{2\pi i/6}\eta'$. And because the right hand side changes by η,

$$e^{2\pi i/6}\eta' = \eta\,. \tag{14}$$

Substituting (13) and (14) in the Legendre formula

$$\eta\kappa' = \eta'\kappa = \frac{\pi i}{2}\,,$$

and introducing the Euler relation

$$\sin z = (e^{iz} - e^{-iz})\,\frac{1}{2i}$$

VOL. 4 1961

gives

$$\eta = \frac{\pi}{2\kappa\sqrt{3}} = \frac{\pi}{p\sqrt{3}}$$

and

$$E_0 = \frac{V}{L}\,\frac{1}{1 - \dfrac{\epsilon_f - 1}{\epsilon_f + 1}\,R^2\,\dfrac{1}{p^2}\,\dfrac{\pi}{\sqrt{3}}} \tag{15}$$

FIELD INTENSITY DISTRIBUTION IN THE DOUBLE GRID OF DIPOLE LINES AND THE EVALUATION OF $\nabla\,|\,\vec{E}\,|^2$.

As a consequence of the relations between Weierstrass' functions ζ and p, the derivative of the potential function, it is simple to write the equation for the conjugate intensity vector

$$\vec{E}^* = -\frac{d\omega}{dz} = -\frac{d}{dz}\left[E_0 z - E_0\,\frac{\epsilon_f - 1}{\epsilon_f + 1}\,R^2\zeta(z)\right] = -E_0\left[\frac{\epsilon_f - 1}{\epsilon_f + 1}\,R^2\mathrm{p}(z) + 1\right].$$

Transformation into polar coordinates gives

$$\left.\begin{aligned}\vec{E}^* &= -E_0\left[\frac{\epsilon_f - 1}{\epsilon_f + 1}\,R^2\mathrm{p}(re^{-i\phi}) + 1\right],\\ \vec{E} &= -E_0\left[\frac{\epsilon_f - 1}{\epsilon_f + 1}\,R^2\mathrm{p}(re^{i\phi}) + 1\right].\end{aligned}\right\} \tag{16}$$

The multiplication $\vec{E}\vec{E}^*$, expansion of $\mathrm{p}(z)$ in series, using the two first terms of it and introducing $e^{ni\phi} + e^{-ni\phi} = 2\cos n\phi$, gives

$$|\vec{E}|^2 = E_0^2 \left[\left(\frac{\epsilon_f - 1}{\epsilon_f + 1}\right)^2 R^4 \left(\frac{1}{r^4} + \frac{60}{p^6} r^2 \cos 6\phi + \frac{900}{p^{12}} r^8\right) + \right.$$
$$\left. + \frac{\epsilon_f - 1}{\epsilon_f + 1} R^2 \left(\frac{1}{r^2} 2 \cos 2\phi + \frac{60}{p^6} r^4 \cos 4\phi + 1\right)\right] \tag{17}$$

The gradient $\nabla |\vec{E}|^2$ is a vector sum of partial derivatives of (17)

$$\nabla |\vec{E}|^2 = \frac{\partial |E|^{2}_{r}}{\partial r} + \frac{\partial |E|^{2}_{\phi}}{\partial r} \frac{1}{r}. \tag{18}$$

The radial and azimuthal components of $\nabla |\vec{E}|^2$ are:

$$\nabla_{rad} |\vec{E}|^2 = 4E_0^2 \left[\left(\frac{\epsilon_f - 1}{\epsilon_f + 1}\right)^2 R^4 \left(-\frac{1}{r^5} + \frac{30}{p^6} r \cos 6\phi + \frac{800}{p^{12}} r^7\right) + \right.$$
$$\left. + \frac{\epsilon_f - 1}{\epsilon_f + 1} R^2 \left(-\frac{1}{r^3} \cos 2\phi + \frac{60}{p^6} r^3 \cos 4\phi\right)\right]. \tag{19}$$

$$\nabla_{az} |\vec{E}|^2 = 4E_0^2 \left[\left(\frac{\epsilon_f - 1}{\epsilon_f + 1}\right)^2 R^4 \frac{-90}{p^6} r^2 \sin 6\phi + \right.$$
$$\left. + \frac{\epsilon_f - 1}{\epsilon_f + 1} R^2 \left(-\frac{1}{r^2} \sin 2\phi - \frac{60}{p^6} r^4 \sin 4\phi\right)\right]. \tag{20}$$

Equation (1) is solved by using equations (15), (16), (19), (20) and (21).

$$\vec{F} = \vec{F}_{rad} + \vec{F}_{az} = \frac{\phi^3}{16} \frac{\epsilon_p - 1}{\epsilon_p + 2} \left(\nabla_{rad} |\vec{E}|^2 + \nabla_{az} |\vec{E}|^2\right), \tag{21}$$

$$\vec{F}_{rad} = -\frac{\phi^3}{4} \frac{\epsilon_p - 1}{\epsilon_p + 2} E_0^2 \left[\left(\frac{\epsilon_f - 1}{\epsilon_f + 1}\right)^2 R^4 \left(\frac{1}{r^5} - \frac{30}{p^6} r \cos 6\phi\right) + \right.$$
$$\left. + \frac{\epsilon_f - 1}{\epsilon_f + 1} R^2 \left(\frac{1}{r^3} \cos 2\phi - \frac{48}{p^6} r^3 \cos 4\phi\right)\right], \tag{22}$$

$$\vec{F}_{az} = -\frac{\phi^3}{4} \frac{\epsilon_p - 1}{\epsilon_p + 2} E_0^2 \left[\left(\frac{\epsilon_f - 1}{\epsilon_f + 1}\right)^2 R^4 \frac{72}{p^6} r \sin 6\phi + \right.$$
$$\left. + \frac{\epsilon_f - 1}{\epsilon_f + 1} R^2 \left(\frac{1}{r^2} \sin 2\phi + \frac{60}{p^6} r^4 \sin 4\phi\right)\right]. \tag{23}$$

On the fibre surface ($r = R$), for $g = \frac{p}{R}$

$$\vec{F}_{\substack{rad \\ r=R}} = -\frac{\phi^3}{4} \frac{\epsilon_p - 1}{\epsilon_p + 2} E_0^2 \frac{1}{R} \left[\left(\frac{\epsilon_f - 1}{\epsilon_f + 2}\right)^2 \cdot \left(1 - \frac{30}{g^6} \cos 6\phi\right) + \right.$$
$$\left. + \frac{\epsilon_f - 1}{\epsilon_f + 1} \left(\cos 2\phi - \frac{60}{g^6} \cos 4\phi\right)\right], \tag{24}$$

and especially for $\phi = 0°$ and $90°$ respectively

$$\vec{F}_{\substack{rad \\ r=R \\ \phi=0}} = -\frac{\phi^3}{4} \frac{\epsilon_p - 1}{\epsilon_p + 2} E_0^2 \frac{1}{R} \left[\left(\frac{\epsilon_f - 1}{\epsilon_f + 1}\right)^2 \cdot \left(1 - \frac{30}{g^6}\right) + \frac{\epsilon_f - 1}{\epsilon_f + 1} \left(1 - \frac{60}{g^6}\right)\right]. \tag{25}$$

$$\vec{F}_{\substack{rad \\ r=R \\ \phi=90}} = +\frac{\phi^3}{4} \frac{\epsilon_p - 1}{\epsilon_p + 2} E_0^2 \frac{1}{R} \left[-\left(\frac{\epsilon_f - 1}{\epsilon_f + 1}\right)^2 \left(1 + \frac{30}{g^6}\right) + \frac{\epsilon_f - 1}{\epsilon_f + 1} \left(1 + \frac{60}{g^6}\right)\right]. \tag{26}$$

For comparative purposes formulae are given for the values of forces $\vec{S_F}$ near to a single fibre. The derivation of the equations is not given because of its simplicity

$$\vec{S_{F_{rad}}} = -\frac{\phi^3}{4} \frac{\epsilon_p - 1}{\epsilon_p + 2} \left(\frac{V}{L}\right)^2 \left[\frac{\epsilon_f - 1}{\epsilon_f + 1} \frac{R^2}{r^3} \cos 2\phi + \left(\frac{\epsilon_f - 1}{\epsilon_f + 1}\right)^2 \frac{R^4}{r^5}\right], \tag{27}$$

$$\vec{S_{\substack{F_{rad} \\ r=R}}} = -\frac{\phi^3}{4} \frac{\epsilon_p - 1}{\epsilon_p + 2} \left(\frac{V}{R}\right)^2 \frac{1}{R} \left[\frac{\epsilon_f - 1}{\epsilon_f + 1} \cos 2\phi + \left(\frac{\epsilon_f - 1}{\epsilon_f + 1}\right)^2\right], \tag{28}$$

$$\vec{S}_{\substack{F_{rad} \\ r=R \\ \phi=0}} = -\frac{\phi^3}{4}\frac{\epsilon_p-1}{\epsilon_p+2}\left(\frac{V}{L}\right)^2\frac{1}{R}\left[\frac{\epsilon_f-1}{\epsilon_f+1}+\left(\frac{\epsilon_f-1}{\epsilon_f+1}\right)^2\right], \tag{29}$$

$$\vec{S}_{\substack{F_{rad} \\ r=R \\ \phi=90}} = +\frac{\phi^3}{4}\frac{\epsilon_p-1}{\epsilon_p+2}\left(\frac{V}{L}\right)^2\frac{1}{R}\left[\frac{\epsilon_f-1}{\epsilon_f+1}-\left(\frac{\epsilon_f-1}{\epsilon_f+1}\right)^2\right], \tag{30}$$

$$\vec{S}_{F_{az}} = -\frac{\phi^3}{4}\frac{\epsilon_p-1}{\epsilon_p+2}\left(\frac{V}{L}\right)^2\frac{\epsilon_f-1}{\epsilon_f+1}\frac{R^2}{r^2}\sin 2\phi\,. \tag{31}$$

In Table 3 are given, as an example, the magnitudes in dynes of some radial components of forces calculated for particle positions G H, I, K (Fig. 8) and parameters $\phi = 1\,\mu$, $R = 1\,\mu$, $p = 4\,\mu$, $\epsilon_p = 2, 5$, $\epsilon_f = 4$, $L = 1$ cm, $V = 10$ kV.

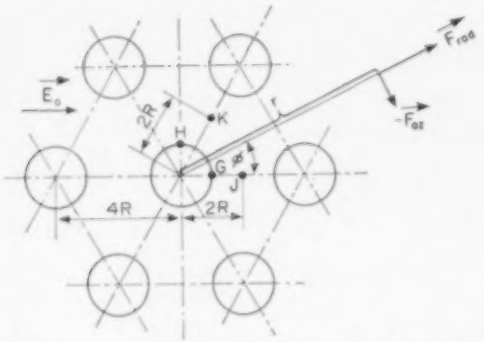

FIG. 8. Scheme of the positions of particles for which the forces are calculated (Table 3).

TABLE 3

Position	G	H	I	K
System of fibres	$-1{,}02 \cdot 10^{-6}$	$+2{,}54 \cdot 10^{-7}$	$-3{,}9 \cdot 10^{-7}$	$-6{,}9 \cdot 10^{-8}$
Single fibre	$-1{,}77 \cdot 10^{-6}$	$+4{,}4 \cdot 10^{-7}$	$-7{,}8 \cdot 10^{-8}$	$+1{,}4 \cdot 10^{-8}$

The distribution of the magnitudes of radial components, along the surface of the fibre, both for a single fibre and for the whole system of fibres is plotted in Fig. 9. They appear to be not only attractive, but repulsive too. The magnitudes of components are plotted radially from the fibre surface; attractive outward, repulsive inward.

DISCUSSION

The previous analysis has dealt with polarization forces acting on single particles and the magnitude of these forces has been derived for various parameters but the retention effect of a filter depends also on the magnitude of the pressure exerted by the gas stream on particles relative to the electric forces. The relationship between these forces is altered if a group of particles is captured by a fibre (Fig. 10) as the polarization forces are additive but the aerodynamic force on the group is much smaller than the sum of pressures on single particles so that even weak polarization forces may be effective when the electric field and air flow are parallel.

VOL. 4 1961

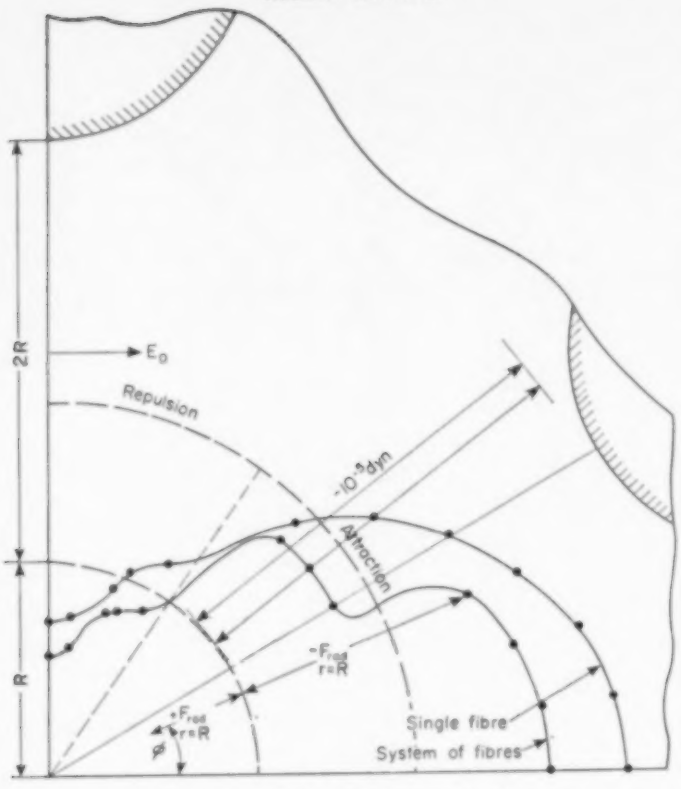

FIG. 9. Distribution of radial forces on the fibre surface.

The equations for the magnitudes of the forces show that the attractive forces increase with decrease of fibre radius. It also follows from the equations that for larger values of $g = \frac{p}{r}$, that is for low filter packing factors, the magnitudes of the polarization forces approach to those round a single fibre, whilst in a densely packed filter the forces in

FIG 10. Action of the electric and Stokes' forces on the collection of particles.

the interstices are smaller. The dependence on the square of the gradient $(V/L)^2$ has already been mentioned and the dependence on other parameters is obvious from the equations.

Acknowledgments—My thanks are due to the management of the Research Institute of Air-technics in Prague where the work was carried out and to Messrs V. FISER, R. SVETNICA, Z. SVOBODA and MRS. Z. GUTENBERG, who were very helpful in the experimental work.

REFERENCES

BECKER (1941). *Theorie der Elektrizität*, p. 79. Leipzig.

OBERHETTINGER-MAGNUS. *Anwendungen der elliptischen Funktionen in Physik und Technik*, p. 68. Berlin.

Int. J. Air and Water Poll. Pergamon Press 1961. Vol. 4, Nos. 3/4, pp. 237–246. Printed in Great Britain.

A NEW ATMOSPHERE IRRADIATION CHAMBER

ROBERT R. AUSTIN, ROGER W. LEWIS and RALPH DONALDSON, Jr.
Robert R. Austin Laboratories, San Gabriel, California
(*Received in final form*, 25 *August* 1960)

Abstract—The irradiation of atmospheric samples of air with ultraviolet light produces oxidants when hydrocarbons and nitrogen dioxide are present and thus permits a measurement of the smog-forming potential of the air.

A new high irradiation intensity chamber using fluorescent ultraviolet lamps has been developed. Data are given for the irradiation of some hydrocarbons in air in the presence of nitrogen dioxide. Some data are also given for atmospheric samples.

The performance of the new chamber is compared to that of the fifty-liter chambers which have been in use in the past. The chamber volume is eight liters. Power required has been reduced from 1600 watts in the fifty-liter chamber to 160 watts. Oxidant levels produced at the same sampling rate on atmospheric samples are approximately equivalent to the levels produced in the fifty-liter chamber.

VOL.
4
1961

INTRODUCTION

THE well-known decrease in such manifestations of Los Angeles air pollution as oxidant values and eye irritation which occurs toward sunset is not an indication of a decrease in total pollution. It reflects instead the end of the photochemical formation of the short-lived species responsible for these effects.

LITTMAN, *et al.* (1956), noting that the compounds responsible for " photochemical smog " remained in the air, introduced the use of artificial irradiation chambers as a means to measure this smog-forming potential, and termed the chemical complex responsible " oxidant precursor ". The most active oxidant precursor is now known to be a mixture of olefinic hydrocarbons and nitrogen dioxide. Precursor concentrations are expressed as the difference between post- and pre-irradiation concentrations of oxidant.

The early work was done with a fifty-liter flask as irradiation chamber and four H 400 E–1 G. E. lamps as light source. Practical problems of heat dissipation and power requirements are met in many instrument locations. A fifty-liter chamber volume reduces the rate of response of the recorder to changes in the concentration of the compounds that produce oxidants on irradiation. Approximately 20 minutes are required for the recorder to reach 85 per cent of its response to a given change in concentration. Thus, corresponding concentration peaks for the direct oxidant measurement and for the irradiated sample will be displaced by about 20 minutes. This factor leads to confusion in interpreting data.

An investigation of more efficient irradiation apparatus has therefore been made and a new chamber developed using tubular fluorescent ultraviolet lamps. In order to preserve the continuity of records, it was more desirable to duplicate the performance of the larger chamber than to bring its behavior into line with the now known atmospheric chemistry of hydrocarbons.

Examination of light output data for available commercial lamps shows the following values for two sources:

TABLE I. LIGHT OUTPUT IN WATTS

Lamp	Middle U.V. 2800–3200	Near U.V. 3200–3800	Visible 4000–6000
40 watt BI 48" tube	·25	8·10	·98
H 400 E-1	·412	22·5	57·26

It will be noted that while the current of the 400 watt lamp is higher by a factor of 10, the output in the near ultraviolet is only increased by a factor of approximately 2¼.

Light input efficiency to the chamber for the 400 watt lamps is not high because of reflection from spherical flask walls and limitations in reflector design. Higher efficiency is attainable with a cylindrical chamber and parallel cylindrical lamps.

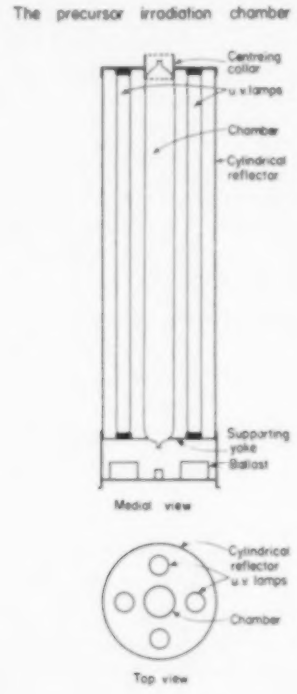

FIG. 1

Two basic chamber designs have been studied. The first was a pyrex cylindrical chamber with a single ultraviolet lamp mounted axially in the chamber. Multiple chambers of this type are used in series to give required residence time. The second type of chamber was a single pyrex tube mounted axially in a metal housing with ultraviolet lamps spaced uniformly around the glass cylinder. The internal housing wall is lined with polished aluminium foil. Highest efficiency was attained with the single chamber and external lamps. This design also offered advantages in ease of lamp replacement and chamber cleaning.

Some data from experimental chambers with internal bulbs bear on the reaction of hydrocarbons to produce oxidant and are also given here. A chamber of the second type was designed for practical use in air monitoring service. A drawing of this chamber is shown in Fig. 1 and data are given for its irradiation characteristics and performance as compared to the fifty-liter flask chamber which has been in general use.

EXPERIMENTAL

Reflector Efficiency

The significance of reflector efficiency and of wall temperature and area was studied with tubular chambers 4 feet long and 80 mm in diameter. Lamps were mounted axially in each chamber.

In these experiments aluminium foil and silver mirror coatings were studied. Aluminium foil was placed first on the outer wall surface and then as a chamber liner on the inner wall surface. The silver mirror coating was formed on the outer wall surface. Data for oxidant concentration reached at a standard flow rate of 3·7 liters/minute are given in Table 2.

TABLE 2. EFFECT OF REFLECTORS ON CHAMBER EFFICIENCY

Date	Reflector	Oxidant Produced (PPHM)
11/5	Al foil outside	35
11/7	„ „ inside	31
11/7	Al foil outside	35
	„ „ inside	37
12/4	Al foil outside	35
	None	5
12/9	Al foil outside	35
	Silver mirror outside	27

Note: (Data are for a mixture in air of Isobutylene 4 p.p.m. and NO_2 1 p.p.m.).

These data show that polished aluminium foil is a practical reflector for ultraviolet and that absorption of ultraviolet in the pyrex wall of the cylinder is not significant. There is a seven-fold increase in oxidant level for the aluminium reflective surface compared with the uncoated glass.

Irradiation Efficiency

Studies of irradiation efficiency were made with 1, 2, 3 and 4 80 mm chambers in series to determine optimum chamber volume and residence time. Flow of air through the chamber is not linear. The residence time given in the tables is actually obtained by dividing the chamber volume by the flow rate and represents average duration of irradiation. Data are given in Table 3.

It will be noted for the second chamber the efficiency is comparable to that of the first, but for the third and fourth chambers, the efficiency falls off. This loss in efficiency is not due to depletion of the raw material or to the attainment of equili-

VOL. 4 1961

brium between the reacting compounds and their products of reaction, since when the flow rate is reduced so as to double the residence time, a higher level of oxidant is developed.

TABLE 3. IRRADIATION EFFICIENCY FOR CHAMBERS IN SERIES

Isobutylene	4 p.p.m.	Normal flow	
Butene	4 p.p.m.	80 mm chamber residence	
NO_2	1 p.p.m.		

Date	Hydrocarbon	No. Chambers	Residence Time	Oxidant p.p.h.m.	Net Oxidant Increase
12/12	Isobutylene	1	1·5 min.	15	15
		2	3·0	35	20
		3	4·5	45	10
		4	6·0	50	5
		4	12·0	62	
12/12	1 Butene	1	1·5	10	10
		2	3·0	21	11
		3	4·5	27	6
		4	6·0	31	4

External Lamps Vs. Internal Lamps

The above data probably indicate high decomposition rates at the relatively hot bulb surface and a relatively high surface-to-volume ratio with internally mounted bulbs. While it is obvious that light reflection will be optimum when the lamp is mounted inside the chamber, it was considered important to study irradiation efficiency with externally mounted lamps.

In this experiment, the chamber was placed in a tubular housing and located axially. Tubes were mounted near the housing wall and spaced evenly. Data are given in Table 4 for experiments with this configuration and for internally mounted lamps.

TABLE 4. IRRADIATION EFFICIENCY DATA FOR CHAMBERS WITH INTERNAL U. V. LAMPS AND EXTERNAL U. V. LAMPS

Date	Chamber	Hydrocarbon	Oxidant	Residence Time (Min.)
1/30	80 mm 4 external lamps 9" housing	1 butene	21	1·8
	3—80 mm chambers with internal lamps	1 butene	13	6
	50-liter	1 butene	29	12

(Butene at approximately 4 p.p.m., NO_2 at approx. 1 p.p.m.)

Oxidant concentration reached in 1·8 min. in one 80 mm chamber was 21 p.p.m., while a concentration of 29 p.p.m. was reached in 12 minutes in the fifty-liter chamber.

A single chamber with external lamps proved to be more efficient than three chambers in series with internal lamps. Experiments with a 100 mm chamber showed that increasing chamber volume by 30 per cent produced a 20 per cent increase in oxidant level at standard flow rate.

It is apparent that further increase in diameter to increase residence time will have diminishing value in increasing oxidant concentration. The 100 mm chamber was therefore adopted for the design of a practical irradiation chamber and housing.

Irradiation Intensity

Comparative light intensity data have been obtained for the fifty-liter flask and for a single 100 mm chamber irradiated by four external lamps spaced evenly in a 9 in. housing.

A barrier layer photocell with a filter passing ultraviolet light in the band from 3000 to 4000 Ångstrom, was used to measure intensity. Measurements were made at points around the circumference of the chamber on the radius common to the chamber cylinder and the lamp and on the radius between lamps. The intensity at the axis of the chamber was also determined. Little difference was observed in the intensity values for the four lamps. Data therefore are given as an average of four readings between lamps and on the radii to the lamps. Three series of measurements were made, one 6 in. from the top of each chamber, one at the midpoint and one 6 in. from the bottom. The data are given in Table 5.

VOL. 4 1961

TABLE 5. U. V. LIGHT INTENSITY DATA FOR TWO CHAMBERS

Radiation intensity in μ amps output of photocell

Chamber	Center	Radius to lamp	Radius between lamps
100 mm tube			
6 in. from bottom	300	400	380
Midpoint	500	500	400
6 in. from top	400	400	400
50-liter flask			
6 in. from bottom	60	71	67
Midpoint	90	92	82
6 in. from top	90	85	80

Measurements of the intensity of direct sunlight at noon in Los Angeles during the first week of March with the same equipment gave photocell currents from 95 to 104 amps. The average intensity is approximately 20 per cent higher than the average intensity in the fifty-liter flask.

The difference in light intensity for the various locations in each chamber is not great. Data are not precise enough to warrant rigorous mathematical treatment to obtain a mean value of intensity. However, the intensity in the small chamber appears to be 4 to 5 times that measured in the fifty-liter chamber. Data for oxidant concentration show that the residence time in the fifty-liter flask is 5 to 6 times that required in the 100 mm chamber for equivalent oxidant levels.

Hydrocarbon Structure Versus Oxidant Production

Data for some representative hydrocarbons and for exhaust gas mixtures irradiated in the various chambers are given in Table 6.

TABLE 6. OXIDANT VALUES FOR VARIOUS HYDROCARBONS IRRADIATED IN THREE CHAMBERS

	Oxidant in p.p.h.m. from Various Chambers with Residence Time as Shown			
Hydrocarbon	100 mm 5·2 min.	100 mm 2·6 min.	50-liter 12 min.	4–80 mm 6 min.
Acetylene	55	37	50	
Isooctane	50	32	48	
Diisobutylene	80	50	65	
Butadiene	100	52	50	
"		38	30	34
Exhaust + NO_2 *		48	54	
Isobutylene		18	17	13

* A second run was made on this mixture in the 100 mm chamber at 20 per cent increase in residence time. Oxidant level was 60 p.p.h.m. Hydrocarbons at approximately 4 p.p.m., NO_2 at approximately 1 p.p.m.

It is well to point out the role of temperature in the two chambers. Heat input to the cylindrical chamber is much lower and convection cooling much more effective because of the greater vertical length of the chamber. Lower residence time is also a factor in reducing decomposition of ozone on the chamber walls.

There is no recorded peak in the oxidant level when a given mixture of olefin and nitrogen dioxide in air flows continuously through the 100 mm chamber at constant rate during the warm-up period after ultraviolet lamps are turned on. The fifty-liter flask shows a marked peak at about 30 min after lights are turned on. The drop in

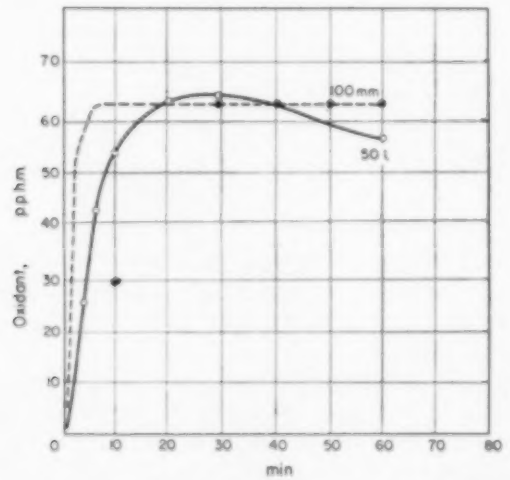

FIG. 2. Irradiation efficiency vs. time auto exhaust + NO_2.

oxidant level after 30 min, observed for the sample irradiated in the fifty-liter flask, appears to be caused by the increase in temperature of the chamber walls.

Curves for the two chambers operating on a mixture of exhaust gas and nitrogen dioxide in air are shown in Fig. 2. It should be noted that in continuous service the fifty-liter chamber will operate at the lower efficiency.

It will be noted that the relatively active olefins such as butadiene and diisobutylene show equivalent or higher oxidant values compared to those obtained in the fifty-liter flask. The less reactive hydrocarbons show relatively less oxidant for the small chamber. These data show that the measurement of oxidant concentration, either direct or after irradiation, is an empirical measurement which includes the contribution of saturated, as well as, unsaturated hydrocarbons.

The cylindrical chamber in practical use will tend to magnify the contribution of reactive hydrocarbons to the oxidant levels in the atmosphere, compared with the present fifty-liter chamber.

The data thus far presented have been recorded by an oxidant recorder of the type introduced by LITTMAN and BENOLIEL (1953). The accuracy in making comparison between chambers was limited by the regulation of input mixture to the chamber and by the liquid flow rate and air sample flow rate regulation of the instrument. It is not considered to be better than + 10 per cent.

Chamber Efficiency Studies with Manual Sampling

Some data have been obtained by sampling manually from the same mixture simultaneously through the two chambers and by determining oxidant colorimetrically with two reagents, potassium iodide and phenolphthalin.

It is possible to measure sample volumes more accurately with manual sampling, and if the mixtures to be irradiated can be maintained at constant composition, the performance of the chambers can be more accurately compared.

VOL. 4 1961

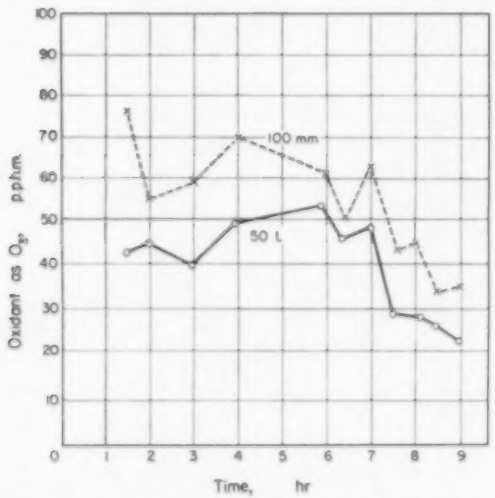

FIG. 3. Irradiation of butene-NO_x-mixtures sample flow 4L per min. Phenolphthalin reagent.

The phenolphthalin reagent, which was introduced by HAAGEN-SMIT (1952) for oxidant measurement, was included in this phase of the study because it was convenient and in order to determine whether there is a significant difference in the oxidant levels developed in the two chambers as measured by the two reagents. Both reagents are in use and while potassium iodide reagent is generally used in recorders where irradiated samples are taken, phenolphthalin reagent may be used in this way in the future.

A mixture of about 200 p.p.m. butene and 50 p.p.m. nitrogen dioxide in nitrogen was prepared in a pressure tank and this mixture fed into the intake air to the irradiation chamber. Flow rate of the concentrated mixture was allowed to vary during the run. Data for phenolphthalin analysis from the two chambers are plotted in Fig. 3.

Data for a similar run using 20 per cent potassium iodide as reagent are plotted in Fig. 4. These data show that oxidant concentrations shown for both reagents were higher for the 8-liter chamber. The effect of more rapid response of the small chamber is also shown.

Data for irradiated atmospheric samples using the phenolphthalin reagent are also given in Fig. 5. The smog-forming potential of the air during the period in which this work was done was relatively low so that accuracy is limited. The data are in general agreement with data for synthetic mixtures given above.

Studies of the Effect of Olefin/Nitrogen Dioxide Ratio

The ratio of olefin to nitrogen dioxide concentration in most mixtures studied in the irradiation experiments has been approximately 4 to 1. Work at Franklin Institute (STEPHEN *et al.*, 1956) has shown that the ratio is important and that the above ratio is near optimum. Some experimental work has been done to determine the importance of the relative concentration of olefin and nitrogen dioxide under the conditions of this experimental work.

An oxidant level was established after irradiation in the 100 mm chamber of a mixture of 1 p.p.m. nitrogen dioxide and 4 p.p.m. olefin. The concentration of each

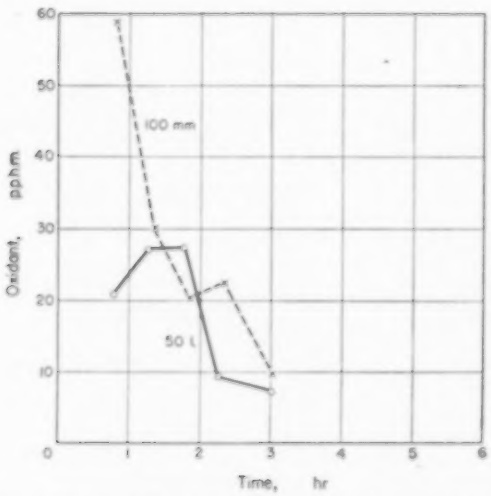

FIG. 4. Irradiation of butene-NO_2-mixtures sample flow 4L per min. reagent 20% KI.

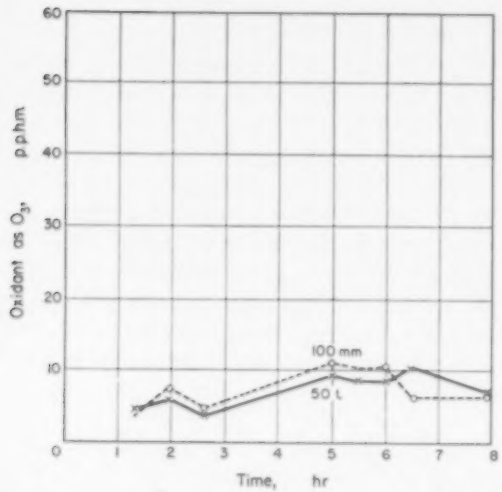

FIG. 5. Irradiation of atmospheric air sample flow 4L per min. Phenolphthalin reagent.

gas in turn was then reduced stepwise in a measured percentage and the percentage change in oxidant level was determined.

Curves are given in Fig. 6 for the percentage change in oxidant versus the per cent change of nitrogen dioxide and of 1 pentene.

These data show that the residual oxidant formation from nitrogen dioxide alone in the absence of olefin is approximately 45 per cent of the oxidant level at 4 p.p.m. olefin. Ten per cent reduction in either component is not shown by these data to reduce the oxidant level.

VOL. 4 1961

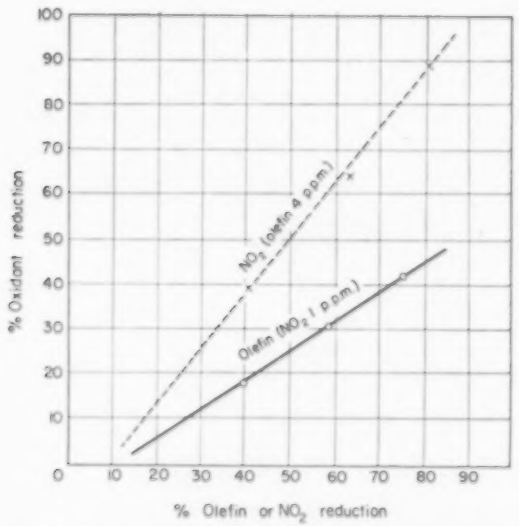

FIG. 6. The effect of olefin/nitrogen dioxide ratio of oxidant production by irradiation.

SUMMARY AND CONCLUSIONS

A new atmosphere irradiation chamber has been developed and performance studies made. This 100 mm cylindrical pyrex chamber is irradiated by four 40 watt 48 in. tubular fluorescent ultraviolet lamps. Performance studies show that oxidant levels for representative olefins for auto exhaust samples in air and for atmospheric samples are equivalent for this chamber to oxidant levels produced in the fifty-liter flask which has been in use. The new chamber operates on 160 watts power and provides, at 3·7 L/minute 2·6 minutes residence time, as compared to 1600 watts power and 12 minutes residence time of the fifty-liter chamber.

Data in this study also show that saturated hydrocarbons can contribute to oxidant values in irradiated mixtures of hydrocarbons and nitrogen dioxide in air.

The shorter irradiation time required in the small chamber will show concentration values for irradiated samples very little displaced in time from corresponding values for direct atmospheric samples.

Acknowledgement—The work has been done as part of Research Grant S–86 from Division of Research Grants, National Institutes of Health, U.S. Public Health Service. The help and co-operation of members of the staffs of the Los Angeles Air Pollution Control District, who supplied an oxidant recorder on loan, and of the Air Pollution Foundation is acknowledged and appreciated.

REFERENCES

LITTMAN F. E., FORD H. W. and ENDOW N. (1956) *Ind. Eng. Chem.* **48**, 1493.
LITTMAN F. E., BENOLIEL H. W. (1953) *Anal. Chem.* **25**, 1480.
HAAGEN-SMIT A. J. (1952) *Ind. Eng. Chem.* **44**, 1342.
STEPHENS E. R., HANST P. L., DOERR R. C. and SCOTT W. E. (1956) *Ind. Eng. Chem.* **48**, 1498.

Int. J. Air and Water Poll. Pergamon Press 1961. Vol. 4, Nos. 3/4, pp. 247–255. Printed in Great Britain.

A QUANTITATIVE STUDY OF THE LIMED FILTER PAPER TECHNIQUE FOR FLUORINE AIR POLLUTION STUDIES*

DONALD F. ADAMS
Division of Industrial Research, Washington State University, Pullman, Washington
(*Received in final form*, 8 *July* 1960)

Abstract—Exposed, lime-treated filter paper will accumulate fluoride from the atmosphere at a finite rate, associated with the relative concentration of pollution at each sampling site. Data are presented which relate (*a*) the rate of fluoride accumulation per unit surface area of the exposed limed paper with (*b*) the fluoride concentration in the air of a plant growth chamber. The data show an average fluoride collection rate of 7·6 $\mu g\ F^-/dm^2/day/\mu g\ F^-/m^3$. The data are discussed in relation to previously published literature relating fluoride accumulation in limed paper exposed to industrial air pollution under field and greenhouse conditions. Additional data are presented which show that the fluoride concentration in a greenhouse atmosphere is significantly decreased over relatively short distances through processes of surface adsorption and foliar pickup.

INTRODUCTION

THE relative fluoride pollution intensity at different distances and directions from a source of a fluoride-containing effluent may be established by analyzing lime-treated filter papers which have been exposed in the area of contamination. The method is predicated on the assumption that the gaseous fluorides will react with and be fixed by the lime at some rate which is related to the atmospheric concentration of fluorides.

The limed paper survey technique involves the simple and inexpensive expedient of exposing lime-impregnated filter papers in protective shelters designed to permit adequate air circulation. The usual exposure period is either one calendar month or 28 days. At the end of the exposure period the papers are then exchanged for fresh papers, the fluorine content of the exposed papers chemically determined and the data reported in terms of micrograms per square decimeter of exposed surface of the treated paper per unit time for each sampling site. The limed paper fluoride level found at each site for each sampling period is an index of the degree of fluoride exposure in the vicinity of each sampling site.

Although this survey method has been widely used in many areas in the United States during the past ten years, limited data of this type has been reported in the literature (ADAMS, 1957; MCINTIRE, *et al.*, 1956; MILLER, *et al.*, 1953; and ROBINSON, 1957). This dearth of information may be attributed to the nature of the technique, that of routine surveillance of suspected areas of pollution. Compilations of routine data are not generally submitted for publication.

The limed paper technique for fluorine survey was first reported by MILLER *et al*, (1953). These authors obtained a 5-year statistical correlation between the fluoride levels in forage grown at lime paper exposure sites during the exposure period and the fluoride content of simultaneously exposed papers. These authors also showed a significant correlation between the extent of fluoride-induced leaf burn on exposed gladiolus and the fluoride accumulated by simultaneously exposed limed filter papers. ADAMS (1957) related the average monthly filter paper fluoride level for the entire

* Presented Division of Water, Sewage and Sanitation, 136th meeting, ACS, Atlantic City, N.J., September 1959.

VOL. 4 1961

growing season (two different years) with the fluoride content of heterogeneous ground cover vegetation available at each of 20 sampling sites. The curvilinear relation had an r value of +0·922. This study further showed that the lime paper technique was quite reliable in measuring the decrease in relative intensity of fluoride pollution following installation of extensive fume control equipment by the major source of fluoride in one of the areas surveyed. The limed papers showed a 65 per cent pollution reduction, whereas the industry stated that a 71 per cent reduction had been achieved. In addition, it was shown that a 5·2 per cent coefficient of variation existed between duplicate limed paper shelters at 5 sampling sites.

ROBINSON (1957) proposed that lime papers respond to the total fluoride brought in contact with it, rather than responding to atmospheric concentrations as do air samplers having constant, positive sampling rates. He then postulated that doubling the air flow will result in bringing roughly double the fluoride into contact with the exposed limed papers.

A similar technique of exposing lead peroxide coated cylinders for delineation of areas of sulfur dioxide pollution has been used in Great Britain since 1932. Certain variables which might affect the rate of absorption of the sulfur dioxide by lead peroxide have been studied by WILSDON and MCCONNELL (1934). These studies included such environmental factors as wind speed, rainfall, humidity and temperature. In the range of air speeds between 1·5 and 9 meters per second (3·3–20·1 m.p.h.) and SO_2 concentrations of 1–6 p.p.m. the rate of reaction was not found to be significantly dependent upon air speed.

Meteorological and topographical factors may combine to increase or decrease the fluoride concentration in the air at various times contacting the treated surface. These factors will produce an equivalent change in the rate of accumulation of fluoride. However, the levels of fluoride accumulated by the limed papers in the vicinity of a given source should be virtually independent of the normal variations in air flow rate. Under conditions of extremely high air flow rates, the contact time would become an important factor in the rate of accumulation. Regardless of the precise role of the inter-related variables of wind speed, diffusion, etc., and the resultant atmospheric concentration or the pollutant flux at a given site, the lime papers are exposed in a manner similar to exposed, adjacent vegetation.

No data, other than that of ROBINSON (1957), have been found in the literature which attempts to relate the fluoride concentrations in the exposed lime papers to known concentrations of atmospheric fluorides in experimental chambers. This present paper reports some statistical relationships which have been found between lime paper fluoride levels and experimental HF atmospheric concentrations at constant air flow rates. These relationships are stated as a function of an exposure factor expressed as a time-concentration product. No direct information is yet available to relate atmospheric concentration and wind speed with fluoride pickup by limed papers.

MATERIALS AND METHODS

The lime-impregnated papers were prepared by dipping Whatman No. 2, 11·0 cm. filter paper in a lime suspension (10 g./l. of Fisher " low in fluorine " lime). (The use of higher concentrations of lime suspensions will result in treated papers which will " flake off " during storage and exposure.) The wet papers were dried in a large Pyrex tray in a forced-draft oven at 50–60° C. The treated papers, six to a set, were hung

from plastic clothes pins in a phytotron plant growth chamber. These papers were not enclosed in a shelter as would be necessary for outdoor exposure.

The chamber in which the filter papers were exposed had the interior dimensions of 8½ ft. × 5 ft. × 7½ ft. Hydrogen fluoride was introduced into the incoming air duct from a fumigator system similar to that described by HILL *et al.* (1958). The fluoride-containing air stream is then divided into two ducts and each stream passes through a ceiling diffuser grille into a 42·5 ft.³ air space above the chamber. The ceiling of the chamber (the floor of the air space) consists of a perforated masonite (peg board) panel which further diffuses the incoming air into the growth area. The air flow rate in the vicinity of the suspended limed papers was approximately 25 lineal ft. per minute (0·3 m.p.h.). This air flow rate remained constant throughout these studies.

The light intensity at the level of the limed papers was approximately 1500 foot-candles. The light source was comprised of twelve 8 ft, 200 watt VHO fluorescent lamps and six 60 watt incandescent bulbs. The on–off cycle of the lights was automatically controlled by a time clock to yield a daily photoperiod of 13 hours duration. The incoming air conditioning unit controlled the air temperature at 10° C ± 2° for the nectoperiod and 30° C ± 2° for the photoperiod. The relative humidity was 42% ± 3% and 74% ± 3% respectively.

Continuous air samples were obtained by withdrawing room air at the approximate rate of 1 ft³/min through distilled water in a fritted glass absorption system (ADAMS *et al.*, 1952). The air sample inlet was placed in the immediate vicinity of the suspended limed papers. The scrubbing solutions were collected twice daily and titrated with thorium nitrate using Alizarin Red S as indicator (ADAMS and KOPPE, 1956 and SMITH and GARDNER, 1950). The atmospheric fluoride concentration for each sampling period was calculated from the total micrograms of fluoride collected and the total volume of air samples as measured with a dry test flow meter. The results were expressed as μg of fluoride per m³ of air.

VOL. 4 1961

At the end of each lime paper exposure period, the papers were removed from the fumigation chamber, dried for 24 hours at 70° C, weighed, ashed, and distilled by a modification of the WILLARD and WINTER (1933) procedure. The distillates were titrated to a photometric end point using a modification (ADAMS and KOPPE, 1956) of the SMITH and GARDNER (1950) thorium nitrate titration. An equal number of unexposed, lime-treated filter papers were used for a blank analysis. The blank values were subtracted from the exposed values prior to calculation.

For comparison with lime paper indexes, the atmospheric fluoride concentrations for each lime paper exposure period have been expressed as weighted averages. The fluoride concentration in μg/m³ for each discrete air sampling period was multiplied by the total length of the respective sampling period in minutes. The sum of the time-concentration products for each lime paper exposure period was then divided by the total minutes to yield the weighted average.

RESULTS

A total of 23 exposure trials were conducted. Each exposure period was different in duration, thus each trial represented a different exposure index with a somewhat different average atmospheric fluoride concentration for each exposure period. Table 1 gives a tabulation of the data obtained from the 23 exposures.

Linear and curvilinear regression equations were calculated from the relationship

between the exposure indexes and the fluoride accumulated in the lime papers. The curvilinear relationship showed a significant improvement over the linear relationship between the variables, as indicated by the obtained " F " value of 14·99. A logarithmic relationship was not observed.

The correlation between the fluoride accumulated by the lime papers and the exposure indexes is quite high as indicated by the linear and curvilinear r values of +0·946 and +0·969. These r values are well in excess of the 0·549 required for significance at the 1 per cent probability level. These results are summarized in Tables 1 and 2 and are graphically presented in Fig. 1.

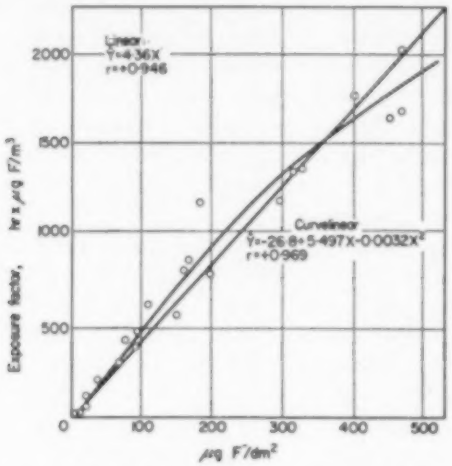

FIG. 1. Limed paper fluorides vs. exposure factors.

From these data it is apparent that there is a high degree of relationship between the fluoride concentration in the atmosphere and the length of the exposure with the fluoride accumulated by the exposed limed papers. In these tests the predicted exposure indexes had a coefficient of variation of ± 10·7 per cent from the measured indexes.

The rate of accumulation of fluoride per unit surface area (both sides) of limed paper exposed was found to range from 3·9 to 30 μg $F^-/dm^2/day/\mu g$ F^-/m^3. The two highest rates of accumulation were associated with average atmospheric fluoride concentrations of 0·04 and 0·14 μg F^-/m^3. The other 21 rates ranging from 3·9 to 8·9 were associated with average atmospheric concentrations between 0·46 and 3·64 μg F^-/m^3.

DISCUSSION

Previously reported studies have shown that a relatively large number of filter paper exposure sites will adequately delineate areas of varying fluoride exposure (ADAMS, 1959; MACINTIRE *et al.*, 1956; MILLER *et al.*, 1953). Not only will the method discriminate between areas of higher and lower exposure intensity, but will reflect major changes in emission rates from known sources within the area of study (ADAMS, 1957.)

The results of the experiment herein reported show that the limed filter paper

TABLE 1. FILTER PAPER TEST DATA

Exposure (Hrs.)	Ave. Air Conc. (μg F^-/m^3	Exposure Factor (μg F^-/m^3) (hrs.)	Filter Paper Conc. (μg F^-/dm^2)	Rate of Fluoride Accumulation μg $F^-/dm^2/day/\mu g$ F^-/m^3
95·0	0·04	3·8.	4·8	30·0
47·8	0·14	6·7	7·8	27·9
72·5	0·46	33·4	12	8·9
46·6	1·4	66·1	24	8·8
67·8	2·0	134·3	22	3·9
118·0	1·8	207·8	36	4·2
168·4	1·8	304·9	68	5·4
112·9	3·6	411·0	91	5·3
221·7	1·9	430·0	82	4·5
263·5	1·9	492·7	96	4·7
225·2	2·6	585·3	150	6·2
270·2	2·4	645·7	110	4·1
292·2	2·8	821·2	199	5·8
359·6	2·3	830·8	160	4·6
364·8	2·4	893·6	165	4·4
486·5	2·4	1157·8	188	3·9
654·6	1·8	1158·7	293	6·0
688·8	2·0	1343·2	316	5·6
726·1	1·9	1357·9	327	5·8
580·0	2·8	1641·5	450	6·6
721·1	2·3	1673·0	468	6·7
642·1	2·8	1772·3	402	5·4
734·6	2·8	2042·0	470	5·5

TABLE 2. COMPARISON OF LINEAR AND QUADRATIC REGRESSION BETWEEN FLUORINE IN LIME PAPER AND ATMOSPHERIC INDEXES

	Linear		Quadratic		
	d.f.	S.S.	d.f.	S.S.	M.S.
Due to Linear Regression (b_1)	1	8,232,293	1	8,232,293	
Due to Quadratic Regression (b_2)			1	202,976	
Total Due to Regression	1	8,232,293	2	8,435,269	
About Regression	21	473,612	20	270,636	13,532
Total	22	8,705,905	22	8,705,905	
r, correlation coefficient		0·946		0·969	
F, value for improvement of fit due to quadratic regression				14·99 *	

* Value of F for 1 per cent significance 8·10.

method may be expected to reflect the exposure intensity within limits of ± 10 per cent.

Studies of the similar lead peroxide method for sulfur dioxide conducted by other workers have shown that the rate of accumulation of SO_2 by lead peroxide is virtually independent of normal changes in humidity of the air, the normal range of wind speeds, concentrations of SO_2 up to 1000 p.p.m. (which is in excess of that normally

VOL. 4 1961

encountered in air pollution studies), etc. The primary source of error introduced by ambient air conditions appeared to involve air temperatures. It was reported that a rise of 10° F increased the reactivity of the treated surface by approximately 2 per cent. Information thus far established for the limed filter paper method is in general agreement with British information developed with the lead peroxide method.

A curvilinear relationship is shown between the exposure index and the level of fluoride accumulated by the exposed paper in this study. This substantiates similar inferences which can be drawn from the data of MILLER *et al.* (1953) which shows that the average fluoride accumulated in 8-week exposures of filter papers was 93 per cent of the total accumulated in two successive 4-week exposures.

These data verify the obvious consideration that the possible number of molecular collisions between the airborne fluoride molecules and the calcium oxide will be decreased as the surface of the treated paper changes from calcium oxide to fluoride. It may be inferred from the data that, up to a concentration in the paper of approximately 200–250 μg F^- per square decimeter, the rate of fluoride accumulation is virtually linear. Above this level of fluoride concentration in the lime papers, the rate of accumulation begins to take on a curvilinear character. Thus should levels exceeding 200–250 μg F^-/square decimeter be found in field studies, the inference would be that a somewhat proportionately higher atmospheric exposure level actually existed than would have been predicted on the basis of a linear arithmetic ratio between sites of higher and lower exposure indexes.

Working in opposition to this trend is the possibility that fluoride is accumulated at a greater rate from absolute air concentrations somewhat below 0·4 μg F^-/m^3. However, this will, undoubtedly, not be observed under many field conditions, since the usually reported low average concentrations are in reality a sampling artifact. This artifact results from the use of sampling techniques which are inadequate to disclose the short term exposure periods of higher concentration produced by meteorological variables. The existence of these artifacts has been demonstrated through development and use of an automatic fluoride analyzer (ADAMS and KOPPE, 1959).

Comparison between the average lime filter paper fluoride collection rates reported by ROBINSON (1957) and the data herein reported show that the calculated average collection rates are of the same order of magnitude even though exposure conditions were somewhat different. Table 3 summarizes the three sets of data.

Although good agreement is shown between ROBINSON's data and the " fumigation chamber " air data herein reported, one may speculate about the cause(s) of the variations in average collection rates obtained. Differences of this magnitude of average

TABLE 3. COMPARISON OF LIMED FILTER PAPER COLLECTION RATES

Exposure Location	Wind Speed (Ave. m.p.h.)	No. of Results	Ave. Collection Rate $\mu g\ F^-/dm/day^2/\mu g\ F^-/m^3$	Range of Exposure Concentrations $\mu g\ F^-/m^3$
Greenhouse Air *	3	11	3·6	0·05–2·1
Outdoor Air *	8	18	8·2	0·14–0·44
Indoor Growth Chamber Air	0·3	23	7·6	0·01–3·6

* Data after ROBINSON (1957)

collection rates, i.e. 3·6 as compared with 7·6–8·2, might possibly result from a spatial relationship which may have existed between the location of exposed filter paper and the nearly point source from which the air samples were obtained in the determination of the air concentration data. No air samples were obtained which related the actual air concentration at the filter paper exposure positions, although it was reported that air samples were independently obtained prior to the exposure of the filter papers indicating that the concentration of fluoride at the greenhouse inlet and outlet were comparable (ROBINSON, 1960). No information is available concerning the comparative density of growing vegetation in the greenhouse during these two samplings.

Dense growing vegetation within the greenhouse could conceivably produce a decrease in the atmospheric fluoride concentration from one end of the greenhouse to the other. Although this may seem doubtful at first glance, marked differences in the foliar fluoride content of greenhouse roses related to the spatial location of the bushes sampled with respect to the alleged source of fluoric contamination have been discovered by the author. HILL *et al.* (1959) also suggests that " abundant vegetation in a chamber may result in differences in the fluoride content of the air in different parts of the chamber ". Tables 4 and 5 give data obtained by the author which relates the

TABLE 4. RELATIONSHIP OF SAMPLE LOCATION TO FOLIAR FLUORIDE CONCENTRATION

House and Bench No.	Rose Leaves p.p.m. F^- (dry wt. basis)
6–2 *	75
5–6	53
3–7	46
3–5	33
2–5	18
2–3	23

* House and benches in order of increasing distance from alleged source.

foliar fluoride content (p.p.m. F^- on a dry wt. basis) of rose leaves of equivalent age and exposed limed filter paper taken from adjacent, interconnected greenhouses with the direction away from the primary alleged source of fluoride located some 3–4 miles away. Adsorption and reaction with the interior greenhouse surfaces also undoubtedly play a significant role in the observed decrease in concentration of atmospheric fluoride through the greenhouse.

Although no air concentration data is directly available to substantiate this rather striking reduction of the foliar and limed paper fluoride level with distance away from the source within the large greenhouse (Table 4), the data indicate that a relatively heavy growth of vegetation and expanse of wall area will effectively remove soluble gaseous air pollutants such as fluoride from a moving flow of air. The air flow through ROBINSON'S greenhouse was reported to be 3 m.p.h., a rate undoubtedly greater than that existing in the greenhouses reported in Table 4. The more rapidly moving air would certainly tend to minimize differences between incoming and outgoing atmospheric fluoride levels, although one is unable to establish the presence or absence of a concentration gradient in this particular instance with the existing data.

Thus, in the absence of evidence to the contrary, one may at least speculate that the

VOL. 4 1961

TABLE 5. RELATIONSHIP OF SAMPLE LOCATION TO LIMED PAPER FLUORIDE CONCENTRATION

House No.	$\mu g\ F^-/dm^2$
6 *	7·6
5	6·4
4	5·0
3	3·6
2	4·8
1	3·8

* Houses in order of increasing distance from alleged source.

lower collection rate which ROBINSON (1957) obtained with the greenhouse-exposed limed papers could be due in part to the existence of lower-than-reported atmospheric fluoride concentrations at the surface of the limed filter papers resulting from removal of the fluoride from the air by the plants growing in the greenhouse.

Although ROBINSON (1957) gave no description of the outdoor exposure conditions, it was subsequently determined that the outdoor samplings were favorably arranged so as to eliminate the possibility for differences in reported and actual air concentrations between the scrubber-type air sampling unit and the exposed filter paper (ROBINSON, 1960).

The possibility for variation between reported and actual atmospheric fluoride concentration was virtually non-existent in the experimental arrangement herein described. The contaminated air entered the plant growth chambers through many small holes in the ceiling and passed down across the suspended filter papers before approaching the surface of the leaves of plants growing on benches 4–5 feet below the air inlet. The inlet of the air sampling tube was at the same level as the filter papers. Thus, conditions for comparison of air concentration and collection were ideal.

It should also be noted that the rate of fluoride collection by the limed filter paper is not a linear function. Thus, differences in observed collection rates could also be partially explained on the basis of possible variations in average atmospheric fluoride levels among these three experimental conditions.

Another source of variation between the exposures of ROBINSON and those herein reported involves the differences in type of atmospheric fluorides being used. ROBINSON (1957) exposed his limed paper to an industrial source of fluoride of unstated molecular composition(s). Hydrofluoric acid was used as the fluoride source in these present studies. No information is available which relates the limed paper collection efficiency for HF vs. the unknown gaseous and/or particulate fluorides of ROBINSON's experiments.

In view of the general agreement obtained between ROBINSON's average collection rates and the average collection rate herein reported, and considering the uncertainties involved in the " greenhouse " exposures, the non-linear collection rate, the widely varying rates of air flow and the unknown heterogeneous character of the fluoride-containing pollutant, the range of average collection rates thus far reported does not appear to indicate the existence of any serious shortcoming attributable to the lime paper survey method *per se*.

CONCLUSIONS

Based on the data thus far reported by the various investigators, the lime paper technique may be used with reliability and low cost (*a*) to delineate areas of fluoride pollution (*b*) to determine the relative intensity of pollution between exposure sites within a given area, (*c*) to reflect changes in pollution intensity which may occur as the result of installation of fluoride fume controls at a source, or (*d*) to indicate the relative contribution of a newly established source of fluoride contamination.

Success in the application of this method will be dependent upon (i) exposing the limed papers in adequate shelters to protect them from rain-leaching or extraneous deposits, (ii) using lime suspension below 10 g/l CaO to prevent flaking off of lime during exposure, (iii) selecting exposure sites according to the best known and published site selection criteria, and (iv) having an adequate number of exposure sites to represent the study area.

Acknowledgements—The author is indebted to T. S. Russell for assistance in statistical analysis and Julia Jowders for chemical analysis of samples for fluoride content. Appreciation is also expressed to D. A. Thomas and V. L. Miller for helpful suggestions and critical review of the manuscript.

REFERENCES

Adams D. F. (1957) Further applications of the limed filter paper technique in fluorine air pollution studies. *APCA J.* **7,** 88–91.

Adams D. F. and Koppe R. K. (1956) Effect of pH on high-salt-thorium fluoride titration. *Anal. Chem.* **28,** 116–117.

Adams D. F. and Koppe R. K. (1959) Automatic atmospheric fluoride pollutant analyzer. *Anal. Chem.* **31,** 1249–1254.

Adams D. F., Mayhew D. J., Gnagy R. M., Richey E. P., Koppe R. K. and Allen I. W. (1952) Atmospheric pollution in the ponderosa pine blight area. *Ind. Eng. Chem.* **44,** 1356–1365.

Hill A. C., Transtrum L. G., Pack M. R. and Winters W. S. (1959) Facilities and techniques for maintaining a controlled fluoride environment in vegetation studies. *APCA J.* **9,** 22–27.

MacIntire W. H., Hardison M. A. and McKenzie D. R. (1956) Spanish moss and filter paper exposures for detection of air-borne fluorides. *J. Agric. and Food Chem.* **4,** 613–620.

Miller V. L., Allmendinger D. F., Johnson F. and Polley D. (1953) Lime papers and indicator plants in fluorine air pollution studies. *J. Agric. and Food Chem.* **1,** 526–529.

Robinson E. (1957) Determining fluoride air concentrations by exposing limed filter paper. *Amer. Ind. Hyg. Assoc. Quart.* **18,** 145–148.

Robinson E. (1960) Personal communication.

Smith F. A. and Gardner D. F. (1950) A comparison of the thorium nitrate back-titration and the salt-acid thorium titration for the determination of fluoride. *Arch. Biochem.* **29,** 311–314.

Willard H. H. and Winter O. B. (1933) Volumetric method for determination of fluorine. *Ind. Eng. Chem., Anal. Ed.* **4,** 7–11.

Wilsdon B. H. and McConnell F. J. (1934) The measurement of atmospheric sulphur pollution by means of lead peroxide. *J. Soc. Chem. Ind.* **53,** 385-T.

VOL. 4 1961

Int. J. Air and Water Poll. Pergamon Press 1961. Vol. 4, Nos. 3/4, pp. 256–266. Printed in Great Britain.

BACTERIAL INDICATORS OF POLLUTION IN HOUSEHOLD WELL WATERS*

F. Rosenberg, N. Dondero and H. Heukelekian

VARIATIONS IN COUNTS OF COLIFORMS, ESCHERICHIA AEROBACTER AND ENTEROCOCCUS OVER A YEAR

Individual household well waters are used as a source of drinking water by approximately 47 million people. The fact that treatment and quality control of these waters is restricted by lack of satisfactory low-cost equipment raises the question of whether it is feasible to maintain standards developed for the control of bacteriological quality of municipal water supplies.

Since the coliform test, which is generally used in the bacteriological analysis of community drinking water supplies, has certain limitations in evaluating recent fecal pollution, it is questionable as to whether it should be directly applied to the well water supplies of individual households. Although there has been considerable interest in the establishment of a procedure in which an organism of fecal origin would be used as an indicator of pollution, such a procedure has been complicated by problems in isolation, as well as by the limited presence of a number of these organisms outside the body. Of the organisms under consideration, *Escherichia* coli and the enterococcus group have been the most promising. Both are of intestinal origin and do not appear to proliferate outside their normal environment. The development of new techniques, such as membrane filtration, has decreased the time required for their isolation and has led to numerous comparative studies of their occurrence in polluted waters of various origins. However, the estimation of similarities and differences of numbers and occurrence of these indicator organisms in regard to pollution in well waters has been limited and generally confined to studies of short duration.

The present study was initiated to determine the relationship between these organisms throughout a year, and to ascertain whether a relationship exists between *Escherichia*, enterococci, *Aerobacter*, and coliforms as determined by the five-tube dilution standard method and the following factors:

(1) precipitation,
(2) the presence of anionic detergents in the water,
(3) depth and temperature of the well water,
(4) type and construction of the well.

Description of Wells

In the first of two surveys basic data was collected from two wells, each of which served a single family from January to December 1959; a third well was added to the study in May 1959 and was sampled until January 1960. A second survey studied a community of 100 wells in Middlebush, New Jersey; it was undertaken in March 1959 and again in August of the same year; results of this second study will be reported in a subsequent paper.

* Paper of the Journal Series, New Jersey Agricultural Experiment Station, Rutgers, the State University of New Jersey, Department of Sanitation, New Brunswick, N.J.

From an extensive preliminary study of wells in the Middlebush and North Brunswick, N.J. areas, two wells, located in different strata, which had shown pollution over a period of time were chosen. The first, an unlined dug well, slightly over 13 feet deep and located in unconsolidated clayey sand will be designated by the letter (V). A tile pipe, 6 inches in diameter, extended 1 foot above the ground, its opening protected by a large tin can. Behind the house and some 50 feet north of the well was a septic tank, the drainage field of which extended away from the well in a northeasterly direction.

The second, a drilled well, 175 feet deep and located in a red shale formation, will be designated by the letter (B). A pump, supplying a 120-gallon pressure tank was directly over the well in the cellar. The 6-inch casing pipe projected about 6 inches above the bottom of a 3-foot square sump, the latter covered by a concrete slab. Although earlier studies had been made on this well by VOELKER (1953), it is no longer possible, since the casing is now sealed, to obtain temperature or depth measurements. The septic tank was 50 feet west of the well and drainage from the tank was in a northwesterly direction away from the well.

An artesian well which previous studies had shown free of pollution, was also studied. This well (designated (C)) was 75 feet deep and in a shale formation. Study of this well was continued in order to determine whether seasonal variations in the number of pollution indicator organisms would occur in a " clean " well.

At the (V) and (C) wells samples were taken in sterile bottles from kitchen taps, and at the (B) well from an outside tap. Temperature and rainfall data were obtained from the monthly United States Weather Bureau reports at New Brunswick. Well temperature readings were made with a thermometer on samples brought to the surface in a metal container. Depth of the water surface was determined by lowering a conductivity device (VOELKER, 1953).

VOL. 4 1961

Bacteriological Methods

Well water samples were analyzed for the presence of coliforms, enterococci, and anionic detergents. Bacteriological analyses were initiated within 3 hours after collection. Coliform analyses were performed according to the procedures described in STANDARD METHODS (1955). In the presumptive test five 10-ml, five 1·0-ml, five 0·1 ml and five 0·01-ml portions were planted in lactose broth and incubated at 37° C for 48 hours. In all cases where gas production occurred within this period, 1-ml portions were transferred to brilliant green bile broth. Evidence of gas formation within 48 hours at 37° C verified the presence of coliforms. The Most Probable Number of coliform organisms per 100 ml was obtained from the (MPN) table given in STANDARD METHODS (1955).

The membrane filter technique FLYNN *et al.* (1958) was used in conjunction with the MPN test in order to: (1) correlate results of the two methods, and (2) determine the number of *Escherichia* and *Aerobacter* organisms present in the sample. Enterococcus determinations were performed solely by means of the membrane filter technique. Membrane culture media were obtained from Baltimore Biological Laboratories.

One hundred ml, 10-ml, 1-ml, and 0·1-ml portions were filtered, the initial one without dilution, the others brought up to 100-ml volume with sterile buffer prior to filtration. Filter membranes were incubated 2 hours at 37° C on pads saturated with M-EHC enrichment broth, after which they were transferred to pads with B-EMB broth and incubated for 18 to 20 hours more.

For the enumeration of enterococci, membranes after filtration of various volumes of the sample were initially incubated at 37° C on absorbent pads containing dextrose broth. After 2 hours the membranes were transferred to pads containing sterile M-Slanetz enterococcus broth, to which 0·01 per cent previously sterilized triphenyl tetrazolium chloride had been added aseptically, and reincubated for an additional 42 ± 2 hours.

High humidity was maintained throughout all incubations by wrapping the petri dishes in moist towels and placing trays of water in the incubator.

After incubation, membranes were examined with a dissecting microscope at magnifications of from 10x–60x. Colonies of Aerobacter appeared mucoid and orange-brown. Generally they were 4–6 mm in diameter, raised, and convex.

Escherichia colonies, on the other hand, were almost always smaller than those of *Aerobacter*. They had dark, almost black, centers, and manipulation of the petri plates to catch the light revealed a greenish metallic sheen.

The enterococcus colonies appeared either glistening, dark red with a pink periphery, or a light pink in color with a rather flat appearance, in agreement with the results of SLANETZ and BARTLEY (1957).

Citrate Utilization. Thirty-two colonies which showed typical *Escherichia coli* characteristics on membrane filters, as described above, were collected over a period of time and tested for their ability to utilize citrate as a sole source of carbon. *Escherichia freundii* and *intermedium*, colonies of which may be confused with *E. coli*, are generally found in soil and water; those bacteria utilize citrate as a sole carbon source whereas *E. coli* does not. Colonies were picked to tubes of Koser's citrate medium. Cultures remaining clear after incubation at 37° C for 36 hours were considered as having originated from *E. coli* colonies.

Soil Samples. Samples of soil obtained from the vicinity of the wells, septic tanks and drainage fields, were analyzed to determine the presence of enterococci, *Escherichia* and *Aerobacter*. Samples of 16 g to 60 g of soil were taken at various times during the study by scraping away the top layer and scooping soil into a sterilized beaker with a sterilized spatula.

The soil was suspended on 100 ml of sterile buffer and shaken for 15 minutes on a Burrell wrist action shaker. Dilutions ranging from one-tenth to one ten-thousandth were prepared, filtered through the membrane filter apparatus, cultured, and incubated as noted above.

Detergent Analysis.

The presence of anionic detergents was determined by the method of DEGENS *et al.* (1953), commonly referred to as the Chicago Method. The principle of the method is that sulfonated or sulfated surface active materials form a blue complex with methylene blue, which is soluble in chloroform. The percentage of detergent may be calculated by measuring the optical density of the extracted solution and comparing with a standard curve.

Statistical Analyses

An analysis of factors influencing the numbers of enterococci found in well (B) was made with the aid of an IBM 650 calculator, using the WOLONTIS (1956) Program.

A similar analysis on the well V was not feasible because of the infrequency of enterococcus isolations.

Chi-square tests were made to determine relationship between other variables.

In the determination of geometric averages, where " less than one " organism was isolated, a logarithmic value of zero was assigned.

RESULTS

Most Probable Number of Coliforms

Seventy-five samples from well (V) were analyzed for coliform density. There was a range of 0–35,000 coliforms per 100 ml. The geometric average for the year was 89 coliforms per 100 ml.

Seventy-three samples from well (B) had a range of 0–18,000 coliforms per 100 ml and the geometric average for the year was 140 per 100 ml.

Twenty-seven analyses of well (C), of which 9 were positive, were made between May, 1959 and January 1960. The MPN never exceeded 5 per 100 ml.

Weekly geometric averages for wells (V) and (B) are plotted in Figs. 1 and 2. The corresponding figures for well (C) were not plotted because of the low values.

An evaluation of MPN data for the year tends to confirm VOELKER's (1953) findings in that the count of the deep well (B) conformed more closely to a basic season trend than did the count from the shallow well; both wells showed a rise in the number of coliforms from a minimum in January to a peak in July and August, thereafter well (B showed a gradual decrease, but the shallow well (V), after reaching a sudden peak

VOL. 4 1961

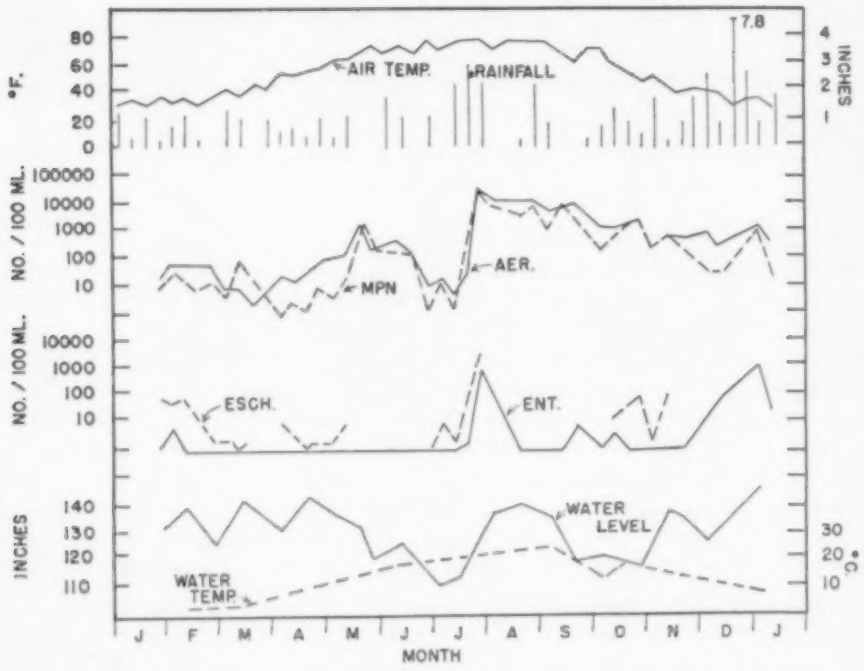

FIG. 1. Variation in bacterial indicators, well characteristics and climatic conditions in shallow dug well (well (V)) in unconsolidated formation.

in July, showed a period of low numbers. This July peak of well (V) corresponded to a heavy rainfall of more than 7 inches; there was a general decline in coliforms from this point to the end of the sampling period in January. Heavy precipitation during the latter part of December again corresponded with a significant rise in organisms. In well (B) also, increased numbers of coliforms corresponded with the July rainfall. Throughout the course of the study well (C), used as a control to determine whether a well having no pollution in the Spring would exhibit seasonal variation, showed no significant changes in coliform density.

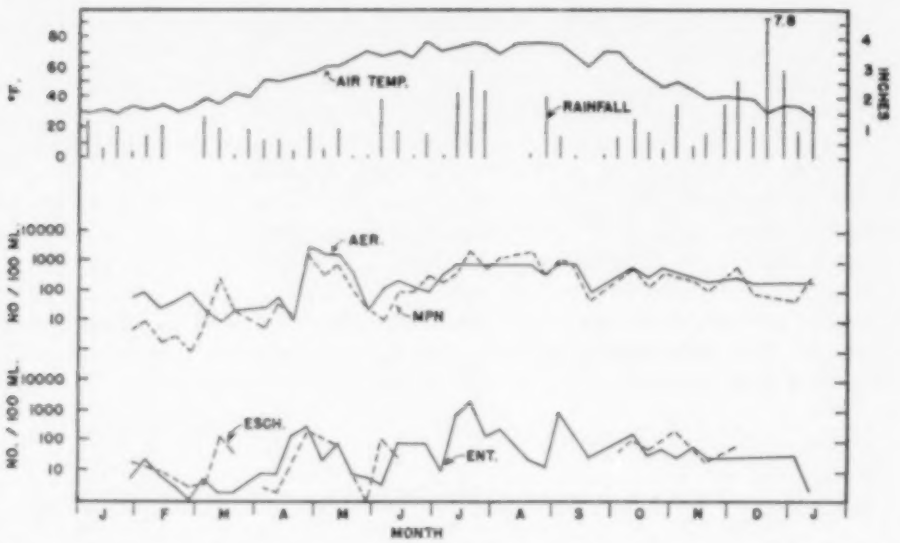

FIG. 2. Variation in bacterial indicators and climatic conditions in deep-driven well (well (B) in shale.

Escherichia and Aerobacter Species

In the Spring of 1959 it became apparent that a situation existed which prevented accurate quantitative determination of Escherichia by the membrane filter method. In many samples, Escherichia colonies could not be counted in 100-ml or 10-ml samples because the membranes on M-EMB medium became completely overgrown with other colonies. Smaller portions of the samples were then negative for Escherichia. Thus, for example, the absence of Escherichia in a 100-ml portion of the sample merely indicated that 0–99 organisms may have been present in the original 100-m. portion. As a result, accurate averages were not obtainable.

Weekly geometric averages of Aerobacter values for wells (V) and (B) are plotted it Figs. 1 and 2. Specific values from Escherichia determinations are also given to show the trend inherent during the year. The discontinuities of the Escherichia curve were caused by the inability to calculate average values for the overgrown samples.

Seventy samples were analyzed for Escherichia and Aerobacter using the membrane filter technique.

In the seventy samples from well (V), the range of Aerobacter was 0–42,000 per 100 ml; the geometric average for the year was 180 per 100 ml.

The range in seventy-five samples in well (B) was 7–6600 aerobacter, per 100 ml; the geometric average for the year was 250 per 100 ml.

Escherichia was never isolated from samples from well (C). Twenty-seven analyses ranged from 0–13 Aerobacter per 100 ml. The geometric average was 1·5 Aerobacter per 100 ml.

Of thirty-two typical Escherichia colonies picked from M-EMB pads, 16 each from wells (B) and (V), only two colonies from each well were able to utilize citrate in Koser's medium, indicating a preponderance of intestinal Escherichia.

A comparison of MPN values and Aerobacter numbers determined by membrane filtration shows a rather close correspondence; where available, Escherichia values showed similar trends.

Enterococci

Weekly averages for enterococcus counts for wells (V) and (B) are plotted in Figs. 1 and 2.

Seventy-two samples from well (V) were analyzed for enterococci; 47 were negative. Between February 12 and July 22, enterococci were isolated from this well only 3 times. The range from 0 to 950 per 100 ml; the average was 2·4 per 100 ml for the year.

In well (B), 70 of 71 samples contained enterococci. Numbers per 100 ml ranged from 0–6,100; the average for the year was 35 per 100 ml.

Ten of 27 samples in well (C) contained enterococci which ranged from 0–48 per 100 ml, the average value obtained from the data for the year being 1·8 per 100 ml. Of the total of 110 enterococci, 82 per cent appeared between July 16 and September 5.

VOL. 4 1961

Statistical Analysis

A statistical analysis of factors affecting variance in counts was undertaken using the WOLONTIS (1956) program and the model 650, International Business Machines calculator.

The initial analysis was designed to detect whether any of the following factors exerted an influence on the variance in numbers of enterococci:

(1) minimum daily temperature;
(2) average monthly temperature;
(3) rainfall on day prior to sampling;
(4) rainfall on day of sampling;
(5) amount of detergents on day of sampling;
(6) amount of detergents in previous sample;
(7) Most Probable Number of coliforms.

Results obtained are shown in Table I.

The *F* value is the ratio of one random variance to another. It is defined as the estimated variance between groups divided by the estimated variance within groups. If the means of groups differ significantly among themselves, they show more variation than can be attributed to random sampling. A value of *F* less than the value given at the probability level in Table 1, could happen by chance with the designated probability.

The results in Table 1 can be interpreted to mean that there was a high degree of

Table 1. Correlation of climatic conditions, detergents and MPN with the enterococcus count in well (B)

Factor	F* Ratio
Minimum daily temperature	0·05
Average monthly temperature	0.5
Rainfall on day prior to sampling	25
Rainfall on day of sampling	7
Detergent content on day of sampling	1·2
Detergent content of previous sample	1·8
MPN	3

* *F* ratio of 2·84 for 10 per cent probability level
F ratio of 4·08 for 5 per cent probability level
F ratio of 7·31 for 1 per cent probability level

probability that the enterococcus count in well (B) was correlated with recent rainfall and with the MPN, but not with temperature or detergent concentration.

The enterococcus count in well (V) remained at or near zero for the first six months of the year. In mid-July after a heavy rain, the MPN, Aerobacter, Escherichia and enterococcus counts all reached their highest values. Enterococcus counts fell rapidly whereas the other organisms decreased at a much slower rate. In early January, after heavy precipitation, MPN and enterococcus counts again reached a peak.

Total Count on M-EMB Medium

The variations in total numbers of organisms growing on M-EMB medium are plotted in Fig. 3. By comparison with the rainfall chart, it can be seen that the total count peaks are closely associated with periods of much precipitation.

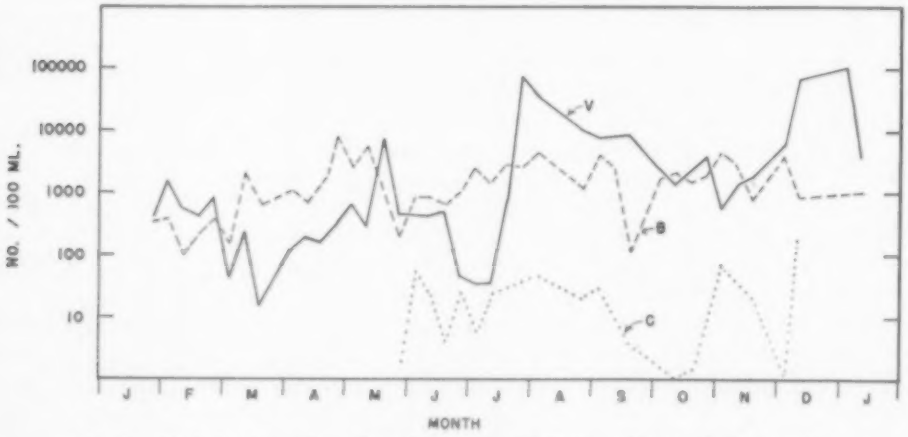

Fig. 3. Variation in total number of organisms M-EMB medium in the three wells.

Soil Sample Analyses

Eleven soil samples, some from each well, were analyzed for pollution indicator organisms in an effort to determine whether pollution appeared to be entering through the soil. The results of the soil analyses are summarized on Table 2. It can be seen

TABLE 2. ANALYSIS OF SOIL SAMPLES FOR POLLUTION INDICATING ORGANISMS

Date	Source and Location	Sample Size	Numbers per Gram		
			Aerobacter sp.	*Escherichia* sp.	Enterococci
July 22	(C)—Septic tank	60 g	17	less than 1 in 1/1000 dil.	5
July 27	(V)—Well	40 g	420	less than 1 in 1/10,000 dil.	110
July 29	(V)—Septic tank	32 g	less than 1 in 1/1000 dil.	less than 1 in 1/1000 dil.	less than 1 in 1/100 dil.
July 31	(V)—Septic tank towards drainage field	28 g	250	less than 1 in 1/1000 dil.	71
July 31	(V)—Well towards drainage field	23 g	830	less than 1 in 1/1000 dil.	35
Aug. 28	(C)—Well	23 g	87	less than 1 in 1/1000 dil.	less than 1 in 1/100 dil.
Aug. 28	(V)—Well	26 g	420	less than 1 in 1/1000 dil.	less than 1 in 1/1000 dil.
Aug. 28	(B)—Well	16 g	190	less than 1 in 1/1000 dil.	less than 1 in 1/100 dil.
Oct. 5	(B)—Well	18 g	56	less than 1 in 1/1000 dil.	280
Oct. 7	(B)—Septic tank	26·5 g	less than 1 in 1/1000 dil.	less than 1 in 1/1000 dil.	less than 1 in 1/1000 dil.
Oct. 15	(V)—Well— 1 ft depth	35 g	3	less than 1 in 1/100 dil.	less than 1 in 1/100 dil.
	Well— 3 ft depth	39 g	3	less than 1 in 1/100 dil.	less than 1 in 1/100 dil.

that the potential for contamination from surface washings, in terms of presence of Aerobacter, was high for all three wells, indeterminate for Escherichia because of the unsuitable dilutions employed, and, for enterococci, probably as high as for Aerobacter.

VOL. 4 1961

Anionic Detergents

The presence of anionic surface active agents was determined in all three well waters. A comparison of results in the three wells is shown in Fig. 4.

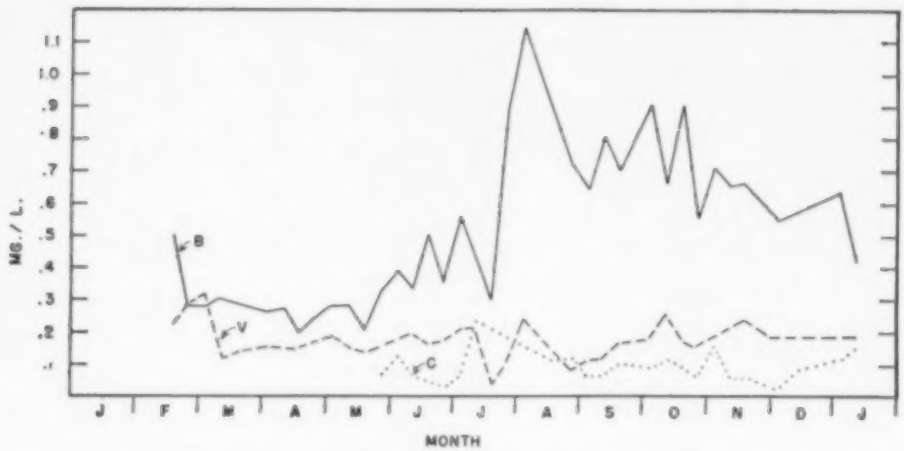

FIG. 4. Variation in concentration of anionic detergents in the three wells.

FLYNN *et al.* (1958) reported that the presence of synthetic detergents in well waters was a direct result of pollution by household sewage discharges. Since most household synthetic detergents are the anionic type, the Chi square test was performed to determine if a positive correlation existed between bacterial contamination and the presence of anionic detergents. No such correlation was found. Results are summarized in Table 3.

DISCUSSION

From the foregoing results, it appears that recent rainfall is closely associated with an increase in numbers of pollution-indicator organisms in the wells which were studied. The shale strata around well (B) allow pollution to enter throughout the year; in summer, pollution is accentuated by heavy rainfall. In well (V), in sandy soil Aerobacter and MPN values are at a somewhat lower level during the summer months, but increase rapidly in response to rainfall. In both wells, enterococci seem less persistent in numbers and very responsive by increase in numbers to rainfall.

It may be observed that the number of aerobacter organisms, by the membrane filter method, generally exceeded the coliform MPN in 68 per cent of cases in well (B), in 73 per cent in well (V), and in 57 per cent in well (C). Aerobacter made up the majority of coliform bacteria in the sample. Since Aerobacter is not generally considered to indicate recent fecal pollution, the value as a pollution indicator of household well waters appears to be limited. *Escherichia coli* and enterococci, both being of fecal origin constitute appropriate indices of pollution. Enterococci were generally found in conjunction with *E. coli* especially when the latter were present. Enterococci alone were sometimes isolated in the absence of *E. coli*, both by virtue of the actual absence of *E. coli* and in cases when *E. coli* was overgrown on M-EMB medium. It

TABLE 3. SUMMARY OF CORRELATION ANALYSES

Variables Tested	χ^2 Value*	
	(V)	(B)
Aerobacter Count and MPN	23·5	3.7
Enterococcus Count and Aerobacter Count	3·3	7·4
Enterococcus Count and MPN	4·7	3†
Total Count and Aerobacter Count	33·5	23·3
Total Count and Enterococcus Count	19·9	13·3
Total Count and MPN	24·4	32·3
Precipitation on Day of Sampling & Aerobacter	14·6	0·2
Precipitation on Day of Sampling & MPN	9·2	3·9
Precipitation on Day of Sampling & Enterococcus	10	7
Precipitation (day-1) and Aerobacter	11·1	0·2
Precipitation (day-1) and MPN	2·4	0·5
Precipitation (day-1) and Enterococci	9·0	25‡
Water Level and Aerobacter	2·8	—
Water Level and Enterococci	2·1	—
Water Level and MPN	1·3	—
Water Temperature and Aerobacter	0·9	—
Water Temperature and Enterococci	3·1	—
Water Temperature and MPN	7·2	—
Detergent Conc. and Aerobacter	2·9	2·0
Detergent Conc. and Enterococci	2·9	1·2†
Detergent Conc. and MPN	5·1	9·9

* 5 per cent probability level, $\chi^2 = 9{\cdot}49$

† ($F = 4{\cdot}08$) Where F value is given, analysis of variance was calculated and F value is given at 5 per cent probability level.

‡ ($F = 2{\cdot}84$).

may thus be concluded that (*a*) culturing enterococci is more sensitive and more selective than culturing Escherichia and (*b*) enterococci are more indicative of fecal pollution than Escherichia.

The membrane filter technique has made easier the estimation of numbers of enterococci than of *E. coli*.

The citrate utilization tests reported here showed that strains of non-fecal Escherichia growing on M-EMB medium were counted as *E. coli* when more complete identification was lacking.

The presence of both Escherichia and enterococci is an indication of recent fecal pollution, as in the presence of Escherichia alone. The absence of enterococci, however, has not been acceptable as the sole criterion of freedom from pollution.

A summary of correlation analyses by the χ^2 method for several combinations of variables for wells (B) and (V) is given in Table 3. χ^2 values above 9·49 indicate positive correlation with only 5 per cent probability that the results were due to chance.

It should be noted that all variables were not related in the same way in both wells. The variables showing positive correlation in both wells were: total count on M-EMB medium with Aerobacter, enterococcus, and MPN values; and precipitation on the day of sampling with enterococcus values.

An analysis to determine the correlation of water level and water temperature with bacteriological quality in well (V) showed no statistically valid results.

VOL. 4 1961

The relationship of enterococcus levels with Escherichia numbers was not calculated for the wells in this study, but will be presented in a second report covering a survey of 100 wells in one community.

SUMMARY AND CONCLUSIONS

One well, situated in sandy soil, and two deep drilled wells, situated in shale, were sampled twice a week for a year, and the most probable numbers of coliforms and the numbers of Aerobacter, Escherichia and enterococci were determined, along with collateral information on rainfall, temperature, level of water in the well and detergent concentrations.

The following conclusions were reached from statistical analysis of the data:

1. *Aerobacter* counts and MPN values increased simultaneously in a shallow dug well in sandy soil (well (V)), but not in a deep-drilled well in shale strata (well (B)).

2. No correlation was shown between numbers of enterococci and either *Aerobacter* or the MPN in the shallow well. In the deep-drilled well, there was no correlation between numbers of enterococci and *Aerobacter*, though for enterococci and the MPN the correlation was slightly less.

3. " Total count ", as determined by the number of organisms growing on M-EMB medium, increased together with *Aerobacter*, enterococcus and MPN values in both wells.

4. Increases in numbers of *Aerobacter*, enterococci, and the MPN in the well (V), as well as enterococci in well (B), were associated with rainfall on day of sampling. No correlation between MPN, *Aerobacter*, and rainfall on day of sampling was found to be present in well (B).

5. No correlation was shown between the MPN and rainfall one day prior to sampling in well (V), nor between *Aerobacter* and MPN values and rainfall one day prior to sampling in the well (B). An increase in *Aerobacter* and enterococci in well (V) was evident. In well (B), enterococcus values were higher than when rain fell on the day of sampling.

6. Water level and temperature in well (V) had no effect on the number of enterococci, *Aerobacter*, and the MPN value.

7. The detergent concentration in the wells showed no valid correlation with the numbers of *Aerobacter* or enterococci in either well.

MPN values increased with increasing detergent concentrations in the well (B). This was not the case in well (V).

Acknowledgement—The study reported herein was supported by a grant from the United States Public Health Service, Division of Research Grants.

REFERENCES

Degens P. N., van der Zee H. and Kommer J. D. (1953) Anionic Syndets in Amsterdam Sewage. *Sewage and Ind. Wastes*, **25**, 20.

Flynn J. M., Andreoli A. and Guerrera A. A. (1958) Study of Synthetic Detergents in Ground Water. *J. Am. Water Works Assoc.*, **50**, 1551.

Slanetz L. W. and Bartley C. H. (1957) Numbers of Enterococci in Water, Sewage and Feces Determined by the Membrane Filter Technique with an Improved Medium. *J. Bacteriol.*, **74**, 591.

Standard Method for the Examination of Water, Sewage and Industrial Wastes (1955) Tenth Ed., *Am. Public Health Assoc.*, New York.

Voelker R. A. (1953) Factors Affecting the Bacteriological and Chemical Quality of Private Home Well Waters in New Jersey. Thesis, Rutgers University.

Wolontis Z. M. (March, 1956) IBM Applied Science Division, Technical Newsletter No. 11.

Int. J. Air and Water Poll. Pergamon Press 1961. Vol. 4, Nos. 3/4, pp. 267-271. Printed in Great Britain.

ABSTRACTS OF PAPERS PUBLISHED IN *STAUB*

Second Quarter 1960

Developments and New Publications in Comminution Technology. D. BEHRENS. (Karlsruhe: Institut für Mechanische Verfahrenstechnik an der Technischen Hochschule.) *Staud*, vol. 20, pp. 101–8, 83 Refs.

A comprehensive review of recent industrial developments and of publications in this field during the past two years.

New Edition of the " V.D.I. Recommendations for particle Size Determination for Technical Dusts ". R. NAGEL. (Offenbach/Main.) *Staub*, vol. 20, pp. 109–12, 3 Refs.

The suggestions in the new " V.D.I. Richtlinien " should make particle size determinations from various laboratories directly comparable.

The Prediction of Overall Efficiencies of Mechanical Dedusting Plant. W. SOLBACH (Lübeck). *Staub*, vol. 20, pp. 113–17, 9 Refs.

The author argues that in his experience, a size cut based on a mean equivalent particle sedimentation rate, affords a better description of cyclone efficiency than the commonly used grade efficiency curves. Small scale experiments on the dusts to be collected are essential as effective particle sizes and agglomeration during collection cannot be accurately predicted.

VOL.
4
1961

Radioactive Aerosols in the Atmosphere. Prof. J. A. SCHEDLING, (Vienna: Physikalisches Institut der Universität). *Staub*, vol. 20, pp. 139–44, 19 Refs.

The various sources of fallout arising from nuclear explosions are reviewed. The author then describes a unit in which air is sampled continuously for 3 or 6 hours before being automatically moved to an activity detection and recording counter. The Sr-90 content and the gamma-spectrum of the samples were measured.

Photometric Determination of Konimeter and other Dust Samples. G. BROOMHEAD, J. R. HODKINSON and Dr. V. SIMMONS (Sheffield: Safety in Mines Research Establishment, Ministry of Power, and the University of Sheffield Mining Department). *Staub*, vol. 20, pp. 144–50, 38 Refs.

Light-field microscope images of konimeter samples of airborne dust were evaluated both by light extinction and by particle counting. Since most of the scattered light was collected, the results depend on absorbtion in the particles. Measurements of scattered light in dark-field images are easier to make, but are more difficult to interpret. They may be used, with an empirical calibration, for dusts of much the same size. In the Tyndalloscope, the light scattered per unit area of black and transparent particles appears to be in the ratio theoretically predicted. Narrow-angle extinction measurements on size selected samples offered the best possibility of surface area determination independent of particle transparency. Supplementary measurements of light scattering through a definite moderate angle then estimated the transparency of the particles.

Konimetric Measurement of the Photometric Dust Concentration. Dr. R. ROEBER (Berlin: V.E.B. Wissenschaftlich Technisches Büro für Gerätebau, Institut für Regelungstechnik). *Staub*, vol. 20, pp. 150–5, 12 Refs.

Photometry by absorbtion measurements is recommended as the most suitable technique for konimeter samples. Details of the technique are given and the limits of accuracy of the experimental data are discussed.

The Measurement of Dusts at the Place of Work and Its Importance to Industrial Hygiene. Prof. A. WINKEL (Bonn: Staubforschungsinstitut der gewerblichen Berufsgenossenschaften, e. V.). *Staub*, vol. 20, pp. 156–60, 13 Refs.

Comparisons of the various methods of measuring dusts (size and concentration) at a place of work by konimeter, thermal precipitator and gravimetric filter apparatus are made. A simple formula is given, which will assess the silicosis hazard from particle counts and from free silica content.

Asbestos Types; Their Investigation by Optical Means and Their Pathological Action. Prof. K. G. SCHMIDT (Bonn: Staubforschungsinstitut der gewerblichen Berufsgenossenschaften, e. V.). *Staub*, vol. 20, pp. 173–80, 43 Refs.

Microscopic phase contrast and polarization techniques lead to the ready identification of eleven types of asbestos. The author suggests that the highly dangerous nature of chrysotile asbestos, amosite and crocidolite is probably due to their soft, pliable fibres entering the alveolar tracts more easily than the hard, needlelike fibres of tremolite and anthophyllite. However, until more is known about the pathological action of these latter asbestos types, they should, in practice, all be considered dangerous.

Particle Size Analysis Using the Slit Ultra-Microscope. Dr. J. OLAF (Essen: Bergbau-Forschung G.m.b.H., Forschungsinstitut des Steinkohlenbergbauvereins). *Staub*, vol. 20, pp. 180–3, 16 Refs.

The particle sizes and concentrations of coal mine dusts have been determined with the slit ultramicroscope using dark-field illumination. The smallest particle that can be measured is 0·2 microns. The individual determinations are fast and can be carried out at the source of the dust. However, to obtain reasonable accuracy, large numbers of measurements are required for statistical evaluation. Moreover, the photographic recording technique has other inherent sources of error, and is time consuming.

Scintillation Spectral Analysis for Aerosols. B. BINEK (Prague: Institute for Physical Chemistry of the Academy of Science). *Staub*, vol. 20, pp. 184–5, 2 Refs.

A spectrometer is briefly described in which aerosol particles can be counted and sized at rates up to 6000 particles per minute.

Third Quarter 1960

The disturbance of sedimentation analyses due to the flow around obstructions in sedimentation vessels.

Dr. W. KAST (Walsum: Laboratorium für Staubphysik und Messtechnik der Bergwerksgesellschaft Walsum m.b.H.). *Staub*, vol. **20**, pp. 205–211, 10 Refs.

In using the conventional Andreasen pipette or the sedimentation balance errors occur because of the flow around the collection tube of the former or the collection pan of the latter. After theoretical and experimental investigation, minor structural modifications which will reduce these errors are suggested for both instruments.

A new method for dust concentration measurements using the deposition of dust in a flow chamber with ionizing radiations.

Dr. D. HASENCLEVER (Bonn: Staubforschungsinstitut.) and H. C. SIEGMANN (München). *Staub*, vol. **20**, pp. 212–218, 14 Refs.

Dust concentrations are measured by passing dust-laden gases through a cylinder in which radiations from a radioactive source (a radium compound) are present. The ionization current from the source passing through dust free air (I_0) is compared electrically to the current passing through the dusty air (I_{st}). The dust concentration is found to be proportional to the logarithm of I_0/I_{st}, and if the average particle size is known, the particle concentration can be obtained. Details of the apparatus and of some initial experimental results are given.

Rationalization of the photometric evaluation of mine konimeter samples by apparatus modification and the the addition of a mechanical computer.
Dr. H. MERTENS (Unna-Königsborn: Klöckner-Bergbau Königsborn-Werne AG.). *Staub*, vol. **20,** pp. 218–220, 1 Ref.

August Edition: Combined conference of the VDI Technical Group on Dusts, the Austrian Engineers and Architects Association and the Austrian Dust (Silicosis) Control Office, Held in Vienna, 4–6 May, 1960. The theme of the conference was: *Trends in the Development of Dust Measurement:* Group I: *Dust Concentration Measurements.* Introduction: P. NOSS, (Essen), *Present position of dust measuring techniques. Staub*, vol. **20,** pp. 243–244.

Dust deposition in thermal and pressure gradients.
Prof. G. STETTER (Vienna: Physikalisches Institut der Universität). *Staub*, vol. **20,** pp. 244–252, 15 Refs.
The basic theories of diffusion are discussed, and it is found that under certain conditions of flow, experimental results agree with theory.

Investigations concerning the accuracy of particle size analyses.
Prof. H. RUMPF (Karlsruhe: Institut für Mechanische Verfahrenstechnik an der Technischen Hochschule). *Staub*, vol. **20,** pp. 253–266, 29 Refs.
A detailed discussion of the theoretical bases of sedimentation.

VOL. 4 1961

Dust measuring equipment indicating or registering weight.
Prof. T. GAST (Walsum). *Staub*, vol. **20,** pp. 266–272, 4 Refs.
An electronic balance designed to measure dust concentrations is described, and the variations for different applications are indicated. Discussion: Dr. T. GAST, Dr. J. L. v. EICHBORN (18 Refs.). Group II: *Dust Deposition Measurement.* Introduction: Dr. K. SCHWARZ (Essen), *Survey of the problems of measuring dust deposition. Staub*, vol. **20,** pp. 275–278, 11 Refs. A review of the methods employed in Germany (solids and SO_2). The paper is largely concerned with funnel methods and the adhesive foil.

The measurement of dust deposition.
Prof. M. DIEM (Karlsruhe). *Staub*, vol. **20,** pp. 278–282, 10 Refs.
Several methods of dust deposition measurement, which were used simultaneously over a period of one year, are compared. The dust concentrations at various heights (up to 500 metres) are also given.

Practical Experience in Dust Deposition Measurement.
Prof. A. HELLER (Berlin-Dahlem: Federal Office of Health for Water, Soil and Air Hygiene). *Staub*, vol. **20,** pp. 282–285, 4 Refs. Discussion: Dr. K. SCHWARZ, H. OELS. Group III: *The Organization of Dust Measurements.* Introduction: F. MARESCH (Vienna, Oestreichische Staub (Silikose) Bekämpfungsstelle).
Aims and Objects of the Austrian Dust and Silicosis Control Centre. *Staub*, vol. **20,** pp. 285–286. *Industrial Dust Control.* W. KITZLER (Leoben: Oestreichische Staub-(Silikose) Bekämpfungsstelle). *Staub*, vol. **20,** pp. 286–289, 5 Refs.

Dust Measurement in Black Coal Mines.

Dr. H. BREUER (Essen: Hauptstelle für Staub und Silikosebekämpfung des Steinkohlenbergbauvereins). *Staub*, vol. **20**, pp. 290–299, 12 Refs.

Since it is only the dust with particle size less than 5 microns which collects in the alveoli of the lungs, the dust measuring devices must be able to classify dusts as coarse (greater than 5 microns) or fine. Because the chemical and mineralogical composition of the dust affects its pathological action, routine measurements differentiate between coal and other dusts. A process for quartz determination is in preparation.

Methods of measurement in powder metallurgy.

Dr. K. TORKAR (Graz, Oestereich: Institut für Anorganische und Physikalische Chemie der Technischen Hochschule). *Staub*, vol. **20**, pp. 299–302.

Origin, behaviour and determination of submicron aerosols in Smog.

Prof. A. GOETZ (Pasadena, Cal.: California Institute of Technology). *Staub*, vol. **20** pp. 303–308, 23 Refs.

Smog generation occurs in large (automobile) traffic and industrial centers. It is contingent upon the coexistence of uncombusted hydrocarbons (HC), NO_2 SO_2 at greater than 10^{-7} concentration in stagnant air masses exposed to intense irradiation. It represents the early phases of a photochemical reaction among these compounds which produces highly polar " oxidant " compounds. Their associate avidity in the presence of natural aerosols causes particle growth well into the 10^{-5} cm range, resulting in visibility reduction and synergistic irritation. This effect increases with the olefine concentration of the hydrocarbon. With age the particle vanishes completely, due to further oxidation to volatile components (CO_2, H_2O, etc.). With the aerosol spectrometer the growth and subsequent decline of the particles can be traced quantitatively. (Author's Abstract).

Mean Special Concentrations and Maximum Allowable Concentrations.

Dr. H. KOCH (Koblenz: Bundesinstitut für Arbeitsschutz). *Staub*, vol. **20**, pp. 308–311.

Discussion as to whether the maximum allowable concentration can be used as a reference point for spot tests at places of work. Discussion: Prof. A. GOETZ, Prof. H. JUNG, Dr. K. EMBER, L. HIRSCH. Group IV: *The Measurement of Radioactive Dusts.* Introduction: Prof. J. A. SCHEDLING, (Vienna). *A survey of the problems of measuring radioactive dusts. Staub*, vol. **20**, pp. 313–319.

Methods of Measuring Radioactive Dusts in Workrooms.

Dr. D. HASENCLEVER (Bonn: Staubforschungsinstitut). *Staub*, vol. **20**, pp. 314–319, 4 Refs.

A detailed discussion of the various types of instruments developed, and used by the author.

Radioactive Pollution in the Atmosphere.

Dr. G. SCHUMANN (Heidelberg: II Physikalisches Institut der Universität). *Staub*, vol. **20**, pp. 319–324, 15 Refs.

The sources of radioactivity in the atmosphere, and the use of radioactive materials as tracers in biological and air pollution work. End of Symposium and Conference.

Regulations governing the erection of plants which may cause air pollution.
H. OELS (Bonn). *Staub*, vol. **20,** pp. 326–329.

Research and Control of Air Pollution in the United States.
Dr. H. W. GEORGII (Frankfurt a. M.). *Staub*, vol. **20,** pp. 329–333, 11 Refs.

The Determinations of SO_2 tolerance Limits in Plantations.
Dr. R. GUDERIAN (Essen: Forschungsinstitut für Luftreinhaltung e.V.). *Staub*, vol. **20,** pp. 334–337, 12 Refs.

Problems connected with air pollution investigations, in particular the damage caused by SO_2 from ore roasters in tree plantations and on other vegetation, are discussed and illustrated.

Dust Removal in Flue Gas Scrubbers.
Dr. E. WEBER (Zweibrücken). *Staub*, vol. **20,** pp. 338–344, 24 Refs.

Calculations show that the spray droplets from nozzles in a blast furnace gas scrubber, for most of the distance they move, are at their terminal velocities. By changing the spray nozzles and the dirty gas velocities the efficiency of the spray tower can be improved.

Translated and Abstracted by W. STRAUSS,
Department of Chemical Engineering,
University of Melbourne, Australia.

VOL.
4
1961

Int. J. Air and Water Poll. Pergamon Press 1961. Vol. 4, Nos. 3/4, pp. 272–274. Printed in Great Britain.

Air Pollution Bibliography

WE are indebted to the compilers of the sources from which the titles listed in this bibliography are selected. The number of papers published is so large that we considered a selection of the more important papers made by one with great experience in the field of air pollution would be of considerable value, a task kindly undertaken by Mr. T. F. Hurley.

Abstracts of the papers listed can be found in *A.P.C.A. Abstracts* April 1960–June 1960 (denoted by " A " code number) of *Public Health Engineering Abstracts* March 1960–June 1960 (denoted by " P ").

GENERAL ASPECTS OF AIR POLLUTION

Towards clean air. *Brit. Med. J.* (London), No. 5161, 1242 (Dec. 5, 1959). [A 3000/1960]

Control of smoke and dust emission from existing coal equipment. H. J. ROSE. *Smokeless Air* (London) **30**, 190–3 (1960). [A 3106/1960]

Air pollution by sulfur dioxide, hydrogen sulfide, and carbon disulfide. L. ROSIVAL and M. STRECHA. *Smokeless Air* (London) **30**, 194–9 (1960). [A 3107/1960]

Future problems in air pollution research. L.A. CHAMBERS. *Ind. Med. and Surg.* **28**, 487–90 (Nov. 1959). [A 3047/1960]

New understanding from current atmospheric pollution research. M. D. THOMAS. *Amer. J. Public Health* **49**, 1664–9 (Dec. 1959). [A 3052/1960]

SOURCE, POLLUTANTS, CONTROL OF AIR POLLUTION

Sulfur dioxide in atmospheric pollution, and methods of control. D. BIENSTOCK, J. H. FIELD and H. E. BENSON. *Natl. Acad. Sci.–Natl. Research Council Publ.* No. **652**, 54–62 (1959). [A 3001/1960]

The concentration of sulfur dioxide in the atmosphere near power stations. W. G. CUMMINGS and M. W. REDFEARN. *J. Inst. Fuel* (London) **32**, 358–63 (Aug. 1959). [A 3003/1960]

Spectroscopic analysis of industrial emissions for nitric oxide, nitrogen dioxide, and sulfur dioxide. A. J. HAAGEN-SMIT, V. D. TAYLOR and MARGARET F. BRUNELLE. *Int. J. Air Poll.* (London) **2**, 159–66 (Oct. 1959). [A 3005/1960]

Atmospheric factors affecting the corrosion of steel. P. J. SEREDA. *Ind. Eng. Chem.* **52**, 157–60 (Feb. 1960). [A 3007/1960]

The reduction of smoke from a vertical boiler fired by an underfeed stoker. D. L. R. BAILEY and L. E. REED. *J. Inst. Fuel.* (London) **33**, 188–92 (Apr. 1960). [A 3111/1960]

Use of a battery of burning chambers to remove industrial wastes from the atmosphere. O primenenii batareinykh kamer dozhiganiia dlia ochistki promyshlennykh vybrosov v atmosfernyi vozdukh. S. P. BELOUSOV, A. S. DUN, and I. I. NIKBERG. *Gigiena i Sanit.* (Moscow) **24**, (4) 70–1 (1959). [A 3112/1960]

The use of heterocyclic tertiary amines for the control of corrosion caused by flue gases. E. B. DAVIES and B. J. ALEXANDER. *J. Inst. Fuel* (London) **33**, 163–73 (Apr. 1960). [A 3115/1960]

The release of sodium aerosols during the combustion of pulverised coal. A laboratory investigation. D. OUNSTED and J. SCHOEN. *J. Inst. Fuel* (London) **33**, 199–206 (Apr. 1960). [A 3118/1960]

Measuring of the dust-content in industrial gases and in the respiratory air; measurements of the dust deposited on the ground. Staubgehaltsmessung in Industriegasen und Atemluft; Staubniederschlagsmessungen im Gelände. K. GUTHMANN. *Stahl u. Eisen* (Düsseldorf) **79**, 1129–41 (Aug. 6, 1959). [A 3054/1960]

Settling chambers for the collection of grit R. JACKSON. *B.C.U.R.A.* (Surrey) **23**, 349–65 (Aug.–Sept. 1960). [A 3055/1960]

Introduction to the use of slag wool filters for cleaning . . . hot gas streams. Part II. LESLIE SILVERMAN, CHARLES KURTER, and CHARLES BILLINGS. *Industrial Wastes*, **4**, 73–74 (July 1959). [P/1960]

Performance of a flue-fed incinerator. E. R. KAISER, J. HALITSKY, M. B. JACOBS, and L. C. MCCABE. *Journal of the Air Pollution Control Association*, **9**, 85–91 (August 1959). [P/1960]

ATMOSPHERIC PHENOMENA, DISPERSION, EMISSION

The areas within concentration isopleths downwind of continuous point source. W. P. ELLIOTT, *Int. J. Air Poll.* (London) **2**, 115–26 (Oct. 1959). [A 3008/1960]

ANALYSIS, DETECTION, MEASUREMENT, MEASUREMENT EQUIPMENT MEASUREMENT METHOD, RESEARCH, SAMPLE, TECHNIQUES, TESTING

Ultraviolet determination of nitrogen dioxide as a nitrite ion. A. P. ALTSHULLER and A. P. WARTBURG. *Anal. Chem.* **32**, 174–7 (Feb. 1960). [A 3009/1960]

Methods of sampling and storage of air containing vapors and gases. R. A. BAKER and R. C. DOERR. *Int. J. Air Poll.* (London) **2**, 142–158 (Oct. 1959). [A 3011/1960]

Note on the exchange of iodine between the atmosphere, land, and sea. B. BOLIN. *Int. J. Air Poll.* (London) **2**, 127–31 (Oct. 1959). [A 3012/1960]

Micrurgic identification of chloride and sulfate. R. D. CADLE. *Natl. Acad. Sci.–Natl. Research Council Publ.* No. **652**, 18–21 (1959). [A 3013/1960]

Measurement of the dust fallout in the vicinity of a single low chimney. M. DIEM, U.K. At. Energy Authority (Ind. Group), Risley, Warrington, Lancashire, Eng. 1959. 9 pp. [A 3015/1960]

Determination of NO_2 and NO in air. W. E. GILL. *Amer. Ind. Hyg. Assoc. J.* **21**, 87–96 (Feb. 1960). [A 3016/1960]

Measurements on the content of non-volatile organic material in atmospheric precipitation. G. H. NEUMANN, S. FONSELIUS and L. WAHLMAN. *Int. J. Air. Poll.* (London) **2**, 132–41 (Oct. 1959). [A 3022/1960]

Spectrophotometric determination of chloride in air. P. W. WEST and H. COLL. *Natl. Acad. Sci.–Natl. Research Council Pub.* No. **652**, 37–42 (1959). [A 3028/1960]

Correction for anisokinetic sampling of gas-borne dust particles. S. BADZIOCH. *J. Inst. Fuel* (London) **33**, 106–10 (Mar. 1960). [A 3123/1960]

Particle size analysis for the chemical engineer. L. COHEN. *Chem. & Process Eng.* (London) **40**, 383–6 (Nov. 1959). [A 3128/1960]

Particle size analysis in routine process control. A. G. PENDLETON. *Chem. & Process Eng.* (London) **41**, 147–8 (Apr. 1960). [A 3136/1960]

Some statistical aspects of dust counting. J. R. ASHFORD. *Brit. J. Appl. Phys.* (London) **11**, 13–21 (Jan. 1960). [A 3060/1960]

Current applications of the reverse-jet filter principle. K. J. CAPLAN. *A.M.A. Arch. Ind. Health* **21**, 200–8 (Mar. 1960). [A 3062/1960]

Some aspects of gas chromatography. P. J. FARENDEN and M. P. MENDOZA. *B.C.U.R.A.* (Surrey) **23**, 366–76 (Aug.–Sept. 1959). [A 3064/1960]

Determination of sulfur trioxide and sulfur dioxide in flue gases. R. S. FIELDER, P. J. JACKSON, and E. RAASK. *J. Inst. Fuel* (London) **33**, 84–9 (Feb. 1960). [A 3066/1960]

A note on the determination of low concentrations of sulfate in rain and other waters. J. K. JOHANNESSON. *New Zealand J. Sci.* (Wellington) **1**, 423–4 (Sept. 1958). [A 3070/1960]

The distribution of a polydispersed aerosol in a turbulent atmosphere at a long distance from an instantaneous point source. O rasseîanii tîazheloi polidispersnoî primesi v turbulentnoî atmosfere na bol'shom rassoîanii ot mgnovennogo tochechnogo istochnika. I. L. KAROL' and IA. PRESSMAN. *Inzhener. Fiz. Zhur.* (Minsk) **2**, (9) 83–91 (Sept. 1959). [A 3071/1960]

A routine sampler for detecting variations in the emission of dust and grit. B. LEES and M. C. MORLEY. *J. Inst. Fuel* (London) **33**, 90–5 (Feb. 1960). [A 3074/1960]

Deposition of aerosols on clothing at low wind speeds. C. L. PUNTE and E. J. OWENS. *Armed Forces Chem. J.* **14**, 25–8 (Mar.–Apr. 1960). [A 3076/1960]

Gas analyser-recorder using chromatography. Analyseur-enregistreur de gaz par voie chromatographique. M. VÉLUT and J. JOURDA. *Rev. Inst. franç pétrol.* (Paris) **13**, 1635–58 (Dec. 1958). [A 3078/1960]

Improved cascade impactor for measuring aerosol particle size in air pollutants, commercial aerosols, cigarette smoke. R. I. MITCHELL and J. M. PILCHER. *Industrial and Engineering Chemistry*, **51**, 1039–42 (Sept. 1959). [P/1960]

The influence of the combustion and type of coal upon the 3,4-benzpyrene content of waste

VOL. 4 1961

gases. B. P. GURINOW. *Gigiena i Sanitariya*, **27**, No. 12, 6–9 (1958). *Staub*, **19**, 306–7 (Aug. 1959). [P/1960]

Progress of the automobile industry in regard to automobile exhaust and air pollution. JAMES M. CHANDLER. *American Industrial Hygiene Association Journal*, **20**, 488–93 (Dec. 1959). [P/1960]

Geometric mean particle size and its application in sampling of airborne dust. S. GURUSWAMY and V. S. NARASIMHACHAR. *J. Sci. & Indus. Research*, **18B**, 319–23 (Aug. 1959). [P/1960]

Measurements on the content of non-volatile organic material in atmospheric precipitation. GEORG HUGO NEUMANN, STIG FONSELIUS and LARS WAHLMAN. *Int. J. of Air Poll.*, **2**, No. 2, 132–41 (Oct. 1959). [P/1960]

The longevity of the phytotoxicant produced from gaseous ozone-olefin reactions. WILFRED NIELS ARNOLD. *Int. J. Air Poll.*, **2**, No. 2, 167–74 (Oct. 1959). [P/1960]

AREA MEASUREMENTS, SURVEYS

Concentration of sulfur-containing pollutants in a major urban area. M. B. JACOBS. *Natl. Acad. Sci.—Natl. Research Council Publ.* No. **652**, 81–7 (1959). [A 3030/1960]

On the correlation of lung cancer with tar in air pollution. E. GORHAM. *Med. Officer* (London) **101**, 178 (Mar. 28, 1959). [A 3139/1960]

The reliability of air pollution measurements in relation to the siting of instruments. MARJORIE CLIFTON, D. KERRIDGE, WINIFRED MOULDS, J. PEMBERTON, and J. K. DONOGHUE. *Int. J. Air Poll.* (London) **2**, 188–96 (Oct. 1959). [A 3081/1960]

Reducing trace substances in the atmosphere. Reduzierende Spurenstoffe in der atmosphäre. H. MROSE. *J. Meteorol.* (Berlin) **13**, 51–8 (Jan.–June 1959). [A 3082/1960]

The spatial distribution of air pollution in Sheffield, 1957–59. J. PEMBERTON, MARJORIE CLIFTON, J. K. DONOGHUE, D. KERRIDGE, and WINIFRED MOULDS. *Int. J. Air Poll.* (London) **2**, 175–87 (Oct. 1959). [A 3083/1960]

Air pollution and cancer mortality in Liverpool hospital region and North Wales. P. STOCKS. *Int. J. Air Poll.* (London **1**, Nos. 1/2, 1–13 (Oct. 1958). Bulletin of Hygiene, **34**, 768–69 (Aug. 1959). [P/1960]

BOOKS, MANUALS, SELECTED PUBLICATIONS, SPECIFICATIONS, STANDARDS, TECHNICAL REPORTS

The chemical analysis of air pollution. M. B. JACOBS. Interscience Publishers, Inc., New York. 1960. $13.50. 430 pp. *Ser. Chemical Analysis* Vol. **10**. [A 3033/1960]

Limits of allowable concentrations of atmospheric pollutants. Book 1, V. A. RYAZANOV, Editor. Transl. by B. S. LEVINE, 59–21173. OTS U.S. Dept. of Commerce, Wash. 25, D.C. $2.75. 135 pp. [A 3091/1960]

Limits of allowable concentration of atmospheric pollutants. Book 2—1955. V. A. RYAZANOV, Editor. Transl. by B. S. LEVINE. 59–21174. OTS U.S. Dept. of Commerce, Wash. 25, D.C. $3.00. 163 pp. [A 3092/1960]

Limits of allowable concentration of atmospheric pollutants. Book 3—1957. V. A. RYAZANOV, Editor. Transl. by B. S. LEVINE. 59–21175. OTS U.S. Dept. of Commerce, Wash, 25, D.C. $3.00. 146 pp. [A 3093/1960]

Sanitary protection of atmospheric air: purification of industrial discharge gases from suspended substances. V. N. UZHOV. Transl. by B. S. LEVINE. 59–21092, 1959. OTS U.S. Dept. of Commerce, Wash. 25, D.C. $3.00. 152 pp. [A 3094/1960]

EFFECTS OF AIR POLLUTION

Lung disease due to inhaled dust. K. M. A. PERRY. *Postgrad. Med. J.* (London) **35**, 470–5 (Aug. 1959). [A 3041/1960]

Some physical and physiological factors controlling the fate of inhaled substances. P. E. MORROW. Wash.—1023, 113–36. OTS U.S. Dept. of Commerce, Washington 25, D.C. [A 3151/1960]

Tolerance and cross-tolerance development to atmospheric pollutants ketene and ozone. R. M. MENDENHALL and H. E. STOKINGER. *Journal of Applied Physiology*, **14**, No. 6, 923–26 (Nov. 1959). [P/1960]

Air pollution and causes of death. CHARLES DALY. *Brit. J. Prevent. and Social Med.*, **13**, 14–27 (1959). Chemical Abstracts, **53**, 22645 (Nov. 25, 1959). [P/1960]

Int. J. Air and Water Poll. Pergamon Press 1961. Vol. 4, Nos. 3/4, p. 275. Printed in Great Britain.

Book Reviews

Modern trends in Occupational Health. Edited by R. S. F. SCHILLING, M.D., M.R.C.P., D.P.H., D.I.H.

THE series of " Modern Trends " publications are now well established as valuable contributions to medical literature and the present volume maintains the high standard. The chapter dealing with the measurement of health by the Editor provides a good summary and introduction to the many excellent contributions which follow. Every aspect of industrial health is covered and the two chapters dealing with industrial pulmonary disease will be of particular interest to those concerned with the effects of inhalation of noxious substances on health. The chapter dealing with industrial radiation hazards is also outstanding and one which merits careful study.

The contributions dealing with the psychological aspects of industrial health are particularly interesting, and Dr. HERON's contribution on ageing and employment gives a clear account of the recent researches which have been carried out on this important subject. The pressing problem of noise is also dealt with, together with many other aspects of this ever-growing subject.

This is a book not only for the specialist but it contains much for every doctor and is well worthy of particular consideration by the many general practitioners who hold industrial appointments. The book is well produced and is easy to read, and can be thoroughly recommended as good value.

ANDREW B. SEMPLE

Water Pollution Research, 1959. H.M. Stationery Office, 1960. 115 pp., 7s.

IT is a matter for congratulation that, in spite of a steady increase in the activity and size of his Laboratory, the Director of Water Pollution Research was able to produce this lengthy and interesting report within six months of the end of the year to which it refers.

Only six years after its opening the Stevenage laboratory is being extended to increase its total research effort by nearly one-half. This is a fair reflection of the widespread public interest in river pollution and of the leading position held by the WPR Laboratory.

The treatment of waste waters continues to be the chief concern of the Laboratory and this work receives considerable financial support from industry through the Federation of British Industries. The best type and size of bacteria-bed medium has, in recent years, become more important as sewage works have become overloaded and the possibility has been considered of converting these works to recirculation or alternating double filtration. To investigate this a large pilot plant has been set up at Stevenage, in the open air, using four types of medium, each in two sizes. Radioactive tracers are to be used to correlate filter efficiency with retention time.

Synthetic detergents have been blamed for all sorts of troubles at sewage works and in streams, and, indeed, there can be no doubt that they are responsible for some of them. For some years past a Standing Technical Committee of the Ministry of Housing and Local Government has been looking into this matter with the active assistance of the WPR Laboratory. In August 1958 the detergent manufacturers started to supply the Luton area with a newly developed detergent which laboratory and pilot tests had shown to be more easily destroyed during sewage treatment. The results were systematically examined by Stevenage.

A great volume of research is being carried on in other fields: aeration in activated sludge, fish toxicity, freshwater streams, instruments for a number of analyses, survey of the Thames estuary, etc. The list of the Laboratory's publications during the year give a useful conspectus of this work.

P.C.G.I.

VOL. 4 1961

Int. J. Air and Water Poll. Pergamon Press 1961. Vol. 4, Nos. 3/4, p. 276. Printed in Great Britain.

Notes and News

Soviet air pollution studies available in English from OTS.

An extensive survey of Russian literature on air pollution and related occupational diseases is being compiled by Dr. BEN S. LEVINE under a U.S. Public Health Service research grant. His first and second volumes of the series are now available from the Office of Technical Services, U.S. Department of Commerce, Washington 25, D.C., U.S.A.

Dr. LEVINE has devoted the last five years to collecting and translating Russian literature on air pollution. The Russian-born scientist is a former U.S. Public Health Service researcher. Now retired, he is devoting full time to surveying and translating Russian works on air pollution for the benefit of American scientists and technicians who want information on air pollution research and development in the U.S.S.R. Dr. LEVINE is now working on the third volume of the new literature survey and he expects the complete survey to fill at least several more volumes, all of which will be published by OTS.

The survey covers the basic concepts of air pollution prevention in the U.S.S.R., explains the methods of approach, outlines the scope and plan of the work, and evaluates the progress made. Dr. LEVINE points out that Soviet interest in air pollution is both hygienic and economic. The survey shows that industrial discharges frequently contain large amounts of valuable byproducts.

Dr. LEVINE has also translated and OTS has published a three-volume series on the limits of allowable concentrations of atmospheric pollutants, plus a volume on sanitary protection of atmospheric air. The latter volume was written by V. N. UZHOV of the Technical Division of the Institute for Making Gas Purifying Equipment in Moscow. Dr. LEVINE selected UZHOV's book for translation after an extensive review of Russian works on the subject. Although the book was first published in 1955, Dr. LEVINE considers it "authoritatively recent".

Dr. LEVINE's translations and literature surveys currently available from OTS are as follows. Please use the order number when ordering. (Dates given below are the dates of publication in the Soviet Union.)

No. 59–21173 Limits of Allowable Concentrations of Atmospheric Pollutants (Book 1), 1952, 135 pages, $2.75.

No. 59–21174 Limits of Allowable Concentrations of Atmospheric Pollutants (Book 2), 1955, 163 pages, $3.

No. 59–21175 Limits of Allowable Concentrations of Atmospheric Pollutants (Book 3), 1957, 146 pages, $3.

No. 59–21092 Sanitary Protection of Atmospheric Air; Purification of Industrial Discharge Gases from Suspended Substances, 1955, 160 pages, $3.

No. 60–21049 U.S.S.R. Literature on Air Pollution and Related Occupational Diseases, **1**, 214 pages, $3.50.

No. 60–21188 U.S.S.R. Literature on Air Pollution and Related Occupational Diseases, **2**, 270 pages, $4.

No. 60–21475 U.S.S.R. Literature on Air Pollution and Related Occupational Diseases, **3**, 265 pages, $4.

USCOMM–DC–62,344

VOL.
4
1961